2012

Chemical characterization of hydrocarbons and transcriptome profiling to elucidate pathway(s) of hydrocarbon biosynthesis in maize, pea, Botryococcus braunii and Emiliania huxleyi

Wenmin Qin
Iowa State University

Chemical characterization of hydrocarbons and transcriptome profiling to elucidate pathway(s) of hydrocarbon biosynthesis in maize, pea, *Botryococcus braunii* and *Emiliania huxleyi*

by

Wenmin Qin

A dissertation submitted to the graduate faculty

in partial fulfillment of the requirements for the degree of

DOCTOR OF PHILOSOPHY

Major: Biochemistry

Program of Study Committee:
Basil J. Nikolau, Major Professor
Alan Dispirito
Jacqueline Shanks
Martin Spalding
Marna Yandeau-Nelson

Iowa State University

Ames, Iowa

2012

TABLE OF CONTENTS

ACKNOWLEDGEMENTS

I would never have been able to finish my dissertation without the guidance of my committee members, help from my lab members, collaborators and friends, and support from my family.

I would like to express my deepest gratitude to my advisor, Dr. Basil Nikolau, for his excellent guidance, caring, patience, and providing me with an excellent atmosphere and financial support for doing research. I would like to thank Dr. Marna Yandeau-Nelson for guiding my research for the past several years and helping me to develop my background in maize physiology and biochemistry. I also would like to thank Dr. Nikolau and Dr. Yandeau-Nelson for their help in the preparation of this dissertation. Dr. Jacqueline Shanks was enthusiastic and always provide insight to my work and available to answer questions in our biweekly hydrocarbon group meeting. I would like to thank other committee members, Dr. Alan Dispirtio and Dr. Martin Spalding and my former committee members, Dr. Tom Bobik, Dr. Volker Brendel and Dr. Reuben Peters for serving on my Program of Study committee.

I would like to thank Dr. Ann Perera and Dr. Zhihong Song teach me how to use GC-MS and identify all the metabolites in all my samples and analyze data generated by GC-MS. Dr. Wolfe Gordon from Univesity of California-Chico teaches me how to grow *Emiliania huxleyi,* which needs special nutrients and growth conditions. I would like to thank Dr. Laura Jarboe for letting me use the Bio-Rad qPCR machine in her lab and Dr. Kumar

Babu Kautharapu for helping me start with the qPCR experiments. Also, I would like to thank our lab manager, Dr. Libuse Brachova for maintaining the lab and make all the experiments possible, Sam Condon, an undergraduate student in our lab for collecting and preparing maize samples, extracting hydrocarbons, preparing media for algae and cell counting of *Emiliania huxleyi* and all other lab members for their suggestion about the my research, for their jokes, like a seasoning of life here and their support.

I would also like to thank my parents, especially my mom, Suzhi Liu, two younger sisters and one younger brother, who always support me and encourage me with their best wishes.

Finally, I would like to thank my husband, Wenzhi Lan, who was always there cheering me up and stood by me through the good times and bad. Our daughter, Lisa Lan, wipes away my stress and gives me strength when I feel tired and weak.

CHAPTER 1: OVERVIEW

INTRODUCTION

Hydrocarbons are compounds comprised of only carbon and hydrogen. Based on their structures, hydrocarbons can be classified into four different types: 1) saturated hydrocarbons (alkanes); 2) unsaturated hydrocarbons with at least one double (alkene) or triple (alkyne) bond between carbon atoms; 3) cycloalkanes containing one or more carbon rings; and 4) aromatic hydrocarbons having one or more aromatic rings.

Simple, linear hydrocarbons such as alkanes and alkenes occur at low levels but are widely distributed in the biosphere. For example, hydrocarbons are found in some bacteria (Han and Calvin 1969a, b; Park 2005) and algae (Dennis and Kolattukudy 1991b; Rieley et al. 1998a) as well as in the cuticles of insects (Endler et al. 2004; Samuels et al. 2008b; Wackett et al. 2007) and plants (Samuels et al. 2008b). Hydrocarbons mainly exist in surface lipids of plants and insects and they serve as a protective barrier against water loss and pathogen attack (Kunst and Samuels 2003b; Kunst and Samuels 2009; PostBeittenmiller 1996; Samuels et al. 2008b). Because aliphatic hydrocarbons are the predominant components of petroleum-based fuels such as gasoline, diesel, and jet fuel, biological-derived hydrocarbons are ideal replacement of transportation fuels (Fortman et al. 2008; Jetter and Kunst

2008; Regalbuto 2009) and thus are potential alternative biorenewable fuel for petroleum (Jetter and Kunst 2008).

Hydrocarbon biosynthesis

Hydrocarbons are thought to be synthesized from very long chain fatty acid (VLCFA) precursors (Tornabene 1982). However, the biological synthesis of hydrocarbons from VLCFAs is poorly understood. Four different hypotheses for the mechanism(s) of hydrocarbon biosynthesis have been proposed (Beller et al. 2010; Frias et al. 2010; Park 2005; Schirmer et al. 2010; Sukovich et al. 2010a; Sukovich et al. 2010b; Templier et al. 1991a, b) (Fig1).

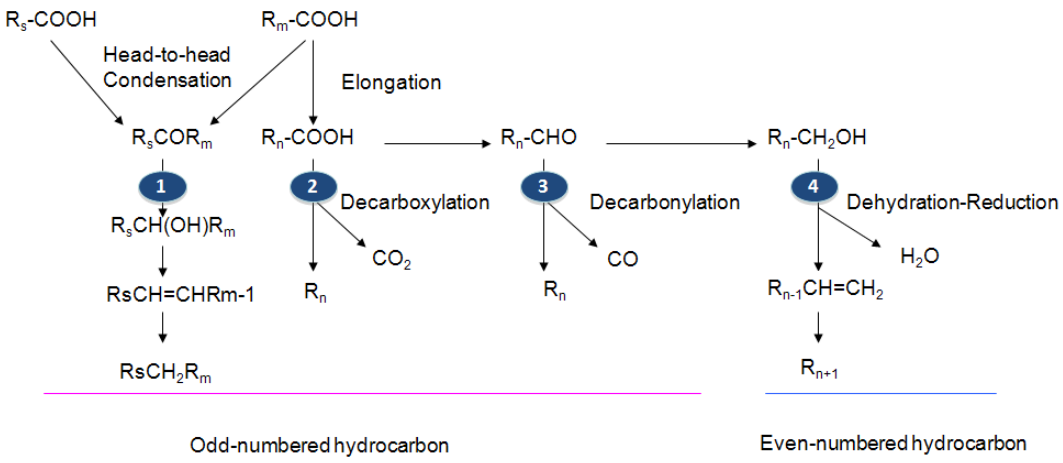

Figure 1. Potential hydrocarbon biosynthesis pathways

The majority of the linear hydrocarbons that are found in biological systems are of odd-number of carbon atoms. Because most fatty acids are assembled by the condensation of 2-carbon units (acetate), theoretically therefore, odd-numbered hydrocarbons (chain length 2n-1) can be derived

from even-numbered fatty acid (2n) by either the loss of a single carbon atom or by the addition of a single carbon. The theory that hydrocarbon biosynthesis occurs via the loss of one carbon is supported by the finding that across many diverse biological systems odd-numbered hydrocarbons (2n-1) occur together with their corresponding even-numbered fatty acid (2n) precursors (Chibnall and Pipe 1934; Largeau et al. 1980a; Major and Blomquist 1978). This theory was further supported by radio-labeling studies in which either the carboxyl group or alkyl chain of a fatty acid was radio-labeled, and it was demonstrated that the labeled carboxyl carbon is lost in the reaction, whereas labeled carbons within the alkyl chain are retained (Cassagne and Lessire 1974; Khan and Kolattukudy 1974; Kolattukudy et al. 1972). However, the mechanism by which the single carbon atom is lost during hydrocarbon biosynthesis is still poorly understood. Four different hydrocarbon biosynthetic mechanisms have been proposed, and these are illustrated in Figure 1, and individually discussed.

1. Direct decarboxylation of a fatty acid: Direct decarboxylation of fatty acid removes a single carbon and results in a 2n-1 hydrocarbon (Largeau et al. 1980a; Templier et al. 1992b; Templier et al. 1984, 1987, 1991a, b). Direct evidence for this mechanism includes decarboxylation of exogenous C_{32} fatty acid in leaf slices of *Brassica oleracea* (Kolattukudy and Buckner 1972), flower petals of *Vicia faba* (Croteau and Kolattukudy 1974; Kolattukudy et al. 1974), cell free extracts from pea leaves (Khan and Kolattukudy 1974) as well

as decarboxylation of exogenous C_{24} acid in *Allium porrum* leaves (Croteau and Kolattukudy 1974). Recently, the *OleT* gene was identified in *Jeotgalicoccus species* and shown to encode a novel P450 fatty acid decarboxylase. Overexpression of *OleT* in *Escherichia coli* results in the production of a terminal alkene (Rude et al. 2011). Similarly, a curacin thioesterase, CurM TE, from a marine cyanobacterium *Lyngbya majuscule*, catalyzes the formation of terminal alkene from β-sulfated acyl-ACP substrates through hydrolysis, decarboxylation, and sulfate elimination (Gehret et al. 2011). These examples demonstrate that very diverse mechanisms exist for the decarboxylation of a fatty acid to generate alkenes.

2. Decarbonylation mechanism: The decarbonylation mechanism, involves the reduction of a fatty acid to an aldehyde, which is subsequently decarbonylated to produce a hydrocarbon through the release of carbon monoxide (Cheesbrough and Kolattukudy 1984b). The decarbonylation mechanism was first proposed based on observations in pea (Buckner and Kolattuky 1973). In the presence of dithioerythritol, which inhibits the conversion of C_{32} fatty acid to C_{31} alkane, C_{32} aldehyde accumulated and no C_{31} alkane was produced (Buckner and Kolattuky 1973). In addition, exogenously labeled C_{18} and C_{24} aldehydes can be converted to alkanes by the microsomal preparation from pea (Bognar et al. 1984). Additional evidence in support of the decarbonylation mechanism has been obtained from a number of systems. For example, microsomal preparations from the uropygial

gland of *Podiceps nigricollis* (the eared grebe water bird) and the algae, *B. braunii* are both able to convert C_{18} aldehyde to C_{17} alkane with the concomitant release of CO (Cheesbrough and Kolattukudy 1988; Dennis and Kolattukudy 1991c). Later, the decarbonylase activity was partially purified from *B. braunii* and it was hypothesized to be a cobalt-porphyrin enzyme, which could convert fatty aldehyde to hydrocarbon and CO under anaerobic conditions (Dennis and Kolattukudy 1992). In insects, (e.g. the fleshfly *Sarcophaga crassipalpis,* the blowfy *Phormia regina,* the German cockroach *Blattella germanica,* the house cricket *Acheta domesticus,* the Mormon cricket *Anabrus simplex,* the dampwood termite *Zootermopsis nevadensis* and the house fly, *Musca domestica*), this activity was found that be a cytochrome P450 enzyme and was able to convert aldehydes to hydrocarbons and CO (Mpuru et al. 1996; Reed et al. 1996; Reed et al. 1995; Reed et al. 1994a; Reed et al. 1994b). In contrast to the putative cobalt-porphyrin enzyme characterized in *B. braunii*, this cytochrome P450 enzyme in insects requires NADPH and oxygen for enzymatic activity and very little hydrocarbon was formed under anaerobic conditions. A putative decarbonylase has also been partially purified from a higher plant, *Pisum sativum* (Schneider-Belhaddad and Kolattukudy 2000). The partially purified aldehyde decarbonylase in pea, like the decarbonylase in *B. braunii*, is a metal-dependent, integral membrane protein, which converts the aldehyde a hydrocarbon and CO (Schneider-Belhaddad and Kolattukudy 2000). This indicates that metals play

an important role in pea decarbonylase activity, as has been demonstrated in *B. braunii*. Simultaneously with these characterizations, the enzyme catalyzing the conversion of the fatty acid to the aldehyde was characterized. This fatty acyl-CoA reductase was partially purified from *B. braunii* and pea leaves (Vioque and Kolattukudy 1997; Wang and Kolattukudy 1995b).

Recently, genes of both the aldehyde decarbonylase and an acyl-ACP reductase, which produces the aldehyde intermediate from fatty acid, have been identified from a cyanobacteria, *Synechococcus elongates* (Schirmer et al. 2010). More recently, in Arabidopsis *cer1* is found to be involved in very long-chain alkane biosynthesis (Bourdenx et al. 2011), and *cer1* is reported to form a complex with *cer3* and this *cer1*/*cer3* complex is responsible for converting very long chain fatty acids to very long chain alkanes (Bernard et al. 2012b).

3. Reduction-Dehydration-reduction mechanism: This mechanism involves the initial double reduction of a fatty acid to the corresponding aldehyde and alcohol, which is then dehydrated, and further reduced to a hydrocarbon. This mechanism was proposed based on the observation in *Vibrio furnissii* M1, that after feeding [1-^{14}C] hexadecanoic acid, radio-labeled even-numbered alkanes and the corresponding radio-labeled alcohol and aldehyde intermediates were detected (Park 2005). However, the recent genome sequencing of *V. furnissii* M1 did not reveal the occurrence of the alkane biosynthesis genes (Park 2005; Wackett et al. 2007). This probably

implies that hydrocarbon biosynthesis in *Vibrio furnissii* may occur via a different mechanism from double reduction-hydration-reduction pathway described by Park (Park 2005).

4. Head-to-head condensation mechanisms: This hypothesis involves the head-to-head decarboxylative condensation of two fatty acid molecules, to generate a ketone that is sequentially reduced, dehydrated and finally reduced to form a hydrocarbon. This mechanism was first proposed in 1929 based on the observation in cabbage that a C_{29} hydrocarbon was present in large amounts, and that the predicted intermediates for head-to-head condensation of two C_{15} fatty acid molecules, the corresponding ketone and secondary alcohol, were also present. However, C_{15} fatty acid precursor was not found (Channon and Chibnall 1929). Later, several modified head-to-head condensation mechanisms were proposed in pyrethrum and string bean (Wanless et al. 1955), tobacco (Kaneda 1968) and in the bacteria, *Sarcina lutea* and *Stenotrophomonas maltophilia* (Albro and Dittmer 1969a, b, c; Tornabene and Peterson 1978). Recently, genes involved in the head-to-head condensation pathway were identified in the bacteria *Micrococcus luteus* and *Shewanella oneidensis* strain MR-1(Beller et al. 2010; Sukovich et al. 2010a; Sukovich et al. 2010b). Expression of a cluster of three genes from *Micrococcus luteus* conferred *E. coli* with the ability to produce long-chain aliphatic hydrocarbons (Beller et al. 2010). Deletion of the *oleABCD* gene cluster in *Shewanella oneidensis* strain MR-1 eliminates the ability of this strain

to produce alkanes and other nonpolar extractable products. Three of these genes (*OleA, C* and D) were shown to be required for catalysis of the head-to-head condensation (Sukovich et al. 2010b). *OleA* catalyzes the formation of the ketones via a non-decarboxylative thiolytic condensation of fatty acyl chains. *OleC* is thought to participate in the conversion of ketones to hydrocarbons, based on the observation that in an *oleC* knock-out mutant the ketone, but not the structurally analogous hydrocarbon was produced (Sukovich et al. 2010a; Sukovich et al. 2010b). However, the function of *OleD* is as yet not clear.

The head-to-head-condensation pathway has been confirmed in the bacteria, *Shewanella oneidensis* and the decarbonylation pathway have been confirmed the cyanobacteria *Synechococcus elongatus* and Arabidopsis (Bernard et al. 2012b; Schirmer et al. 2010; Sukovich et al. 2010a; Sukovich et al. 2010b), In plants, like maize and pea, and green algae, *B. braunii*, the present literature suggest that decarbonylation pathway is responsible for hydrocarbon biosynthesis. In Arabidopsis, *cer1*/*cer3* complex convert fatty acids to alkanes. CER1 is the decarbonylase and CER3 converts fatty acids to aldehyde or other intermediates (Bernard et al. 2012b).

Hydrocarbons in maize silk

In *Zea mays* ssp. Mays (maize), hydrocarbons are prevalent in the cuticular surface lipids covering numerous organs including the coleoptile, leaves from seedlings and mature plants, ear husk leaves, pollen and silks

(Bianchi et al. 1990; Blaker and Greyson 1988; Perera 2005a). The surfaces of silks and pollen are especially rich sources of hydrocarbons (Bianchi et al. 1990), which account for ~89% of the surface lipids on these organs (Perera 2005a). The surface lipids on silks from the maize inbred B73 are composed primarily of C_{27}, C_{29} and C_{31} n-alkanes and alkenes and comprise ~2% of the dry weight of silks (Perera et al. 2010c). These cuticular hydrocarbons are thought to serve as a protective barrier against water loss, insect herbivory and pathogen invasion (Kunst and Samuels 2003a; PostBeittenmiller 1996; Samuels et al. 2008a, b).

Hydrocarbon accumulation differs between two portions of silks, those that are encased by husk leaves versus the portion that have emerged from the husk leaves and are exposed to the environment. The cuticle of silks that have emerged from the ear husks accumulate hydrocarbons over an 8-day period, with accumulation occurring most rapidly 2-3 days post-emergence (Perera et al. 2010c). Up to 3-fold more hydrocarbons accumulate on emerged silks as compared to silks that are encased within the ear husks. Total hydrocarbon accumulation also varied 2- to 3-fold between two maize inbreds, cultivars B73 and Mo17, with some hydrocarbon constituents represented 2-50 fold more in emerged silks from inbred B73 (Perera et al. 2010c).

Saturated and unsaturated C_{16} and C_{18} fatty acids are predominant in maize pollen (Bianchi et al. 1990; Seppanen et al. 1989), which is also true for

maize silk (Perera et al. 2010b). This suggests that C_{16} and C_{18} fatty acids can be elongated to fatty acid with chain length up to C_{32} to be used as the precursors for hydrocarbon biosynthesis in maize pollen and silk. In addition, the double bond positions in $C_{18:1}$, $C_{18:2}$ and $C_{18:3}$ are consistent with the double bond positions in maize silks (Perera et al. 2010c). Characterization of the lipid constituents of maize silk cuticle suggests that three parallel pathways generate the unsaturated fatty acids and fatty aldehydes that are the precursors of the alkenes and dienes series of hydrocarbons (Perera et al. 2010c). This includes: 1) elongation-isomerization-decarbonylation, in which a 2-enoyl-CoA intermediate from fatty acid elongation is isomerized to 3-enoyl-CoA to generate 5-monounsaturated acids, followed by reduction and decarbonylation to form 4-alkenes; 2) elongation-desaturation-decarbonylation, in which the fatty acid is first elongated to a very long chain fatty acid and it is then desaturated, reduced and decarbonylated to an alkene; and 3) desaturation-elongation-decarbonylation, which starts with the desaturation of a C18 fatty acid to 18:1Δ12, 18:2 Δ9, 12 and 18:2 Δ6,9 unsaturated fatty acids, which are then elongated to very long chain fatty acids and reduced to aldehydes and decarbonylated to generate alkenes and dienes, and these processes produce a series of unsaturated alkenes of different chain lengths, containing double bonds at the 4th, 6th, or 9th, and dienes with double bonds at the 6th and 9th, and 9th and 12th positions (Perera et al. 2010c).

Hydrocarbons in pea epidermis

Alkanes are very abundant in the surface lipids of leaves (Buschhaus et al. 2007a, b; Cassagne and Lessire 1975; Gniwotta et al. 2005; Riedel et al. 2007). For example, C_{29} alkane comprises ~30% of total surface lipids on leaves from *Brassica oleracea* (Eigenbrode et al. 1991). Like in other plants, surface lipids on pea leaves also play a role in resistance to environmental stresses, such as drought (Sanchez et al. 2001), pathogens and insect predators (Chang et al. 2004; Chang et al. 2006; Gniwotta et al. 2005; Gorb et al. 2008; Rutledge and Eigenbrode 2003; White and Eigenbrode 2000a).

In pea, surface lipids on leaves are reported to be composed of alkanes, esters, aldehydes, primary and secondary alcohols and free fatty acids (Holloway et al. 1977; Kolattukudy 1970; Macey and Barber 1970b). Relative compositions of surface lipids vary between the adaxial (i.e. upper) and abaxial (i.e. lower) sides of the leaf (Gniwotta et al. 2005; Holloway et al. 1977). The abaxial leaf epidermis contains more alkanes (~73% of total surface lipids) whereas the adaxial leaf epidermis has more alcohols (~71% of total surface lipids) (Halloway PJ 1977). Accordingly, surface lipid ultrastructures of abaxial and adaxial epidermis differ and were ribbon-shaped and platelet-shaped, respectively (Gniwotta et al. 2005). The biological importance of this difference in surface lipid composition between the upper and lower surface of the leaf are not clear. However, data suggests that specific compositions of surface lipids may be resistant to pathogens. For

example, the abaxial (lower) surface of pea leaves, which accumulates a significant amount of hydrocarbons, is more resistant to the pathogen, *Erysiphe pisi*, as evidenced by a lower rate of spore germination and hyphae formation (Gorb et al. 2008). Moreover, the pea leaf surface with reduce surface lipids, the insect attachment force to leaf considerably enhances (Chang et al. 2004; Chang et al. 2006; White and Eigenbrode 2000a, b). Similarly, the pea leaf surface with more surface lipids, the insect and pathogen density decreased (Donkin et al. 1982; Hey et al. 1997; Jewer et al. 1982; Jewer et al. 1985; Pemadasa 1981, 1982). In addition, the abaxial leaf surface contains more stomata and the stomata can open greater in abaxial than in adaxial epidermis of leave (Macey and Barber 1970b; Vassilevska-Ivanova and Naidenova 2006). The high levels of alkanes in the abaxial leaf epidermis might contribute to prevent water loss when the stomata open for gas exchange.

The change of a single gene can affect the composition and amount of surface lipids in pea (Holloway et al. 1977; Vassilevska-Ivanova and Naidenova 2006). For example, the *wa*, *was*, *wb*, *wel*, *win*, *wlo,* and *wsp* mutants each have a waxless phenotype (Marx 1987a). However, the affected genes in these mutants have not been identified or cloned. Among them, the *wachslos* (*wlo*) mutation normally suppresses wax deposition on the adaxial surfaces of leaflets (Tsukahara and Sawayama 2005).

As discussed in the hydrocarbon biosynthesis pathway section, hydrocarbons in pea might be biosynthesized by the decarbonylation pathway. However, genes involved in hydrocarbon biosynthesis in pea have yet to be identified and characterized.

Hydrocarbons in *Botryococcus braunii*

B. braunii, a unicellular photosynthetic microalgae, has attracted a lot of interest because of its high hydrocarbon content and thus potential application and profitability for liquid fuel production (Rao et al. 2007). Based on the chemical structures of hydrocarbons produced, three races of *B. braunii* have been documented (Races A, B and L). Race A is dominated by unbranched, odd-numbered n-alkadienes ranging from C_{25} to C_{31} and comprising 16-70% of cellular dry weight (Okada et al. 2000; Okada et al. 2004). Race B predominantly produces isoprenoid hydrocarbons, known as botryococcenes (C_nH_{2n-10}), with chain lengths between C_{30} to C_{37} and accounting for 27-86% of cellular dry weight (Metzger et al. 1990). Race L produces lycopadiene, a C_{40} tetraterprene, which accounts for 2-8% of cellular dry weight (Largeau et al. 1980a). Race A is of particular interest in this thesis because this strain produces simple, linear hydrocarbons.

Hydrocarbons accumulate in two distinct sites in *B. braunii*. The bulk of hydrocarbons occurs in an external pool in the trilaminar outer walls and associated globules, and this is thought to be the main site of hydrocarbon accumulation (Wolf and Cox 1981). A second internal pool is present in

cytoplasmic inclusion bodies (Largeau et al. 1980b). Hydrocarbons within these pools could potentially be metabolized and mobilized. A study in which *B. braunii* was incubated with labeled palmitic acids, resulted in the labeling of hydrocarbons; after several weeks, the labeled hydrocarbons from both internal and external pools did not decrease (Templier et al. 1992a). This result indicates that hydrocarbons in these two pools are irreversibly stored and not further metabolized (Templier et al. 1992a). However, later, a third pool, a small internal pool, was found to be involved in metabolism of alkenylepoxides and alkadienones (An et al. 2003; Dayananda et al. 2005; Tran et al. 2010; Weetall 1985).

It has been generally established that carbon, nitrogen and phosphorous are required for growth and replication (Ge et al. 2011b; Ranga Rao and Ravishankar 2007; Tanoi et al. 2011). Specific concentrations of these nutrients can impact hydrocarbon production. For example, providing 2% CO_2 to *B. braunii* increases hydrocarbon production in different strains (e.g. LB572, CFTRI-Bb-2, CFTRI-Bb-1 and N-836) (Shifrin and Chisholm 1981). Although nitrogen is required for cellular growth, nitrogen deficient conditions can stimulate lipid storage (Choi et al. 2011). For example, for *B. braunii* strain UTEX 572, reducing nitrate from 3.66 to 0.04 mM results in the doubling of lipid content (Casadevall et al. 1985). In contrast, excess phosphate can noticeably increase hydrocarbon production (Casadevall et al. 1985). The high concentration of phosphate might be used to maintain N:P ratio, which is

known to influence the lipid content of various algae (Dennis and Kolattukudy 1992; Wang and Kolattukudy 1995a).

As aforementioned, both the fatty acyl-CoA reductase, responsible for generating aldehydes, and the decarbonylase that subsequently converts the aldehyde to a hydrocarbon, were partially purified from *B. braunii* (Kayano and Shiraiwa 2009). This suggests that a decarbonylation pathway is active in *B. braunii*. However, the associated genes have yet to be identified and characterized.

Hydrocarbons in *Emiliania huxleyi*

The coccolithophore *Emiliania huxleyi* (*E. huxleyi*) is a unicellular alga that produces an intricate calcium carbonate platelet exoskeleton (i.e. coccoliths) (Paasche 2001). *E. huxleyi* has colonized almost every photic zone of the oceans and constitutes a high portion of the marine biomass. *E. huxleyi* plays a major role in global carbon cycling by regulating the exchange of CO_2 across the ocean-atmosphere interface through calcium carbonate precipitation and photosynthesis (Timmermans et al. 2001; Westbroek et al. 1993), and deposition of carbon deep within the ocean (Conte et al. 1994; Conte et al. 1995).

Of particular palaeoceanographic interest, *E. huxleyi* produces neutral lipids consisting of a series of polyunsaturated long-chain (C_{31}–C_{39}) alkenones, alkenoates, and alkenes (collectively termed, PULCA) (Conte et al. 1992; Conte et al., 1994; Bell and Pond, 1996; Sawada et al., 1996). These

compounds are widely used as biomarkers, indicating the existence of such algae in paleo-environments (Eglinton et al., 1992). C_{31} alkadienes, C_{33} alkadiene, triene and tetraenes, and C_{37} and C_{38} alkatrienes have been observed in different strains of *E. huxleyi* and the alkene distributions differ among strains (Conte et al. 1995; Grossi et al. 2000; Rieley et al. 1998b). For example, some strains (e.g. CCAP920/2, CH25/90, 92E, VAN 55, VAN56 and GO1) contain a mixture of C_{31}, C_{33}, C_{37} and C_{38} alkenes while others (e.g. CS-57, G1779GE, M181, 88E and EH2) lack the C_{37} and C_{38} hydrocarbons (Sawada and Shiraiwa 2004; Volkman et al. 1980). In addition, $C_{29:1}$ and $C_{21:6}$ alkenes have also been found in some *E. huxleyi* strains (Rieley et al. 1998b). The double bond positions of alkenes from some strains have been identified. For example, 1,22-, 2,22-, 3,22-, 2,24-$C_{31:2}$ and 2,24-$C_{33:2}$ were identified in strain CCAP 920/2, and 1,22-$C_{31:2,}$ 1,15,22-$C_{37:3}$ and 1,16,23-$C_{38:3}$ were characterized in strain VAN 556 (Rieley et al. 1998b). In addition, in these two *E. huxleyi* strains, double bonds in C_{31} and C_{33} alkenes were *cis* isomers, whereas in C_{37} and C_{38} alkatrienes they were *trans* (Paasche 1998, 2001; Paasche and Brubak 1994; Sekino et al. 1996; Sekino and Shiraiwa 1994). Although double bond positions are known for some alkenes in *E. huxleyi*, the information about the double bond positions of other alkenes is still unknown. Thus, it is necessary to identify the double bond position in these alkenes to provide chemical structure information to understand the hydrocarbon biosynthesis pathway.

The growth of *E. huxleyi* is greatly influenced by availability of nutrients (Sekino and Shiraiwa 1994). *E. huxleyi* can produce large quantities of organic matter by fixing dissolved inorganic carbon (Sekino et al. 1996) (Herfort et al. 2002, 2003), but cell growth is inhibited when inorganic carbon supplies (e.g. bicarbonate) are limiting (Shiraiwa 2003a). However, high concentrations of bicarbonate can suppress cell growth and the mechanism of this suppression is not yet fully understood (Egge and Heimdal 1994). However, it has been proposed that in the presence of excess bicarbonate, coccolith formation may be favored over photosynthesis (Pond and Harris 1996), which could thereby suppress growth. In addition to carbon, availability of phosphorous and nitrogen is also important for growth and for hydrocarbon production. An analysis of algae blooms showed that *E. huxleyi* grows well at low concentrations of phosphate. Cells were most dense when grown in an N:P ratio of 16:0.2, whereas cell growth was inhibited when grown at an N:P ratio of 16:5 (Epstein 1998; Prahl et al. 2003). In addition, the PULCAs in *E. huxleyi* increased in stationary phase (Eltgroth et al. 2005) and under N and P limitation, PULCA accumulation increased up to 10-20% (Grossi et al. 2000; Shiraiwa 2003a).

The physiological functions of alkenes and their biosynthetic pathways in *E. huxleyi* cells remain elusive. Alkenes might serve as an energy reserve, similar to other neutral lipids in *E huxleyi* and *Isochrysis galbana* (Rontani et al. 2006). In addition, these alkenes may play an important role in the acclimatization to

low temperatures by regulating membrane fluidity, which could explain the huge blooms observed in high-latitude waters where the temperature is 10-15 ℃ (Rontani et al. 2006).

Most of the alkenes which have been identified in *E. huxelyi* have the n-9 (ω 9) position. This suggests that they might be derived from an oleic acid (cis-9-$C_{18:1}$) precursor followed by chain elongation and desaturation (Grossi et al. 2000; Rontani et al. 2006). In addition, the corresponding methyl C_{37} and C_{38} alkenones have been identified in *E. huxleyi* strain CS-57 (Rontani et al. 2006). This might suggest that in *E. huxleyi* CS-57, 15,22-$C_{37:2}$ and 15,22-$C_{38:2}$ are derived from their corresponding methyl C_{37} and C_{38} alkenones by reduction to alkenols, followed by dehydration to alkatrienes and a second reduction to C_{37} and C_{38} alkadienes (Sukovich et al. 2010a; Sukovich et al. 2010b). The C_{37} and C_{38} alkenones with the same double bonds positions are thought to be derived from fatty acid precursors that are elongated followed by Δ^{14} and Δ^{15} desaturation (Schirmer et al. 2010). Collectively, these observations suggest that there are multiple hydrocarbon biosynthesis pathways that function in in *E. huxleyi*. However, at present, no genes and proteins involved in hydrocarbon biosynthesis in *E. huxleyi* have been identified.

RESEARCH GOAL

A goal of this research is to provide metabolic profiling and transcriptome profiling data from which the hydrocarbon biosynthesis pathway can be

dissected via the isolation and characterization of genes involved in hydrocarbon biosynthesis in different biological systems. Maize, pea, *B. braunii* and *E. huxleyi* have been chosen as the biological systems to investigate the mechanism of hydrocarbon biosynthesis not only because they are rich of simple hydrocarbons but also because their genome sequences are available or will be available soon. The genomes of maize and *E. huxyeli* have been sequenced (www.maizesequence.org; genome.jgi-psf.org/Emihu1/Emihu1.home.html) and EST sequencing of *B. braunii* is being carried out by DOE Joint Genome Institute (www.jgi.doe.gov/sequencing/why/bbraunii.hmtl) and ~8200 pea ESTs are available in Genbank (http://pgrc.ipk-gatersleben.de/cr-est/files/).

In this thesis conditions for the hyper- and hypo-accumulation of hydrocarbons were established (Chapter 2, 3, 5, 6 and 7). The physiological conditions that induce the hyper- and hypo-accumulation of hydrocarbons conditions were used to simultaneously collect RNA for transcriptome sequencing analysis. Simultaneously, the hydrocarbons were analyzed in the four biological systems, specifically to identify the positions of double bonds in alkenes (Appendix A, Chapter 6 and 7). The comparative transcriptome profiling of cells that hyper- and hypo-accumulate hydrocarbon in all four biological systems is being used to identify genes that are differentially expressed between these two conditions. This thesis covers the entire pipeline for maize (Chapter 2, 3 and 4). Chapter 4 takes advantage of differential

hydrocarbon accumulation between stages of silk development in maize, and mines transcriptomes of these silks for candidate genes involved in hydrocarbon biosynthesis. This comparative transcriptome profiling approach is also being applied to pea epidermis, and the two algae, *B. braunii* and *E. huxleyi*.

These accomplishments have set the stage for comparative transcriptome profiling to identify candidate genes involved in the hydrocarbon biosynthetic pathway(s) in these four biological systems. In addition, sequence similarity networks can be built from these four biological systems by pairwise blast. The within system networks can then be clustered to identify highly inter-connected modules using the Markov Chain Clustering (Archer and McLellan) method. Then, modules without any genes increasing their expression in the direction of hydrocarbon accumulation and genes without increasing expression in the direction of hydrocarbon accumulation will be filtered out. By this cross-system analysis, the candidate genes involved in hydrocarbon biosynthetic pathway(s) shared by maize silk, pea epidermis, *B. braunii* and *E. huxleyi* can be discovered. In addition, the systems that have been set up and characterized in this body of work can also be used to identify the hydrocarbon biosynthetic pathways specific to each of the individual biological systems.

Addressing these research goals will add to the current understanding of how hydrocarbons are biosynthesized in different biological systems. This

fundamental understanding has the potential of impacting the development of alternative advanced biofuels that can be used in place of petroleum-sourced fuels. It is widely recognized that the current use of fossil-carbon as an energy source is unsustainable because of depleting supplies and the accumulation of carbon dioxide in the environment. Because biologically-sourced hydrocarbons have chemical structures that are nearly identical to petroleum, they ultimately could have an application in the development of advanced biofuels.

DISSERATION ORGANIZATION

This dissertation is organized into eight chapters, consisting of six journal papers (Chapters 2-7) and general conclusions (Chapter 8). Chapter 1 includes a literature review that provides a general introduction to the chemical nature of hydrocarbons, current knowledge regarding the biosynthesis of hydrocarbons and a brief description of the biological systems that produce hydrocarbons (e.g. the silk of maize, the epidermal layer of pea, and within the algae, *B. braunii* and *E. huxleyi*). Chapters 2, 3 and 4 focus on the natural variation of hydrocarbon accumulation observed in different organs of maize across numerous genotypes. Chapter 2 describes the natural variation of hydrocarbon accumulation in two organs in maize (pollen and silks) that produce relatively large amounts of hydrocarbons across a very genetically diverse set of maize inbreds, including 26 founders of the nested-association

mapping population (Benjamini and Hochberg 1995) and 14 inbreds with diverse genetic backgrounds . Chapter 3 extends the analysis of maize by examining hydrocarbon accumulation on pollen and silks in a select set of maize inbreds and hybrid progeny generated from genetic crossing among these inbreds. Chapter 4 describes the comparative transcriptome profiling between encased and emerged maize silks to elucidate differential expression of genes involved in surface lipid production on maize silks. Dr. Marna Yaudeau-Nelson and I planted and collected all the maize silks materials in fields used in Chapter 2, 3 and 4. I have done all the preparation for maize silks, hydrocarbon extraction and analysis and data analysis with help of an undergraduate student, Sam Condon, who lyophilized and ground maize samples and did hydrocarbon extractions of some maize sample in Chapter 2, 3 and 4. A BCB graduate student, Adarsh Jose did all the bioinformatics analysis in Chapter 4. The approach of comparative transcriptome profiling has also been applied to other three organisms, pea epidermis and two algae, *B. braunii* and *E. huxleyi*. I have prepared all the RNA samples from cells with hyper- and hypo-accumulated hydrocarbons in all of the four organisms. How the transcriptomics data were generated was described in Appendix A. Transcriptome data obtained from these RNA samples are now being analyzed in collaboration with Adarsh Jose.

Chapter 5 describes the different spatial and temporal accumulation of hydrocarbons in epicuticular lipids from leaves and stipules of *Pisum sativum*,

using a mutant that allows for efficient isolation of the epidermis from the underlying tissue. I have done all the work in this chapter with help of ~10 undergraduates, who peel pea epidermis with me.

Chapters 6 and 7 describe hydrocarbon accumulation patterns in the algae, *B. braunii* and *E. huxleyi*, grown in different carbon, nitrogen and phosphate nutrient availability, which modulates hydrocarbon accumulation. I have done all the work in these two chapters with help of Sam Condon, who prepared media for *B. braunii* and *E. huxleyi* and counted cells of *E. huxleyi*.

Chapter 8 is a general summary and conclusion of this work and it integrates the conclusion from Chapter 2-7 and discusses the impact and future directions of the research.

References

Albro PW, Dittmer JC (1969a) The biochemistry of long-chain, nonisoprenoid hydrocarbons. 3. The metabolic relationship of long-chain fatty acids and hydrocarbons and other aspects of hydrocarbon metabolism in Sarcina lutea. Biochemistry 8:1913-1918

Albro PW, Dittmer JC (1969b) The biochemistry of long-chain, nonisoprenoid hydrocarbons. I. Characterization of the hydrocarbons of Sarcina lutea and the isolation of possible intermediates of biosynthesis. Biochemistry 8:394-404

Albro PW, Dittmer JC (1969c) The biochemistry of long-chain, nonisoprenoid hydrocarbons. IV. Characteristics of synthesis by a cell-free preparation of Sarcina lutea. Biochemistry 8:3317-3324

An JY, Sim SJ, Lee JS, Kim BW (2003) Hydrocarbon production from secondarily treated piggery wastewater by the green alga Botryococcus braunii. J Appl Phycol 15:185-191

Archer K, McLellan F (2002) Controversy surrounds proposed xenotransplant trial. Lancet 359:949-949

Beller HR, Goh EB, Keasling JD (2010) Genes Involved in Long-Chain Alkene Biosynthesis in Micrococcus luteus. Appl Environ Microb 76:1212-1223

Benjamini Y, Hochberg Y (1995) Controlling the False Discovery Rate - a Practical and Powerful Approach to Multiple Testing. J Roy Stat Soc B Met 57:289-300

Bernard A, Domergue F, Pascal S, Jetter R, Renne C, Faure JD, Haslam RP, Napier JA, Lessire R, Joubes J (2012) Reconstitution of Plant Alkane Biosynthesis in Yeast Demonstrates That Arabidopsis ECERIFERUM1 and ECERIFERUM3 Are Core Components of a Very-Long-Chain Alkane Synthesis Complex. Plant Cell 24:3106-3118

Bianchi G, Murelli C, Ottaviano E (1990) Maize Pollen Lipids. Phytochemistry 29:739-744

Blaker TW, Greyson RI (1988) Developmental Variation of Leaf Surface Wax of Maize, Zea-Mays. Can J Bot 66:839-846

Bognar AL, Paliyath G, Rogers L, Kolattukudy PE (1984) Biosynthesis of Alkanes by Particulate and Solubilized Enzyme Preparations from Pea Leaves (Pisum-Sativum). Archives of Biochemistry and Biophysics 235:8-17

Buckner JS, Kolattuky PE (1973) Specific Inhibition of Alkane Synthesis with Accumulation of Very Long-Chain Compounds by Dithioerythritol, Dithiothreitol, and Mercaptoethanol in Pisum-Sativum. Arch Biochem Biophys 156:34-45

Buschhaus C, Herz H, Jetter R (2007a) Chemical composition of the epicuticular and intracuticular wax layers on adaxial sides of Rosa canina leaves. Ann Bot-London 100:1557-1564

Buschhaus C, Herz H, Jetter R (2007b) Chemical composition of the epicuticular and intracuticular wax layers on the adaxial side of Ligustrum vulgare leaves. New Phytol 176:311-316

Casadevall E, Dif D, Largeau C, Gudin C, Chaumont D, Desanti O (1985) Studies on Batch and Continuous Cultures of Botryococcus-Braunii - Hydrocarbon Production in Relation to Physiological-State, Cell Ultrastructure, and Phosphate Nutrition. Biotechnology and Bioengineering 27:286-295

Cassagne C, Lessire R (1974) Studies on alkane biosynthesis in epidermis of *Allium porrum*
L. leaves.
. Arch Biochem Biophys
165

Cassagne C, Lessire R (1975) Studies on Alkane Biosynthesis in Epidermis of Allium-Porrum-L Leaves .4. Wax Movement into and out of Epidermal-Cells. Plant Sci Lett 5:261-268

Chang GC, Neufeld J, Durr D, Duetting PS, Eigenbrode SD (2004) Waxy bloom in peas influences the performance and behavior of Aphidius ervi, a parasitoid of the pea aphid. Entomol Exp Appl 110:257-265

Chang GC, Neufeld J, Eigenbrode SD (2006) Leaf surface wax and plant morphology of peas influence insect density. Entomol Exp Appl 119:197-205

Channon HJ, Chibnall AC (1929) The ether-soluble substances of cabbage leaf cytoplasm: The isolation of n-nonacosane and di-n-tetradecyl ketone. Biochem J 23:168-175

Cheesbrough TM, Kolattukudy PE (1984) Alkane biosynthesis by decarbonylation of aldehydes catalyzed by a particulate preparation from Pisum sativum. Proc Natl Acad Sci U S A 81:6613-6617

Cheesbrough TM, Kolattukudy PE (1988) Microsomal preparation from an animal tissue catalyzes release of carbon monoxide from a fatty aldehyde to generate an alkane. J Biol Chem 263:2738-2743

Chibnall A, Pipe SH (1934) The metabolism of plant and insect waxes.
. Biochemical Journal 28

Choi GG, Kim BH, Ahn CY, Oh HM (2011) Effect of nitrogen limitation on oleic acid biosynthesis in Botryococcus braunii. J Appl Phycol 23:1031-1037

Conte MH, Thompson A, Eglinton G (1994) Primary Production of Lipid Biomarker Compounds by Emiliania-Huxleyi - Results from an Experimental Mesocosm Study in Fjords of Southwestern Norway. Sarsia 79:319-331

Conte MH, Thompson A, Eglinton G, Green JC (1995) Lipid Biomarker Diversity in the Coccolithophorid Emiliania-Huxleyi (Prymnesiophyceae) and the Related Species Gephyrocapsa-Oceanica. J Phycol 31:272-282

Croteau R, Kolattukudy PE (1974) Biosynthesis of hydroxyfatty acid polymers. Enzymatic synthesis of cutin from monomer acids by cell-free preparations from the epidermis of Vicia faba leaves. Biochemistry 13:3193-3202

Dayananda C, Sarada R, Bhattacharya S, Ravishankar GA (2005) Effect of media and culture conditions on growth and hydrocarbon production by Botryococcus braunii. Process Biochem 40:3125-3131

Dennis M, Kolattukudy PE (1992) A cobalt-porphyrin enzyme converts a fatty aldehyde to a hydrocarbon and CO. Proc Natl Acad Sci U S A 89:5306-5310

Dennis MW, Kolattukudy PE (1991a) Alkane biosynthesis by decarbonylation of aldehyde catalyzed by a microsomal preparation from Botryococcus braunii. Arch Biochem Biophys 287:268-275

Dennis MW, Kolattukudy PE (1991b) Alkane biosynthesis by decarbonylation of aldehyde catalyzed by a microsomal preparation from Botryococcus braunii. Arch Biochem Biophys 287:268-275

Donkin ME, Travis AJ, Martin ES (1982) Stomatal Responses to Light and Co2 in the Argenteum Mutant of Pisum-Sativum. Z Pflanzenphysiol 107:201-209

Egge JK, Heimdal BR (1994) Blooms of Phytoplankton Including Emiliania-Huxleyi (Haptophyta) - Effects of Nutrient Supply in Different N-P Ratios. Sarsia 79:333-348

Eigenbrode SD, Stoner KA, Shelton AM, Kain WC (1991) Characteristics of Glossy Leaf Waxes Associated with Resistance to Diamondback Moth (Lepidoptera, Plutellidae) in Brassica-Oleracea. J Econ Entomol 84:1609-1618

Eltgroth ML, Watwood RL, Wolfe GV (2005) Production and cellular localization of neutral long-chain lipids in the haptophyte algae Isochrysis galbana and Emiliania huxleyi. J Phycol 41:1000-1009

Endler A, Liebig J, Schmitt T, Parker JE, Jones GR, Schreier P, Holldobler B (2004) Surface hydrocarbons of queen eggs regulate worker reproduction in a social insect. Proceedings of the National Academy of Sciences of the United States of America 101:2945-2950

Epstein BL, D' Hondt, S., Quinn, J. G., Zhang, J. & Hargraves, P. E. (1998) The effect of dissolved nutrient concentrations on alkenone-based temperature estimates. . Paleoceanography 13:122-126

Fortman JL, Chhabra S, Mukhopadhyay A, Chou H, Lee TS, Steen E, Keasling JD (2008) Biofuel alternatives to ethanol: pumping the microbial well. Trends Biotechnol 26:375-381

Frias JA, Goblirsch BR, Wackett LP, Wilmot CM (2010) Cloning, purification, crystallization and preliminary X-ray diffraction of the OleC protein from Stenotrophomonas maltophilia involved in head-to-head hydrocarbon biosynthesis. Acta Crystallogr F 66:1108-1110

Ge YM, Liu JZ, Tian GM (2011) Growth characteristics of Botryococcus braunii 765 under high CO(2) concentration in photobioreactor. Bioresource Technol 102:130-134

Gehret JJ, Gu LC, Gerwick WH, Wipf P, Sherman DH, Smith JL (2011) Terminal Alkene Formation by the Thioesterase of Curacin A Biosynthesis STRUCTURE OF A DECARBOXYLATING THIOESTERASE. J Biol Chem 286:14445-14454

Gniwotta F, Vogg G, Gartmann V, Carver TLW, Riederer M, Jetter R (2005) What do microbes encounter at the plant surface ? Chemical composition of pea leaf cuticular waxes. Plant Physiol 139:519-530

Gorb E, Voigt D, Eigenbrode SD, Gorb S (2008) Attachment force of the beetle Cryptolaemus montrouzieri (Coleoptera, Coccinellidae) on leaflet surfaces of mutants of the pea Pisum sativum (Fabaceae) with regular and reduced wax coverage. Arthropod-Plant Inte 2:247-259

Grossi V, Raphel D, Aubert C, Rontani JF (2000) The effect of growth temperature on the long-chain alkenes composition in the marine coccolithophorid Emiliania huxleyi. Phytochemistry 54:393-399

Halloway PJ HG, Baker EA, Macey MJK (1977) Chemical composition and ultrastructure of the epicuticular wax in four mutants of *Pisum sativum* (L). Chem Phys Lipids 20:141-155

Han J, Calvin M (1969a) Hydrocarbon Distribution of Algae and Bacteria, and Microbiological Activity in Sediments. P Natl Acad Sci USA 64:436-&

Han J, Calvin M (1969b) Hydrocarbon distribution of algae and bacteria, and microbiological activity in sediments. Proc Natl Acad Sci U S A 64:436-443

Herfort L, Thake B, Roberts J (2002) Acquisition and use of bicarbonate by Emiliania huxleyi. New Phytol 156:427-436

Herfort L, Thake B, Roberts J (2003) Acquisition and use of bicarbonate by Emiliania huxleyi (vol 156, pg 427, 2002). New Phytol 158:225-225

Hey SJ, Bacon A, Burnett E, Neill SJ (1997) Abscisic acid signal transduction in epidermal cells of Pisum sativum L Argenteum: Both dehydrin mRNA accumulation and stomatal responses require protein phosphorylation and dephosphorylation. Planta 202:85-92

Holloway PJ, Grace M, Hunt EA, Baker, Macey MJK (1977) Chemical composition and ultrastructure of the epicuticular wax in four mutants of *Pisum sativium* (L). Chemistry and Physics of Lipids 20:141-155

Jetter R, Kunst L (2008) Plant surface lipid biosynthetic pathways and their utility for metabolic engineering of waxes and hydrocarbon biofuels. Plant J 54:670-683

Jewer PC, Incoll LD, Shaw J (1982) Stomatal Responses of Argenteum - a Mutant of Pisum-Sativum-L with Readily Detachable Leaf Epidermis. Planta 155:146-153

Jewer PC, Neales TF, Incoll LD (1985) Stomatal Responses to Carbon-Dioxide of Isolated Epidermis from a C-3 Plant, the Argenteum Mutant of Pisum-Sativum-L and a Crassulacean-Acid-Metabolism Plant Kalanchoe-Daigremontiana Hamet and Perr. Planta 164:495-500

Kaneda T (1968) Biosynthesis of Long-Chain Hydrocarbons .2. Studies on Biosynthetic Pathway in Tobacco. Biochemistry 7:1194-&

Kayano K, Shiraiwa Y (2009) Physiological Regulation of Coccolith Polysaccharide Production by Phosphate Availability in the Coccolithophorid Emiliania huxleyi. Plant Cell Physiol 50:1522-1531

Khan AA, Kolattukudy PE (1974) Decarboxylation of long chain fatty acids to alkanes by cell free preparations of pea leaves (Pisum sativum). Biochem Biophys Res Commun 61:1379-1386

Kolattukudy PE (1970) Composition of the surface lipids of pea leaves (Pisum sativum). Lipids 5:398-402

Kolattukudy PE, Buckner JS (1972) Chain elongation of fatty acids by cell-free extracts of epidermis from pea leaves (pisum sativum). Biochem Biophys Res Commun 46:801-807

Kolattukudy PE, Buckner JS, Brown L (1972) Direct evidence for a decarboxylation mechanism in the biosynthesis of alkanes in B. oleracea. Biochem Biophys Res Commun 47:1306-1313

Kolattukudy PE, Croteau R, Brown L (1974) Structure and Biosynthesis of Cuticular Lipids: Hydroxylation of Palmitic Acid and Decarboxylation of C(28), C(30), and C(32) Acids in Vicia faba Flowers. Plant Physiol 54:670-677

Kunst L, Samuels AL (2003a) Biosynthesis and secretion of plant cuticular wax. Progress in Lipid Research 42:51-80

Kunst L, Samuels AL (2003b) Biosynthesis and secretion of plant cuticular wax. Prog Lipid Res 42:51-80

Kunst L, Samuels L (2009) Plant cuticles shine: advances in wax biosynthesis and export. Curr Opin Plant Biol 12:721-727

Largeau C, Casadevall E, Berkaloff C (1980a) The Biosynthesis of Long-Chain Hydrocarbons in the Green-Alga Botryococcus-Braunii. Phytochemistry 19:1081-1085

Largeau C, Casadevall E, Berkaloff C, Dhamelincourt P (1980b) Sites of Accumulation and Composition of Hydrocarbons in Botryococcus-Braunii. Phytochemistry 19:1043-1051

Macey MJK, Barber HN (1970) Chemical Genetics of Wax Formation on Leaves of Pisum-Sativum. Phytochemistry 9:5-&

Major MA, Blomquist GJ (1978) Biosynthesis of Hydrocarbons in Insects - Decarboxylation of Long-Chain Acids to Normal-Alkanes in Periplaneta. Lipids 13:323-328

Marx GA (1987) A suite of mutants that modify pattern formation in pea leaves. Plant Molecular Biology Reporter 5:311-335

Metzger P, Allard B, Casadevall E, Berkaloff C, Coute A (1990) Structure and Chemistry of a New Chemical Race of Botryococcus-Braunii (Chlorophyceae) That Produces Lycopadiene, a Tetraterpenoid Hydrocarbon. Journal of Phycology 26:258-266

Mpuru S, Reed JR, Reitz RC, Blomquist GJ (1996) Mechanism of hydrocarbon biosynthesis from aldehyde in selected insect species: Requirement for O-2 and NADPH and carbonyl group released as CO2. Insect Biochemistry and Molecular Biology 26:203-208

Okada S, Devarenne TP, Chappell J (2000) Molecular characterization of squalene synthase from the green microalga Botryococcus braunii, race B. Arch Biochem Biophys 373:307-317

Okada S, Devarenne TP, Murakami M, Abe H, Chappell J (2004) Characterization of botryococcene synthase enzyme activity, a squalene synthase-like activity from the green microalga Botryococcus braunii, Race B. Arch Biochem Biophys 422:110-118

Paasche E (1998) Roles of nitrogen and phosphorus in coccolith formation in Emiliania huxleyi (Prymnesiophyceae). Eur J Phycol 33:33-42

Paasche E (2001) A review of the coccolithophorid Emiliania huxleyi (Prymnesiophyceae), with particular reference to growth, coccolith formation, and calcification-photosynthesis interactions. Phycologia 40:503-529

Paasche E, Brubak S (1994) Enhanced Calcification in the Coccolithophorid Emiliania-Huxleyi (Haptophyceae) under Phosphorus Limitation. Phycologia 33:324-330

Park MO (2005) New pathway for long-chain n-alkane synthesis via 1-alcohol in Vibrio furnissii M1. J Bacteriol 187:1426-1429

Pemadasa MA (1981) Abaxial and Adaxial Stomatal Behavior and Responses to Fusicoccin on Isolated Epidermis of Commelina-Communis L. New Phytol 89:373-384

Pemadasa MA (1982) Differential Abaxial and Adaxial Stomatal Responses to Indole-3-Acetic-Acid in Commelina-Communis L. New Phytol 90:209-219

Perera MA (2005) Molecular and chemical characterization of genes involved in maize cuticular wax biosynthesis. Dissertation, Iowa State University

Perera MA, Qin W, Yandeau-Nelson M, Fan L, Dixon P, Nikolau BJ (2010a) Biological origins of normal-chain hydrocarbons: a pathway model based on cuticular wax analyses of maize silks. Plant J 64:618-632

Perera MADN, Qin WM, Yandeau-Nelson M, Fan L, Dixon P, Nikolau BJ (2010b) Biological origins of normal-chain hydrocarbons: a pathway model based on cuticular wax analyses of maize silks. Plant J 64:618-632

Pond DW, Harris RP (1996) The lipid composition of the coccolithophore Emiliania huxleyi and its possible ecophysiological significance. J Mar Biol Assoc Uk 76:579-594

PostBeittenmiller D (1996) Biochemistry and molecular biology of wax production in plants. Annu Rev Plant Phys 47:405-430

Prahl FG, Wolfe GV, Sparrow MA (2003) Physiological impacts on alkenone paleothermometry. Paleoceanography 18

Ranga Rao A, Ravishankar GA (2007) Influence of CO2 on growth and hydrocarbon production in Botryococcus braunii. J Microbiol Biotechn 17:414-419

Rao AR, Dayananda C, Sarada R, Shamala TR, Ravishankar GA (2007) Effect of salinity on growth of green alga Botryococcus braunii and its constituents. Bioresour Technol 98:560-564

Reed JR, Hernandez P, Blomquist GJ, Feyereisen R, Reitz RC (1996) Hydrocarbon biosynthesis in the house fly, Musca domestica: Substrate specificity and cofactor requirement of P450hyd. Insect Biochemistry and Molecular Biology 26:267-276

Reed JR, Quilici DR, Blomquist GJ, Reitz RC (1995) Proposed mechanism for the cytochrome P450-catalyzed conversion of aldehydes to hydrocarbons in the house fly, Musca domestica. Biochemistry 34:16221-16227

Reed JR, Vanderwel D, Blomquist JG, Reitz RC (1994a) Evidence for the Involvement of a Cytochrome-P450 Enzyme in a Novel Mechanism for Hydrocarbon Biosynthesis in the House-Fly, Musca-Domestica. Faseb Journal 8:A1381-A1381

Reed JR, Vanderwel D, Choi S, Pomonis JG, Reitz RC, Blomquist GJ (1994b) Unusual mechanism of hydrocarbon formation in the housefly: cytochrome P450 converts aldehyde to the sex pheromone component (Z)-9-tricosene and CO2. Proc Natl Acad Sci U S A 91:10000-10004

Regalbuto JR (2009) Cellulosic Biofuels-Got Gasoline? Science 325:822-824

Riedel M, Eichner A, Meimberg H, Jetter R (2007) Chemical composition of epicuticular wax crystals on the slippery zone in pitchers of five Nepenthes species and hybrids. Planta 225:1517-1534

Rieley G, Teece MA, Peakman TM, Raven AM, Greene KJ, Clarke TP, Murray M, Leftley JW, Campbell C, Harris RP, Parkes RJ, Maxwell JR (1998a) Long-chain alkenes of the haptophytes Isochrysis galbana and Emiliania huxleyi. Lipids 33:617-625

Rieley G, Teece MA, Peakman TM, Raven AM, Greene KJ, Clarke TP, Murray M, Leftley JW, Campbell CN, Harris RP, Parkes RJ, Maxwell JR (1998b) Long-chain alkenes of the haptophytes Isochrysis galbana and Emiliania huxleyi. Lipids 33:617-625

Rontani JF, Prahl FG, Volkman JK (2006) Re-examination of the double bond positions in alkenones and derivatives: Biosynthetic implications. J Phycol 42:800-813

Rude MA, Baron TS, Brubaker S, Alibhai M, Del Cardayre SB, Schirmer A (2011) Terminal Olefin (1-Alkene) Biosynthesis by a Novel P450 Fatty Acid Decarboxylase from Jeotgalicoccus Species. Appl Environ Microb 77:1718-1727

Rutledge CE, Eigenbrode SD (2003) Epicuticular wax on pea plants decreases instantaneous search rate of Hippodamia convergens larvae and reduces attachment to leaf surfaces. Can Entomol 135:93-101

Samuels L, Kunst L, Jetter R (2008a) Sealing plant surfaces: cuticular wax formation by epidermal cells. Annu Rev Plant Biol 59:683-707

Samuels L, Kunst L, Jetter R (2008b) Sealing plant surfaces: Cuticular wax formation by epidermal cells. Annu Rev Plant Biol 59:683-707

Sanchez FJ, Manzanares M, de Andres EF, Tenorio JL, Ayerbe L (2001) Residual transpiration rate, epicuticular wax load and leaf colour of pea plants in drought conditions. Influence on harvest index and canopy temperature. Eur J Agron 15:57-70

Sawada K, Shiraiwa Y (2004) Alkenone and alkenoic acid compositions of the membrane fractions of Emiliania huxleyi. Phytochemistry 65:1299-1307

Schirmer A, Rude MA, Li XZ, Popova E, del Cardayre SB (2010) Microbial Biosynthesis of Alkanes. Science 329:559-562

Schneider-Belhaddad F, Kolattukudy P (2000) Solubilization, partial purification, and characterization of a fatty aldehyde decarbonylase from a higher plant, Pisum sativum. Arch Biochem Biophys 377:341-349

Sekino K, Kobayashi H, Shiraiwa Y (1996) Role of coccoliths in the utilization of inorganic carbon by a marine unicellular coccolithophorid, Emiliania huxleyi: A survey using intact cells and protoplasts. Plant Cell Physiol 37:123-127

Sekino K, Shiraiwa Y (1994) Accumulation and Utilization of Dissolved Inorganic Carbon by a Marine Unicellular Coccolithophorid, Emiliania-Huxleyi. Plant Cell Physiol 35:353-361

Seppanen T, Laakso I, Wojcicki J, Samochowiec L (1989) An Analytical Study on Fatty-Acids in Pollen Extract. Phytother Res 3:115-116

Shifrin NS, Chisholm SW (1981) Phytoplankton Lipids - Interspecific Differences and Effects of Nitrate, Silicate and Light-Dark Cycles. J Phycol 17:374-384

Shiraiwa Y (2003) Physiological regulation of carbon fixation in the biosynthesis and calcification of coccolithophorids Comparative biochemistry and Physiology Part B 136:775-783

Sukovich DJ, Seffernick JL, Richman JE, Gralnick JA, Wackett LP (2010a) Widespread Head-to-Head Hydrocarbon Biosynthesis in Bacteria and Role of OleA. Appl Environ Microb 76:3850-3862

Sukovich DJ, Seffernick JL, Richman JE, Hunt KA, Gralnick JA, Wackett LP (2010b) Structure, Function, and Insights into the Biosynthesis of a Head-to-Head Hydrocarbon in Shewanella oneidensis Strain MR-1. Appl Environ Microb 76:3842-3849

Tanoi T, Kawachi M, Watanabe MM (2011) Effects of carbon source on growth and morphology of Botryococcus braunii. J Appl Phycol 23:25-33

Templier J, Diesendorf C, Largeau C, Casadevall E (1992a) Metabolism of n-alkadienes in the A race of Botryococcus braunii. Phytochemistry 31:113-120

Templier J, Diesendorf C, Largeau C, Casadevall E (1992b) Metabolism of Normal-Alkadienes in the a Race of Botryococcus-Braunii. Phytochemistry 31:113-120

Templier J, Largeau C, Casadevall E (1984) Hydrocarbon Formation in the Green-Alga Botryococcus-Braunii .4. Mechanism of Non-Isoprenoid Hydrocarbon Biosynthesis in Botryococcus-Braunii. Phytochemistry 23:1017-1028

Templier J, Largeau C, Casadevall E (1987) Hydrocarbon Formation in the Green-Alga Botryococcus-Braunii .5. Effect of Various Inhibitors on Biosynthesis of Non-Isoprenoid Hydrocarbons in Botryococcus-Braunii. Phytochemistry 26:377-383

Templier J, Largeau C, Casadevall E (1991a) Biosynthesis of Normal-Alkatrienes in Botryococcus-Braunii. Phytochemistry 30:2209-2215

Templier J, Largeau C, Casadevall E (1991b) Nonspecific Elongation Decarboxylation in Biosynthesis of Cis-Alkadienes and Trans-Alkadienes by Botryococcus-Braunii. Phytochemistry 30:175-183

Timmermans KR, Snoek J, Gerringa LJA, Zondervan I, de Baar HJW (2001) Not all eukaryotic algae can replace zinc with cobalt: Chaetoceros calcitrans (Bacillariophyceae) versus Emiliania huxleyi (Prymnesiophyceae). Limnol Oceanogr 46:699-703

Tornabene TG (1982) Microorganisms as Hydrocarbon Producers. Experientia 38:43-46

Tornabene TG, Peterson SL (1978) Pseudomonas maltophilia: identification of the hydrocarbons, glycerides, and glycolipoproteins of cellular lipids. Can J Microbiol 24:525-532

Tran HL, Kwon JS, Kim ZH, Oh Y, Lee CG (2010) Statistical Optimization of Culture Media for Growth and Lipid Production of Botryococcus braunii LB572. Biotechnol Bioproc E 15:277-284

Tsukahara K, Sawayama S (2005) Liquid fuel production using microalgae. Journal of the Japan Petroleum Institute 48:251-259

Vassilevska-Ivanova R, Naidenova N (2006) Assessment of the stability and adaptability of waxbloom and waxless pea (Pisum sativum L.) mutant lines. Sci Hortic-Amsterdam 109:15-20

Vioque J, Kolattukudy PE (1997) Resolution and purification of an aldehyde-generating and an alcohol-generating fatty acyl-CoA reductase from pea leaves (Pisum sativum L). Arch Biochem Biophys 340:64-72

Volkman JK, Eglinton G, Corner EDS, Forsberg TEV (1980) Long-Chain Alkenes and Alkenones in the Marine Coccolithophorid Emiliania-Huxleyi. Phytochemistry 19:2619-2622

Wackett LP, Frias JA, Seffernick JL, Sukovich DJ, Cameron SM (2007) Genomic and biochemical studies demonstrating the absence of an alkane-producing phenotype in Vibrio furnissii M1. Appl Environ Microb 73:7192-7198

Wang X, Kolattukudy PE (1995a) Solubilization and Purification of Aldehyde-Generating Fatty Acyl-Coa Reductase from Green-Alga Botryococcus-Braunii. Febs Lett 370:15-18

Wang X, Kolattukudy PE (1995b) Solubilization and purification of aldehyde-generating fatty acyl-CoA reductase from green alga Botryococcus braunii. FEBS Lett 370:15-18

Wanless GG, King WH, Ritter JJ (1955) Hydrocarbons in Pyrethrum Cuticle Wax. Biochemical Journal 59:684-690

Weetall HH (1985) Studies on the Nutritional-Requirements of the Oil-Producing Alga Botryococcus-Braunii. Appl Biochem Biotech 11:377-391

Westbroek P, Brown CW, Vanbleijswijk J, Brownlee C, Brummer GJ, Conte M, Egge J, Fernandez E, Jordan R, Knappertsbusch M, Stefels J, Veldhuis M, Vanderwal P, Young J (1993) A Model System Approach to Biological Climate Forcing - the Example of Emiliania-Huxleyi. Global Planet Change 8:27-46

White C, Eigenbrode SD (2000a) Effects of surface wax variation in Pisum sativum on herbivorous and entomophagous insects in the field. Environ Entomol 29:773-780

White C, Eigenbrode SD (2000b) Leaf surface waxbloom in Pisum sativum influences predation and intra-guild interactions involving two predator species. Oecologia 124:252-259

Wolf FR, Cox ER (1981) Ultrastructure of Active and Resting Colonies of Botryococcus-Braunii (Chlorophyceae). Journal of Phycology 17:395-405

CHAPTER 2. THE NATURAL VARIATION IN HYDROCARBON ACCUMULATION IN POLLEN AND SILKS FROM A DIVERSE SET OF MAIZE INBREDS

Wenmin Qin, Sam Condon, MarnaYandeau-Nelson, Basil J. Nikolau.
Center for Metabolic Biology, Plant Science Institute
Center for Biorenewable Chemicals
Department of Biochemistry, Biophysics and Molecular Biology
Iowa State University, Ames, IA 50010
Email: dimmas@iastate.edu
Telephone: 515-294-0347
Fax number: 515-294-0534

Abstract

Total hydrocarbon accumulation and relative abundances of individual constituents were investigated in pollen and silks of a diverse set of maize inbreds. This includes 26 inbred founders of the nest-associated mapping population, and 14 inbreds with diverse genetic backgrounds. The latter set of inbreds together capture ca. 30% of the allelic diversity that occurs in a collection of 260 inbreds. These analyses indicate that hydrocarbons abundances vary in maize silks among a diverse inbreds and also vary between two different tissues, pollen and silk in the same inbred. In addition to this genetic-based and organ-specific effect on hydrocarbons, we observed that the the emerged silks produce 2 to 3 fold more hydrocarbons that silks encased within the husk leaves. This latter pattern of hydrocarbon accumulation may be due to environmental signals and/or organ development, because silk emergence integrates silk development and exposure to higher stress levels as silks emerge outside the husk leaves.

Keywords: *Zea mays*, Poaceae, maize, metabolomics, pollen, silk, hydrocarbons, surface lipids

1. Introduction

Simple, linear hydrocarbons such as alkanes and alkenes occur at low levels in discrete places in biological systems (Han and Calvin 1969a; Park 2005; Samuels et al. 2008a; Wackett et al. 2007). One of the most accessible biological systems to study these hydrocarbons is the cuticle of insects and plants (Greene and Gordon 2003; Samuels et al. 2008b). Hydrocarbons are rich in the cuticule surface lipids of plants, and they serve as a protective barrier against water loss and pathogen attack (Kunst and Samuels 2003b; Kunst and Samuels 2009; PostBeittenmiller 1996; Samuels et al. 2008b).

The cuticle of silks from the maize inbred B73 is composed primarily of C_{27}, C_{29} and C_{31} n-alkanes and alkenes, and these metabolites comprise about 2% of the dry weight of this organ (Perera et al. 2010c). The cuticle hydrocarbon lipid-pool of silks rapidly expands as the silks emerge from the ear husks over an 8-day period, with accumulation increasing by about 3-fold during this period (Perera et al. 2010c). In addition, there appears to be considerable natural variation within the maize germplasm. For example, the silks of the inbred B73 accumulate 2- to 3-fold more hydrocarbons than the inbred Mo17, with considerable more complexity in hydrocarbon profiles in B73 than Mo17 (Perera et al. 2010c) .

In addition to silks, the cuticles of other maize organs (e.g. seedling leaf, coleoptile, mature leaf, ear husk and pollen) also contain hydrocarbons (Bianchi et al. 1990; Blaker and Greyson 1988; Perera 2005b). Among these, pollen produces a cuticle that is rich in hydrocarbons; ~89% of the pollen cuticle surface lipids are hydrocarbons (Perera 2005b).

Maize is a genetically diverse crop species, encompassing extensive genome polymorphism in DNA sequences (Liu et al. 2010; Sa et al. 2010; Ware et al. 2006), and expressing tremendous variation in morphological traits. Metabolic diversity within maize germplasm has also been noted, including diversity in such metabolites as carotenoids (Kuhnen et al. 2011; Menkir et al. 2008), phenolics (Lopez-Martinez et al. 2009), anthocyanins (Kuhnen et al. 2011; Lopez-Martinez et al. 2009), fatty acids (Flint-Garcia et al. 2009) and amino acids (Flint-Garcia et al. 2009); many of these metabolic traits are also affected by the environmental modifiers (Harrigan et al. 2007). Specifically, in maize silks, such diversity has been found in secondary metabolites, for example anthocyanins, polyphenols, protocatechuic acid, gallic acid, cinnamic acid, syringic acid and caffeic acid (Kuhnen et al. 2010).

Nested association mapping (Benamotz et al.) populations (McMullen et al. 2009; Yu et al. 2008) are a good resource to investigate the inheritance of morphological and metabolic diversity among maize inbreds. The NAM populations are derived from a set of 26 inbred lines that represent the genetic allelic diversity in maize inbreds. NAM populations consist of 25 families, each

consisting of 200 recombinant inbred lines (RILs). Each family uses the inbred B73 as the common parent, crossed by 25 diverse founder lines (25FL). Among these 25FL parents, more than half are tropical in origin, nine are temperate lines, two are sweet corn lines (representing Northern Flint), and one is a popcorn inbred line (McMullen et al. 2009; Yu et al. 2008). In addition to the NAM population founder lines, in this study 14 maize inbreds covering ca. 30% of maize genetic diversity (Liu et al. 2003) were also surveyed for hydrocarbon production in silks and/or pollens. We found that both quantitative and qualitative differences in hydrocarbon constituents among different maize inbreds and between silk and pollen in the same maize inbreds.

2. Results and Discussion

2.1 **Quantitative and qualitative differences in hydrocarbon profiles in silks among different maize inbreds**

The purpose of this study was to assess the amount of variation in hydrocarbon accumulation (i.e. total amount of hydrocarbons and composition of those hydrocarbons) in silks across a diverse set of maize germplasm. Analyzing two sets of maize inbreds accessed this diversity. The first set, which were cultivated and analyzed in the summer of 2009, were chosen from a collection of 260 diverse inbred lines (Liu et al. 2003). The selected 14 inbred lines (Table 1) captures ca. 30% of the allelic diversity that has been observed at 2039 genetic loci among the entire collection of the 260 inbreds (Liu et al. 2003). The second set of inbreds, which were grown and analyzed in the

summer of 2010, encompassed the 26 inbreds that are the founder parents for the NAM populations (Yu et al. 2008). Across the two sets of inbreds analyzed, eight inbreds were grown in both seasons, which provided us with the ability to assess environmental modifiers that affect hydrocarbon accumulation (Table 1).

The majority of the hydrocarbons detected in both encased and emerged silks from all tested inbreds were odd-numbered hydrocarbons, including C_{23}, C_{25}, , $C_{27,}$, C_{29}, C_{31} and C_{33} alkanes, and $C_{27:2}$, $C_{27:1}$, $C_{29:2}$, $C_{29:1}$, $C_{31:2}$ and $C_{31:1}$ alkenes. Collectively these metabolites accounted for ~ 90% of the total hydrocarbons of each sample, which is consistent with previous studies of surface lipids on silks from different inbreds (Miller et al. 2003; Perera et al. 2010b; Yang et al. 1992). However, very low abundances of even-numbered hydrocarbons, including C_{24}, C_{26}, $C_{28:1}$, C_{28} and C_{30} were also detected, which has not been reported previously (Fig 1). Those even-numbered hydrocarbons might be biosynthesized by a different pathway from odd-numbered hydrocarbons (Park 2005), which suggests that there are two different hydrocarbon biosynthesis pathways in maize.

In the 2009 study, which encompassed 14 different inbreds, we found that at the 6-day post-silk emergence (PSE) time-point, hydrocarbon content of silks was either similar to or increased by ca. 1.5-fold, as compared the silks that were sampled at 3-days PSE (Fig. 2a and Fig. 2b). Therefore, in the 2010 study we sampled silks from the 26 inbred founders of the NAM populations, at

only 3-days PSE. Total hydrocarbons content was widely diverse among the 26 inbred founders. For instance, the Ky21 inbred (5.51 μmol/g dry weight) produced around 6 fold more hydrocarbons than Ms71 (0.56 μmol/g dry weight) (Fig 3). In addition, over the two-year study, we found that the emerged silks of the majority of the tested inbreds produce about 2 to 3 folds more hydrocarbons as compared to the encased silks (Fig. 2a, 2b, and 3).

To study the effect of silk development on hydrocarbon accumulation, in the summer 2009 season, silks were sampled at both 3- and 6-days post-silk emergence (PSE), and at both sampling times, silks that were encased or emerged from the husk leaves were collected separately (Fig 2a and Fig 2b). The quantity of total hydrocarbons that accumulated in the silks varied considerably among the 14 inbreds tested. Specifically, at 3-days PSE, B73 silks produced the largest amount of hydrocarbons (7.86 μmol/g dry weight) ($p<0.05$), which is approximately 4-fold higher than that found in CML5, which produced the smallest amount of hydrocarbons (2.13 μmol/g dry weight) (Fig 2a). At 6-days PSE, B73 silks were also the highest accumulators of hydrocarbons (7.86 μmol/g dry weight), but the lowest accumulator was Mo17, which produced 1/3 of the amount of B73 (2.62 μmol/g dry weight) (Fig 2b).

In addition to the variation in total hydrocarbon amount produced among 33 tested inbreds, the relative abundances of individual hydrocarbons out of the total hydrocarbons also varied among different maize inbreds and the ranges of relative percentages are listed in Table 2a and Table 2b. Minor

constituents, like C_{22}, C_{24}, $C_{25:2}$, $C_{25:1}$, $C_{27:2}$, $C_{28:2}$, $C_{28:1}$, $C_{29:2}$, $C_{30:2}$, $C_{30:1}$, $C_{31:2}$, $C_{33:1}$, C_{33}, are missing in some inbreds but present in other inbreds. Also, the major constituents are also different from 2 to more than 10 folds. For the 14 inbreds tested in 2009, most of them produced more (p value<0.05) alkanes than alkenes in both 3- and 6- day-old encased and emerged silks (Supplemental Table 1, 2, 3 and 4) except Tzi18 3-day old encased silks, which produce more alkenes than alkanes and CML5, Mo17 and Tzi8 3-day old encased maize silks, B73 3-day old emerged maize silk, B37, Tzi8 6-day-old encased maize silks, and Tzi8 6-day-old emerged maize silks, which produce similar amount of alkanes and alkenes. All of the 26 founders of NAM population produced more alkanes than alkenes in both 3-day-old encased and emerged maize silks except CML333, which produced similar amount of alkanes and alkenes (p-value >0.05) (Supplemental Table 5 and 6).

Using the data on the silk hydrocarbon composition profiles from the summer 2009 study, the 14 maize inbreds were statistically clustered using Manhattan Distance as the measure of statistical distance (Perera et al. 2010c) (Figure 4a and Fig 4b). These statistical analyses of the hydrocarbon composition data indicate that the 14 inbreds can be classified into 3 groups; but the inbreds cluster somewhat differently from hydrocarbon composition data gathered at 3 and 6-days PSE. The features common to both these hierarchical dendrograms however were: 1) the inbreds are distributed among three major clades; 2) the clade containing the inbred B73 is most

distinct from the other clades; 3) the majority of the inbreds cluster relatively close to each other. The three major clades in each hierarchical tree are labeled A-C (Fig. 4), and of these, clade A (A1 for 3-day PSE and A2 for 6-day PSE), which contains B73, appears to represent the inbreds that express the highest levels and most chemically diverse hydrocarbons in the silk. The differences between the two trees are somewhat subtle, but indicate that there are genetic-based differences in the hydrocarbon profiles in the silks of different ages. These differences could reflect dissimilar developmental programs among the inbreds, or may reflect the fact that among the inbreds there are dissimilar responses to the change in environment as silks emerge from the protective shield of the husk to the much more stress condition outside the husks.

Using the data on the silk hydrocarbon composition profiles from the summer 2010 study, 26 founders of NAM population can be clustered mainly into 2 groups (Clades I and II, Fig. 5a), the higher hydrocarbon-expressing clade contains inbreds Ky21, B73, NC358, Ki11, Tx303, NC350, CML52, Ki3, CML338, Oh7B, Tzi8 and IL14H, and the lower hydrocarbon-expressing clade contains inbred Oh43, Mo17, B97, CM103, CML322, CML333, CML247, Mo18W, M37W,Hg301, PG39, CML96, M162W, CML277 and MS71. Comparing the grouping of two sets of inbreds based on hydrocarbons to that based on the genetic structure of the inbreds (Flint-Garcia et al. 2005; Liu et al. 2003) are shown in Fig 4a, 4b, 4d, Fig 5a and Fig 5b. This kind of

comparison for both of 2 sets of inbreds indicates that the relationship between the underlying genetics is not linearly related to the metabolic outcome of silk hydrocarbon chemotypes. This would reflect therefore that in addition to the genetic-based differences among the inbreds, environmental modification factors also play an important role in how hydrocarbon accumulation is expressed in maize silks.

2.2 **Organ-specific differences in hydrocarbon profiles is differentially expressed among maize inbreds**

Hydrocarbons were also analyzed in pollen from 13 maize inbreds (these are from the same collection as analyzed in Figure 2, but pollen from the missing inbred CML5, could not sampled as it flowered late in the season). Among the 13 inbreds analyzed, inbred CML322 expressed the highest amounts of hydrocarbons on the pollen surface, and this is 2-fold higher than the inbred H99, which had the lowest level of hydrocarbons ($p<0.05$) (Fig. 2c). All the major hydrocarbon constituents were identified on the pollen surfaces all 13 inbred lines. However some minor constituents (less than ~1%), namely, C_{22}, C_{23}, C_{24}, $C_{25:2}$, $C_{25:1}$, $C_{27:2}$, $C_{33:1}$, C_{33}, C_{34} were not present in maize pollen. Other minor constituents, like $C_{28:2}$, $C_{28:1}$, C_{28}, $C_{30:1}$, C_{30} and $C_{31:2}$ are present in some inbreds but absent in other inbreds. The relative abundances of major constituents differed from 2 to 5 folds among inbreds (Supplemental Table 5). C_{25}, C_{27} and C_{29} were the predominant alkane and $C_{29:1}$ and $C_{31:}$were the primary alkene constituents in maize pollen of all the 13 inbred lines, which

is consistent with hydrocarbon composition reported for pollen from inbreds B37, NY821, K55 and Mo506 (Bianchi et al. 1990).

In both tissues, pollen and silk, hydrocarbon constituents comprise ~89% of lipids (Yang et al., 1992; Perera et al., 2010; (Perera 2005a). This is drastically higher than the ca. 1% hydrocarbon content been observed in surface lipids on seedling maize leaves, which is predominantly comprised of long-chain alcohols, aldehydes and esters (Bianchi et al. 1985). Although silk has the same hydrocarbon constituents as found in pollen, the total quantity and composition of hydrocarbons differs greatly between the two organs. Pollen produced 2 (A632) to 7 (CML322) folds of surface hydrocarbons of those in encased silk in all of the 13 inbreds. Pollen from B37, C103, Tzi18, M37W and Mo17 produced more and up to 2-fold hydrocarbons of emerged silk while pollen from H99, Tzi8 and A632 produced the same amount of hydrocarbons as emerged silk. The only inbred that produced more hydrocarbons in emerged silk than pollen is B73. In addition, pollen from CML322, CML91, Oh43 and CML52 produced more hydrocarbons than 3 days PSE silk but same amount of hydrocarbons as 6 days PSE silks (Fig 2).

For pollen, B73, CML91 and Mo17 showed a 1:1 alkane to alkene ratio (Table 3a) as was previously reported for other inbreds (Bianchi et al. 1990). However, A632, B73 and C103 produced more alkenes than alkanes while M37W, Oh43, CML322, CML52, H99, Tzi18 and Tzi8 produced more alkanes

than alkenes. The relative abundances of hydrocarbon constituents often varied between pollen and silks within a given inbred. For example, surface hydrocarbons on pollen (26.9% to 39.3%) produced more $C_{29:1}$ (8.93% to 29.6%) than silks but produced less C_{29} (4.74-13.47% in pollen and 15.8-39.7% in silk) (Supplemental table 1, 2, 3, 4 and 7). Except for major constituents, minor individual constituents also vary between organs. For example, C_{24} alkanes and $C_{25:1}$ and $C_{33:1}$ alkenes comprise ca. 5% of total hydrocarbons from both encased and emerged silks from diverse inbreds, whereas these constituents are undetectable in pollen (Supplemental table 1, 2, 3, 4 and 7).

In addition to pollen-stigma recognition (Piffanelli et al. 1998) and withstanding environmental stress (Wiermann and Gubatz 1992) like surface lipids in maize silk, pollen coat also plays a significant role in pollen dispersal (Piffanelli et al. 1998). This function difference between silk surface lipids and pollen coat might explain why the hydrocarbon amounts and relative abundances of individual constituents are different between them.

Using the data on the pollen hydrocarbon composition profiles from the summer 2009 study, the 13 maize inbreds clustered as illustrated in Figure 4c. These statistical analyses of the hydrocarbon composition data indicate that the 13 inbreds can be classified into 3 groups. The hierarchical dendrogram displayed that the clade containing the inbred CML322 is most distinct from the other clades and the majority of the inbreds cluster relatively close to each other. In addition, the grouping based on pollen hydrocarbons is different

from that based on encased and emerged silk hydrocarbons. In silk, the clade with B73 is highest hydrocarbon accumulator however in pollen; the clade with CML322 is the highest hydrocarbon accumulator. In addition, the grouping based on hydrocarbons in silks and pollen is different from the grouping according to the genetic structures in maize inbreds (Fig 4c) (Flint-Garcia et al. 2005; Liu et al. 2003). Comparison of the grouping based on genetic structures and based on hydrocarbons in silks and pollen, the features we can find for these four hierarchical dendrograms were: 1). Inbreds in the same group according to genetic structures distribute in different clades except for the SS group based hydrocarbons in pollen (Fig 4); 2) B73 and A632, belonging to the SS groups, are in the clade with highest hydrocarbon accumulation in both 3-day and 6-day emerged silks; 3) Tzi 8, CML322 and CML52 in the TS group in the clade with highest hydrocarbon accumulation in pollen. The difference of groupings based on hydrocarbons (chemotypes) between pollen and silks could reflect dissimilar organ-specific programs and the developmental effect on hydrocarbons in inbreds. In addition, the difference of groupings based on hydrocarbons (chemotypes, Fig 4c) and genetic structure (genotypes, Fig 4d) suggests that in addition to the genetic-based differences among the inbreds, other factors, like environmental modification factors, also affect how hydrocarbon accumulation is expressed in pollen, which is same as what we have observed in maize silks.

2.3 **Environmental modifiers of hydrocarbon profiles is differentially expressed among maize inbreds**

The inbreds Mo17, CML52, C103, M37W, CML322, Tzi8, Oh43 and B73 were grown in two separate years (Table 1). Tzi 8 and CML 52 produced the same amount of total hydrocarbon in year 2009 and 2010. However, for all the other 6 inbreds grown in both years, total hydrocarbon accumulation was ~2-fold higher in emerged silks and~1.5 fold higher in encased silks from each inbred in Summer 2009 as compared to Summer 2010 ($p<0.05$) (Fig.6). Although Tzi 8 and CML 52 accumulated the same amount of total hydrocarbon amount in two different years, the relative abundances of individual hydrocarbons were different. The relative abundances of C_{24}, $C_{27:2}$, $C_{28:2}$, $C_{28:1}$, $C_{30:1}$, $C_{31:2}$, $C_{33:1}$ and C_{33} remained consistent between year 2009 and 2010 while the relative ratio of other detected constituents changed from year to year in the 8 tested inbreds. Among them, C_{22}, C_{30} and C_{34} were present in maize silks of year 2009 but absent from those of year 2010. $C_{31:1}$ was higher in both encased and emerged silks in 2009 than those in 2010 in all of the 8 inbreds ($p<0.05$). Relative abundances of other hydrocarbons were higher in year 2009 in some inbred and lower in year 2009 in other inbreds. For example, ratios of C_{31} and C_{29} were higher in year 2009 in C103 but lower in year 2009 in Tzi 8, CML322 and CML52 and stayed the same in other inbreds (Supplemental Table 8).

Our results are consistent with previous report that hydrocarbon content in maize silk varied from year to year (Miller et al. 2003; Yang et al. 1992). The larger changes between seasons in hydrocarbon content in emerged silks, suggests environmental impact on hydrocarbon accumulation. Therefore, we examined temperature highs and low, soil temperature 4inches below the surface, daily precipitation, average relative humidity and solar radiation in July and August for both 2009 and 2010, which are measured at Ames [AWM station] and maintained at mesonet.agron.iastate.edu. Among them, temperature highs and low, soil temperature 4 inches below the surface, average relative humidity and solar radiation were similar between year 2009 and 2010. However, daily precipitation varied greatly between the summers of 2009 and 2010. In July, the average daily precipitation in 2010 is around 85 folds of that in 2009 and in August it is around 85 and 94 folds of that in 2009 (Supplemental Fig 1).

Using the data on the silk hydrocarbon composition profiles from the summer 2009 and 2010 study of these 8 inbreds, the encased and emerged silks from the summer 2009 and 2010 study of eight maize inbreds clustered as illustrated in Figure 7. These statistical analyses of the hydrocarbon composition data indicate that some inbreds (Oh43, CML322, C103 and Mo17) can be clearly classified into 4 groups, encased silks from the summer 2009, encased silks from the summer 2010, emerged silks from the summer 2009 and emerged silks from the summer 2010 while other inbreds are hard to

distinguished between replications from year 2009 and 2010. This difference among inbreds indicates that some inbreds are more accessible to the influence of environmental factors than other inbreds.

3. Conclusion

The surface lipids on maize silk not only prevents excessive water loss but also defends against attack by external agents(Samuels et al. 2008a). The hydrocarbon amount and the relative abundances of individual hydrocarbons were different in the same maize inbreds from year to year. This is probably due to the environment since each year there might be different fungus and/or insects in the field and the weather are different, which might trigger different genes to modify the hydrocarbon amount and relative abundances of hydrocarbon compositions to protect maize silk from these fungus and/or insects and moisture loss. The quantitative trait of hydrocarbon may be attributable to large numbers of genes with small effects instead of a few genes. Differential expression of several genes among the maize inbreds might cause the different relative hydrocarbon amount among them. And the genes affecting the very early step of hydrocarbon biosynthesis might influence the total hydrocarbon amounts in different maize inbreds. By providing the hydrocarbon metabolic profiling will contribute our understanding of hydrocarbon biosynthetic mechanism in maize if we can establish the correlated networks of transcripts, proteins and hydrocarbon metabolites.

4. Experimental

4.1 General Experimental Procedures

Seeds of 14 maize (*Zea mays*) inbreds, and 26 founders of NAM population were bought from maize genetics cooperation stock center and were grown in field in summer 2009 and 2010 respectively. The hexane (HPLC grade) used for hydrocarbon purification and internal standard, hexacosane were bought from Fisher Scientific and Fluka Analytical respectively. The 40-140 mesh silica gel used for hydrocarbon purification was bought from Mallinckrodt Baker, Inc.

4.2 Plant material

All analyses were conducted on the silks and pollen of 13 inbred cultivars of maize *(Zea mays* ssp. mays L.), listed in Table 1. A total of 14 maize inbreds were grown at the Iowa State University Agronomy Farm (Boone, IA) in 2009 and a set of 26 inbreds were grown at Iowa State University Curtiss Farm (Ames, IA) in 2010. Eight inbreds were examined in two locations over two different years (i.e. Mo17, CML52, C103, M37W, CML322, Tzi8, Oh43 and B73).

Ear shoots were bagged prior to silking and ears were harvested between 10am and 12pm either 3- or 6-days after first silk emergence and were transported to the laboratory on ice. Emerged and encased silks were harvested from each ear, flash frozen in liquid nitrogen and store at -80℃. Before usage, maize silks were lyophilized using a FreeZone 4.5 Liter Freeze

Dry System (Labconco Corporation, MO) and lyophilized tissue was powderized using a Genogrinder 2000 (Spex CertiPrep, NJ).

4.3 Extraction of hydrocarbons

Immediately prior to hydrocarbon extraction, 10 μg of hexacosane (1 mg/mL) (Fluka, WI) was applied directly to the plant material (ca. 100 mg of tissue) as an internal standard. Hydrocarbons from each sample were extracted with 1.5 mL HPLC grade hexane (Fisher Scientific, NJ) with sonication for 15 min and centrifuged at 13000 g for 1 mins. Supernatant was collected after centrifugation and this extraction step was reported for two more times.

The combined supernatant was passed through a column containing 0.6 g silica gel (J.T. Baker, NJ) that was pre-washed with 10 mL hexane. After elution the column was washed with 10 mL hexane. The combined eluents were dried in a rotary nitrogen evaporator (Organomation Associates, Inc., MA) at 30 ℃. The dried hydrocarbon samples were dissolved in 1 mL hexane.

4.4 Hydrocarbon analysis

Chromatographic analysis was performed with a GC (Model 6890 series, Agilent Technologies, Palo Alto, CA), equipped with a mass detector Model 5973 (Agilent Technologies, Palo Alto, CA). Chromatography was conducted with a HP-5MS cross-linked (5%)-diphenyl-(95%)-dimethyl polysiloxane column (30 m length, 0.25 mm inner diameter) using helium as the carrier gas. The injection temperature was at 280 ℃. The oven temperature was initially at

200 ℃, was increased to 280 ℃ at a rate of 4 ℃/min, further increased to 320 ℃ at a rate of 20 ℃/min and held at this temperature for 3 min. Constituent peaks were identified by comparing to the NIST library (http://www.sisweb.com/software/nist-gc-library.htm). To quantify hydrocarbon constituents, the response of the mass-spectrometer was calibrated to the hexacosane internal standard in each sample.

4.5 Statistical methods

All metabolite data were gathered from a minimum of three biological replicates. Metabolite abundances are the average of these multiple determinations (±s.e.). Where appropriate, a student's t-test assuming unequal variance was conducted to determine whether the metabolite abundances are statistically different between genotypes. To compare the hydrocarbon composition and amount difference among the maize inbreds, the dissimilarity between a pair of genotypes was computed using a weighted Manhattan distance measure (Dixon et al., 2009; Perera et al., 2010).

References

Bianchi, A., Bianchi, G., Avato, P., Salamini, F., 1985. Biosynthetic Pathways of Epicuticular Wax of Maize as Assessed by Mutation, Light, Plant-Age and Inhibitor Studies. Maydica 30, 179-198.

Bianchi, G., Murelli, C., Ottaviano, E., 1990. Maize Pollen Lipids. Phytochemistry 29, 739-744.

Blaker, T. W., Greyson, R. I., 1988. Developmental Variation of Leaf Surface Wax of Maize, Zea-Mays. Can J Bot 66, 839-846.

Flint-Garcia, S. A., Bodnar, A. L., Scott, M. P., 2009. Wide variability in kernel composition, seed characteristics, and zein profiles among diverse maize inbreds, landraces, and teosinte. Theor Appl Genet 119, 1129-1142.

Flint-Garcia, S. A., Thuillet, A. C., Yu, J. M., Pressoir, G., Romero, S. M., Mitchell, S. E., Doebley, J., Kresovich, S., Goodman, M. M., Buckler, E. S., 2005. Maize association population: a high-resolution platform for quantitative trait locus dissection. Plant Journal 44, 1054-1064.

Greene, M. J., Gordon, D. M., 2003. Social insects - Cuticular hydrocarbons inform task decisions. Nature 423, 32-32.

Han, J., Calvin, M., 1969. Hydrocarbon Distribution of Algae and Bacteria, and Microbiological Activity in Sediments. P Natl Acad Sci USA 64, 436-&.

Harrigan, G. G., Stork, L. G., Riordan, S. G., Reynolds, T. L., Ridley, W. P., Masucci, J. D., MacIsaac, S., Halls, S. C., Orth, R., Smith, R. G., Wen, L., Brown, W. E., Welsch, M., Riley, R., Mcfarland, D., Pandravada, A., Glenn, K. C., 2007. Impact of genetics and environment on nutritional and metabolite components of maize grain. J Agr Food Chem 55, 6177-6185.

Kuhnen, S., Bernardi Ogliari, J., Dias, P. F., da Silva Santos, M., Ferreira, A. G., Bonham, C. C., Wood, K. V., Maraschin, M., 2010. Metabolic fingerprint of Brazilian maize landraces silk (stigma/styles) using NMR spectroscopy and chemometric methods. J Agric Food Chem 58, 2194-2200.

Kuhnen, S., Lemos, P. M. M., Campestrini, L. H., Ogliari, J. B., Diasc, P. F., Maraschin, M., 2011. Carotenoid and anthocyanin contents of grains of Brazilian maize landraces. J Sci Food Agr 91, 1548-1553.

Kunst, L., Samuels, A. L., 2003. Biosynthesis and secretion of plant cuticular wax. Progress in Lipid Research 42, 51-80.

Kunst, L., Samuels, L., 2009. Plant cuticles shine: advances in wax biosynthesis and export. Current Opinion in Plant Biology 12, 721-727.

Liu, K. J., Goodman, M., Muse, S., Smith, J. S., Buckler, E., Doebley, J., 2003. Genetic structure and diversity among maize inbred lines as inferred from DNA microsatellites. Genetics 165, 2117-2128.

Liu, Z. Z., Guo, R. H., Zhao, J. R., Cai, Y. L., Wang, F. G., Cao, M. J., Wang, R. H., Shi, Y. S., Song, Y. C., Wang, T. Y., Li, Y., 2010. Analysis of Genetic

Diversity and Population Structure of Maize Landraces from the South Maize Region of China. Agr Sci China 9, 1251-1262.

Lopez-Martinez, L. X., Oliart-Ros, R. M., Valerio-Alfaro, G., Lee, C. H., Parkin, K. L., Garcia, H. S., 2009. Antioxidant activity, phenolic compounds and anthocyanins content of eighteen strains of Mexican maize. Lwt-Food Sci Technol 42, 1187-1192.

McMullen, M. D., Kresovich, S., Villeda, H. S., Bradbury, P., Li, H. H., Sun, Q., Flint-Garcia, S., Thornsberry, J., Acharya, C., Bottoms, C., Brown, P., Browne, C., Eller, M., Guill, K., Harjes, C., Kroon, D., Lepak, N., Mitchell, S. E., Peterson, B., Pressoir, G., Romero, S., Rosas, M. O., Salvo, S., Yates, H., Hanson, M., Jones, E., Smith, S., Glaubitz, J. C., Goodman, M., Ware, D., Holland, J. B., Buckler, E. S., 2009. Genetic Properties of the Maize Nested Association Mapping Population. Science 325, 737-740.

Menkir, A., Liu, W. P., White, W. S., Mazlya-Dixon, B., Rocheford, T., 2008. Carotenoid diversity in tropical-adapted yellow maize inbred lines. Food Chem 109, 521-529.

Miller, S. S., Reid, L. M., Butler, G., Winter, S. P., McGoldrick, N. J., 2003. Long chain Alkanes in silk extracts of maize genotypes with varying resistance to Fusarium graminearum. J Agr Food Chem 51, 6702-6708.

Park, M. O., 2005. New pathway for long-chain n-alkane synthesis via 1-alcohol in Vibrio furnissii M1. J Bacteriol 187, 1426-1429.

Perera, M. A., 2005a. Molecular and chemical characterization of genes involved in maize cuticular wax biosynthesis. Dissertation, Iowa State University.

Perera, M. A., Qin, W., Yandeau-Nelson, M., Fan, L., Dixon, P., Nikolau, B. J., 2010a. Biological origins of normal-chain hydrocarbons: a pathway model based on cuticular wax analyses of maize silks. Plant J 64, 618-632.

Perera, M. A. D. N., 2005b. Molecular and chemical characterization of genes involved in maize cuticular wax biosynthesis. Ph.D Dissertation.

Perera, M. A. D. N., Qin, W. M., Yandeau-Nelson, M., Fan, L., Dixon, P., Nikolau, B. J., 2010b. Biological origins of normal-chain hydrocarbons: a pathway model based on cuticular wax analyses of maize silks. Plant Journal 64, 618-632.

Piffanelli, P., Ross, J. H. E., Murphy, D. J., 1998. Biogenesis and function of the lipidic structures of pollen grains. Sex Plant Reprod 11, 65-80.

PostBeittenmiller, D., 1996. Biochemistry and molecular biology of wax production in plants. Annu Rev Plant Phys 47, 405-430.

Sa, K. J., Park, J. Y., Park, K. J., Lee, J. K., 2010. Analysis of genetic diversity and relationships among waxy maize inbred lines in Korea using SSR markers. Genes Genom 32, 375-384.

Samuels, L., Kunst, L., Jetter, R., 2008a. Sealing plant surfaces: cuticular wax formation by epidermal cells. Annu Rev Plant Biol 59, 683-707.

Samuels, L., Kunst, L., Jetter, R., 2008b. Sealing plant surfaces: Cuticular wax formation by epidermal cells. Annu Rev Plant Biol 59, 683-707.

Wackett, L. P., Frias, J. A., Seffernick, J. L., Sukovich, D. J., Cameron, S. M., 2007. Genomic and biochemical studies demonstrating the absence of an alkane-producing phenotype in Vibrio furnissii M1. Appl Environ Microb 73, 7192-7198.

Ware, D., Zhao, W., Canaran, P., Jurkuta, R., Fulton, T., Glaubitz, J., Buckler, E., Doebley, J., Gaut, B., Goodman, M., Holland, J., Kresovich, S., McMullen, M., Stein, L., 2006. Panzea: a database and resource for molecular and functional diversity in the maize genome. Nucleic Acids Res 34, D752-D757.

Wiermann, R., Gubatz, S., 1992. Pollen Wall and Sporopollenin. Int Rev Cytol 140, 35-72.

Yang, G., Wiseman, B. R., Espelie, K. E., 1992. Cuticular Lipids from Silks of 7 Corn Genotypes and Their Effect on Development of Corn-Earworm Larvae [Helicoverpa-Zea (Boddie)]. J Agr Food Chem 40, 1058-1061.

Yu, J. M., Holland, J. B., McMullen, M. D., Buckler, E. S., 2008. Genetic design and statistical power of nested association mapping in maize. Genetics 178, 539-551.

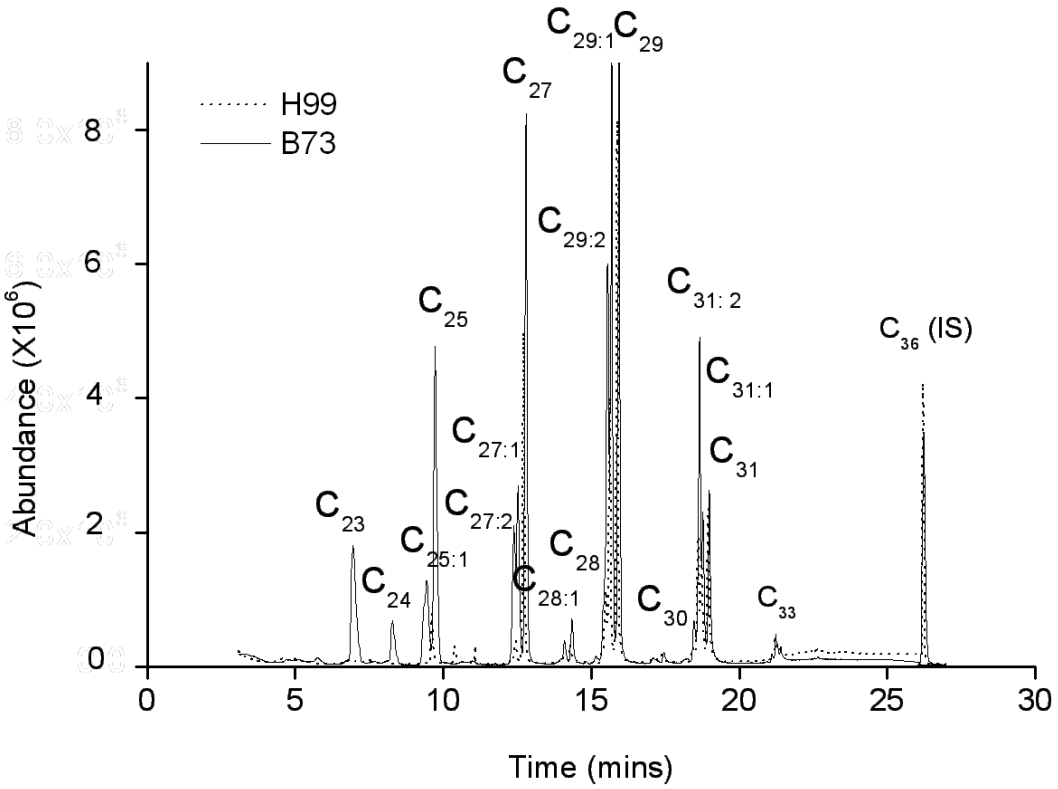

Figure 1. Gas chromatograph of emerged B73 and H99 maize silks

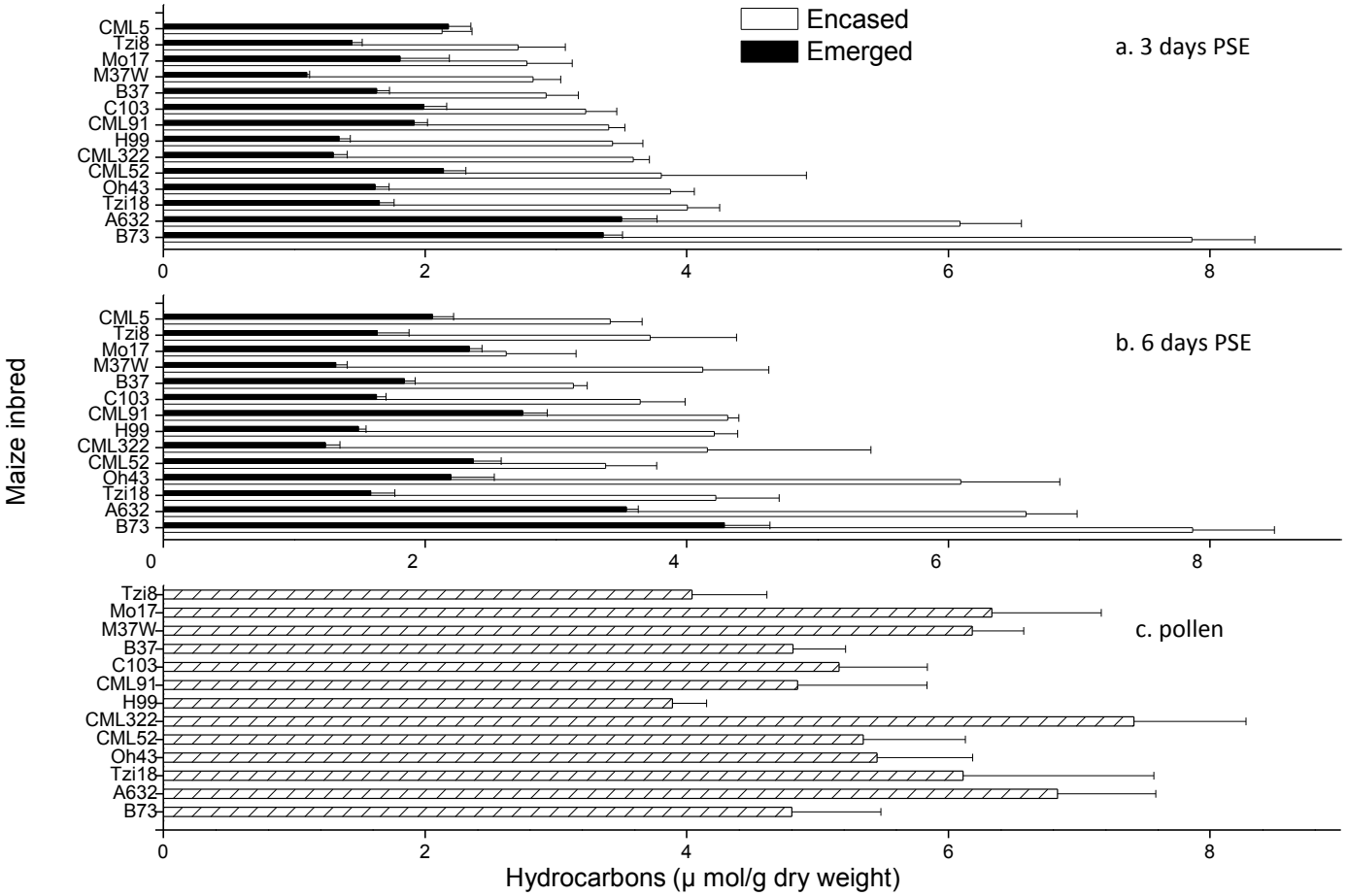

Figure 2. Total hydrocarbon accumulation of encased and emerged silks and pollen in 14 maize inbreds.

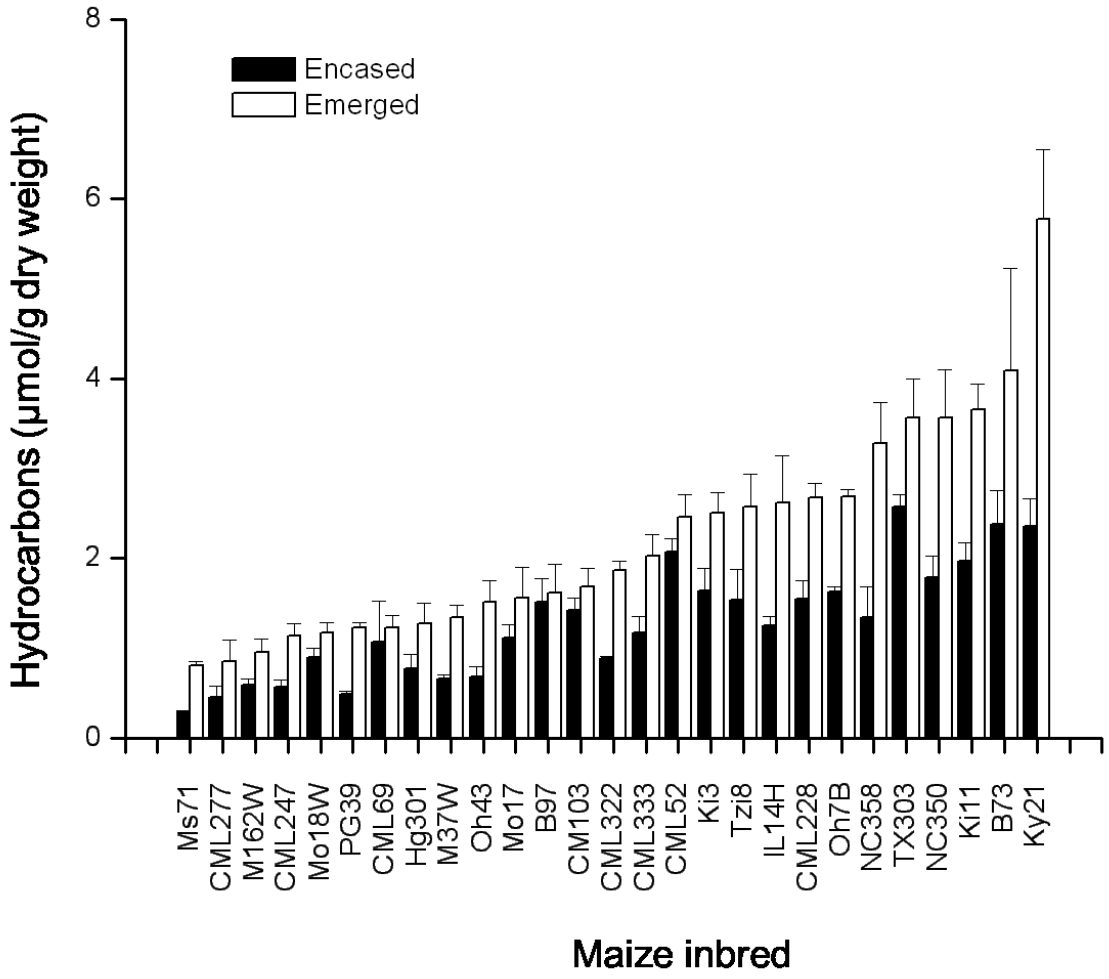

Figure 3. Total hydrocarbon amount in both 3-day-old encased and emerged maize silk of 26 founders of NAM population.

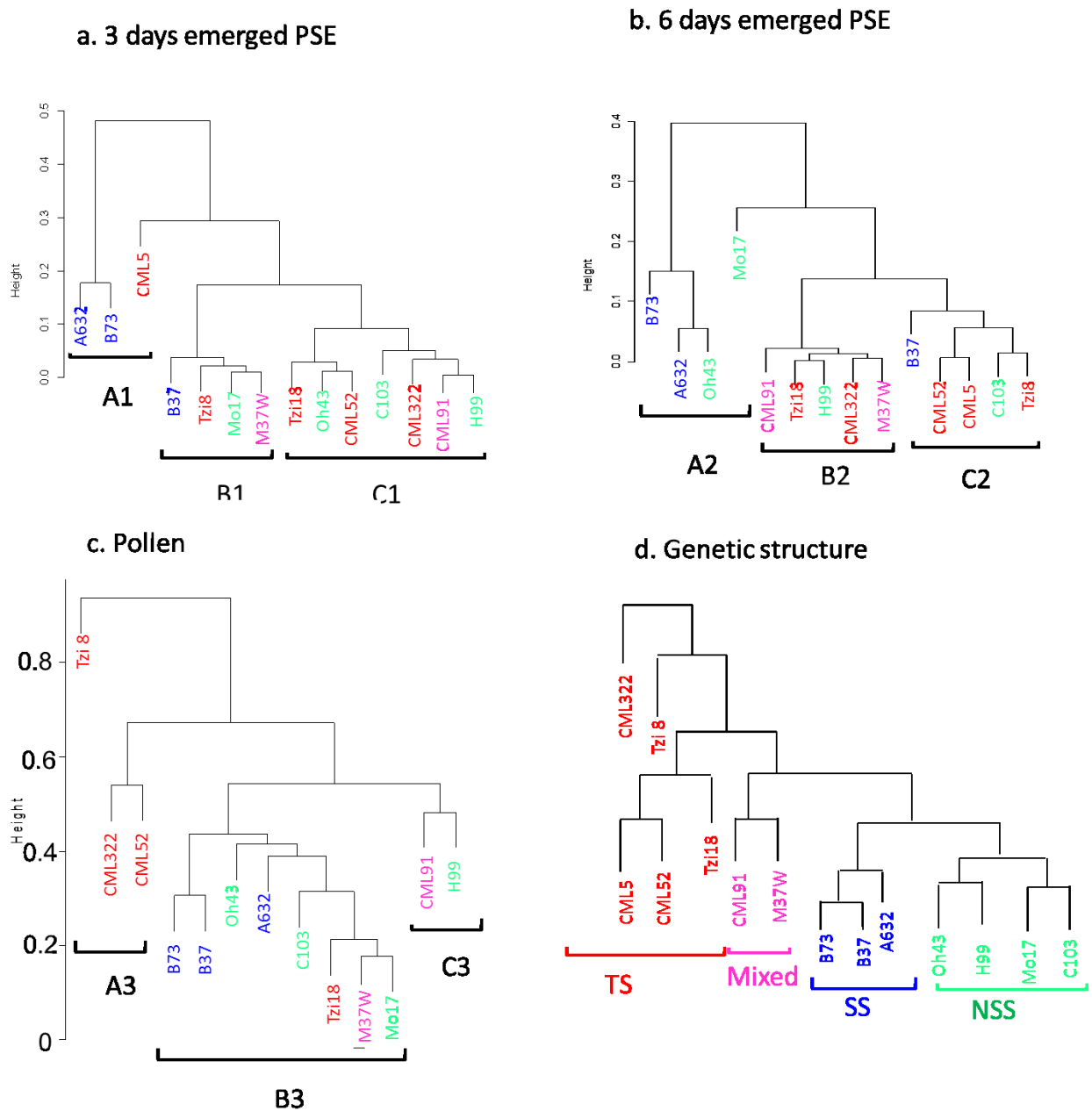

Figure 4. Cluster dendrogram of 14 inbreds grown in summer at year 2009 based on hydrocarbons from 3 days (a) and 6-days (b) PSE silks, pollen (c) and genetic structures (d) by using average linkage.
TS, the tropical lines are labeled read, SS, the stiff stalk lines are labeled blue, NSS, non-stiff stalk lines are labeled green and Mixed, lines with <80% membership for any subgroup, are labeled purple.

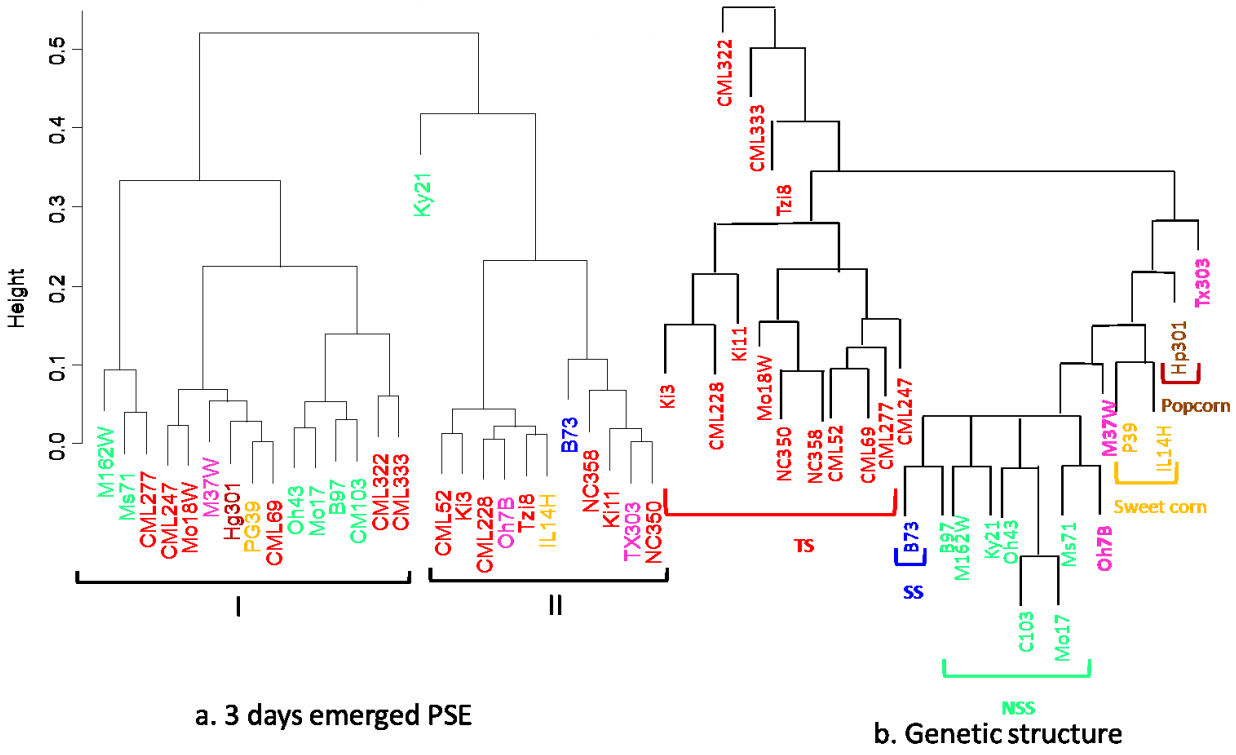

Figure 5. Cluster dendrogram of 26 founders of NAM population based on total hydrocarbons from 3 days PSE silks (a) and genetic structure (b) by using average linkage. TS, the tropical lines are labelled red, SS, the stiff stalk lines are labeled blue, NSS, non-stiff stalk lines are labelled green, Mixed, lines with <80% membership for any subgroup, are labeled purple, sweet corn lines are labeled orange and popocorn line is labeled brown.

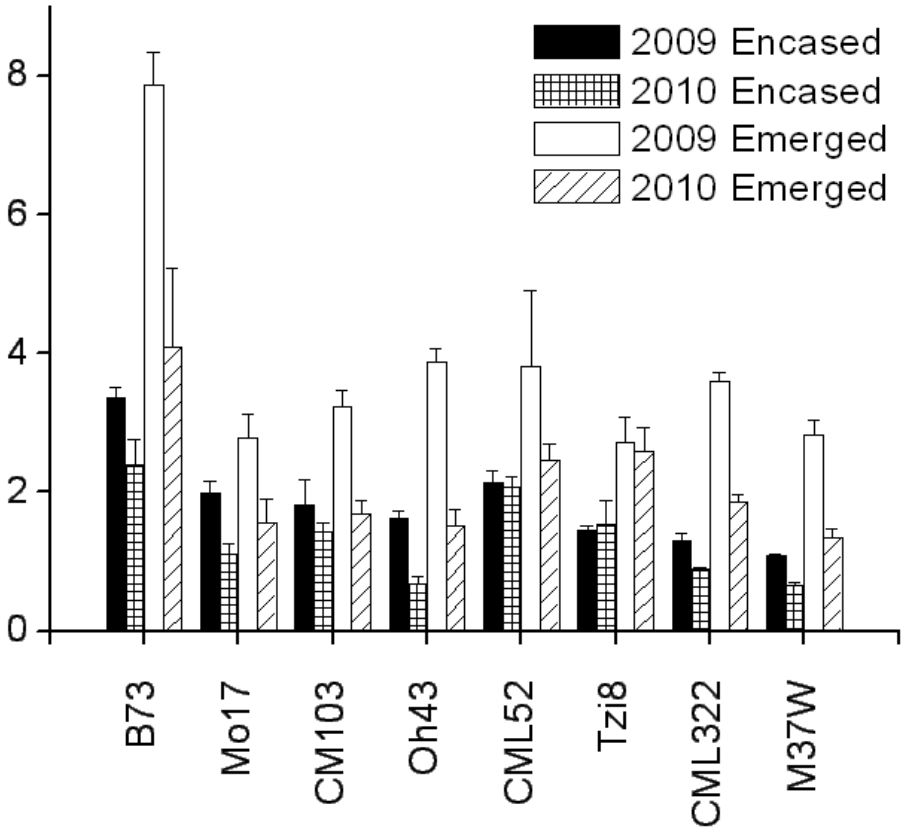

Figure 6. Comparison of total hydrocarbon in diverse maize inbreds between year 2009 and 2010.

a. B73

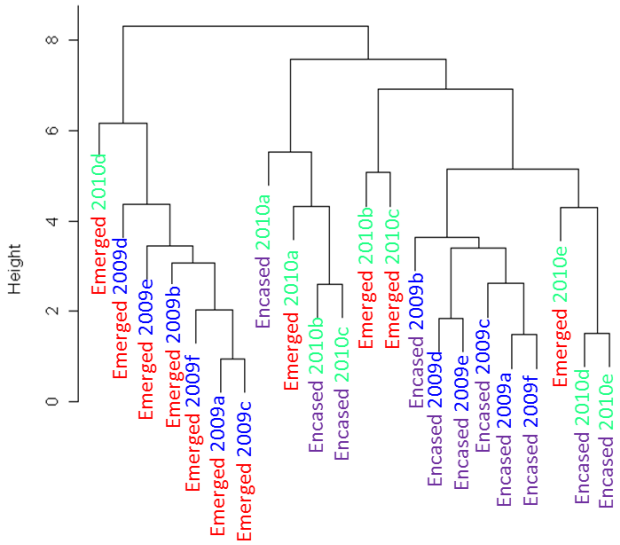

b. C103

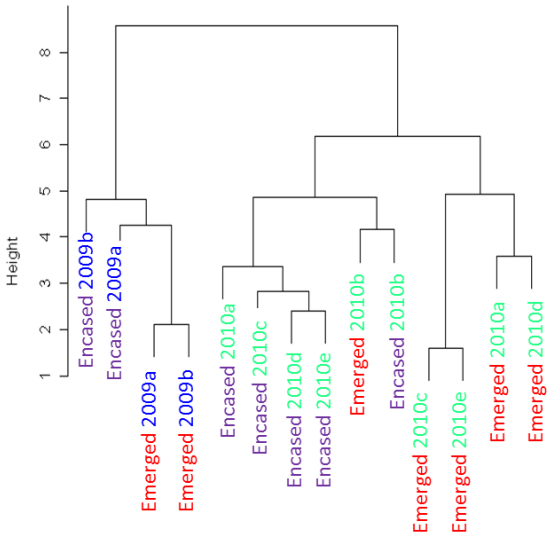

c. CML52

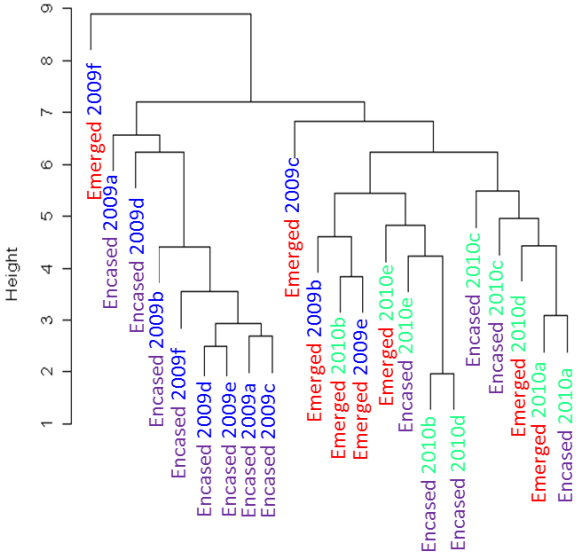

d. Tzi8

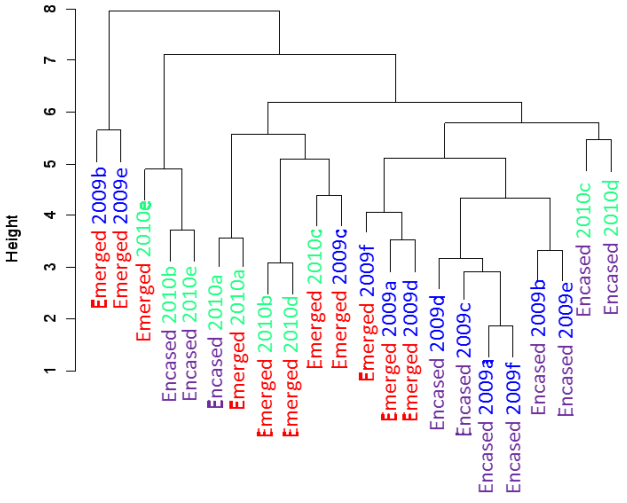

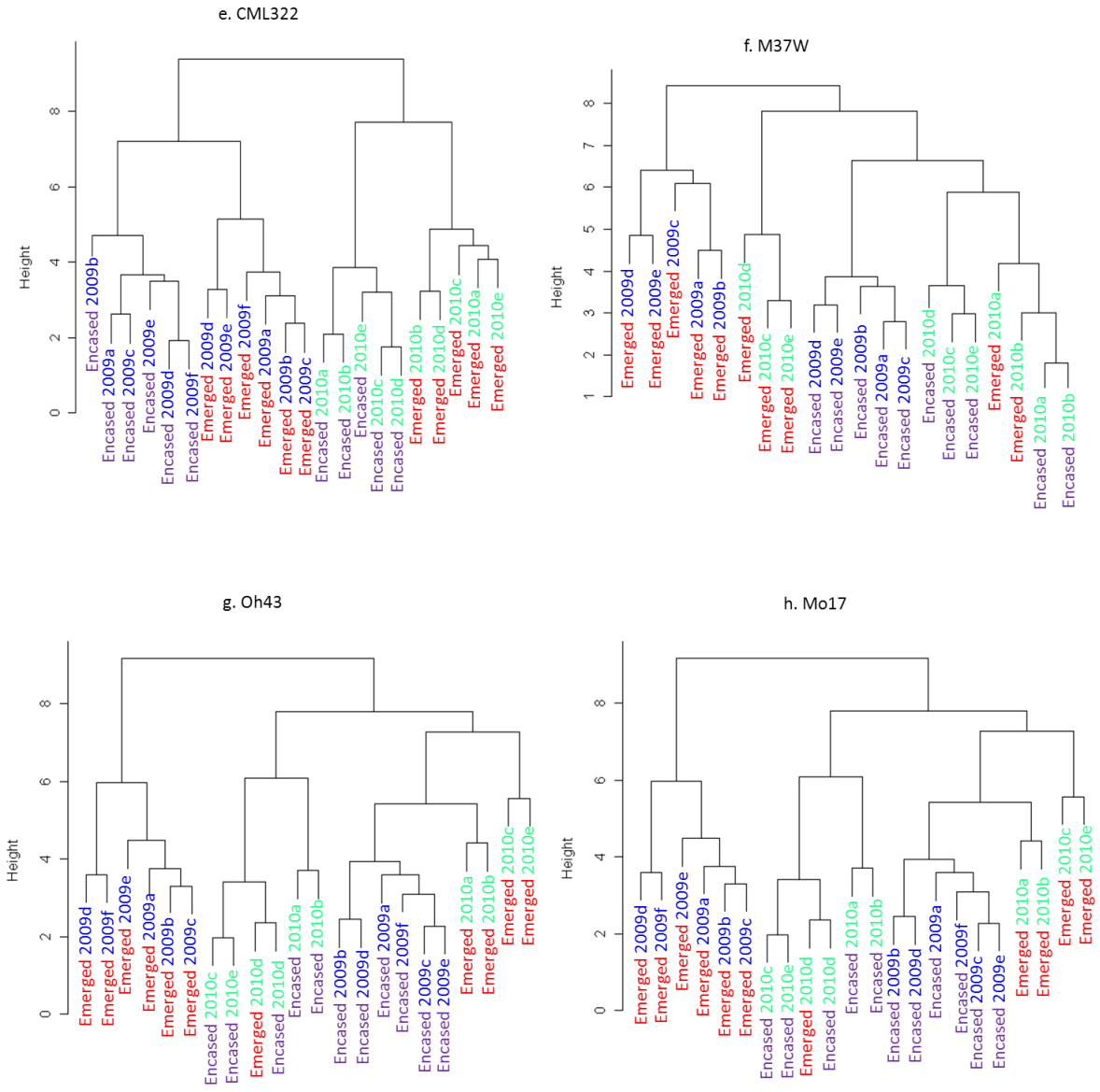

Figure 7. Cluster dendrogram of hydrocarbons in 8 maize inbreds in both 2009 and 2010.

Table 1. 14 maize inbreds planted in 2009.

Inbred[a]	Group[b]	Subgroup[c]	Season[d]
A632	SS	B14A	2009
B37	SS	B37	2009
B73	SS	B73	2009; 2010
B97*	NSS	NSS-mixed	2010
C103	NSS	C103	2009
CML103*	TS	CML-late	2010
CML228*	TS	Suwan	2010
CML247*	TS	CML-early	2010
CML322*	TS	CML-early	2009; 2010
CML333*	TS	CML-P	2010
CML5	TS	CML-late	2009
CML52*	TS	TZI	2009; 2010
CML69*	TS	Suwan	2010
CML91	Mixed		2009
H99	NSS	NSS-mixed	2009
Hp301*	Popcorn		2010
Il14H*	Sweet corn		2010
Ki11*	TS	Suwan	2010
Ki3*	TS	Suwan	2010
Ky21*	NSS	K64W	2010
M162W*	NSS	K64W	2010
M37W*	Mixed		2009; 2010
Mo17	NSS	C109:Mo17	2009; 2010
Mo18W*	Mixed		2010
MS71*	NSS	NSS-X	2010
NC350*	TS	NC	2010
NC358*	TS	TZI	2010
Oh43*	NSS	M14:Oh43	2009; 2010
Oh7B*	Mixed		2010
P39*	Sweet corn		2010
Tx303*	Mixed		2010
Tzi18	TS	TZI	2009
Tzi8*	TS	TZI	2009; 2010

a. Inbreds denoted with asterisks are founder inbreds that generated the NAM population (Yu et al., 2008)
b. Groups are listed as defined in Liu et al. (2003); Stiff Stalk (SS), Non-Stiff Stalk (NSS), Tropical or Semi-tropical (Wettstein - Knowles)
c. Subgroups are listed as defined in Liu et al. (2003)
d. Field season when inbred was evaluated.

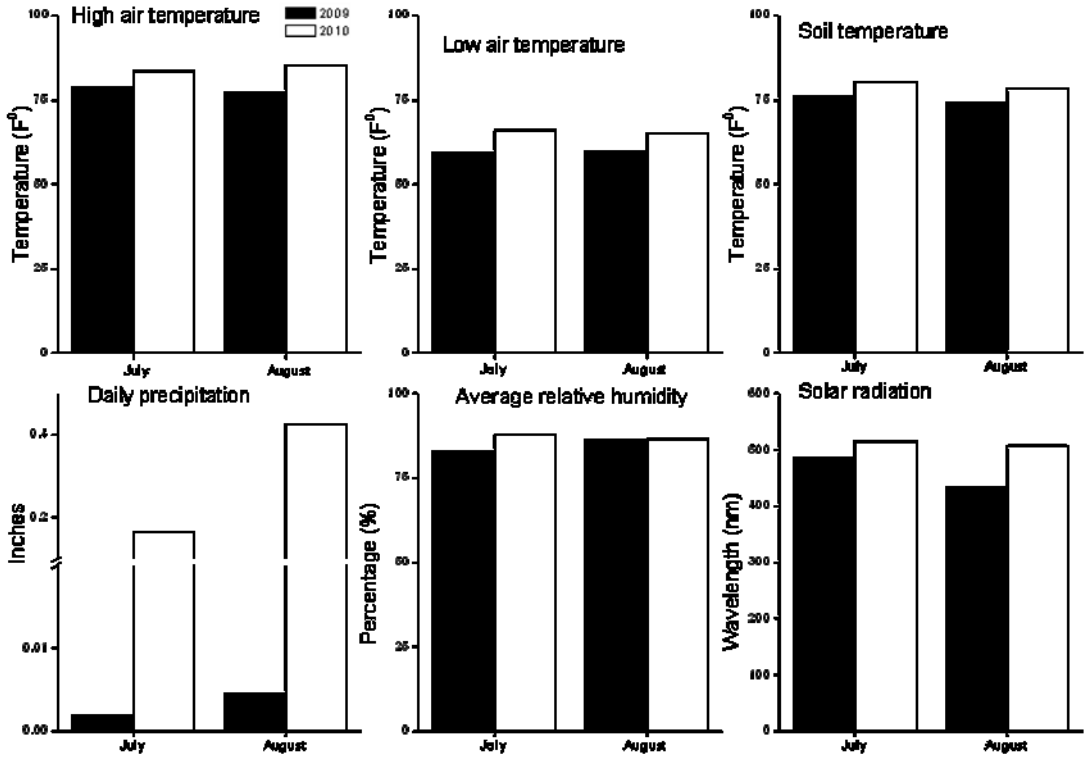

Supplemental Figure 1. Climate comparison between year 2009 and 2010 from May to August

Supplemental Table 1
Supplemental Table 2
Supplemental Table 3
Supplemental Table 4
Supplemental Table 5
Supplemental Table 6
Supplemental Table 7
Supplemental Table 8
(..\Desktop\Supplemental Tables for Chapter 2.xlsx)

CHAPTER 3. INHERITANCE PATTERNS OF HYDROCARBON ACCUMULATION EXHIBIT DIFFERENTIAL HETEROTIC EFFECTS IN POLLEN AND SILKS OF MAIZE HYBRIDS

Wenmin Qin, Samson Condon, Marna D. Yandeau-Nelson, Basil J. Nikolau.
Center for Metabolic Biology, Plant Science Institute
Center for Biorenewable Chemicals
Department of Biochemistry, Biophysics and Molecular Biology
Iowa State University, Ames, IA 50010
Email: dimmas@iastate.edu
Telephone: 515-294-0347
Fax number: 515-294-0534

Abstract

Simple non-isoprenoids hydrocarbons (Perera et al. 2010c) occur in low amounts in discrete parts of the biosphere (e.g. bacteria, algae, and the cuticles of plants and insects). However, these molecules are major constituents of the cuticular lipids of many plants, but their biosynthetic origins has become of interest for biofuel applications. Hydrocarbon profiling of surface cuticular lipids in four maize inbred lines (LH1, LH123HT, PHG39, and PHG84) and their genetic hybrids demonstrate heterotic inheritance patterns. Specifically, in pollen this heterosis is expressed as overdominance, whereas in silks this trait displays underdominance. The phenomena that hydrocarbon inheritance pattern is different among the organs of maize implies that different pathways/genes/alleles or genetic regulation networks play a role in hydrocarbon biosynthesis in silks and pollens.

Key words: *Zea mays*, heterosis, hydrocarbons, pollen, silk

Introduction

Simple hydrocarbons (e.g., alkanes, alkenes and dienes) are relatively rare, but are widely distributed in the biosphere. For example, hydrocarbons are found in some bacteria (Han and Calvin 1969b; Park 2005) and algae (Dennis and Kolattukudy 1991b; Rieley et al. 1998a) as well as in the cuticles of insects (Endler et al. 2004; Samuels et al. 2008b; Wackett et al. 2007) and plants (Samuels et al. 2008b). Hydrocarbons mainly occur as components of the surface lipids of plants and insects, serving as a protective barrier against water loss and pathogens (Samuels et al. 2008b). In addition, they are a potential alternative biorenewable fuel (Jetter and Kunst 2008).

In maize, hydrocarbons are prevalent in the surface cuticular lipids covering all aerial organs of the plant, including pollen and silks (Bianchi et al. 1990; Blaker and Greyson 1988; Perera 2005a). The surface of silks and pollen are especially rich sources of hydrocarbons (Bianchi et al. 1990), which accounts for ~89% of the surface lipids (Perera 2005a). In pollen collected from different maize inbreds, 15-40% of the cuticular lipids are comprised of hydrocarbons (Bianchi et al. 1990). In silks from the inbred B73, hydrocarbons constitute >90% of the cuticular lipids and the emerged maize silk produces ca. 2-3 fold more hydrocarbons as compared to silks still encased within the husk leaves (Perera et al. 2010a).

A number of different mechanisms have been suggested for the biosynthesis of hydrocarbons. All of these begin with fatty acids, and

suggested mechanisms for converting the fatty acids to a hydrocarbon include: 1) the head-to-head condensation of two fatty acids to form a ketone, followed by reduction and dehydration/reduction (Sukovich et al. 2010a); 2) double reduction of a fatty acid to a primary alcohol, followed by dehydration and reduction (Park 2005); 3) decarboxylation of a fatty acid (Cheesbrough and Kolattukudy 1984a; Largeau et al. 1980a; Rude et al. 2011; Templier et al. 1992b; Templier et al. 1984, 1987, 1991a, b); and 4) reduction of a fatty acid to a fatty aldehyde, followed by decarbonylation (Schirmer et al. 2010). It's generally believed that hydrocarbons of plant cuticles are synthesized by the decarbonylation pathway (Aarts et al. 1995; Schneider-Belhaddad and Kolattukudy 2000). Until recently, CER1/CER3 are found to be responsible for very long chain alkanes biosynthesis in Arabidopsis and coexpression of CYTB5s can increase 3 folds of CER1/CER3 alkane production (Bernard et al. 2012a). This process is envisioned to produce saturated alkanes by reducing saturated fatty acids and subsequently decarbonylating the resulting saturated aldehyde. Characterization of the lipid constituents of maize silk cuticle suggests that three parallel pathways generate the unsaturated fatty acids and fatty aldehydes that are the precursors of the alkenes and dienes series of hydrocarbons (Perera et al. 2010a). This includes: 1) elongation-isomerization-decarbonylation; 2) elongation-desaturation-decarbonylation; and 3) desaturation-elongation-decarbonylation, and these processes produce a

series of unsaturated alkenes of different chain lengths, containing double bonds at the 4^{th}, 6^{th}, or 9^{th}, and dienes with double bonds at the 6^{th} and 9^{th}, and 9^{th} and 12^{th} positions (Perera et al. 2010a).

Historically, heterosis in maize has been observed for traits associated either with yield (e.g., biomass, plant height, kernel row or rank number, kernel weight, etc.) or traits that are easily measured (Birchler et al. 2003; Birchler et al. 2010; Goff 2011; Hochholdinger and Hoecker 2007; Springer and Stupar 2007). Based on an earlier study (Perera et al. 2010a) that indicated a heterotic response in the accumulation of hydrocarbons in the hybrids between the inbreds B73 and Mo17, in this study, we explored this phenomena in the silks and pollen of the hybrids among the inbreds LH1, LH123HT, PHG84 and PHG39. The observation that hydrocarbon accumulation showed overdominance in pollen but underdominance in silks implies that the hydrocarbon biosynthetic pathways are probably differentially regulated between these two organs.

Materials and Methods

Plant material and hydrocarbon extraction

Four inbred lines (LH1, LH123HT, PHG39 and PHG84) (Table 1) were crossed to generate six sets of hybrid progeny (LH1xLH123HT, LH1xPHG39, LH1xPHG84, LH123HTxPHG39, LH123HTxPHG84, PHG39xPHG84). Parental inbreds and their hybrid progeny were planted and grown at the Iowa State University Agronomy Farm (Boone, IA) during the summer, 2009.

Ear shoots were covered with a paper bag prior to silking to prevent pollination. Silks were collected six days after their first emergence from the ear husks. Ears were harvested from the field between 9am-10am and for extraction and analysis they were transported to the lab on ice around noon. Emerged silks were dissected in to two sections, those that had emerged from, and those that were still encased in the husk; the encased silks were stripped from the cob. Samples were flash-frozen in liquid nitrogen. Pollen was collected and flash frozen between 11am and 1pm from tassels that had emerged anthers on at least half of the main spike and branches. All silk and pollen samples were stored at -80℃. Prior to hydrocarbon extraction, silks and pollen were lyophilized in a FreeZone 4.5 Liter Freeze Dry System (Labconco, MO) and powderized with a Genogrinder 2000 (Spex CetriPrep, NJ).

Immediately prior to extraction of hydrocarbons, 10 µg of the internal standard, hexacosane (1 mg/mL) (Fluka, WI) was applied directly to ~100 mg of tissue. HPLC-grade hexane (Fisher Scientific, NJ; 1.5 mL) was added to the tissue and samples were sonicated for 15 min and centrifuged at 13000g for 1 min. The supernatant was collected. This extraction step was repeated two more times. The combined supernatant for each sample was passed over a silica gel (J.T.Baker, NJ) column and the column was washed with 10 mL hexane. The eluent was collected and dried in a rotary nitrogen evaporator (Organomation Associates, INC, MA) at 30 ℃. The dried hydrocarbon sample was dissolved in 1 mL hexane for GC-MS analysis.

Gas chromatography-mass spectrometric analysis

Chromatographic analysis was performed with a gas chromatograph (Model 6890 series, Agilent Technologies, Palo Alto, CA), equipped with a mass detector Model 5973 (Agilent Technologies, Palo Alto, CA). Chromatography was conducted using a HP-5MS cross-linked (5%)-diphenyl-(95%)-dimethyl polysiloxane column (30 m length, 0.25 mm inner diameter), using helium as the carrier gas. The injection temperature was at 280℃. The oven temperature was initially at 200 ℃, was increased to 280 ℃ at a rate of 4 ℃/min, and further increased to 320 ℃ at a rate of 20 ℃/min and held at this temperature for 3 min.

Statistical methods

All metabolite data were gathered from a minimum of five biological replicates. Metabolite abundances are the average of these multiple determinations (± standard error). Where appropriate, a student's t-test was conducted to determine whether the metabolite abundances are statistically different among samples. To compare the global hydrocarbon composition among the maize inbred lines and F1 hybrids, the weighted Manhattan distance (D_j) (Dixon et al., 2009) was used to measure the dissimilarity between a pair of genotypes (Perera et al. 2010a). For classifying and visualizing similarities among different maize inbreds and their hybrids, hierarchical clustering with average linkage was applied based upon the

weighted Manhattan distance. The cluster agglomeration method average linkage computes cluster distances as average distance between objects from the first cluster and objects from the second cluster.

Results

Hydrocarbon accumulations in maize pollen and silk of parent inbreds LH1, LH123HT, PHG39 and PHG84

The inbreds LH1 and PHG39 belong to the Stiff Stalk (SS) heterotic group, whereas inbreds LH123HT and PHG84 belong to different lineages in the Non-Stiff Stalk (NSS) heterotic group (Table 1) (Nelson et al. 2008). Hydrocarbons of pollen, and silks that were emerged from or still encased within ear husks were characterized from these four inbreds. For all four inbreds, the major hydrocarbon constituents identified in these samples are predominantly odd-numbered alkanes and alkenes of chain lengths ranging from 23 and 31 carbons, in combination with minor amounts of even-numbered hydrocarbons with chain length ranging from 24 to 30 carbons (less than 1%) (Supplemental Tables 1, 2 and 3). The major hydrocarbon constituents (i.e. ~96% of the total hydrocarbons) of all three of these biological organs are C_{25}, $C_{27:1}$, C_{27}, $C_{29:1}$, C_{29}, $C_{31:1}$ and C_{31}, where C_{25} and C_{27}, and C_{29} is the predominant alkane, and $C_{29:1}$ is the predominant alkene. In both encased and emerged silks, LH1, LH123HT and PHG84 alkanes (~50%) and alkenes (~50%) accumulate to relatively equal levels, whereas PHG39 expresses a higher level of alkanes (~56% for emerged silks and ~55% for encased silks)

as compared to alkenes (~44% for emerged silks and ~45% for encased silks) (p value <0.05). In pollen, LH1, PHG39 and PHG84 have similar amounts of alkanes (~50%) and alkenes (~50%), whereas in LH123HT pollen there are more alkanes (~61%) than alkenes (~38%) (p value <0.05).

The total amount of hydrocarbons (ranging from 5.5 to 6.5 μmol/g dry silk for emerged silks and 5.6 to 6.1 μmol/g dry pollen) (Fig. 1) as well as most of hydrocarbon constituents (Supplemental Table 1 for emerged silks and Supplemental Table 2 for pollen) did not differ significantly among the emerged silks and pollen of the four inbreds (p>0.05). However relative abundances of some minor hydrocarbon constituents did vary among the inbreds. For example, C22, C29:2 are present in emerged silks of LH1, LH123HT but absent in those of PHG39 and PHG84 (Supplemental Table 1); $C_{25:1}$, $C_{28:2}$ and C_{28} are absent in pollen of LH1 but present in the other three inbreds (Supplemental Table 2).

For each of the four inbreds, the emerged silks had ~2-3-fold higher amounts of hydrocarbons (~6 μmol/g dry silk) as compared to the encased silks, which is similar to a previous observation for silks of the inbred B73 (Perera et al., 2010). Total hydrocarbons in encased silks differed 2-fold among inbreds (p-value <0.05), with PHG39 accumulating the most (~3.2 μmol/g dry silk; Fig. 1) and LH1 accumulating the least (~1.5 μmol/g dry silk; Fig. 1).

In addition, in the encased silk samples the relative abundances of the major hydrocarbon constituents differed among the inbreds (Supplemental Table 3). The relative abundances of all the major hydrocarbons, C_{25}, $C_{27:1}$, C_{27}, $C_{29:1}$, C_{29}, $C_{31:1}$ and C_{31} in LH1 encased silks are considerably different from those in PHG39 and PHG84 encased silks (p-value <0.05) (Supplemental Table 3), while relative abundances of $C_{29:1}$ and C_{29} did not differ between LH1 and LH123HT. Minor constituents also vary among inbreds in encased silks (Supplemental Table 3). The differences in constituent profiles may be due to fact that LH1 and PHG39 belongs to the Stiff-Stalk (SS) group while PHG84 and LH123HT belong to Non-Stiff Stalk (NSS) group.

Using the data of hydrocarbon composition profiles from pollen, encased and emerged silks, the 4 parental maize inbreds were statistically clustered using Manhattan Distance as the measure of statistical distance (Perera et al. 2010a)(Figure 2). These statistical analyses of the hydrocarbon composition data indicate that the four parents can be classified into two clades, but the inbred distribution among these clades is different depending on the organ whose chemotype is compared. The relationship among the four inbreds is very similar based on hydrocarbon profiles from encased and emerged silks, with PHG39 and LH123HT being in the same clade, and LH1 and PHG84 are in the same second clade that is distinct from the first. However, based on hydrocarbon profiles from pollen, the inbreds LH1, PHG39 and LH123HT are in one clade, and PHG84 is in another clade. These classifications of the

inbreds based on hydrocarbon profiles from silks and pollen are different from the grouping based on the 768 single nucleotide polymorphism (SNP) markers, in which PHG39 and LH1 are in the same clade while PHG84 and LH123HT in the same but separate clade (Nelson et al. 2008). This differences between the genotypes of the inbreds and the expressed chemotypic traits that are different among the different organs reflect the fact that each inbred has a different developmental program for regulating the expression of hydrocarbons

Heterotic effects on hydrocarbon accumulation in maize pollen

To gain insight into the genetic interactions that impact pollen and silk hydrocarbon accumulation and composition, we profiled these constituents in six F1 hybrids generated by intercrossing the LH1, LH123HT, PHG39 and PHG84 inbreds. As with the four parental inbreds, the predominant hydrocarbons identified on the pollen of the six hybrids were C_{23}, C_{25}, $C_{27:1}$, C_{27}, $C_{29:1}$, C_{29}, $C_{31:2}$, $C_{31:1}$ and C_{31}, which comprised more than 96% of all the hydrocarbons detected, and among these, C_{25}, C_{27} and $C_{29:1}$ are the predominant constituents accounted for more than 68% percent of the hydrocarbons.

In the hybrids all genetic loci will be in the heterozygous state and given that in this heterozygous state the functionality of the two alleles at each locus is additive, the expectation is that traits (hydrocarbon constituents) will be expressed at the midpoint between the two parents. Therefore, we statistically evaluated the abundance of each cuticular wax component and tested this

prediction. These analyses indicate that the accumulation pattern of the individual hydrocarbon components could be classified as one of three types (Birchler et al. 2003; Crow 1948; Swanson-Wagner et al. 2006): 1) additive, accumulation in the hybrid is at the mid-parent level; 2) high- or low-parent dominant, accumulation in the hybrid is at a level comparable to either one of the two parents; and 3) over- or under-dominant, accumulation is at a level above the high-parent or below the low-parent, respectively. For example, the total hydrocarbon content of the pollen of the three hybrids, LH1×PHG39, LH1×LH123HT, LH123HT×PHG39 were significantly higher than both of their individual parents, and therefore this trait showed overdominance (Fig. 3). The majority of individual hydrocarbon constituents showed either overdominance or high-parent dominance (Supplemental Table 3) in the hybrids LH1 ×PHG39 (i.e. C_{27}, C_{29}, $C_{29:1}$, $C_{31:2}$, $C_{31:1}$ and $C_{31:2}$ constituents), LH1×LH123HT (i.e. C_{25} and C_{27}, C_{29}, $C_{29:1}$, $C_{31:2}$, $C_{31:1}$ and $C_{31:2}$ constituents) and PHG39×PHG84 (i.e. C_{25}, $C_{27:1}$, C_{27}, $C_{31:2}$, $C_{31:1}$ and C_{31} constituents) hybrids (Supplemental Table 3). In addition to these constituents, which are all odd-numbered and major hydrocarbon components, some even-numbered hydrocarbons (e.g., $C_{30:1}$ in LH1 ×PHG39 and C_{24} in LH1×LH123HT and PHG39×PHG84) also showed heterotic effects in the hybrids (Supplemental Table 3). Interestingly, the C_{23} and C_{24} hydrocarbon showed under-dominance effects in the three hybrids, LH1×PHG39, LH1×LH123HT, LH123HT×PHG39.

Although heterotic effects were not observed for the total hydrocarbon content of pollen from the three hybrids, LH1×PHG84, LH123HT×PHG84 and PHG39×PHG84 (Fig 3), some individual constituents in each of these hybrids did exhibit heterosis. For example, overdominance was observed for the C_{29} hydrocarbon in the LH1×PHG84 hybrid, and for the C_{25}, C_{27}, C_{31} and $C_{33:1}$ constituents in the PHG39×PHG84 hybrid (Supplemental Table 3); high parent dominance, was observed for the C_{25}, C_{27} and C_{31} hydrocarbon constituents in the LH123HT×PHG84 hybrid (Supplemental Table 3).

Under-dominance of hydrocarbon accumulation in maize silks

In contrast to the heterotic inheritance patterns of hydrocarbon accumulation observed in pollen, the majority of hydrocarbon constituents of silks of the hybrids derived from LH1, LH123HT, PHG39, and PHG84 showed under-dominance, that is the hybrids exhibited a lower hydrocarbon accumulation as compared to either of the parents. Hybrids, LH1×PHG84 and PHG39×PHG84 exhibited under-dominance and LH1×PHG39 showed low-parent dominance with hydrocarbons from both encased and emerged silks. The other three hybrids, LH1×LH123HT, LH123HT×PHG39 and LH123HT×PHG84, which had LH123HT as the common parent displayed a different heterotic patterns between encased and emerged maize silks (Fig 3). Although most of the hydrocarbon constituents showed underdominace (high or low parent) or additive accumulation (Supplemental Table 1 and 3), a few hydrocarbons showed heterosis. For instance, $C_{25:1}$ and C_{25} showed

overdominace in hybrids LH1×LH123HT and LH123HT×PHG84, $C_{27:1}$ exhibited high-parent dominance in LH1×LH123HT and $C_{29:1}$ showed high-parent dominance in LH123HT×PHG84 (Supplemental Table 3).

Heterotic pattern in hybrid PHG39×PHG84 is consistent over two different seasons

Because environmental conditions may impact hydrocarbon accumulation patterns (Jetter and Kunst 2008), hydrocarbons were analyzed on silks from the hybrid PHG39xPHG84 and its inbred parents over two growing seasons. For all genotypes tested hydrocarbon accumulation in either encased or emerged silks was higher in 2009 than 2010. Specifically, for all three genotypes the total hydrocarbon accumulation in emerged silks was 2-3 fold higher in 2009 than in 2010 (p-value <0.05). For the encased silks, hydrocarbon levels in PHG39 and PHG39×PHG84 was 3- and 9-fold higher in materials grown in 2009 as compared to 2010 grown material. The only exception to this trend was the hydrocarbons in the encased silks of PHG84, which were at similar levels in both years (p-value >0.05) (Fig. 4). In addition to producing higher levels of hydrocarbons, PHG39, PHG84 and their hybrid also produced more unsaturated hydrocarbons, $C_{29:1}$ and $C_{31:1}$ in year 2009 than 2010, and this is the case for both encased and emerged silks (Fig 5). Despite these differences in hydrocarbon accumulation between the two growth seasons, both total hydrocarbon accumulation and individual constituent

amounts exhibited clear under-dominance in the hybrid as compared to the inbred parents in both seasons (Fig 4 and Fig 5).

These differences in hydrocarbon accumulation may be attributable to differences in environmental conditions between the two seasons. To assess how the environment may have been different between the two growth seasons, we accessed daily weather data that were gathered from May to August in 2009 and 2010 at the Ames station (AMW station) (mesonet.agron.iastate.edu). This weather station is situated within 2.2 miles from the genetic field where our maize plants were grown. There is no obvious difference between the maximum and minimum daily temperatures, soil temperature 4 inches below the surface, average relative humidity and solar radiation during this period between 2009 and 2010. However, daily precipitation varied greatly between the two summers. In July and August, 2010 the average daily precipitation was ~84 and 94-fold higher than in 2009, respectively (Table 2). Therefore, more hydrocarbons were accumulated in a drier season (2009). This is consistent with the physiological function of hydrocarbons, prevention of water loss on the plant cuticle surface (Samuels et al. 2008b).

Discussion

Hydrocarbons accumulation in hybrids differs between maize pollen and silk.

Until recently, heterotic traits that have been studied in maize have primarily been associated with yield (Smith et al. 1990) or traits could be easily measured (i.e., phenotypes) (Stupar et al. 2008). Recently, heterotic effects of metabolic traits have been observed in developing seeds from maize and faba bean (Meitzel et al. 2011; Romisch-Margl et al. 2010), as well as in Arabidopsis seedlings (Lisec et al. 2009). This study applied metabolite (hydrocarbons) profiling to inbreds LH1, LH123HT, PHG39 and PHG84 and their hybrids to understand heterosis phenomenon in maize pollen and silks. Among the six hybrids in this study, total hydrocarbon accumulation and the majority of hydrocarbon constituents from pollen of the three hybrids (LH1×LH123HT, LH1×PHG39 and LH123HT×PHG39) showed overdominance, whereas hydrocarbons in the other three hybrids (LH1×PHG84, LH123HT×PHG84 and PHG39×PHG84) showed additive effects, in which the hybrid producing similar amount of hydrocarbons to the average of its two parents (Fig.3 and Supplemental Table 3). Although the lipids extracted from maize silk have a composition similar to that found for maize pollen, total hydrocarbons from both encased and emerged silks in each of the hybrids (with the exception of encased silks from the hybrid LH1×LH123HT) instead showed underdominance. Different heterotic patterns between maize silk and pollen (underdominance in maize silk but overdominance in maize pollen) in the same hybrid suggests that different

hydrocarbon biosynthesis pathways or different genetic regulation network for hydrocarbon biosynthesis exists in maize silk and pollen.

Hydrocarbons in pollen of the four inbreds in this study comprised of equal portions of alkanes (mainly C_{25}, C_{27} and C_{29}) and alkenes (mainly $C_{27:1}$, $C_{29:1}$ and $C_{31:1}$), very similar to hydrocarbon constituents found on pollen derived from maize inbreds B37, NY821, K55 and Mo506 (Bianchi et al. 1990). However, trace amounts of even-numbered hydrocarbons were also observed in LH1, LH123HT, PHG39 and PHG84 (Supplemental Table 3). In the LH1×PHG39, LH123HT×PHG39 and LH1×LH123HT hybrids, hydrocarbons with chain lengths of 25-carbons or greater showed overdominance dominance with each individual hydrocarbon showing either overdominance or high-parent dominance whereas hydrocarbons with chain lengths equal to or less than 25-carbons showed underdominance, as we previously observed for hydrocarbons on silks from the B73xMo17 hybrid (Perera et al. 2010a), with each individual hydrocarbon showing either additive effects or underdominance. Hydrocarbons with different chain length have been demonstrated to follow different heterotic patterns in 3 hybrids of maize pollen as well as B73×Mo17 maize silk (Perera et al. 2010a). The remaining three hybrids (i.e. LH1×PHG84, LH123HT×PHG84 and PHG39×PHG84), all of which share the PHG84 parent in common, total hydrocarbon accumulation showed additive effects in pollen. However, some individual hydrocarbons

showed underdominance, high-parent dominance or overdominance (Supplemental Table 3).

Contrary to maize pollen, underdominance or low-parent dominance was observed for total hydrocarbons in emerged maize silks for the six hybrids and in encased silk for four hybrids in this study (Fig 3). The underdominance phenomenon observed for these hybrids is quite different from the heterotic pattern described for hydrocarbons that accumulate on the silks of the B73xMo17 hybrid, which shows heterosis instead of underdominance (Perera et al. 2010a). In addition, no individual constituents showed heterosis in encased and emerged silks. Instead, all of them showed additive effect, low-parent dominance or underdominance (Supplemental Table 1 and Supplemental Table 2). Different genetic backgrounds and environmental conditions might contribute to the different hereditary trait in the same organ in maize.

Not only did the current study use four inbreds that have different lineages and fit into different heterotic groups (Table 1) than the B73 (Iowa Stiff Stalk Synthetic heterotic group) and Mo17 (Lancaster Sure Crop heterotic group) inbreds used by Perera et al. (2010), the experiments were conducted over separate growing seasons. Differences in environmental conditions could play a role in hydrocarbon accumulation patterns. Hydrocarbons are thought to provide a hydrophobic barrier that can prevent water loss (Samuels et al. 2008b), which could be less necessary in wet conditions. Indeed, rainfall

measurements were >60-fold higher in the summer of 2010 where hydrocarbon accumulation was much less than in the drier 2009 season.

Furthermore, hierarchical cluster analysis for both encased and emerged silks by using the average linkage illustrate that LH1 is closer to PHG39 and LH123HT is closer to PHG84 by counting all the constituents (Fig 2a and Fig 2b) while in maize pollen, PHG84 is the far from the other three inbreds (Fig 2c). These differences in the relationship among parent inbreds might also play a role in an unknown way. Underdominant traits have previously been observed in hybrid maize. For example, in developing B73xMo17 hybrid kernels, levels of specific amino acids as well as total protein content were depressed as compared with the B73 and Mo17 parental inbreds (Romisch-Margl et al. 2010).

In studies of twelve maize hybrids, differences in nonadditive gene and protein expression were observed between primary roots and shoot apical meristems in a single hybrid (Hoecker et al. 2008; Paschold et al. 2010). Whereas these observations were at the transcript and protein level, in the current study differences in heterotic effects were observed for metabolites accumulating on two different organs. In the three of six hybrids characterized in this study, hydrocarbons in maize pollen showed overdominance whereas hydrocarbon accumulation on silks showed underdominance. Organ-specific patterns of nonadditive gene expression in maize hybrids might contribute to the manifestation of different degree of heterosis in different organs in maize

(Paschold et al. 2010). Perera et. al. (Perera et al. 2010a) proposed three different putative biosynthetic pathways for maize silk hydrocarbons (i.e. the elongation-isomerization pathway, elongation-desaturation-decarboxylation pathway and elongation-desaturation-decarbonylation pathway). Our results, which show that maize pollen exhibits overdominance, while maize silks show underdominance might imply that the proposed different pathways or different regulatory systems exist in maize pollen and silks.

References

Aarts MGM, Keijzer CJ, Stiekema WJ, Pereira A (1995) Molecular characterization of the CER1 gene of arabidopsis involved in epicuticular wax biosynthesis and pollen fertility. Plant Cell 7:2115-2127

Bernard A, Domergue F, Pascal S, Jetter R, Renne C, Faure JD, Haslam RP, Napier JA, Lessire R, Joubes J (2012) Reconstitution of Plant Alkane Biosynthesis in Yeast Demonstrates That Arabidopsis ECERIFERUM1 and ECERIFERUM3 Are Core Components of a Very-Long-Chain Alkane Synthesis Complex. Plant Cell

Bianchi G, Murelli C, Ottaviano E (1990) Maize Pollen Lipids. Phytochemistry 29:739-744

Birchler JA, Auger DL, Riddle NC (2003) In search of the molecular basis of heterosis. Plant Cell 15:2236-2239

Birchler JA, Yao H, Chudalayandi S, Vaiman D, Veitia RA (2010) Heterosis. Plant Cell 22:2105-2112

Blaker TW, Greyson RI (1988) Developmental Variation of Leaf Surface Wax of Maize, Zea-Mays. Can J Bot 66:839-846

Cheesbrough TM, Kolattukudy PE (1984) Alkane Biosynthesis by Decarbonylation of Aldehydes Catalyzed by a Particulate Preparation from Pisum-Sativum. P Natl Acad Sci-Biol 81:6613-6617

Crow JF (1948) Alternative Hypotheses of Hybrid Vigor. Genetics 33:477-487

Dennis MW, Kolattukudy PE (1991) Alkane biosynthesis by decarbonylation of aldehyde catalyzed by a microsomal preparation from Botryococcus braunii. Arch Biochem Biophys 287:268-275

Endler A, Liebig J, Schmitt T, Parker JE, Jones GR, Schreier P, Holldobler B (2004) Surface hydrocarbons of queen eggs regulate worker reproduction in a social insect. Proceedings of the National Academy of Sciences of the United States of America 101:2945-2950

Goff SA (2011) A unifying theory for general multigenic heterosis: energy efficiency, protein metabolism, and implications for molecular breeding. New Phytol 189:923-937

Han J, Calvin M (1969) Hydrocarbon distribution of algae and bacteria, and microbiological activity in sediments. Proc Natl Acad Sci U S A 64:436-443

Hochholdinger F, Hoecker N (2007) Towards the molecular basis of heterosis. Trends Plant Sci 12:427-432

Hoecker N, Lamkemeyer T, Sarholz B, Paschold A, Fladerer C, Madlung J, Wurster K, Stahl M, Piepho HP, Nordheim A, Hochholdinger F (2008) Analysis of nonadditive protein accumulation in young primary roots of a maize (Zea mays L.) F(1)-hybrid compared to its parental inbred lines. Proteomics 8:3882-3894

Jetter R, Kunst L (2008) Plant surface lipid biosynthetic pathways and their utility for metabolic engineering of waxes and hydrocarbon biofuels. Plant J 54:670-683

Largeau C, Casadevall E, Berkaloff C (1980) The Biosynthesis of Long-Chain Hydrocarbons in the Green-Alga Botryococcus-Braunii. Phytochemistry 19:1081-1085

Lisec J, Steinfath M, Meyer RC, Selbig J, Melchinger AE, Willmitzer L, Altmann T (2009) Identification of heterotic metabolite QTL in Arabidopsis thaliana RIL and IL populations. Plant J 59:777-788

Meitzel T, Radchuk R, Nunes-Nesi A, Fernie AR, Link W, Weschke W, Weber H (2011) Hybrid embryos of Vicia faba develop enhanced sink strength, which is established during early development. Plant J 65:517-531

Nelson PT, Coles ND, Holland JB, Bubeck DM, Smith S, Goodman MM (2008) Molecular characterization of maize inbreds with expired US plant variety protection. Crop Sci 48:1673-1685

Park MO (2005) New pathway for long-chain n-alkane synthesis via 1-alcohol in Vibrio furnissii M1. J Bacteriol 187:1426-1429

Paschold A, Marcon C, Hoecker N, Hochholdinger F (2010) Molecular dissection of heterosis manifestation during early maize root development. Theor Appl Genet 120:383-388

Perera MA (2005) Molecular and chemical characterization of genes involved in maize cuticular wax biosynthesis. Dissertation, Iowa State University

Perera MA, Qin W, Yandeau-Nelson M, Fan L, Dixon P, Nikolau BJ (2010a) Biological origins of normal-chain hydrocarbons: a pathway model based on cuticular wax analyses of maize silks. Plant J 64:618-632

Perera MADN, Qin WM, Yandeau-Nelson M, Fan L, Dixon P, Nikolau BJ (2010b) Biological origins of normal-chain hydrocarbons: a pathway model based on cuticular wax analyses of maize silks. Plant Journal 64:618-632

Rieley G, Teece MA, Peakman TM, Raven AM, Greene KJ, Clarke TP, Murray M, Leftley JW, Campbell C, Harris RP, Parkes RJ, Maxwell JR (1998) Long-chain alkenes of the haptophytes Isochrysis galbana and Emiliania huxleyi. Lipids 33:617-625

Romisch-Margl L, Spielbauer G, Schutzenmeister A, Schwab W, Piepho HP, Genschel U, Gierl A (2010) Heterotic patterns of sugar and amino acid components in developing maize kernels. Theor Appl Genet 120:369-381

Rude MA, Baron TS, Brubaker S, Alibhai M, Del Cardayre SB, Schirmer A (2011) Terminal Olefin (1-Alkene) Biosynthesis by a Novel P450 Fatty Acid Decarboxylase from Jeotgalicoccus Species. Appl Environ Microb 77:1718-1727

Samuels L, Kunst L, Jetter R (2008) Sealing plant surfaces: Cuticular wax formation by epidermal cells. Annu Rev Plant Biol 59:683-707

Schirmer A, Rude MA, Li XZ, Popova E, del Cardayre SB (2010) Microbial Biosynthesis of Alkanes. Science 329:559-562

Schneider-Belhaddad F, Kolattukudy P (2000) Solubilization, partial purification, and characterization of a fatty aldehyde decarbonylase from a higher plant, Pisum sativum. Arch Biochem Biophys 377:341-349

Smith OS, Smith JSC, Bowen SL, Tenborg RA, Wall SJ (1990) Similarities among a Group of Elite Maize Inbreds as Measured by Pedigree, F1 Grain-Yield, Grain-Yield, Heterosis, and Rflps. Theoretical and Applied Genetics 80:833-840

Springer NM, Stupar RM (2007) Allelic variation and heterosis in maize: How do two halves make more than a whole? Genome Research 17:264-275

Stupar RM, Gardiner JM, Oldre AG, Haun WJ, Chandler VL, Springer NM (2008) Gene expression analyses in maize inbreds and hybrids with varying levels of heterosis. Bmc Plant Biol 8

Sukovich DJ, Seffernick JL, Richman JE, Gralnick JA, Wackett LP (2010) Widespread Head-to-Head Hydrocarbon Biosynthesis in Bacteria and Role of OleA. Appl Environ Microb 76:3850-3862

Swanson-Wagner RA, Jia Y, DeCook R, Borsuk LA, Nettleton D, Schnable PS (2006) All possible modes of gene action are observed in a global comparison of gene expression in a maize F-1 hybrid and its inbred parents. P Natl Acad Sci USA 103:6805-6810

Templier J, Diesendorf C, Largeau C, Casadevall E (1992) Metabolism of Normal-Alkadienes in the a Race of Botryococcus-Braunii. Phytochemistry 31:113-120

Templier J, Largeau C, Casadevall E (1984) Hydrocarbon Formation in the Green-Alga Botryococcus-Braunii .4. Mechanism of Non-Isoprenoid Hydrocarbon Biosynthesis in Botryococcus-Braunii. Phytochemistry 23:1017-1028

Templier J, Largeau C, Casadevall E (1987) Hydrocarbon Formation in the Green-Alga Botryococcus-Braunii .5. Effect of Various Inhibitors on Biosynthesis of Non-Isoprenoid Hydrocarbons in Botryococcus-Braunii. Phytochemistry 26:377-383

Templier J, Largeau C, Casadevall E (1991a) Biosynthesis of Normal-Alkatrienes in Botryococcus-Braunii. Phytochemistry 30:2209-2215

Templier J, Largeau C, Casadevall E (1991b) Nonspecific Elongation Decarboxylation in Biosynthesis of Cis-Alkadienes and Trans-Alkadienes by Botryococcus-Braunii. Phytochemistry 30:175-183

Wackett LP, Frias JA, Seffernick JL, Sukovich DJ, Cameron SM (2007) Genomic and biochemical studies demonstrating the absence of an alkane-producing phenotype in Vibrio furnissii M1. Appl Environ Microb 73:7192-7198

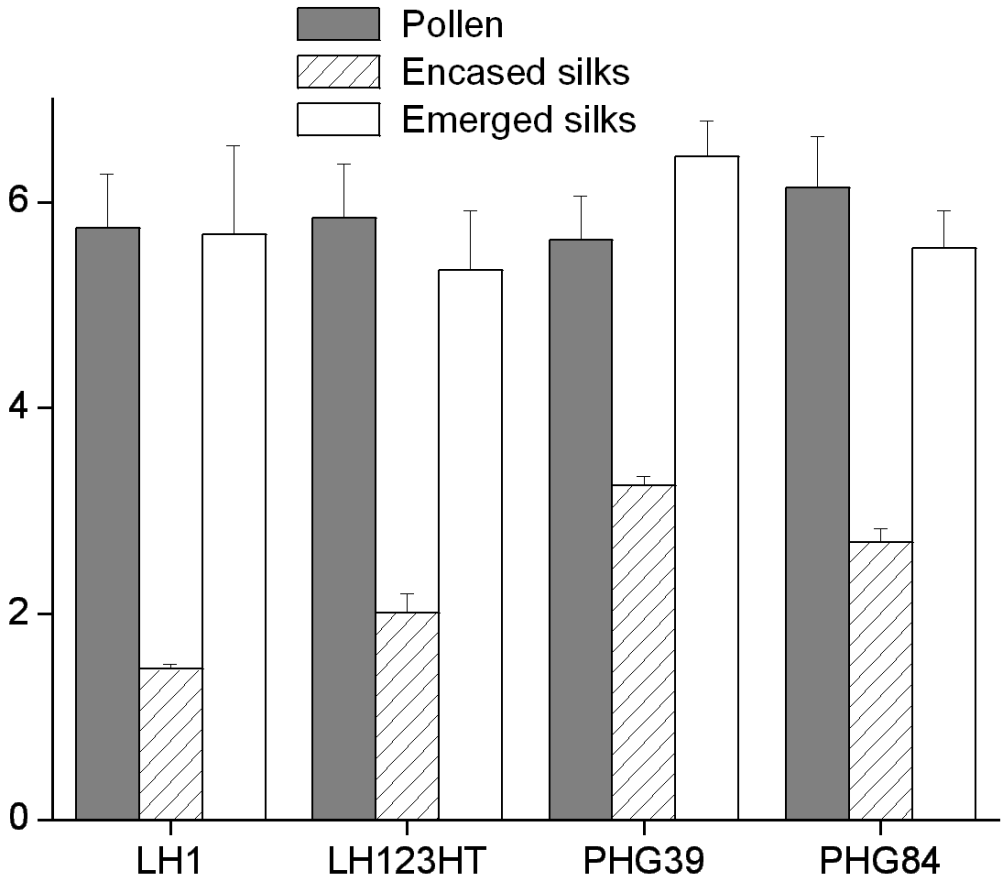

Figure 1. Total hydrocarbon in maize pollen, encased and emerged silks in four parents LH1, LH123HT, PHG39 and PHG84.

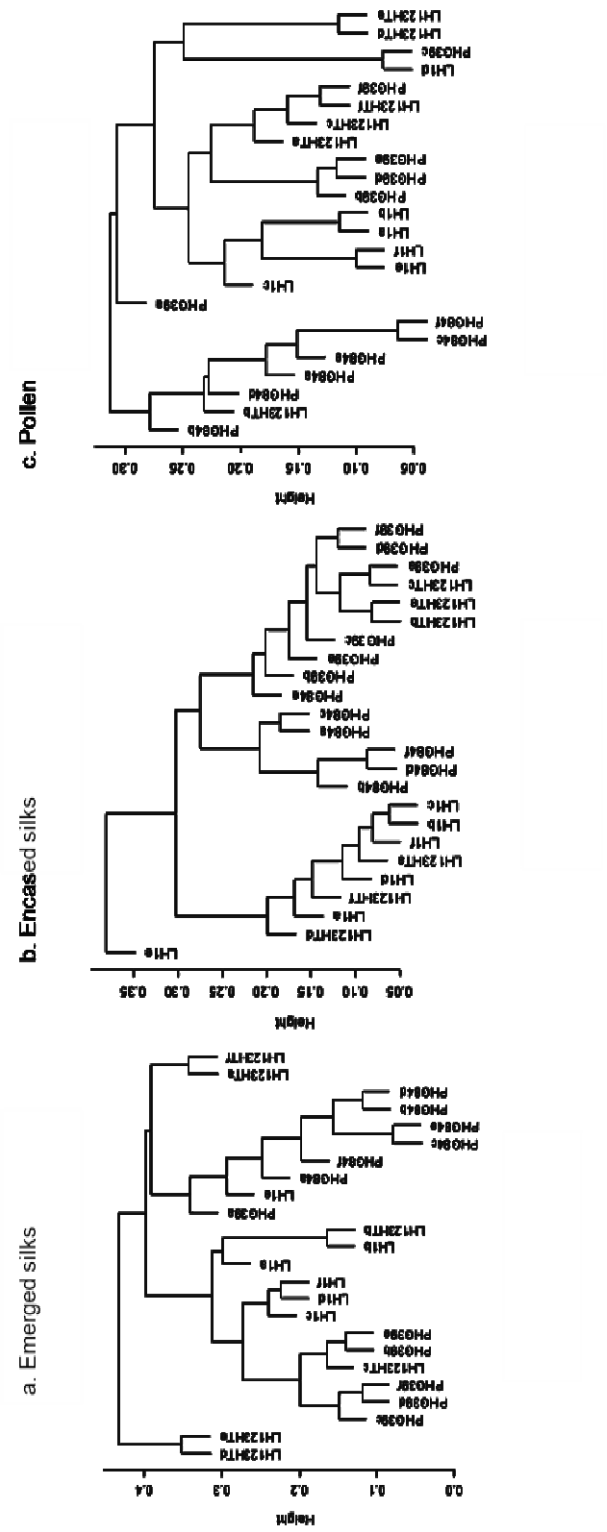

Figure 2. Hierarchical agglomerative clustering of hydrocarbonpattern in encased (a) and emerged (b) maize silks and maize pollen (c) using average linkage agglomeration and Manhattan distance.

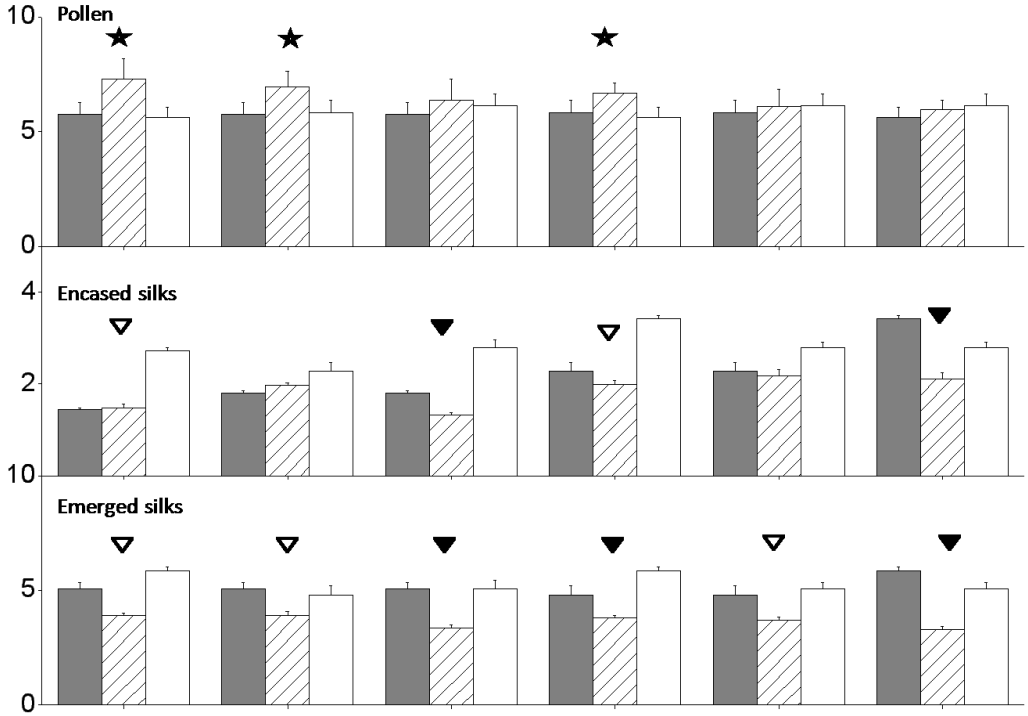

Figure 3. Heterotic and underdominance pattern of total hydrocarbon in maize pollen and silk. ★ -Heterotic effects; ▼ - underdominance ; ▽ - low-parent dominance. Each row have the same hybrids order and in each triplet, the one in the middle is the hybrids and the other two on both sides of the hybrid is its parental lines

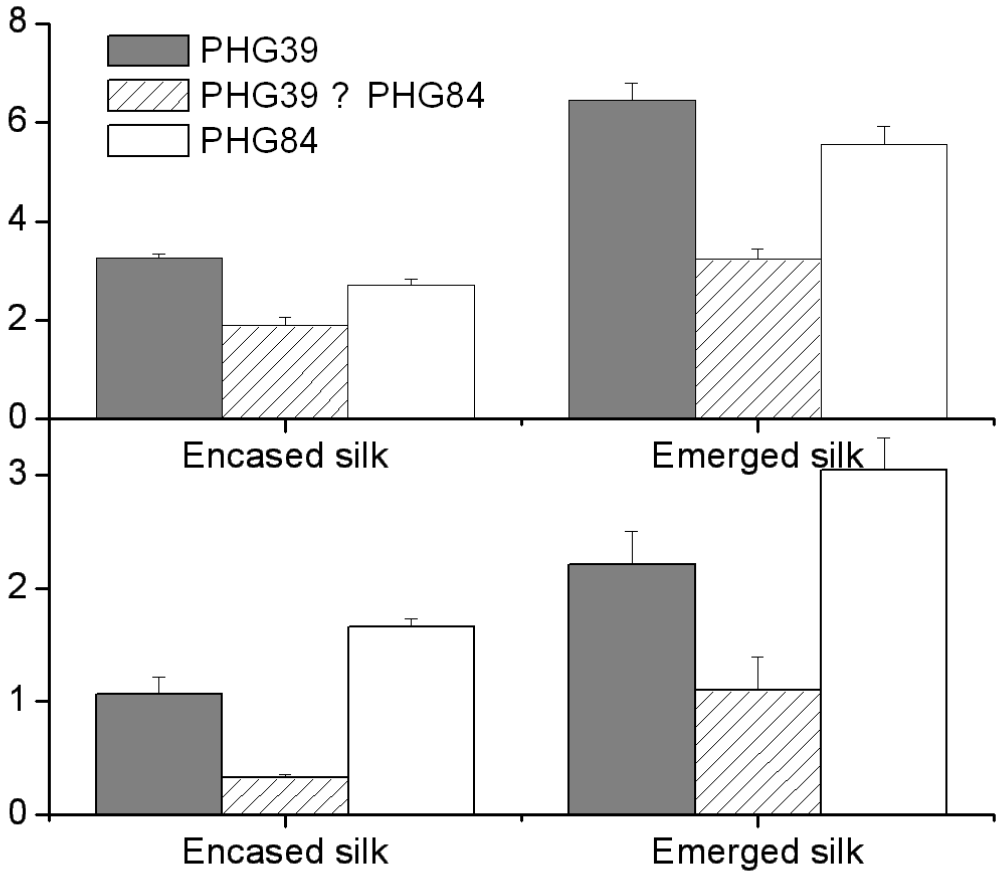

Figure 4. Underdominance pattern for total hydrocarbons is consistent between year 2009 and 2010

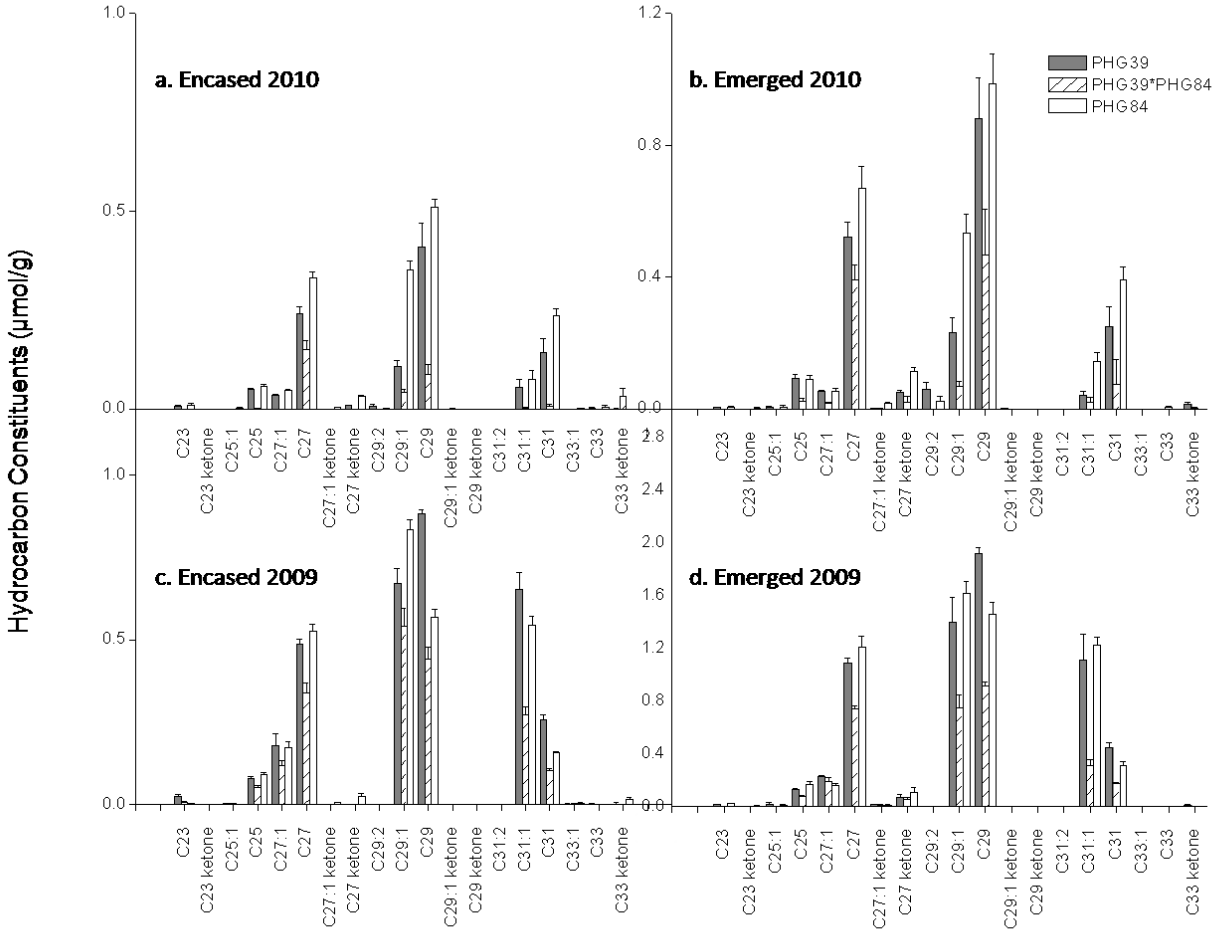

Figure 5. Underdominance patterns for individual consistituents in encased (a) and emerged (b) silks for year 2010 and year 2009 (c, encased and d, emerged).

Table 1. Parental inbred lines

Inbred Line[a]	Lineage-inferred Background[b]	Marker-inferred background[c]	Pedigree
PHG39	Argentine MaizAmargo	B37/A632	PHA33GB4xPHA34CB4
PHG84	Oh7-Midland	Mixed/PH207	PH848xPH595
LH1	Iowa Stiff Stalk Synthetic	B37/PH207	(B37x644)xB37
LH123HT	Pioneer hybrid 3535-derived (PH3535)	Oh43/Mo17/Mixed	Pioneer hybrid 3535

a. Inbred lines designated as “PH” and “LH” originated from Pioneer Hi-Bred, Int. and Holden Foundation Seeds, respectively.
b. Grouping based on lineage and the most predominant genetic backgrounds in that lineage (Mikel& Dudley)
c. The genetic backgrounds of widely used commercial and public inbreds were classified based on 768 single nucleotide polymorphism (SNP) markers (Nelson et al. Crop Sci 2008). In the cases where multiple parent inbreds contributed significant genetic material to the generation of an inbred, these backgrounds are listed in descending order of genetic contribution. Mixed denotes derivation from a population of mixed backgrounds.

Table 2. Daily precipitation of May, June, July and August in year 2009 and 2010 (Barlow et al.)

	2009	2010
July	0.049	4.17
August	0.115	10.848

Supplemental Table 1
Supplemental Table 2
Supplemental Table 3
(..\Desktop\supplement tables for chapter 3.xlsx)

CHAPTER 4. COMPARATIVE TRANSCRIPTOME PROFILING OF SILKS FROM MAIZE INBRED B73 FOR THE IDENTIFICATION OF GENES INVOLVED IN THE BIOSYNTHESIS OF SURFACE LIPIDS

Wenmin Qin, Adarsh Jose, Marna Yaudeau-Nelson, Basil J. Nikolau

Center for Metabolic Biology, Plant Science Institute
Center for Biorenewable Chemicals
Department of Biochemistry, Biophysics and Molecular Biology
Iowa State University, Ames, IA 50010

Abstract

To gain insights into how hydrocarbons are biosynthesized in maize silks, Illumina sequencing was applied to investigate the transcriptome of encased and emerged silks in the maize inbred B73. The emerged silks produce about 2 fold more hydrocarbons as compared to the encased silks. In contrast to hydrocarbon accumulation, encased silks produce ~10% more fatty acids than the emerged silks. Based on transcriptome sequencing read statistics, we found enzymes involved in producing VLCFAs as precursors for hydrocarbons are differentially expressed between encased and emerged silks. Transcripts encoding plastid-located ACCase, the enzyme catalyzing an important limiting step of fatty acid initiation, and KAS, which catalyzes a condensation reaction in fatty acid synthesis are expressed 2-3 folds higher in emerged silks than encased silks. Transcripts encoding a cytosolic-located ACCase, and ACL subunits, which generate substrates for fatty acid elongation, are elevated 2-fold and three KCS transcripts (GRMZM2G167438_T01, GRMZM2G137694_T01 and

GRMZM2G445602_T01) in fatty acid elongation expressed 1-fold higher in emerged silks than encased silks except for one KCS transcript (GRMZM2G167438_T01) with a 25-fold expression in emerged silks of encased silks. On the contrary, another three cytosolic ACCase transcripts (GRMZM5G854500_T01, GRMZM2G375116_T01 and GRMZM2G375116_T02), one KAS transcript (GRMZM2G569948_T01) and another three KCS transcripts (GRMZM2G151476_T01, GRMZM2G149636_T01 and GRMZM2G104626_T01) in fatty acid elongation have higher expression in encased silks than emerged silks. A transcript homologous to *cer1* of Arabidopsis, which is involved in generating hydrocarbons, expressed 7-fold higher in emerged silks than encased silks whereas another transcript (GRMZM2G099097_T03) homologous to *cer1* in Arabidopsis expressed 4-fold higher in encased silks than emerged silks. In addition, desaturases controlling the unsaturation of fatty acids are differentially expressed between the encased and emerged silks. Finally a small pool of candidate genes involved in surface lipid biosynthesis has been identified.

Introduction

Simple, linear hydrocarbons such as alkanes and alkenes occur at low levels in discrete places in biological systems (Han and Calvin 1969a; Park 2005; Samuels et al. 2008a; Wackett et al. 2007). One of the most accessible biological systems for studying these hydrocarbons is the cuticle of

insects and plants (Greene and Gordon 2003; Samuels et al. 2008b). The surface of stigmatic silks of maize are especially rich sources of hydrocarbons (Bianchi et al. 1990), and on this organ the hydrocarbons account for ~89% of the surface lipids (Perera 2005a). The hydrocarbons on maize silks might serve as a protective barrier against water loss and pathogen attack (Kunst and Samuels 2003b; Kunst and Samuels 2009; PostBeittenmiller 1996; Samuels et al. 2008b). During the development of the silks, they are initially totally encased by husk leaves, and as they elongate the tips of the silks emerge from the encasing husk leaves into the external environment. In the maize inbred B73, the emerged silks produce ca. 2-3 fold more hydrocarbons as compared to silks that are still encased within the husk leaves. The surface lipids on B73 silks are composed primarily of C_{27}, C_{29} and C_{31} n-alkanes and alkenes and they comprise 2% of the dry weight of the silks (Perera et al. 2010c).

Hydrocarbons are thought to be synthesized from fatty acid precursors (Tornabene 1982). In plants, fatty acids of chain lengths up to 18 carbons are synthesized via *de novo* synthesis within the plastids by type II fatty acid synthase (FAS). FAS is a collection of four distinct enzymes, which catalyze four sequential and reiterative reactions: 1) ketoacyl-ACP synthase; catalyzes the condensation of a malonyl-ACP and an acetyl-CoA to generate a β–ketoacyl-ACP; 2) ketoacyl-ACP reductase; catalyzes the reduction of the

ketone group to a hydroxyl group; 3) hydroxyacyl-ACP dehydratase; catalyzes the dehydration of the hydroxyl group to form a 2,3 double bond; 4) enoyl-ACP reductase; catalyzes a second reduction reaction to remove the double bond (Ohlrogge and Jaworski, 1997). Very long chain fatty acids (VLCFAs) with chain lengths greater than C_{18}, are synthesized by the elongation of preexisting fatty acids, which occurs in the membranes of the endoplasmic reticulum (ER). The biosynthesis of VLCFAs occurs in a manner analogous to *de novo* fatty acid biosynthesis (Stumpf, 1984, von Wettstein-Knowles, 1995), but utilizes CoA intermediates.

Numerous *glossy* mutant loci have been shown to affect the quantity and/or the composition of surface lipids on the surfaces of seedling leaves in maize (Post-Beittenmiller 1998). Among them, two *GL8* paralogs, with 96% identity, encoding 3-ketoacyl-CoA reductase, are involved in the elongation of VLCFA precursors for hydrocarbons (Xu et al. 1997).

Saturated and unsaturated C_{16} and C_{18} fatty acids are dominant in maize silk, but VLFAs (C_{20}, C_{22} and C_{24} fatty acids) also occur at lower levels (Perera et al. 2010b). These VLFAs, produced by fatty acid elongation are the presumed precursors for hydrocarbon biosynthesis in maize silk, by, subsequent decarbonylation. This process is envisioned to produce saturated alkanes by acting on saturated fatty acids precursors. Three parallel pathways are thought to generate the unsaturated fatty acids and fatty aldehydes that are the precursors of the alkenes and dienes series of hydrocarbons (Perera et

al. 2010c). These parallel pathways include: 1) elongation-isomerization-decarbonylation; 2) elongation-desaturation-decarbonylation; 3) desaturation-elongation-decarbonylation. In the first pathway a 2-enoyl-CoA intermediate from fatty acid elongation is isomerized to 3-enoyl-CoA for hydrocarbon biosynthesis. In the second and third pathways, the order of elongation and desaturation is different. These processes produce a series of unsaturated alkenes of different chain lengths, containing double bonds at the 4^{th}, 6^{th}, or 9^{th} positions, and dienes with double bonds at the 6^{th} and 9^{th}, and 9^{th} and 12^{th} positions (Perera et al. 2010c).

Recently, the *cer1*/*cer3* complex has been shown to catalyze the conversion fatty acid to hydrocarbons in Arabidopsis (Bernard et al. 2012b). However, no genes involved in the hydrocarbon biosynthetic pathway have been identified and characterized in maize.

In this study, we profiled the transcriptomes of silks from the maize inbred B73 that were emerged from or encased by husk leaves, which hyper- or hypo-accumulate hydrocarbons, respectively. Via this approach we have identified a pool of candidate genes, including key enzymes in fatty acid initiation, synthesis and elongations, and homologs to *cer* genes, and *glossy* genes, which are known to affect surface lipids in Arabidopsis and maize (Post-Beittenmiller 1998).

2. Experimental

2.1 Biological Materials

Zea mays L. (maize) inbred B73 plants were grown at Iowa State University Curtiss Farm in summer, 2008. Ear shoots were covered prior to silking to prevent pollination. Silks were collected three days after first emergence from the encasing ear husks; prior study had shown that 3-day-old emerged silk are still at the stage actively accumulating hydrocarbons (Perera et al. 2010c). Emerged silks were cut at the point of emergence and encased silks were stripped from the cob. Samples were flash-frozen and powderized in liquid nitrogen for metabolite analysis and RNA extraction.

2.2 Extraction of hydrocarbons

Immediately prior to hydrocarbon extraction, 10 μg of hexatriacontane (1 mg/mL) (Fluka, WI) was applied directly to the plant material (ca. 100 mg of tissue) as an internal standard. Hydrocarbons from each sample were extracted with 1.5 mL HPLC grade hexane (Fisher Scientific, NJ) with sonication for 15 min and centrifuged at 13000 g for 1 min. Supernatant was collected after centrifugation and this extraction step was repeated two more times. The combined supernatant was passed through a column containing 0.6 g silica gel (J.T. Baker, NJ) that was pre-washed with 10 mL hexane. After elution the column was washed with 10 mL hexane. The combined eluents were dried in a rotary nitrogen evaporator (Organomation Associates, Inc., MA) at 30 ℃. The dried hydrocarbon samples were dissolved in 1 mL hexane.

2.3 Extraction and derivatization of fatty acids

Immediately prior to fatty acid extraction, 10 µg of nonadecanoic acid (1 mg/mL) (Sigma-Aldrich, MO) was applied directly to the plant material (ca. 100 mg of tissue) as an internal standard. Fatty acids from each sample were extracted with 500 uL of 10% barium hydroxide (Sigma-Aldrich, MO) at 110 ℃ for 24 hours. Before recovery of the fatty acids, each sample was cooled and acidified with 6M HCl to pH<4. The fatty acids were recovered by extracting with three aliquots of 3 mL HPLC grade hexane (Fisher Scientific, NJ), and vortexing the mixtures for 1 min each time. Following centrifugation at 13000 g for 1 mins to separate the phases, the combined hexane-phases was dried and silylated with 70 uL of bis-trimethyl silyl trifluoroacetamide with 1% trimethylchlorosilane (BSTFA+1%TMC) at 60℃ for 30-mins for GC-MS analysis (Miwa 1971).

2.4 Hydrocarbon and fatty acid analysis

Chromatographic analysis was performed with a GC (Model 6890 series, Agilent Technologies, Palo Alto, CA), equipped with a mass detector Model 5973 (Agilent Technologies, Palo Alto, CA). Chromatography was conducted with a HP-5MS cross-linked (5%)-diphenyl-(95%)-dimethyl polysiloxane column (30 m length, 0.25 mm inner diameter) using helium as the carrier gas. The injection temperature was at 280 ℃. The oven temperature was initially at 200 ℃, was increased to 280 ℃ at a rate of 4 ℃/min, further increased to 320 ℃ at a rate of 20 ℃/min and held at this temperature for 3 min. Constituent peaks were identified by comparing to the

NIST library (http://www.sisweb.com/software/nist-gc-library.htm). To quantify hydrocarbon and fatty acid constituents, the response of the mass-spectrometer was calibrated to the internal standards, hexatriacontane and nonadecanoic acid respectively in each sample.

2.5 RNA isolation and RNA-seq Library Construction

RNA was extracted from frozen silk tissue using RNA^{TM} PureLink reagent according to manufacturer's instruction (Invitrogen). The crude RNA sample was treated with 2M $LiCl_2$ (Barlow et al. 1963) to remove DNA by precipitation, and RNA quality was tested using the Agilent 2100 Bioanalyzer and associated RNA 6000 Nano assay kit according to manufacturer's instructions.

RNA samples with RIN numbers >8.0 were used for cDNA library construction according to the protocol provided by Illumina, Inc. Poly(A) mRNA was first isolated from the RNA sample and then added to Dynal oligo(dT) beads (Invitrogen). The cDNA library was built by using the mRNA-seq sample preparation kit provided by Illumina, Inc according to manufacturer's guide.

2.6 Sequencing of cDNA library, alignment of reads from RNA-Seq and identification of genes with differential expression

Each cDNA sample was subjected to 75-bp pair-ended sequencing, which was performed by the Iowa State University DNA facility on a Genome Analyzer II system (Illumina). For each biological sample (i.e. encased or emerged silks), two biological replicates were subjected to Illumina sequencing.

The reads produced by the Ilumina Genome AnalyzerII system were first filtered by fastx toolkit (http://hannonlab.cshl.edu/fastx_toolkit/). In a read, all the bases having less than a quality score of 25 form the 3' end were trimmed. The artifact reads and reads less than 25 bases long or with less than 50 % of its bases with a quality score less than 25 after trimming, are removed. The filtered reads were mapped to the genome sequenced from maize inbred B73 (ZmB73_Ref_v2) with TopHat spliced read mapping software (Trapnell et al. 2009), using three different sets of criteria: (1) mapping to entire B73 genome; (2) mapping only to the working gene set, which contains sequences that a combination of evidence based genes and those predicted ab-initio by Fgenesh (Salamov and Solovyev 2000) on repeat-masked genome sequences. (3) mapping only to the filtered gene set, which is a subset of the working gene set, from which transposons, pseudogenes, contaminants, and low-confidence annotations were removed (http://gbrowse.maizegdb.org/gb2/gbrowse/maize_v2/?display_citation=Gene_models).

Insert size distribution of 200 +/- 100 and maximum intron size of 5000 for all the samples were used. All genes with at least 1 read mapping to them in at least one if the four samples, were used for downstream statistical analysis by cufflinks package. ~80-85 % of the reads mapped uniquely to the gene models and were quantified as Fragments per Kilo Base per Million Fragments (where a read-pair is defined as the Fragment) and analyzed to

identify differential expression (q-value < 0.05) using the Cufflinks package (Langmead et al. 2009).

2.7 Normalization and Statistical analysis

Pairwise comparison between hyper- and hypo- hydrocarbon accumulated maize silks were performed using the Bioconductor package DESeq (Anders and Huber 2010). The genes were thought to be differentially expressed with a <0.05 q-value, which is a corrected p-value for multiple tests by controlling the false discovery rate (FDR) for all analyses at 0.05% using Benjamini and Hochberg's method (Benjamini and Hochberg 1995).

All metabolite data were gathered from a minimum of five biological replicates. Metabolite abundances are the average of these multiple determinations (± standard error). Where appropriate, a student's t-test was conducted to determine whether the metabolite abundances are statistically different among samples.

2.8 Quantitative Real-Time PCR Analysis

To verify RNA-seq results, real-time PCR was conducted using SYBR green (Quanta Biosciences). Total RNA samples for RT-PCR analyses represented three biological replicates of B73 encased and emerged silks and were comparable to those used for the DGE library construction. A total of three technical replicates were run for each RNA sample per assay using Bio-Rad iCycler iQ real-time PCR detection system (Bio-Rad). The thermal cycling conditions were 50°C for 3 min (reverse transcription step), 95°C for 3

min (initial melt), and then 40 cycles of 94°C for 15 s and 60°C for 1 min. The linear dynamic range was determined using a standard curve generated from 1, 0.75, 0.5, 0.25 and 0.125 ng of RNA from three replicates in each assay. The reference genes, 18sRNA, actin and ubiquitin, were used as normalization controls. The primers used were listed in Supplemental Table 1.

2.9 Functional Categorization for differentially expressed genes

The assembled transcripts were assigned functions based on their sequence similarity to previously annotated sequences available in NCBI GenBank (Benson et al. 1993), Uniprot (Bairoch et al. 2005), Gene Ontology (Ashburner et al. 2000), KEGG (Kanehisa and Goto 2000), KOG (Tatusov et al. 2003) and BioCyc (http://biocyc.org/) databases. In addition, the TopGO (Alexa et al. 2006) R-package was used to identify GO terms enriched in maize silks.

3. **Results**

To understand the pathway(s) by which surface lipids are synthesized in maize silks, hydrocarbons and fatty acids were analyzed from encased and emerged silks that differentially express these lipids, and in parallel short-read transcriptome profiling was conducted to identify genes that are differentially expressed between these same silk samples.

Very long chain fatty acid and hydrocarbon accumulation differed markedly between encased and emerged maize silks.

As illustrated in Figure 1, both encased and emerged maize silks (harvested three days after first emerged from the husk leaves) produce alkenes (including $C_{25:2}$, $C_{25:1}$, $C_{27:2}$, $C_{27:1}$, $C_{29:2}$, $C_{29:1}$, $C_{31:2}$ and $C_{31:1}$), and odd-numbered alkanes (C_{23}, C_{25}, C_{27}, C_{29} and C_{31}). This observation is consistent with surface lipid accumulation previously characterized from the silks of several different maize inbreds (Miller et al. 2003; Perera et al. 2010b; Yang et al. 1992). In addition to odd-numbered hydrocarbons, however, small amounts (approximately 2% of total hydrocarbons) of even-numbered alkanes and alkenes including C_{24}, C_{28} and C_{30} were also detected, which has not been reported before.

Hydrocarbon accumulation in silks that had emerged from the husk leaves was approximately 2.5-fold higher than in silks that were still encased by the husk leaves (Fig 2). The accumulation of individual hydrocarbon constituents in emerged silks are up to 3-fold higher as compared to encased silks. These individual constituents fall into four major classes of hydrocarbons based on the level of saturation and the number of carbon atoms within the chain (e.g. even- or odd-numbered hydrocarbons; saturated or unsaturated hydrocarbons). This result is similar to a previous study that investigated the hydrocarbons as constituents of the surface lipids of the silks of the inbred B73 (Perera et al. 2010c). In this study that extracted hydrocarbons from the entire silk tissue samples of the same inbred indicate that the hydrocarbons are mainly composed of homologous series of alkanes, alkenes and dienes of

odd-number carbon atoms, ranging between 19 and 33 carbon atoms and the emerged silks produced around 2-3 fold more hydrocarbons as compared to encased silks (Perera et al. 2010c). Odd-numbered hydrocarbons (alkanes and alkenes) predominate in both emerged and encased silks, comprising approximately 98% of hydrocarbon constituents. In both encased and emerged silks, more alkanes were produced than alkenes. However, the emerged silk had higher relative abundances of alkene (~35%) as compare to encased silks (~25%) (Table 1). This might indicate that more fatty acids are desaturated to form alkenes in emerged silks than in encased silks. Also, the relative abundances of some individual constituents vary between emerged and encased tissues. For example, the relative abundance percentage of C_{24} alkane is higher in emerged silk (~1.27%) than in encased silk (~0.07%), whereas there is little difference in accumulation of other even-numbered hydrocarbons (e.g. C_{28} and C_{30} alkane and $C_{30:1}$ alkene) (Table 1).

Because the ultimate precursor of each hydrocarbon is thought to be a homologous fatty acids (Samuels et al. 2008b), the fatty acids were also analyzed in encased and emerged maize silk. Maize silks that had emerged and those that were still encased within the husk leaves mainly produced C_{14}, $C_{16:1}$, C_{16}, $C_{18:2}$, $C_{18:1}$ and C_{18} fatty acids, which are consistent with previous observations (Perera et al. 2010c). Different from the accumulation of hydrocarbons, which display a 2-3 fold difference between encased and emerged maize silks, the encased silks only produced ~10% more fatty acids

as compared to the emerged silks (Fig 2). In addition to total fatty acids, encased and emerged B73 silks have different amount of some individual fatty acids. C_{14} and $C_{18:2}$ fatty acids are ~15% higher in encased silks than emerged silks while other specific fatty acid constituents were more abundant in emerged silks, including an approximately 10% increase in the unsaturated fatty acids, $C_{16:1}$ and $C_{18:1}$ (Fig 3 and Table 2). The trienoic acid $C_{18:3}$, however was not observed, whereas a prior study found that two isoforms of this fatty acid comprised ~8% of the fatty acids in emerged B73 silks (Perera et al). Elongated VLCFAs (e.g., $C_{20:0}$, $C_{22:0}$ and $C_{24:0}$) were also not observed in this study, but was reported to comprise ~ 12.5% of the fatty acids of silks (Perera et al. 2010c). These differences of fatty acid composition might due to the fact that B73 was planted in different locations and in different years, which experienced different growth conditions.

Transcriptome analysis of encased and emerged silks

To ascertain genes that are differentially expressed between emerged and encased silks, and correlate these with the observed hydrocarbon and fatty acid differences in these tissues, comparative transcriptomic analyses were conducted between these two silk tissues. Emerged and encased silks for which hydrocarbon accumulation patterns were already characterized (see above) were subjected to transcriptome sequencing via Illumina technology. Between 11 to 15 million pairs of reads were obtained from each of the samples. Approximately 9 to 12 million reads were retained after quality

filtering by fastx (http://hannonlab.cshl.edu/fastx_toolkit/), and these were mapped to three different assemblies and annotations of the maize genome. These were the B73 reference genome (B73_RefGen_v2) (ftp.maizesequence.org), the Working Gene Set and the Filtered Gene Set. The criteria used to establish these latter two sets are described in the Materials and Methods.

By controlling the false discovery rate (FDR) at 0.05% and using Benjamini and Hochberg's method (Benjamini and Hochberg 1995), we identified 1104 genes that are expressed in both emerged and encased silks, but their levels of expression is different between the two tissue samples. Among these genes, ~2.4% (27 genes) are expressed at more than 10-fold higher levels in the emerged silks as compared to encased silks, and ~7.8% (86 genes) are expressed at more than 10-fold higher levels in the encased silks as compared to emerged silks. Moreover, ~0.5% (5 genes) and ~1.5% (17 genes) are expressed either only in the emerged or encased silks, respectively (Table 3).

To evaluate the reliability of our RNA-Seq results, we performed quantitative RT-PCR (qRT-PCR) on 10-targeted genes. These 10 genes can be classified into 4 categories: 1) genes that are highly expressed in emerged silks with known biochemical functions; e.g., acyl-CoA synthase gene; 2) genes expressed at the same level in encased and emerged silks with known

function; e.g., the *glossy1* gene; 3) genes highly expressed in encased silks with known function; e.g., a cytochrome P450 gene and the *senescence15* gene; and 4) four genes of unknown functions, one highly expressed in emerged silks, one highly expressed in encased silks, and two with similar expression level between the encased and emerged silks. Among these 10 genes that were evaluated, the expression patterns of 8 of them agreed very well between the mRNA-Seq and qRT-PCR datasets (Table 4). The results for two of the test-genes, GRMZM2G077375_T01 (which encodes a wax synthase) and GRMZM2G167438_T03 (which encodes 3-ketoacyl CoA synthase), disagree between the mRNA-Seq and qRT-PCR assays (Table 4). The wax synthase gene (GRMZM2G077375_T01) cannot be detected by mRNA-Seq, but can be detected by qRT-PCR. Thus, the disagreement might be caused by the low expression level of the wax synthase gene in these silk samples. In the case of the 3-ketoacyl synthase gene, the discrepancy may be due to the fact that there are 24 paralogs for this enzyme in the B73 maize sequence. Hence, some reads in the mRNA-Seq data may have mapped to more than one 3-ketoacyl synthase paralog, and this would make it difficult for the Cufflinks algorithm to map those reads to the correct paralog, producing inconsistent expression values.

The rationale for the transcriptome sequencing experiment is to correlate changes in gene expression with changes in hydrocarbon accumulation. However, alternative signals may be the causes of differential

gene expression between encased and emerged silks, and these include: (1) exposure to pathogens (e.g., fungi, insects) on the emerged silks; (2) the desiccation of the emerged silks; (3) developmental factors; (4) exposure to sunlight and/or UV. We therefore explored our dataset to not only identify genes involved in lipid biosynthesis, but also genes involving in these other factors, such as defense response to exogenous pathogens, prevention of water-loss and exposure to UV/light. The enrichment patterns for genes differentially expressed between encased and emerged silks were listed in Table 5. In this chapter we focused only on differentially expressed genes involved in lipid biosynthesis.

Differential expression of genes involved in fatty acid initiation (Alrefai et al.) and synthesis (FAS) between encased and emerged maize silks

Fatty acids are the presumed precursors that are utilized for the biosynthesis of hydrocarbons. Multiple processes are required to generate the VLCFAs that are the precursors of the hydrocarbons. These include plastid-localized *de novo* fatty acid synthesis and ER-localized fatty acid elongation. The former process can be further dissected into fatty acid initiation (FAI) and fatty acid synthesis (FAS). As indicated in Figure 4, FAI encompasses three enzymatic reactions, acetyl-CoA carboxylase (ACCase), malonyl-CoA transacylase and β-ketoacyl-ACP synthase. Our mRNA-Seq data identified evidence for the expression of 6, 1, and 1 transcripts, respectively, of these enzymes (MaizeCyc;

pathway.gramene.org/MAIZE/NEW-IMAGE?type=NIL&object=PWY-4381&redirect=T). Two of the plastid-located ACCase transcripts, (GRMZM5G858094_T02 and GRMZM2G377341_T01), express two fold higher in emerged silks as compared to encased silks, while the other four transcripts have similar expression levels between the encased and emerged maize silks (Fig. 4, Supplemental Table 2). The higher levels of ACCase expression in the emerged silks is consistent with the many studies that have indicated that this enzyme plays a critical role in controlling the rate of fatty acid synthesis (Ohlrogge and Jaworski 1997), and thus correlates with fatty acid accumulation levels in the silks.

Fatty acid synthesis is an iterative process catalyzed by four enzymes that generate 16- and 18-carbon fatty acids: 3-ketoacyl-ACP synthase (Ashburner et al.), 3-ketoacyl-ACP reductase (KAR), hydroxyacyl ACP dehydratase (Schneider-Belhaddad and Kolattukudy) and enoyl ACP reductase (EAR) (Fig 5). The maize genome contains 8, 11, 4 and 3 gene for KAS, KAR, HAD and EAR, respectively (Supplemental Table 3). Four KAS transcripts are present in maize silks and one of the transcripts (GRMZM2G072205_T01) has a two-fold higher expression in emerged silks than encased silks whereas another transcript (GRMZM2G569948_T01) is opposite, and the other two transcripts (shown in normal font in Fig 5) don't show significant differential expression between encased and emerged silks. Ten KAR transcripts, 3 HAD transcripts and 2 EAR transcripts are present in

silks, but they do not show differential expression between the encased and emerged silks (Fig 5 and Supplemental Table 3).

Key fatty acid elongation pathway genes

Fatty acid elongation (FAE) occurs in the membranes of the endoplasmic reticulum (ER), in a manner analogous to *de novo* fatty acid biosynthesis (Stumpf, 1984, von Wettstein-Knowles, 1995). However, in contrast to FAS, which uses ACP to carry the intermediates of the process, FAE utilizes CoA to carry the intermediates. The FAE cycle is composed of iterations of 4 reaction, each catalyzed by ketoacyl-CoA synthase (KCS), 3-ketoacyl CoA reductase (KCR), 3-hydroxyl CoA dehydrotase (HCD) and enoyl-CoA reductase (ECR) (Fig. 6). The maize genome contains 25, 5, 14 and 6 transcripts, respectively, for KCS, KCR, HCD and ECR (Fig 6 and Supplemental Table 4). Among them, 18, 2, 6 and 4 transcripts, respectively for KCS, KCR, HCD and ECR, are expressed in maize silks (Fig 6 and Supplemental Table 4).

KCS catalyzes the condensation reaction in FAE that generates a new carbon-carbon bond as the acyl-chain is elongated (Millar and Kunst 1997). Among the 18 KCS transcripts that are expressed in maize silks, 12 transcripts (identified in normal font in Fig 6) have similar expression patterns between the encased and emerged silks, 3 transcripts (GRMZM2G167438_T01, GRMZM2G137694_T01 and GRMZM2G445602_T01) are highly expressed in emerged maize silks, and 3 transcripts (GRMZM2G151476_T01,

GRMZM2G149636_T01 and GRMZM2G104626_T01) are highly expressed in encased silks (Fig 6 and Supplemental Table 4). The transcripts that encode the 3 other enzymes needed for fatty acid elongation (namely, KCR, HCD and ECR) are expressed at similar levels in both encased and emerged silks (q-value>0.05) (Fig 6 and Supplemental Table 4).

In addition to the reiterative cycle of FAE, the pathway that provides the cytosolic malonyl-CoA needed for FAE was also investigated. This two-reaction pathway requires is sequential reactions catalyzed by ATP-citrate lyase (ACL) (Fatland et al. 2005) and the cytosolic isozyme of ACCase (Yanai et al. 1995) (Fig 6). There are 10 and 5 transcripts for ACL and cytosol-located ACCase present in emerged silks respectively (Fig 6). Among the 10 ACL transcripts, 2 transcripts, (GRMZM2G002416_T01 and GRMZM2G107082_T01), have a twofold expression difference between emerged silks and encased silks, and the other 8 (indicated by the normal font in Fig 6) are not significantly expressed at differential levels between encased and emerged silks. Among the 5 ACCase transcripts, one transcript (GRMZM2G377341) is highly expressed in emerged silks, one (AC197672.3_FG002) has the same expression level between encased and emerged silks while the other 3 transcripts (GRMZM5G854500_T01, GRMZM2G375116_T01 and GRMZM2G375116_T02) are highly expressed in the encased silks (Fig 6).

Desaturases affecting degree of unsaturation in fatty acids and hydrocarbons

We examined the expression of fatty acid desaturases, which generate the unsaturated fatty acids needed for the biosynthesis of alkenes and dienes, which account for a large portion of the hydrocarbon fraction of silks. Homologs to desaturases in Arabidopsis (Supplemental Table 5) were investigated. There are 26 desaturase transcripts in B73 maize genome. Among them, 20 are present in maize silks and14 of these transcripts (identified in normal in Table 6) have similar expression levels between the encased and emerged silks. However, 6 transcripts (GRMZM5G883417_T01, GRMZM2G078569_T04, GRMZM2G056252_T05, GRMZM2G128971_T03, GRMZM2G074401_T01 and GRMZM2G128971_T01) are differentially expressed between encased and emerged maize silks (Table 6). Among these 6 differentially expressed transcripts, two of them that encode stearoyl-ACP desaturase (GRMZM5G883417_T01), and plastidial oleate desaturase (GRMZM2G078569_T04), are expressed to higher levels in emerged silks. The other 4 desaturase transcripts encode 1) fatty acid desaturase 1 (GRMZM2G056252_T05) 2) ER-located oleate desaturase (GRMZM2G128971_T03); 3) plastidial-located linoleate desaturase (GRMZM2G074401_T01 and GRMZM2G128971_T01), and all of these transcripts accumulate at higher levels in the encased silks (Table 6).

Key genes affecting surface lipids

By taking advantage of the knowledge gained from Arabidopsis research, we identified 90 genes that are predicted to be involved in surface lipid biosynthesis in Arabidopsis (http://aralip.plantbiology.msu.edu/enzymes). These include genes involved in generating precursors for fatty acid elongation, FAE pathways, desaturase genes, genes involved in lipid metabolism, trafficking and transportation, and cuticular lipid biosynthesis (Supplemental Table 6).

Using BLAST, homologs of these genes were identified in the silks transcriptome data. This analysis identified a set of 30 genes that exhibit differential expression between encased and emerged silks and share >70% sequence similarity with the Arabidopsis homologs (Supplemental Table 6). This list of transcripts in maize encode a diverse set of enzymes (Table 7), including: 1) ATP citrate lyase (ACL) which generates precursor acetyl-CoA for FAE (Fatland et al. 2005); 2) acetyl-CoA carboxylase (ACCase), which converts acetyl-CoA to malonyl-CoA; 3) Enzymes involved in FAS and FAE; 4) homologs to *CER1*; 5) fatty acid reductase; and 6) fatty acid hydroxylase superfamily. Among these, ACL, ACCase and enzymes involved in FAS and FAE have been discussed previously.

In Arabidopsis, CER1/CER3 appear to form a complex to catalyze the conversion of fatty acids to alkanes (Bernard et al. 2012b). A homolog of the Arabidopsis CER1 gene (GRMZM2G062151_T01) shows ~7 fold higher

expression in emerged silks than encased silks, whereas another homolog of CER1 (GRMZM2G099097_T03) display a ~6 fold higher expression in encased silks as compared to emerged silks. However, no homologs of CER3 was found to be differentially expressed between the two silk samples. Instead, two homologs to fatty acid reductase (GRMZM2G173387_T05 and GRMZM2G020500_T02) show 2- and 6-fold expression differences between emerged silks as compared to encased silks. The fatty acid reductase reduces fatty acyl CoA to a fatty aldehyde and then in a second reduction to a fatty alcohol (Doan et al. 2012); the fatty aldehyde could be used as the precursor for hydrocarbon biosynthesis. In addition, two transcripts (GRMZM2G099097_T03 and GRMZM2G099097_T04) that encode enzymes belonging to the fatty acid hydroxylase superfamily are also differentially expressed between encased and emerged silks. One (GRMZM2G099097_T03) of these is expressed only in emerged silks, while the other transcript (GRMZM2G099097_T04) is expressed 5-fold higher in encased silks than in emerged silks (Table 7).

Identification of genes of extreme differential expression pattern between encased and emerged silks

A pool of genes has been identified that are differentially expressed between the emerged and encased silks (Table 3). Nearly 400 genes are expressed at >2-fold higher expression levels in emerged silks as compared to encased silks, and nearly 700 genes show the opposite expression pattern, being at a higher level in encased silks. The top 20 genes that are most

highly expressed in encased maize silks or most highly expressed in emerged silks are listed in Table 8.

Among the top 20 genes highly expressed in emerged silks, five gene only present in emerged silks and the ratio of transcript abundance between emerged and encased silks for the other 15 genes range from 11-fold to 466-fold. Two transcripts (GRMZM2G141325 and GRMZM2G057027) are annotated as being involved in response to freezing, three transcripts (GRMZM2G016890, GRMZM5G882852 and GRMZM5G828987) in carbohydrate metabolic process and eight transcripts (GRMZM2G384780, GRMZM2G478414, GRMZM2G003368, GRMZM2G158205, GRMZM5G898755, GRMZM2G104847, GRMZM5G812228 and GRMZM2G167438) in lipid metabolism. One transcript (GRMZM2G105335) encodes a growth regulating factor, one transcript (GRMZM2G147051) encodes a protein kinase and the other five transcripts (GRMZM2G019586, GRMZM2G090744, GRMZM2G001223, GRMZM2G160541 and GRMZM2G046070) encode proteins with unknown function (Table 8).

Among the top 20 genes highly expressed in encased silks, 17 genes are only present in encased silks and the ratio of transcript abundance between emerged and encased silks for the other 3 genes range from 63-fold to 909-fold. Twelve transcripts encode proteins with unknown function. One transcript (GRMZM2G007012), one transcript (GRMZM2G083841), one

transcript (GRMZM2G339091), one transcript (GRMZM2G374302), one transcript (GRMZM2G355752), one transcript (GRMZM2G099678), one transcript (GRMZM2G163054) and one transcript (GRMZM2G050076) encodes glucosyltransferase, phosphoenolpyruvate carboxylase, serine-type carboxypeptidase, arginine decarboxylase, early light-induced protein, vegetative storage protein, transcription factor and a protein involved in steroid biosynthetic process respectively. All the other 12 transcripts in table 8 under the category of top 20 genes highly expressed in encased silks encode protein with unknown function (Table 8).

Discussion

In this study we compared the accumulation of hydrocarbons and their fatty acid precursors to the global transcript expression patterns between the encased and emerged silks. This comparison revealed a number of new insights regarding global regulation of genes involved in lipid biosynthesis in maize.

The higher accumulation of hydrocarbon lipids in emerged silks is associated with increased gene expression for key enzymes in FAI, FAS, FAE and surface lipid biosynthesis. Two ACCase transcripts (GRMZM2G377341_T01 and GRMZM5G858094_T01), one KAS transcript (GRMZM2G072205_T01) in FAS are expressed at higher levels in emerged silks. Two ACL transcripts (GRMZM2G002416_T01 and GRMZM2G10708_T01) and one ACCase transcript (GRMZM2G377341), providing acetyl-CoA and

malonyl-CoA primers for FAE, 3 KCS transcripts (GRMZM2G167438_T01, GRMZM2G137694_T01 and GRMZM2G445602_T01), encoding the chain elongation function of FAE, one transcript homologous to *CER1* (GRMZM2G062151_T01), encoding the aldehyde decarbonylase in Arabidopsis are also expressed at higher levels in emerged silks. Taken together, these findings implicate that during silk emergence there is programmed higher expression of certain genes that can support the generation of elevated levels of VLCFAs, which can be utilized to synthesize hydrocarbons that accumulate at higher levels in the emerged silks. The fact that VLCFAs do not accumulate in this organ suggests that these intermediates are efficiently converted to hydrocarbons immediately after they are produced, and thus only very small amount of VLCFAs are present in silks.

In maize many of the enzymes that are involved in the production of hydrocarbons are encoded by gene families, for example ACCase, KAS and KCS. It's interesting to note that a subgroup of these paralogs are associated with the higher accumulation of hydrocarbons in emerged silks, whereas alternative paralogs (3 for ACCase: GRMZM5G854500_T01, GRMZM2G375116_T01 and GRMZM2G375116_T02; 1 for KAS: GRMZM2G569948_T01 and 3 for KCS: GRMZM2G151476_T01, GRMZM2G149636_T01 and GRMZM2G104626_T01) are expressed at higher levels in the encased silks that accumulate lower levels of hydrocarbons. This indicates that different isoforms of these enzymes, encoded by different

paralogs/transcripts are differentially expressed between encased and emerged silks. A possible explanation for these phenomena may be that different isoforms perform the same general function, but possibly with different substrate specificities. For example, different KCS isoforms may be responsible for elongating fatty acyl-CoAs of different chain-lengths. The variety of VLCFA chain lengths and degree of saturation/unsaturation indicate that KCS enzymes with different substrate specificities and expression patterns may be needed in FAE.

The relatively high abundance of unsaturated hydrocarbons in emerged silks is related to the high expression of fatty acid desaturases. Consistent with the finding that alkenes that have a double bond at the 9th position are higher in emerged silks than encased silks (Perera et al. 2010c), we found that a stearoyl-ACP desaturase transcript (GRMZM5G883417_T01), which introduces a double bond in the 9th position of 18:0 to produce 18:1 (Shanklin and Somerville 1991), is expressed at two-fold higher levels in emerged silks as compared to encased silks. In addition, a transcript (GRMZM2G078569_T04) encoding plastidial oleate desaturase is highly expressed in emerged silks. In contrast, two plastidial linoleate desaturase transcripts (GRMZM2G074401_T01 and GRMZM2G128971_T01), an ER-located oleate desaturase (fad2) transcript (GRMZM2G128971_T03) along with the FAD1 transcript (GRMZM2G056252_T05) are highly expressed in encase silks.

These latter desaturases that are expressed at higher levels in encased silks are involved in glycerolipid metabolism (Hernandez et al. 2008) and may not be directly involved in surface lipid biosynthesis.

Reference

Alexa A, Rahnenfuhrer J, Lengauer T (2006) Improved scoring of functional groups from gene expression data by decorrelating GO graph structure. Bioinformatics 22:1600-1607

Alrefai R, Berke TG, Rocheford TR (1995) Quantitative Trait Locus Analysis of Fatty-Acid Concentrations in Maize. Genome 38:894-901

Anders S, Huber W (2010) Differential expression analysis for sequence count data. Genome Biol 11

Ashburner M, Ball CA, Blake JA, Botstein D, Butler H, Cherry JM, Davis AP, Dolinski K, Dwight SS, Eppig JT, Harris MA, Hill DP, Issel-Tarver L, Kasarskis A, Lewis S, Matese JC, Richardson JE, Ringwald M, Rubin GM, Sherlock G, Consortium GO (2000) Gene Ontology: tool for the unification of biology. Nature Genetics 25:25-29

Bairoch A, Apweiler R, Wu CH, Barker WC, Boeckmann B, Ferro S, Gasteiger E, Huang HZ, Lopez R, Magrane M, Martin MJ, Natale DA, O'Donovan C, Redaschi N, Yeh LSL (2005) The universal protein resource (UniProt). Nucleic Acids Res 33:D154-D159

Barlow JJ, Mathias AP, Williamson R, Gammack DB (1963) A Simple Method for the Quantitative Isolation of Undegraded High Molecular Weight Ribonucleic Acid. Biochem Biophys Res Commun 13:61-66

Benjamini Y, Hochberg Y (1995) Controlling the False Discovery Rate - a Practical and Powerful Approach to Multiple Testing. J Roy Stat Soc B Met 57:289-300

Benson D, Lipman DJ, Ostell J (1993) Genbank. Nucleic Acids Res 21:2963-2965

Bernard A, Domergue F, Pascal S, Jetter R, Renne C, Faure JD, Haslam RP, Napier JA, Lessire R, Joubes J (2012) Reconstitution of Plant Alkane Biosynthesis in Yeast Demonstrates That Arabidopsis ECERIFERUM1 and ECERIFERUM3 Are Core Components of a Very-Long-Chain Alkane Synthesis Complex. Plant Cell 24:3106-3118

Bianchi G, Murelli C, Ottaviano E (1990) Maize Pollen Lipids. Phytochemistry 29:739-744

Doan TTP, Domergue F, Fournier AE, Vishwanath SJ, Rowland O, Moreau P, Wood CC, Carlsson AS, Hamberg M, Hofvander P (2012) Biochemical characterization of a chloroplast localized fatty acid reductase from Arabidopsis thaliana. Bba-Mol Cell Biol L 1821:1244-1255

Fatland BL, Nikolau BJ, Wurtele ES (2005) Reverse genetic characterization of cytosolic acetyl-CoA generation by ATP-citrate lyase in Arabidopsis. Plant Cell 17:182-203

Greene MJ, Gordon DM (2003) Social insects - Cuticular hydrocarbons inform task decisions. Nature 423:32-32

Han J, Calvin M (1969) Hydrocarbon Distribution of Algae and Bacteria, and Microbiological Activity in Sediments. P Natl Acad Sci USA 64:436-&

Hernandez ML, Guschina IA, Martinez-Rivas JM, Mancha M, Harwood JL (2008) The utilization and desaturation of oleate and linoleate during glycerolipid biosynthesis in olive (Olea europaea L.) callus cultures. J Exp Bot 59:2425-2435

Kanehisa M, Goto S (2000) KEGG: Kyoto Encyclopedia of Genes and Genomes. Nucleic Acids Res 28:27-30

Kunst L, Samuels AL (2003) Biosynthesis and secretion of plant cuticular wax. Progress in Lipid Research 42:51-80

Kunst L, Samuels L (2009) Plant cuticles shine: advances in wax biosynthesis and export. Curr Opin Plant Biol 12:721-727

Langmead B, Trapnell C, Pop M, Salzberg SL (2009) Ultrafast and memory-efficient alignment of short DNA sequences to the human genome. Genome Biol 10

Millar AA, Kunst L (1997) Very-long-chain fatty acid biosynthesis is controlled through the expression and specificity of the condensing enzyme. Plant J 12:121-131

Miller SS, Reid LM, Butler G, Winter SP, McGoldrick NJ (2003) Long chain Alkanes in silk extracts of maize genotypes with varying resistance to Fusarium graminearum. J Agr Food Chem 51:6702-6708

Miwa TK (1971) Jojoba Oil Wax Esters and Derived Fatty Acids and Alcohols - Gas Chromatographic Analyses. J Am Oil Chem Soc 48:259-&

Ohlrogge JB, Jaworski JG (1997) Regulation of fatty acid synthesis. Annu Rev Plant Phys 48:109-136

Park MO (2005) New pathway for long-chain n-alkane synthesis via 1-alcohol in Vibrio furnissii M1. J Bacteriol 187:1426-1429

Perera MA (2005) Molecular and chemical characterization of genes involved in maize cuticular wax biosynthesis. Dissertation, Iowa State University

Perera MA, Qin W, Yandeau-Nelson M, Fan L, Dixon P, Nikolau BJ (2010a) Biological origins of normal-chain hydrocarbons: a pathway model based on cuticular wax analyses of maize silks. Plant J 64:618-632

Perera MADN, Qin WM, Yandeau-Nelson M, Fan L, Dixon P, Nikolau BJ (2010b) Biological origins of normal-chain hydrocarbons: a pathway model based on cuticular wax analyses of maize silks. Plant J 64:618-632

Post-Beittenmiller D (1998) The cloned Eceriferum genes of Arabidopsis and the corresponding Glossy genes in maize. Plant Physiol Bioch 36:157-166

PostBeittenmiller D (1996) Biochemistry and molecular biology of wax production in plants. Annu Rev Plant Phys 47:405-430

Salamov AA, Solovyev VV (2000) Ab initio gene finding in Drosophila genomic DNA. Genome Res 10:516-522

Samuels L, Kunst L, Jetter R (2008a) Sealing plant surfaces: cuticular wax formation by epidermal cells. Annu Rev Plant Biol 59:683-707

Samuels L, Kunst L, Jetter R (2008b) Sealing plant surfaces: Cuticular wax formation by epidermal cells. Annu Rev Plant Biol 59:683-707

Shanklin J, Somerville C (1991) Stearoyl-Acyl-Carrier-Protein Desaturase from Higher-Plants Is Structurally Unrelated to the Animal and Fungal Homologs. P Natl Acad Sci USA 88:2510-2514

Tatusov RL, Fedorova ND, Jackson JD, Jacobs AR, Kiryutin B, Koonin EV, Krylov DM, Mazumder R, Mekhedov SL, Nikolskaya AN, Rao BS, Smirnov S, Sverdlov AV, Vasudevan S, Wolf YI, Yin JJ, Natale DA (2003) The COG database: an updated version includes eukaryotes. Bmc Bioinformatics 4

Tornabene TG (1982) Microorganisms as Hydrocarbon Producers. Experientia 38:43-46

Trapnell C, Pachter L, Salzberg SL (2009) TopHat: discovering splice junctions with RNA-Seq. Bioinformatics 25:1105-1111

Wackett LP, Frias JA, Seffernick JL, Sukovich DJ, Cameron SM (2007) Genomic and biochemical studies demonstrating the absence of an alkane-producing phenotype in Vibrio furnissii M1. Appl Environ Microb 73:7192-7198

Xu XJ, Dietrich CR, Delledonne M, Xia YJ, Wen TJ, Robertson DS, Nikolau BJ, Schnable PS (1997) Sequence analysis of the cloned glossy8 gene of maize suggests that it may code for a beta-ketoacyl reductase required for the biosynthesis of cuticular waxes. Plant Physiology 115:501-510

Yanai Y, Kawasaki T, Shimada H, Wurtele ES, Nikolau BJ, Ichikawa N (1995) Genomic Organization of 251 Kda Acetyl-Coa Carboxylase Genes in Arabidopsis - Tandem Gene Duplication Has Made 2 Differentially Expressed Isozymes. Plant Cell Physiol 36:779-787

Yang G, Wiseman BR, Espelie KE (1992) Cuticular Lipids from Silks of 7 Corn Genotypes and Their Effect on Development of Corn-Earworm Larvae [Helicoverpa-Zea (Boddie)]. J Agr Food Chem 40:1058-1061

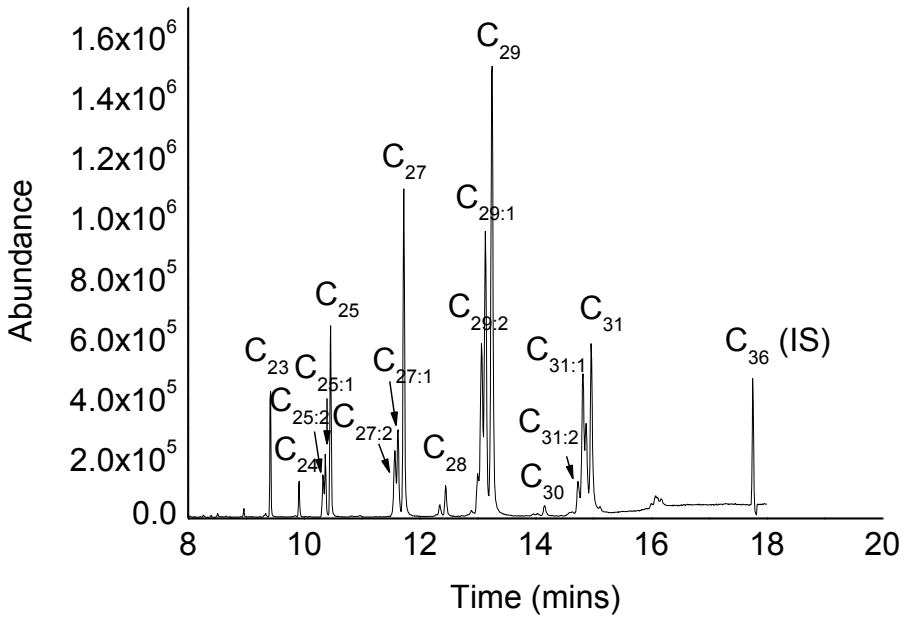

Figure 1. Gas chromatograph of B73 emerged maize silks

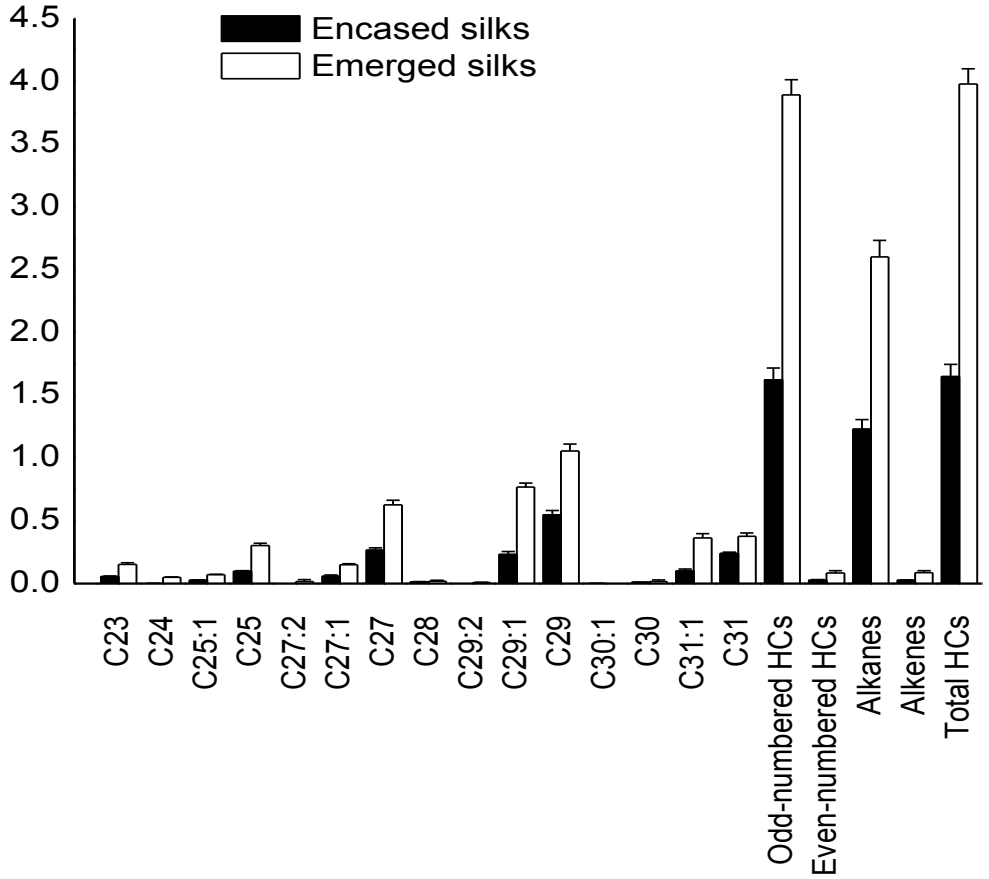

Figure 2. Hydrocarbons in emerged and encased maize silks

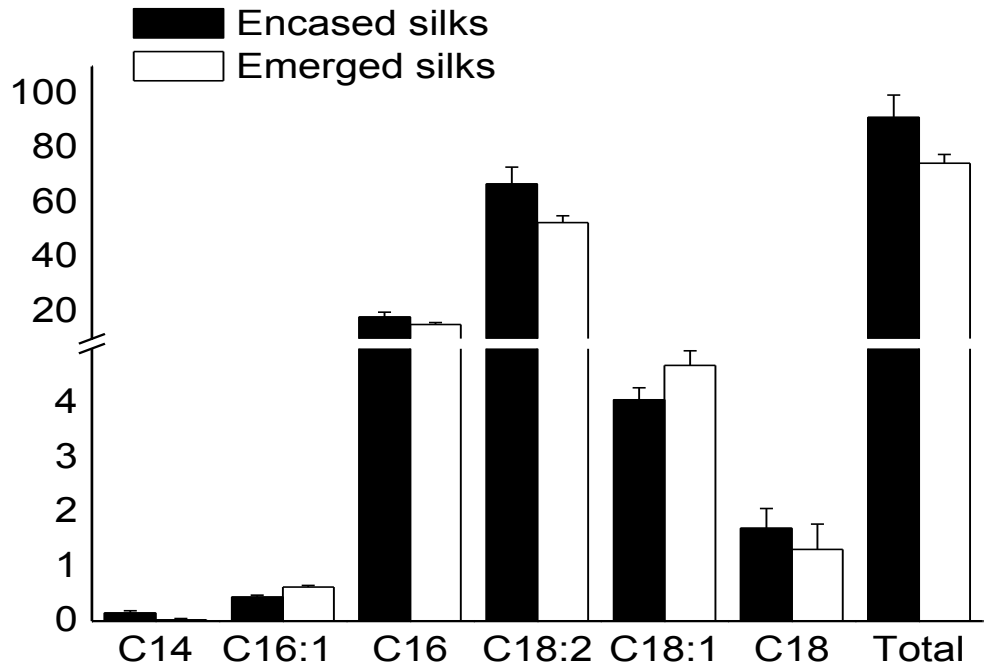

Figure 3. Fatty acids in emerged and encased maize silks

Gene ID for ACCase	Emerged/Encased	q-value
GRMZM2G377341_T01	**3.27**	**5.E-05**
GRMZM5G858094_T02	**2.56**	**2.E-03**
GRMZM2G308860_T01	2.51	0.40
GRMZM5G858094_T01	1.86	0.95
GRMZM2G308860_T02	1.03	1.11
GRMZM5G890665_T02	0.39	0.37

Gene ID for MAT	Emerged/Encased	q-value
GRMZM2G029543	1.20	0.92

Gene ID for KAS	Emerged/Encased	q-value
GRMZM2G003190	0.55	0.99

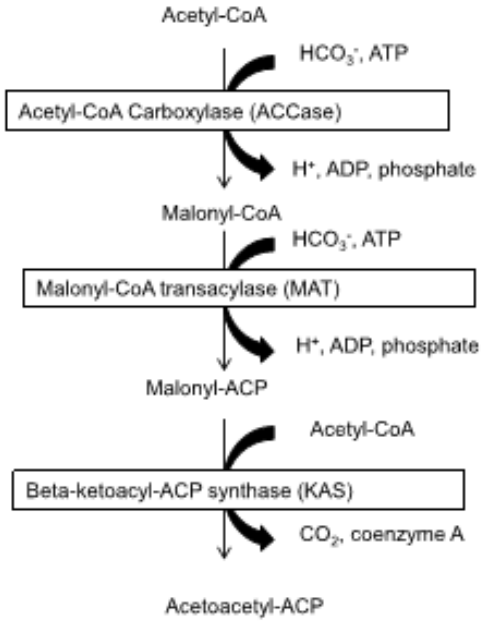

Figure 4. Key enzymes involved in fatty acid synthesis initiation

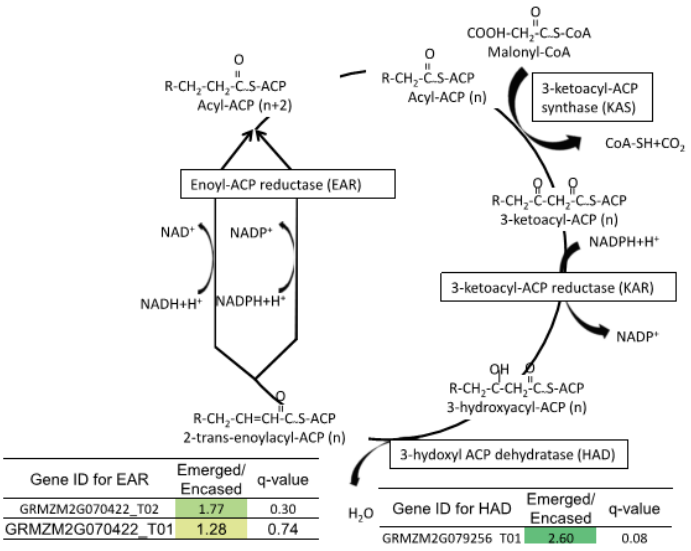

Gene ID for KAS	Emerged/Encased	q-value
GRMZM2G072205_T01	**2.55**	**0.01**
GRMZM2G012863_T02	2.53	0.85
GRMZM2G380650_T02	0.92	1.09
GRMZM2G569948_T01	*0.41*	*0.01*

Gene ID for KAR	Emerged/ Encased	q-value
GRMZM2G043602_01	2.99	0.22
GRMZM2G027059_T01	1.33	1.10
GRMZM2G152105_T01	1.32	0.67
GRMZM2G099696_T01	1.03	1.11
GRMZM2G075140_T01	0.91	1.07
AC233893.1_FGT003	0.84	1.00
GRMZM2G135498_T01	0.80	0.99
GRMZM2G124335_T02	0.78	0.76
GRMZM2G152105_T02	0.65	0.70
GRMZM2G451861_T01	0.60	0.20

Gene ID for EAR	Emerged/ Encased	q-value
GRMZM2G070422_T02	1.77	0.30
GRMZM2G070422_T01	1.28	0.74

Gene ID for HAD	Emerged/ Encased	q-value
GRMZM2G079256_T01	2.60	0.08

Figure 5. Key enzymes involved in fatty acid syntheses

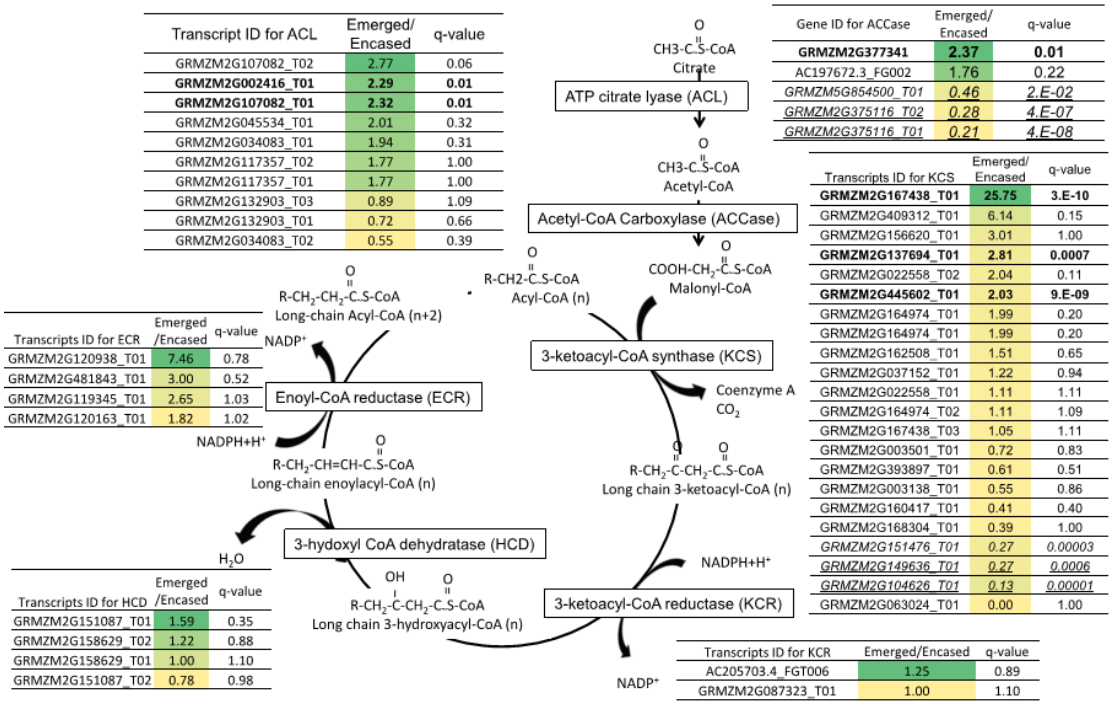

Transcript ID for ACL	Emerged/ Encased	q-value
GRMZM2G107082_T02	2.77	0.06
GRMZM2G002416_T01	**2.29**	**0.01**
GRMZM2G107082_T01	**2.32**	**0.01**
GRMZM2G045534_T01	2.01	0.32
GRMZM2G034083_T01	1.94	0.31
GRMZM2G117357_T02	1.77	1.00
GRMZM2G117357_T01	1.77	1.00
GRMZM2G132903_T03	0.89	1.09
GRMZM2G132903_T01	0.72	0.66
GRMZM2G034083_T02	0.55	0.39

Gene ID for ACCase	Emerged/ Encased	q-value
GRMZM2G377341	**2.37**	**0.01**
AC197672.3_FG002	1.76	0.22
GRMZM5G854500_T01	*0.46*	*2.E-02*
GRMZM2G375116_T02	*0.28*	*4.E-07*
GRMZM2G375116_T01	*0.21*	*4.E-08*

Transcripts ID for KCS	Emerged/ Encased	q-value
GRMZM2G167438_T01	**25.75**	**3.E-10**
GRMZM2G409312_T01	6.14	0.15
GRMZM2G156620_T01	3.01	1.00
GRMZM2G137694_T01	**2.81**	**0.0007**
GRMZM2G022558_T02	2.04	0.11
GRMZM2G445602_T01	**2.03**	**9.E-09**
GRMZM2G164974_T01	1.99	0.20
GRMZM2G164974_T01	1.99	0.20
GRMZM2G162508_T01	1.51	0.65
GRMZM2G037152_T01	1.22	0.94
GRMZM2G022558_T01	1.11	1.11
GRMZM2G164974_T02	1.11	1.09
GRMZM2G167438_T03	1.05	1.11
GRMZM2G003501_T01	0.72	0.83
GRMZM2G393897_T01	0.61	0.51
GRMZM2G003138_T01	0.55	0.86
GRMZM2G160417_T01	0.41	0.40
GRMZM2G168304_T01	0.39	1.00
GRMZM2G151476_T01	*0.27*	*0.00003*
GRMZM2G149636_T01	*0.27*	*0.0006*
GRMZM2G104626_T01	*0.13*	*0.00001*
GRMZM2G063024_T01	0.00	1.00

Transcripts ID for ECR	Emerged /Encased	q-value
GRMZM2G120938_T01	7.46	0.78
GRMZM2G481843_T01	3.00	0.52
GRMZM2G119345_T01	2.65	1.03
GRMZM2G120163_T01	1.82	1.02

Transcripts ID for HCD	Emerged /Encased	q-value
GRMZM2G151087_T01	1.59	0.35
GRMZM2G158629_T02	1.22	0.88
GRMZM2G158629_T01	1.00	1.10
GRMZM2G151087_T02	0.78	0.98

Transcripts ID for KCR	Emerged/Encased	q-value
AC205703.4_FGT006	1.25	0.89
GRMZM2G087323_T01	1.00	1.10

Figure 6. Key enzymes involved in fatty acid elongation

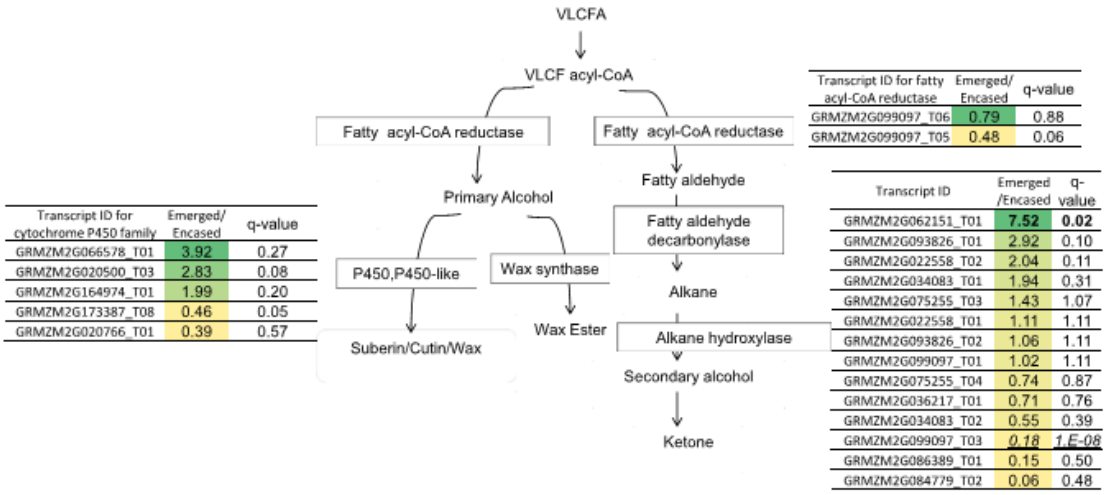

Transcript ID for cytochrome P450 family	Emerged/ Encased	q-value
GRMZM2G066578_T01	3.92	0.27
GRMZM2G020500_T03	2.83	0.08
GRMZM2G164974_T01	1.99	0.20
GRMZM2G173387_T08	0.46	0.05
GRMZM2G020766_T01	0.39	0.57

Transcript ID for fatty acyl-CoA reductase	Emerged/ Encased	q-value
GRMZM2G099097_T06	0.79	0.88
GRMZM2G099097_T05	0.48	0.06

Transcript ID	Emerged /Encased	q-value
GRMZM2G062151_T01	**7.52**	**0.02**
GRMZM2G093826_T01	2.92	0.10
GRMZM2G022558_T02	2.04	0.11
GRMZM2G034083_T01	1.94	0.31
GRMZM2G075255_T03	1.43	1.07
GRMZM2G022558_T01	1.11	1.11
GRMZM2G093826_T02	1.06	1.11
GRMZM2G099097_T01	1.02	1.11
GRMZM2G075255_T04	0.74	0.87
GRMZM2G036217_T01	0.71	0.76
GRMZM2G034083_T02	0.55	0.39
GRMZM2G099097_T03	*0.18*	*1.E-08*
GRMZM2G086389_T01	0.15	0.50
GRMZM2G084779_T02	0.06	0.48

Figure 7. Key enzymes involved in surface lipids biosynthesis

Table 1. Relative abundances of hydrocarbons in emerged and encased maize silks

	Encased	Emerged	p-value for T-test
C23	3.5%±0.3%	3.8%±0.3%	0.47
C24	**0.07%±0.07%**	**1.27%±0.04%**	**0.00001**
C25:1	1.6%±0.3%	1.79%±0.08%	0.52
C25	**5.9%±0.1%**	**7.6%±0.3%**	**0.005**
C27:2	0.005%±0.001%	0.4%±0.4%	0.39
C27:1	3.4%±0.5%	3.8%±0.2%	0.56
C27	16.1%±0.3%	15.7%±0.5%	0.53
C28	0.7%±0.2%	0.5%±0.2%	0.42
C29:2	0.008%±0.002%	0.2%±0.1%	0.19
C29:1	**14%±1%**	**19%±1%**	**0.01**
C29	**33%±1%**	**26.5%±0.6%**	**0.0002**
C30:1	0.08%±0.08%	0.009%±0.004%	0.37
C30	0.66%±0.05%	0.4%±0.4%	0.56
C31:1	**6%±1%**	**9%±1%**	**0.04**
C31	**14.5%±0.3%**	**9.4%±0.5%**	**0.0002**
Odd-numbered HCs	98.5%±0.2%	97.8%±0.5%	0.29
Even-numbered HCs	1.5%±0.2%	2.2%±0.5%	0.29
Alkanes	**75%±1%**	**65%±1%**	**0.002**
Alkenes	**25%±1%**	**35%±1%**	**0.002**

Table 2. Relative abundances of fatty acids in emerged and encased maize silks

Fatty acids	Encased	Emerged	p-value
C_{14}	0.16%±0.03%	0.07%±0.04%	0.14
$C_{16:1}$	**0.50%±0.06%**	**0.84%±0.04%**	**0.002**
C_{16}	19.8%±0.6%	20.3%±0.3%	0.48
$C_{18:2}$	**73.23%±0.8%**	**70.6%±0.6%**	**0.04**
$C_{18:1}$	**4.5%±0.3%**	**6.3%±0.5%**	**0.03**
C_{18}	1.8%±0.3%	1.9%±0.6%	0.94

Table 3. Number of genes showing differential expression between encased and emerged maize silks

Fold Change (Emerged/Encased)	Number of genes identified in the working gene set[1]	Number of genes identified in filtered gene set[2]	Number of Homologs to 90 genes involved in lipid biosynthesis in Arabidopsis
Emerged only	5	5	0
>10	24	22	3
2<FC<10	443	394	3
0.5<FC<2	17	15	1
0.1<FC<0.5	639	582	15
<0.1	86	69	4
Encased only	22	17	0
Total	1,236	1,104	31

Notes: 1-The Working Gene Set (WGS) provides an overall representation of non-overlapping candidate gene elements across the maize genome sequence. It was constructed by complementing evidence-based genes predicted by GeneBuilder with ab initio gene models predicted by FGENESH on Repeat Masked sequence. Only FGENESH models that do not overlap with the evidence-based genes are used in the set; 2-The Filtered Gene Set (FGS) is a subset of the Working Gene Set intended to exclude transposons, pseudogenes, contaminants, and other low-confidence structures.

Table 4. Comparison of expression patterns of 10 genes as determined by RNA-Seq and qPCR

Transcript ID	Protein	mRNA-Seq		qPCR	
		Fold change (Emerged/Encased)	Differentially expressed?	Fold change (Emerged/Encased)	Differentially expressed?
GRMZM2G077375_T01	ws	N. D.* in either sample	No	30.66±5.92	Yes
GRMZM2G167438_T03	kcs	14.29	Yes	0.05±0	Yes
GRMZM2G114642_T01	Gl1	0.4	No	1.22±0.11	NO
GRMZM2G104847	Acyl-CoA synthase	39.54	Yes	54.2±13.99	Yes
GRMZM2G062151	P450	7.52	Yes	20.52±1.58	Yes
GRMZM2G104626	Sen15	0.13	Yes	0.48±0.12	Yes
GRMZM2G149636	Unknown function protein 1	0.27	Yes	0.37±0.02	Yes
GRMZM2G130953	Unknown function protein 2	4.51	Yes	2.79±0.65	Yes
GRMZM2G035417	Unknown function protein 3	1.04	No	1.28±0.1	No
GRMZM2G032910	Unknown function protein 4	0.92	No	0.84±0.07	NO

Note: * Not Detectable

Table 5. Enrichment patterns of GO terms for highly expressed genes

Encased silk	Emerged silk
GO Terms	
Anatomical and structural development and cell growth Processes: Syntheses, Assembly and Organization of Chromosome, Chromatin, Nucleotides, Cell wall, Cellulose Components: Organelles (non-membrane bound), Chromatin, Nucleosome Functions: Auxin stimulus response	**Stress response** Processes: Response to Defense, Heat, Biotic Stress, Fungus, Temperature and Light Components: Intracellular Organelles, Mitochondrial Membrane, Plastids and Stroma Functions: Cellular Lipid Metabolism, Phosphatase Activity and Hydrolase Activity
Pathways (Maize-Cyc)	
Development – Syntheses and metabolism of amino acids and nucleotides.	**Metabolism and Degradation** of Sugar, Cellulose and Glucose **Exposure to light** - photorespiration, aerobic respiration, Calvin-Benson cycle. **Biosynthesis** of fatty acids, amino acids, Coenzyme-A, Vitamins, NAD and heme. **Metabolism** - TCA cycle, glyoxylate **Water-loss prevention** (Suberin) Response to **abiotic stress** (Jasmonic acid) **Defense** – GDP- Mannose biosyntheses. Senescence-related (Glutathion
Transcription Factors	

Gibberellin signaling (WRKY69, involved in cell elongation).l	Glycolysis regulation
Morphogenesis and development (Rolled leaf1).	Heat response regulator (WRKY51)
Pathogen defense (WRKY53).l	Ethylene-responsive (B6T5Z6)
Homoiothermy, response to freezing. l	Sensitivity to bacteria (MADS-X)
Control, development and organ identity (B6TDB4, MADS-box)	

Table 6. Relative transcript abundances of desaturase genes in encased and emerged maize silks

Transcript ID	Protein	Transcript abundance (FPKM*)		Ratio of transcript abundance (Emerged/Encased)	adjusted p-value	Significantly different?
		Encased silks	Emerged Silks			
GRMZM2G027673_T01	Stearoyl-ACP desaturase	0.00	0.00	NA	1.01	no
GRMZM2G027673_T02		0.00	0.00	NA	1.01	no
GRMZM2G027673_T03		0.00	0.00	NA	1.01	no
GRMZM2G027673_T04		0.00	0.00	NA	1.01	no
GRMZM2G316362_T01		0.28	1.94	6.99	0.14	no
GRMZM2G316362_T02		0.27	1.91	6.99	0.14	no
GRMZM5G883417_T01		**12.10**	**26.08**	**2.15**	**0.05**	**yes**
GRMZM2G316362_T03		0.03	0.04	1.51	1.11	no
GRMZM2G026793_T01		3.94	4.89	1.24	0.96	no
AC215690.3_FGT002		18.97	20.59	1.09	1.08	no
GRMZM2G180399_T01		3.67	3.19	0.87	1.05	no
GRMZM5G852502_T01		4.60	2.30	0.50	0.32	no
GRMZM2G119305_T01		0.06	0.00	0.00	1.00	no
GRMZM2G056252_T01	FAD1	0.00	0.00	NA	1.08	no
GRMZM2G056252_T03		0.81	0.00	0.00	0.42	no
GRMZM2G056252_T04		214.07	225.56	1.05	1.11	no
GRMZM2G056252_T05		*1215.45*	*1137.31*	*0.94*	*0.03*	*yes*
GRMZM2G128971_T03	ER Oleate Desaturase (fad2)	*49.79*	*16.71*	*0.34*	*0.00*	*yes*
GRMZM2G078569_T04	Plastidial Oleate Desaturase(fad6)	**11.94**	**25.06**	**2.10**	**0.03**	**yes**
GRMZM2G078569_T01		17.05	14.25	0.84	0.93	no
GRMZM2G078569_T02		18.52	12.87	0.69	0.56	no
GRMZM2G078569_T03		4.12	0.26	0.06	0.34	no
GRMZM2G074401_T01	Plastidial Linoleate Desaturase(fad7/fad8)	*6.25*	*1.18*	*0.19*	*0.00*	*yes*
GRMZM2G128971_T01		*36.04*	*9.78*	*0.27*	*2.E-05*	*yes*
GRMZM2G128971_T02		0.51	0.62	1.21	1.11	no
GRMZM2G129209_T01		0.00	0.00	NA	1.00	no

Note: * FPKM-Fragments Per Kilobase of transcript per Million mapped reads

Table 7. Relative transcript abundances of genes invovlved in surface lipid biosynthesis in maize silks

Transcript ID	Proteins	Transcript abundance (FPKM*)		Ratio of transcript abundance	q-value	Significantly different?
		Encased silks	Emerged Silks			
AC197672.3_FGT002	ACCase	19.07	33.47	1.76	0.22	No
GRMZM2G141256_T02		N.D	N.D	N.A.	1.00	No
GRMZM2G351023_T01		1.17	2.13	1.83	0.76	No
GRMZM2G377341_T01		**5.30**	**17.35**	**3.27**	**5.E-05**	**Yes**
GRMZM5G858094_T01		54.00	100.48	1.86	0.95	No
GRMZM5G858094_T02		**6.32**	**16.19**	**2.56**	**2.E-03**	**Yes**
GRMZM5G890665_T02		1.24	0.48	0.39	0.37	No
GRMZM2G029543_T01	MAT	16.99	20.39	1.20	0.92	No
GRMZM2G003190_T01	ketoacyl ACP synthase	0.26	0.15	0.55	0.99	No
GRMZM2G022563_T01		0.22	0.10	0.44	1.00	No
GRMZM2G111677_T01		N.D	N.D	N.A.	1.00	No
GRMZM2G380650_T02	KAS	2.56	2.35	0.92	1.09	No
GRMZM2G072205_T01		**43.38**	**110.66**	**2.55**	**0.01**	**Yes**
GRMZM2G012863_T01		20.19	19.11	0.95	1.10	No
GRMZM2G012863_T02		0.27	0.68	2.53	0.85	No
GRMZM2G168956_T01		N.D	N.D	N.A.	1.00	No
GRMZM2G060481_T01		N.D	N.D	N.A.	1.00	No
GRMZM2G465868_T01		N.D	N.D	N.A.	1.00	No
GRMZM5G853065_T01		N.D	N.D	N.A.	1.00	No
GRMZM2G024482_T02	HAD	40.03	42.26	1.06	1.10	No
GRMZM2G055667_T01		0.18	N.D	0.00	1.00	No
GRMZM2G079256_T01		3.55	9.24	2.60	0.08	No
GRMZM2G125052_T01		0.48	0.46	0.96	1.00	No
GRMZM2G070422_T01	EAR	25.82	33.11	1.28	0.74	No
GRMZM2G070422_T02		5.84	10.35	1.77	0.30	No
GRMZM2G467242_T01		N.D	N.D	N.A.	1.00	No
AC233893.1_FGT003		7.72	6.51	0.84	1.00	No
GRMZM2G027059_T01		0.10	0.14	1.33	1.10	No
GRMZM2G043602_T01		0.71	2.12	2.99	0.22	No

Table 8. Top 20 genes highly epxressed in emerged silks and top 20 genes highly epxressed in encased silks

Highly expressed in emerged or encased silks?	Gene	Number of paralogs in maize genome	Possible function based on GO terms	Transcript abundance		Ratio of transcript abundance (Emerged/Encased)	Ratio of transcript abundance (Encased/Emerged)	q-value
				Encased silks	Emerged silks			
Top 20 genes highly expressed in emerged silks	GRMZM2G019586	2	uncharacterized protein	0.00	1.71	Infinity		2.E-02
	GRMZM2G090744	1	uncharacterized protein	0.00	3.88	Infinity		4.E-02
	GRMZM2G105335	2	growth regulating factor	0.00	1.71	Infinity		1.E-02
	GRMZM2G141325	2	response to freezing	0.00	1.78	Infinity		2.E-02
	GRMZM2G384780	5	lipid metabolism	0.00	10.26	Infinity		3.E-03
	GRMZM5G898755	1	Non-specific lipid transfer protein	0.15	68.17	466.21		7.E-03
	GRMZM5G828987	1	carbohydrate metabolic process	0.17	5.77	34.90		2.E-02
	GRMZM2G478414	1	lipid metabolism	4.47	131.94	29.53		0.E+00
	GRMZM2G104847	1	Acyl CoA synthase	0.86	24.24	28.11		5.E-07
	GRMZM2G003368	1	fatty acid metabolism	0.19	5.16	27.22		6.E-03
	GRMZM2G001223	1	uncharacterized protein	0.29	7.64	26.36		2.E-02
	GRMZM2G160541	2	uncharacterized protein	0.60	11.77	19.76		2.E-10
	GRMZM5G812228	1	Acyl CoA synthase like protein	1.18	21.02	17.81		1.E-13
	GRMZM2G158205	1	Lipid metabolism	42.03	688.34	16.38		0.E+00
	GRMZM2G167438	1	Acyltransferase	1.22	19.73	16.11		2.E-07
	GRMZM5G882852	3	carbohydrate metabolic process	1.33	20.26	15.19		8.E-11
	GRMZM2G147051	1	protein kinase	0.61	8.22	13.58		2.E-05
	GRMZM2G016890	8	carbohydrate metabolic process	8.58	114.82	13.39		0.E+00
	GRMZM2G057027	6	response to freezing	0.62	7.85	12.75		9.E-04
	GRMZM2G046070	1	uncharacterized protein	2.66	30.02	11.30		9.E-12
Top 20 genes highly expressed in encased silks	AC207189.4_FG002	1	uncharacterized protein	14.03	0.00		Infinity	1.E-02
	GRMZM2G007012	3	glucosyltransferase	1.79	0.00		Infinity	2.E-03
	GRMZM2G045638	1	uncharacterized protein	1.98	0.00		Infinity	4.E-02
	GRMZM2G050076	1	steroid biosynthetic process	1.81	0.00		Infinity	5.E-03
	GRMZM2G062458	1	uncharacterized protein	2.36	0.00		Infinity	2.E-02
	GRMZM2G064530	2	uncharacterized protein	7.68	0.00		Infinity	4.E-05
	GRMZM2G077375	1	uncharacterized protein	3.92	0.00		Infinity	1.E-03
	GRMZM2G078595	1	uncharacterized protein	4.89	0.00		Infinity	3.E-04
	GRMZM2G083841	3	Phosphoenolpyruvate carboxylase	8.26	0.00		Infinity	8.E-10
	GRMZM2G090028	6	uncharacterized protein	3.35	0.00		Infinity	6.E-05
	GRMZM2G119209	8	uncharacterized protein	2.38	0.00		Infinity	1.E-03
	GRMZM2G132875	2	uncharacterized protein	1.76	0.00		Infinity	1.E-02
	GRMZM2G137891	1	uncharacterized protein	2.36	0.00		Infinity	1.E-02
	GRMZM2G163054	1	transcription factor	2.97	0.00		Infinity	4.E-02
	GRMZM2G339091	1	serine-type carboxypeptidase	5.51	0.00		Infinity	1.E-02
	GRMZM2G355752	1	early light-induced protein	3.87	0.00		Infinity	3.E-05
	GRMZM2G425729	1	uncharacterized protein	6.84	0.00		Infinity	2.E-04
	GRMZM2G374302	1	arginine decarboxylase	2983.26	3.28		909.11	0.E+00
	GRMZM2G099678	1	Vegetative storage protein	18.48	0.18		100.36	3.E-03
	GRMZM2G005954	1	uncharacterized protein	28.70	0.45		63.41	5.E-11

Note: * FPKM-Fragments Per Kilobase of transcript per Million mapped reads

Supplemental Table 1. Primers used for qPCR

Gene product	Transcript ID	Forward primer	Reverse primer
18S rRNA	**GRMZM2G114613_T01**	**5'-CGTGTTGACCTGACCGAATA-3'**	**5'-TTGGTGACCACATGGCATAC-3'**
Actin	**GRMZM2G126010**	**5'-TGTCTTCGCTTGCTTCCTTT-3'**	**5'-ATCCTCGTCAGCCATTCTCA-3'**
UBC	**GRMZM2G132759**	**5'-GGACCACCTGACAGTCCCTA-3'**	**5'-GGCTCCACTGCTCTTTGAGA-3'**
ws	GRMZM2G077375_T01	**5'-AGCGTCCAGGTGGTAAATGA-3'**	**5'-GACGACACGTAGTCCTCCAG-3'**
kcs	GRMZM2G167438_T03	**5'-TTTGGCAACAACAAGAGCAG-3'**	**5'-TTCACGATCACCTTCAGCAG-3'**
Gl1	GRMZM2G114642_T01	**5'-GGACAACCTCGGCTTCTACA-3'**	**5'-CCACTCCTTGTCGATCTGGT-3'**
Acyl-CoA synthase	GRMZM2G104847	**5'-GCACACACGAAAGCAAGCTA-3'**	**5'-CTGCTCTTGTTGTTGCCAAA-3'**
P450	GRMZM2G062151	**5'-AGACGCTGGGAATTCAATGT-3'**	**5'-CAAATCCAGCTAGATCGCAAA-3'**
Sem15	GRMZM2G104626	**5'-GGACGTCAAGTCGTTCAACC-3'**	**5'-ATGCAGTTGGAGAGGAGCAT-3'**
Unknown function protein 1	GRMZM2G149636	**5'-TTGCCGTGAGTAGACAGTGC-3'**	**5'-GCGTCTAGAACGCCAAAGAG-3'**
Unknown function protein 2	GRMZM2G130953	**5'-CTTCGCCTGATGAAAGGTTC-3'**	**5'-CAAGCCAAGCCACTAAAAGC-3'**
Unknown function protein 3	GRMZM2G035417	**5'-TCTTGACATGGGTGGTGGTA-3'**	**5'-GGCCTGCTGATTTGTTTGTT-3'**
Unknown function protein 4	GRMZM2G032910	**5'-CCGAAGGCGTTCTTGGTG-3'**	**5'-GTAGAATCCTTCGGGCATGA-3'**

Supplemental Table 2. Relative transcript abundances of genes involved in fatty acid initiation in maize silks

Gene ID	Enzyme	Whether present in maize silks?	Transcript abundance (FPKM*)		Ratio of transcript abundance (Emerged/Encased)	q-value	Significantly different?
			Encased silks	Emerged silks			
AC197672.3_FGT002	ACCase	Yes	19.07	33.47	1.76	0.22	No
GRMZM2G141256_T02	ACCase	No	N.D	N.D	N.A.	1.00	No
GRMZM2G351023_T01	ACCase	Yes	1.17	2.13	1.83	0.76	No
GRMZM2G377341_T01	**ACCase**	**Yes**	**5.30**	**17.35**	**3.27**	**5.E-05**	**Yes**
GRMZM5G858094_T01	ACCase	Yes	54.00	100.48	1.86	0.95	No
GRMZM5G858094_T02	**ACCase**	**Yes**	**6.32**	**16.19**	**2.56**	**2.E-03**	**Yes**
GRMZM5G890665_T02	ACCase	Yes	1.24	0.48	0.39	0.37	No
GRMZM2G029543	MAT	Yes	16.99	20.39	1.20	0.92	No
GRMZM2G022563	KAS	No	0.22	0.10	0.44	1.00	No
GRMZM2G003190	KAS	Yes	0.26	0.15	0.55	0.99	No
GRMZM2G111677	KAS	No	0.00	0.00	NA	1.00	No

Note: * FPKM-Fragments Per Kilobase of transcript per Million mapped reads

Supplemental Table 3. Relative transcript abundances of genes involved in fatty acid biosynthesis in maize silks

Gene ID	Enzyme	Whether present in maize silks?	Transcript abundance (FPKM*)		Ratio of transcript abundance (Emerged/Encased)	q-value	Significantly different?
			Encased silks	Emerged silks			
GRMZM2G380650_T02	KAS	Yes	2.56	2.35	0.92	1.09	No
GRMZM2G072205_T01		Yes	**43.38**	**110.66**	**2.55**	**0.01**	**Yes**
GRMZM2G012863_T01		Yes	20.19	19.11	0.95	1.10	No
GRMZM2G012863_T02		Yes	0.27	0.68	2.53	0.85	No
GRMZM2G168956_T01		No	N.D	N.D	N.A.	1.00	No
GRMZM2G060481_T01		No	N.D	N.D	N.A.	1.00	No
GRMZM2G465868_T01		No	N.D	N.D	N.A.	1.00	No
GRMZM5G853065_T01		No	N.D	N.D	N.A.	1.00	No
AC233893.1_FGT003	KAR	Yes	7.72	6.51	0.84	1.00	No
GRMZM2G027059_T01		Yes	0.10	0.14	1.33	1.10	No
GRMZM2G043602_T01		Yes	0.71	2.12	2.99	0.22	No
GRMZM2G075140_T01		Yes	160.77	147.06	0.91	1.07	No
GRMZM2G099696_T01		Yes	55.40	57.22	1.03	1.11	No
GRMZM2G124335_T02		Yes	36.42	28.41	0.78	0.76	No
GRMZM2G135498_T01		Yes	2.20	1.77	0.80	0.99	No
GRMZM2G152105_T01		Yes	22.67	29.91	1.32	0.67	No
GRMZM2G152105_T02		Yes	2.56	1.67	0.65	0.70	No
GRMZM2G451861_T01		Yes	47.51	28.33	0.60	0.20	No
GRMZM2G152105_T03		No	N.D	N.D	N.A.	1.02	No
GRMZM2G024482_T02	HAD	Yes	40.03	42.26	1.06	1.10	No
GRMZM2G055667_T01		No	0.00	N.D	0.00	1.00	No
GRMZM2G079256_T01		Yes	3.55	9.24	2.60	0.08	No
GRMZM2G125052_T01		Yes	0.48	0.46	0.96	1.00	No
GRMZM2G079256	EAR	Yes	3.55	9.24	2.60	0.08	No
GRMZM2G070422		Yes	25.82	33.11	1.28	0.74	No
GRMZM2G125052		No	0.48	0.46	0.96	1.00	No

Note: * FPKM-Fragments Per Kilobase of transcript per Million mapped reads

Supplemental Table 4. Relative transcript abundances of genes involved in fatty acid elongation in maize silks

Transcripts ID	Enzymes	Sources	Whether present in maize silks?	Transcript abundance		Ratio of transcript abundance (Emerged/Encased)	q-value	Significantly different?
				Encased silks	Emerged silks			
GRMZM2G036927_T03	KCS	Alexis	NO	0.00	0.00	0.00	1.00	No
GRMZM2G063024_T01			NO	0.00	0.00	NA	1.00	No
GRMZM2G128445_T01			NO	0.00	0.00	NA	1.00	No
GRMZM2G133793_T01			NO	0.00	0.00	NA	1.00	No
GRMZM2G168956_T01			NO	0.00	0.00	NA	1.00	No
GRMZM2G167438_T01			**Yes**	**0.86**	**22.23**	**25.75**	**3.E-10**	**Yes**
GRMZM2G409312_T01			Yes	0.25	1.55	6.14	0.15	No
GRMZM2G156620_T01			Yes	0.13	0.41	3.01	1.00	No
GRMZM2G137694_T01			**Yes**	**14.87**	**41.78**	**2.81**	**0.0007**	**Yes**
GRMZM2G022558_T02			Yes	69.78	142.62	2.04	0.11	No
GRMZM2G445602_T01			**Yes**	**963.07**	**1957.57**	**2.03**	**9.E-09**	**Yes**
GRMZM2G164974_T01			Yes	168.98	336.10	1.99	0.20	No
GRMZM2G162508_T01			Yes	102.78	154.84	1.51	0.65	No
GRMZM2G022558_T01			Yes	0.54	0.60	1.11	1.11	No
GRMZM2G164974_T02			Yes	1.39	1.54	1.11	1.09	No
GRMZM2G167438_T03			Yes	0.46	0.49	1.05	1.11	No
GRMZM2G003501_T01			Yes	3.20	2.30	0.72	0.83	No
GRMZM2G393897_T01			Yes	5.78	3.54	0.61	0.51	No
GRMZM2G003138_T01			Yes	0.61	0.34	0.55	0.86	No
GRMZM2G160417_T01			Yes	1.08	0.44	0.41	0.40	No
GRMZM2G569948_T01			*Yes*	*34.29*	*14.00*	*0.41*	*0.01*	*Yes*
GRMZM2G168304_T01			NO	0.23	0.09	0.39	1.00	No
GRMZM2G151476_T01			*Yes*	*34.35*	*9.44*	*0.27*	*0.00003*	*Yes*
GRMZM2G149636_T01			*Yes*	*12.55*	*3.43*	*0.27*	*0.0006*	*Yes*
GRMZM2G104626_T01			*Yes*	*5.14*	*0.66*	*0.13*	*0.00001*	*Yes*
GRMZM2G060481_T01			NO	0.00	0.00	0.00	1.00	No
AC205703.4_FGT006	KCR	Alexis	Yes	10.54	13.16	1.25	0.89	No
GRMZM2G389110_T01			NO	0.00	0.00	NA	1.00	No
GRMZM2G465868_P01		MaizeCyc	No	0.00	0.00	NA	1	No
GRMZM2G087323_T01			Yes	3.05	3.04	1.00	1.10	No
GRMZM2G090733_T01			No	0.00	0.00	NA	1.00	No
GRMZM2G151087_T01	HCD	Alexis	Yes	103.76	165.32	1.59	0.35	No
GRMZM2G033491_T01		MaizeCyc	Yes	0.00	0.00	NA	1.01	No
GRMZM2G158629_T01			Yes	0.76	0.77	1.00	1.10	No
GRMZM2G158629_T02			Yes	97.07	118.61	1.22	0.88	No
GRMZM2G158629_T03			Yes	0.00	0.20	NA	0.53	No
GRMZM2G151087_T02			Yes	2.19	1.71	0.78	0.98	No
GRMZM2G181266_P01			No	0.00	0.00	NA	1.00	No
GRMZM2G132903_P01			No	0.00	0.00	NA	1.00	No
GRMZM2G177404_P01			No	0.00	0.00	NA	1.00	No
GRMZM2G105245_P01			No	0.00	0.00	NA	1.00	No
GRMZM2G459755_P01			No	0.00	0.00	NA	1.00	No
GRMZM2G398500_P01			No	0.00	0.00	NA	1.00	No
GRMZM2G094655_P01			No	0.00	0.00	NA	1.00	No
GRMZM2G854613_P01			No	0.00	0.00	NA	1.00	No
GRMZM2G481843_T01	ECR	Alexis	Yes	0.31	0.93	3.00	0.52	No
AY106269		MaizeCyc	No	0.00	0.00	NA	1.00	No
GRMZM2G467242_T01			No	0.00	0.00	NA	1.00	No
GRMZM2G119345_T01		AraCyc	Yes	0.07	0.19	2.65	1.03	No
GRMZM2G120163_T01			Yes	0.05	0.10	1.82	1.02	No
GRMZM2G120938_T01			Yes	0.04	0.28	7.46	0.78	No

Note: * FPKM-Fragments Per Kilobase of transcript per Million mapped reads

Supplemental Table 5. Gene IDs of desaturases in Arabidopsis

Protein	Gene ID
Stearoyl-ACP desaturase	At1g43800
Stearoyl-ACP desaturase	At2g43710
Stearoyl-ACP desaturase	At3g02610
Stearoyl-ACP desaturase	At3g02620
Stearoyl-ACP desaturase	At3g02630
Stearoyl-ACP desaturase	At5g16230
Stearoyl-ACP desaturase	At5g16240
FAD1	At5g03430
ER Oleate Desaturase (FAD2)	At3g12120
ER Linoleate Desaturase (FAD3)	At2g29980
FAD4	AT4G27030
Monogalactosyldiacylglycerol Desaturase (palmitate-specific, FAD5)	At3g15850
Plastidial Oleate Desaturase (FAD6)	At4g30950
Plastidial Linoleate Desaturase (FAD7)	At3g11170
Plastidial Linoleate Desaturase (FAD8)	At5g05580
delta 9 desaturase (ADS1)	At1g06080
fatty acid desaturase family protein (ADS1)	At1g06090
fatty acid desaturase family protein (ADS1)	At1g06100
fatty acid desaturase family protein (ADS1)	At1g06120
fatty acid desaturase family protein (ADS1)	At1g06350
fatty acid desaturase family protein (ADS1)	At1g06360
delta 9 desaturase (ADS2)	At2g31360
fatty acid desaturase family protein (ADS2)	At3g15870

Supplemental Table 6. List of Arabidopsis genes with putative functions in surface lipid biosynthesis

Function	Arabidopsis Target	Protein
Form Acetyl-CoA by an ATP-dependent reaction from citrate	ACLA-1/AT1G10670	ATP citrate synthase
	ACLA-2/AT1G60810	ATP citrate synthase
	ACLA-3/AT1G09430	ATP citrate synthase
	ACLB-1/AT3G06650	ATP citrate synthase
	ACLB-2/AT5G49460	ATP citrate synthase
Form Malonyl-CoA from acetyl-CoA	ACC1/AT1G36160	acetyl-CoA carboxylase
	ACC2/AT1G36180	acetyl-CoA carboxylase
Fatty acid elongation	FAE1/AT4G34520	fatty acid elongase
	FIDDLEHEAD/AT2G26250	beta-ketoacyl-CoA synthase (also, acyltransferase/ catalytic/ transferase, transferring acyl groups other than amino-acyl groups)
	CUT1(CER6)/AT1G68530	(3-KETOACYL-COA SYNTHASE 6) very-long-chain fatty acid condensing enzyme (also, fatty acid elongase)
	CER60/AT1G25450	(3-KETOACYL-COA SYNTHASE 10) very-long-chain fatty acid condensing enzyme CUT1 (also, catalytic/ transferase, transferring acyl
	KCS1/AT1G01120	(3-KETOACYL-COA SYNTHASE 5) acyltransferase/ fatty acid elongase
	KCS/AT2G26640	(3-KETOACYL-COA SYNTHASE 9) acyltransferase/ catalytic/ transferase, transferring acyl groups other than amino-acyl groups
	KCS/AT1G04220	(3-KETOACYL-COA SYNTHASE 2); fatty acid elongase
	KCS/AT1G19440	(3-KETOACYL-COA SYNTHASE 4); acyltransferase/ catalytic/ transferase, transferring acyl groups other than amino-acyl groups
	KCS/AT5G43760	(3-KETOACYL-COA SYNTHASE 20); fatty acid elongase
	KCS/AT2G16280	(3-KETOACYL-COA SYNTHASE 9) acyltransferase/ catalytic/ transferase, transferring acyl groups other than amino-acyl groups
	KCS/AT2G46720	(3-KETOACYL-COA SYNTHASE 13); acyltransferase/ catalytic/ transferase, transferring acyl groups
	KCS/AT4G34510	(3-KETOACYL-COA SYNTHASE 17); acyltransferase/ catalytic/ transferase, transferring acyl groups other than amino-acyl groups
	KCS/AT2G15090	(3-KETOACYL-COA SYNTHASE 8); acyltransferase/ catalytic/ transferase, transferring acyl groups other than amino-acyl groups
	KCS/AT4G34250	(3-KETOACYL-COA SYNTHASE 16); acyltransferase/ catalytic/ transferase, transferring acyl groups other than amino-acyl groups
	KCS/AT1G71160	(3-KETOACYL-COA SYNTHASE 7); acyltransferase/ catalytic/ transferase, transferring acyl groups other than amino-acyl groups
	KCS/AT5G49070	(3-KETOACYL-COA SYNTHASE 21); acyltransferase/ catalytic/ transferase, transferring acyl groups other than amino-acyl groups
	KCS/AT3G52160	(3-KETOACYL-COA SYNTHASE 15); acyltransferase/ catalytic/ transferase, transferring acyl groups other than amino-acyl groups
	KCS/AT2G28630	(3-KETOACYL-COA SYNTHASE 12); acyltransferase/ catalytic/ transferase, transferring acyl groups other than amino-acyl groups
	KCS/AT1G07720	(3-KETOACYL-COA SYNTHASE 3); acyltransferase/ catalytic/ transferase, transferring acyl groups other than amino-acyl groups
	KCS/AT5G04530	(3-KETOACYL-COA SYNTHASE 19); acyltransferase/ catalytic/ transferase, transferring acyl groups other than amino-acyl groups
	KCR	HTH (HOTHEAD); FAD binding / aldehyde-lyase/ mandelonitrile lyase
	KCR/AT1G24470	Short-chain dehydrogenase/reductase (SDR) family protein
	KCR/YDR036C(YEAST)	3-hydroxyisobutyryl-CoA hydrolase, member of a family of enoyl-CoA hydratase/isomerases; non-tagged
	KCR/AT1G67730	
	ECR/AT3G55360	3-oxo-5-alpha-steroid 4-dehydrogenase/ fatty acid elongase/ trans-2-enoyl-CoA reductase (NADPH)
	ELO/YJL96C(ELO1+ELO2+ELO3)YEAST	Elongation of fatty acids protein 1
	ELO/AT3G0647	GNS1/SUR4 membrane family protein
	ELO/AT3G0646	GNS1/SUR4 membrane family protein
	ELO/AT4G36830	GNS1/SUR4 membrane family protein
	ELO/AT1G75000	GNS1/SUR4 membrane family protein
Wax synthase converting a fatty acid and an alcohol to form a wax ester	WS/AT5G55340	Long-chain-alcohol O-fatty-acyltransferase family protein / wax synthase family protein
	WS/AT5G55350	Membrane bound O-acyl transferase (MBOAT) family protein / wax synthase-related
	WS/AT5G55360	Long-chain-alcohol O-fatty-acyltransferase family protein / wax synthase family protein
	WS/AT1G34500	Membrane bound O-acyl transferase (MBOAT) family protein / wax synthase-related
	WS/AT5G55330	Membrane bound O-acyl transferase (MBOAT) family protein / wax synthase-related
	WS/AT1G34490	Membrane bound O-acyl transferase (MBOAT) family protein / wax synthase-related
	WS/AT5G55370	Long-chain-alcohol O-fatty-acyltransferase family protein / wax synthase family protein
	WS/AT5G51420	Long-chain-alcohol O-fatty-acyltransferase family protein / wax synthase family protein
	WS/AT5G55380	Membrane bound O-acyl transferase (MBOAT) family protein / wax synthase-related
	WS/AT5G5532	Membrane bound O-acyl transferase (MBOAT) family protein / wax synthase-related
	WS/AT1G3452	Long-chain-alcohol O-fatty-acyltransferase family protein / wax synthase family protein
	WS(jojoba)/AAD38040	acyl CoA reductase [synthetic construct]
	WS/AT3G51970	wax synthase-like protein (also, AtSAT1 (Arabidopsis thaliana sterol O-acyltransferase 1); acyltransferase)
	WS/DGAT(ACINETOBACTER	bifunctional wax ester synthase/acyl-CoA; diacylglycerol (organism ACINETOBACTER CALCOACETICUS)
	WS/DGAT-Like/AT5G12420	Hypothetical protein (From BNqueryFile WS/DGAT-Like)
Bifunctional enzyme: Converting fatty acid to fatty aldehyde and fatty alcohol.	MS2/AT3G44540	FAR4 (FATTY ACID REDUCTASE 4); binding / catalytic/ oxidoreductase, acting on the CH-CH group of donors
	MS2/AT3G44550	FAR5 (FATTY ACID REDUCTASE 5); binding / catalytic/ oxidoreductase, acting on the CH-CH group of donors
	MS2/AT5G2242	FAR7 (FATTY ACID REDUCTASE 7); binding / catalytic/ oxidoreductase, acting on the CH-CH group of donors
	MS2/AT3G44560	FAR8 (FATTY ACID REDUCTASE 8); fatty acyl-CoA reductase (alcohol-forming)/ oxidoreductase, acting on the CH-CH group of donors
	MS2/AT3G56700	FAR6 (FATTY ACID REDUCTASE 6); fatty acyl-CoA reductase (alcohol-forming)/ oxidoreductase, acting on the CH-CH group of donors,
	MS2/AT4G33790	CER4 (ECERIFERUM 4); fatty acyl-CoA reductase (alcohol-forming)/ oxidoreductase, acting on the CH-CH group of donors
	MS2/AT3G11980	(MALE STERILITY 2); fatty acyl-CoA reductase (alcohol-forming)/ oxidoreductase, acting on the CH-CH group of donors, NAD or NADP as
	MS2/AT5G22500	FAR1 (FATTY ACID REDUCTASE 1); fatty acyl-CoA reductase (alcohol-forming)/ oxidoreductase, acting on the CH-CH group of donors
	(OH)formingAcCoAreductase(jojoba)/AF149910	
Possible decarbonylase	CER1/AT1G022050	CER1 (ECERIFERUM 1); octadecanal decarbonylase
	CER1	Alternative Splicing of CER1 (ECERIFERUM 1); octadecanal decarbonylase
	YORE-YORE/AT1G02190A	CER1 protein, putative
	YORE-YORE/AT1G02190B	CER1-like protein
	YORE-YORE/AT5G28280	(Probably a CER1-like protein, putative)
Homologs to Wax 2 in maize.The N-terminal portion of WAX2 is homologous with members	YORE-YORE/AT5G57800	CER3 (ECERIFERUM 3); binding / catalytic/ iron ion binding / oxidoreductase (RecName, Protein YORE-YORE)
	YORE-YORE/AT5G57800	CER3 (ECERIFERUM 3); binding / catalytic/ iron ion binding / oxidoreductase (RecName, Protein YORE-YORE)
	YORE-YORE/AT2G37700	Catalytic/ iron ion binding / oxidoreductase
Elongation C30 to C32 fatty acids	CER2/AT4G24510	CER2 (ECERIFERUM 2); transferase/ transferase, transferring acyl groups other than amino-acyl groups
	CER2-Like/AT4G13840	Transferase family protein (Also, fatty acid elongase - like protein (cer2-like))
	CER2-Like/AT3G23840	transferase family protein
Wax secretion	CER5/AT1G51500	CER5 (ECERIFERUM 5); ATPase, coupled to transmembrane movement of substances
Suberin biosynthesis	P450(CYP86A1)/AT5G58860	CYP86A1 (CYTOCHROME P450 86 A1); fatty acid (omega-1)-hydroxylase/ oxygen binding
	P450(CYP86A8)/AT2G45970	CYP86A8; fatty acid (omega-1)-hydroxylase/ oxygen binding
	P450-Like/AT2G45970	CYP78A7; electron carrier/ heme binding / iron ion binding / monooxygenase/ oxygen binding
	P450-Like/AT1G63710	CYP86A7; fatty acid (omega-1)-hydroxylase/ oxygen binding
	P450-Like/AT1G01600	CYP86A4; fatty acid (omega-1)-hydroxylase/ oxygen binding
	P450(CYP94A1)/AT3G56630	CYP94D2; electron carrier/ heme binding / iron ion binding / monooxygenase/ oxygen binding
	P450-Like/AT5G63450	CYP94B1; electron carrier/ heme binding / iron ion binding / monooxygenase/ oxygen binding
	P450-Like/AT4G00360	CYP86A2 (CYTOCHROME P450 86 A2); fatty acid (omega-1)-hydroxylase/ oxygen binding
	P450-Like/AT1G01280	CYP703A2 (CYTOCHROME P450, FAMILY 703, SUBFAMILY A, POLYPEPTIDE 2); oxidoreductase, acting on paired donors, with
	P450-Like/AT5G09970	CYP78A7; electron carrier/ heme binding / iron ion binding / monooxygenase/ oxygen binding
Cutin synthesis	LACS2/AT1G49430	LACS2 (LONG-CHAIN ACYL-COA SYNTHETASE 2); long-chain-fatty-acid-CoA ligase
MKS	MKS1/AY701570	MKS1 [Lycopersicon hirsutum f. glabratum] (exact matc hwith AAV87156.1)
Lipid metabolic process	ACBP/AT5G53470	ACBP1 (ACYL-COA BINDING PROTEIN 1); acyl-CoA binding / lead ion binding
Epidermis surface formation	ALE1(SUBTILISIN-LIKE	ALE1 (ABNORMAL LEAF-SHAPE 1); serine-type endopeptidase
Affecting epidermis cells	HOTHEAD	HTH (HOTHEAD); FAD binding / aldehyde-lyase/ mandelonitrile lyase
Cuticule	RST1/AT3G27670	RST1 (RESURRECTION1); binding
Cutin biosynthesis	BDG/AT1G64670	BDG1 (BODYGUARD1); hydrolase

CHAPTER 5. DIFFERENT SPATIAL AND TEMPORAL ACCUMULATION OF SURFACE LIPIDS ON LEAFLETS BUT NOT ON STIPULES IN AN *ARG* MUTANT OF *PISUM SATIVUM*

Wenmin Qin, Marna D. Yandeau-Nelson, Basil J. Nikolau.

Center for Metabolic Biology, Plant Science Institute

Center for Biorenewable Chemical

Department of Biochemistry, Biophysics and Molecular Biology

Iowa State University, Ames, IA 50010

Email: dimmas@iastate.edu

Telephone: 515-294-0347

Fax number: 515-294-0534

Abstract

Surface lipids that accumulate on the epidermis of pea leaflets are primarily comprised of linear hydrocarbons with chain lengths from 25 to 31 carbon atoms (predominantly C_{31} hydrocarbon), fatty acids ranging from C_{10} to C_{24}, alcohols from C_{26} to C_{30} together with C_{18} alcohol and C_{26} aldehydes. Detailed analyses of hydrocarbons on the adaxial and abaxial epidermal surfaces of stipules and leaflets were conducted on the *Argentum* mutant of *Pisum sativum* 17667, from which the epidermis is easily separable from the underlying tissue. The abaxial epidermis accumulates 20-fold more C_{31} alkane as compared to the adaxial epidermis of the leaflet, whereas accumulation of hentriacontane does not differ between the abaxial and

adaxial epidermis of the stipule. Further analyses showed that abaxial epidermis of leaflet and the epidermis of the stipules accumulate ca. 50% hydrocarbons and 40% alcohols, whereas the adaxial epidermis of the leaflet accumulates less than 10% hydrocarbons and ca. 90% of alcohols, which are mainly C_{26} and C_{28} alcohols. In addition to the spatial difference of hydrocarbon accumulation, there is also temporal difference in surface lipids accumulation increases as the age of the leaflets increase, and these surface lipids include fatty acids, alcohols, hydrocarbons and aldehydes. Although the underlying mechanisms of these spatial and temporal differences are not clear, these molecules might function to protect the plant from pathogens and prevent water loss.

1. Introduction

The plant epidermis, a cell layer composed of epidermal cells, trichomes and guard cells, forms the cellular interface between a plant and its environment. It is covered with surface lipids, which can prevent non-stomatal water loss and provide resistance to insects and other pathogens (Reina-Pinto and Yephremov 2009). Some biochemical features of epidermal cells have been well studied, mainly by chemical analysis and microscopy (Buschhaus et al. 2007a, b; Caffrey et al. 1998; Dragota and Riederer 2007; Nikolau et al. 1984; Riedel et al. 2007; Shin et al. 2010; Wen et al. 2006; Wurtele and Nikolau 1986; Wurtele et al. 1984). In most cases, surface lipids are a complex mixture of hydrophobic components, cutin (a polyester matrix)

and soluble lipids (Merida et al. 1981). The soluble lipids are composed of very long chain aliphatic components, such as n-alkanes, fatty acids, primary and secondary alcohols, aldehydes, ketones or n-alkyl esters (Javelle et al. 2011), which vary among diverse species (Buschhaus and Jetter 2011; Gniwotta et al. 2005). Alkanes are relatively abundant on leaf surfaces (Buschhaus et al. 2007a, b; Cassagne and Lessire 1975; Gniwotta et al. 2005; Riedel et al. 2007). For example, C_{29} alkane accounts for ~30% of total surface lipids on leaves from *Brassica oleracea* (Eigenbrode et al. 1991; Macey and Barber 1970a).

Pea leaves are compound leaves, composed of basal, foliaceous, leaf-like stipules, up to three pairs of proximal leaflets and distal tendrils (Kumar et al. 2009; Mikić et al. 2011). Surface lipids on leaves from *Pisum sativum* (pea) have been investigated (Chang et al. 2006; Gniwotta et al. 2005; Gorb et al. 2008; Macey and Barber 1970b). In these studies, the surface lipids found on leaves were removed using Arabic gum and analyzed (Gniwotta et al. 2005). These analyses demonstrated that the surface lipids are composed of alkanes (50%), esters and aldehydes (18%), primary alcohols (19%), secondary alcohols (7%) and free acids (6%) (Macey and Barber 1970b). Whereas most studies report only the average composition of lipids from the combined abaxial and adaxial sides of the leaf, (Gniwotta et al. 2005) reported that the abaxial epidermis consisted of 73% alkanes whereas the adaxial epidermis contained 71% primary alcohols . Accordingly, ultrastructures of the

epicuticular wax of abaxial and adaxial epidermis are ribbon-shaped and platelet-shaped, respectively (Halloway et al. 1977). While differences have been shown in surface lipids between the abaxial and adaxial leaf surfaces, little is known about how these compositions may vary during leaf development. In addition, the surface lipids on stipules, which are distinct from leaflets (Kumar et al. 2009), and occur in pairs on either side of the junction of the leaf blade petiole and stem, have not be characterized.

The *Argentum* mutant of pea (Hoch et al. 1980) can greatly aid in studies of epidermal leaf tissue. The *Arg* mutant harbors a dominant mutation that has not yet been assigned to a genetic locus and is characterized by a gray-green, silvery cast to the leaves and stipules (Jewer et al. 1982). The nature of the silvery cast is due to an extensive intercellular air space between the epidermis and palisade parenchyma (Grimbly 1977; Hoch et al. 1980), which allows for easy removal of the epidermis from underlying tissue. It has been demonstrated that epidermis removed from *Arg* leaves is free of palisade cell wall fragments, whereas epidermis from wild-type leaves contains remnants of palisade cells (Jewer et al. 1985). In this study we Used the *Arg* mutant, W6 17667, and surface lipids were characterized from the abaxial and adaxial surfaces of leaflets and stipules at different stages of development to define the spatial and temporal resolution of surface lipid accumulation.

2. Results

2.1 Fatty acids, aldehydes, alcohols and hydrocarbons on abaxial and adaxial leaf epidermis and stipule epidermis of *Arg* pea plant

Epidermal tissue from the adaxial and abaxial surfaces of leaves and stipules were easily removed with forceps from the *Arg* mutant leaflets and stipules. Non-polar lipid metabolites were extracted with hexanes, purified by chromatography over a silica gel column, and analyzed via GC-MS as described in the Methods. The predominant hydrocarbon is C_{31} alkane, and minor components include odd-numbered, linear alkanes, of 25-29 carbon chain length (Fig 1). Other, more polar metabolites were identified by GC analysis of the hexane extracts without the silica gel purification step. These GC-MC analyses identified a series of even-numbered saturated fatty acids (from C_{10} to $C_{24,}$), the unsaturated fatty acids $C_{18:1}$ (oleic acid) and $C_{18:2}$ (linoleic acid), a C26 aldehyde, and a series of alcohols, including $C_{18,}$ and those between C_{26} to C_{30} (Fig 2).

The metabolite profiles associated with the abaxial leaflet epidermis and combined abaxial and adaxial stipule epidermis are quite similar. Both the abaxial leaflet epidermis and stipule epidermis contain higher levels of hydrocarbons (50% of total constituents), but fewer alcohols (40% of total constituents) as compared to the adaxial leaf epidermis; the latter is comprised of <10% hydrocarbons and ~90% alcohols (Fig 3a). Similar results were obtained by the analysis of the purified hydrocarbon fraction, which consists predominantly of a C_{31} alkane, along with minor quantities of C_{25}, C_{27} and C_{29}

alkanes. The predominant, C_{31} alkane accounted for more than 90% of the hydrocarbons in the abaxial surface of the leaf and stipule epidermis. However, on adaxial leaf epidermis the C_{31} alkane was only ~60% of the hydrocarbons (Fig 3b).

Fatty acids are minor constituents of the surface lipids, comprising ca. 2% of the metabolites detected in each of the tissues. Even-numbered fatty acids with chain lengths from C_{10} to C_{24} were found, and among these, C_{16} (palmitic acid), C_{18} (stearic acid) and C_{24} fatty acids accounted for 70% of the fatty acids. In addition to saturated fatty acid, unsaturated fatty acids, $C_{18:1}$ (oleic acid) and $C_{18:2}$ (linoleic acid) were also identified (Fig 3c).

For alcohols, the C_{26} and C_{28} alcohol constituents comprised ~90% of the alcohol fraction, with C_{18}, C_{27}, C_{29} and C_{30} present in small amounts (Fig 3d). Abaxial and adaxial leaf epidermis produced more C_{26} alcohol and less C_{28} alcohol, which is opposite to stipule epidermis (Fig 3d). Only C_{26} aldehyde is found in leaf and stipule epidermis. The abaxial leaf epidermis produces more C_{26} aldehydes than adaxial leaf and stipule epidermis (Fig 3e).

2.2 Hydrocarbon accumulation between abaxial and adaxial surfaces does not differ in the stipules but substantially differs in leaflets during plant development

Pea leaves are compound leaves, composed of basal, foliaceous, leaf-like stipules, with up to three pairs of proximal leaflets and distal tendrils (Kumar et al. 2009; Mikić et al. 2011). Because pea leaf development occurs in an

acropetal fashion, the leaflets at the base of the petiole develop first and are, therefore, older than the leaflets at the tip of the petiole. Figure 4 illustrates how the stipules and leaves were labeled to account for this developmental gradient. The stipule and leaflets on the first petiole from the bottom of the pea plant are labeled as L1, and L1_1, L1_2, and so on; the pairs of leaflets on a compound leaf that is closest to the stem is labeled as L1_1 and the distal pair is labeled as L1_2 (Fig 4). The petioles rising up the stem are younger and were labeled L1, L2, etc. (Fig. 4).

Hydrocarbons of the abaxial and adaxial epidermis from *Arg* pea leaves and stipules were collected and analyzed from petioles located at different positions on the stem, which represents different stages of development (Fig 5). The predominant constituent for both the abaxial leaf surface and the stipule is the C_{31} alkane, which comprises >95% of the hydrocarbons. This C_{31} alkane accounts for only ~60% of the hydrocarbons of the adaxial leaf epidermis, the remainder being comprised of C_{25}, C_{27} and C_{29} alkanes (Table 1). The total amount of hydrocarbons did not differ between the stipule's abaxial and adaxial epidermis, whereas in leaves the abaxial epidermis accumulates ~20-fold more hydrocarbons than the adaxial epidermis (p-value>0.05) (Fig 5). Since there was no difference in hydrocarbon accumulation between the abaxial and adaxial stipule epidermis, these tissues were collectively analyzed from the 7th, 11th and 15th petiole positions. These

analyses indicate that there is little if any effect of stipule development in the accumulation of hydrocarbons in the epidermis of these organs (Fig 4).

2.3 C_{31} alkane differentially accumulates between the abaxial and adaxial surfaces and among abaxial epidermis from leaves at different developmental stages

Hydrocarbon accumulation was analyzed in the abaxial and adaxial leaflet epidermises of pairs of leaflets from the 7th, 9th, 11th, 13th and 15th petioles. On some of the petioles (e.g., 11th, 13th and 15th), multiple pairs of leaflets were accessible, and the epidermises from all available pair of leaflets were collected but analyzed separately. Accumulation of C_{25}, C_{27} and C_{29} alkanes does not differ between the abaxial and adaxial leaf epidermis, and among adaxial and abaxial leaf epidermis at different developmental stages (Supplemental Table 1). Only the dominant C_{31} alkane differentially accumulates as the abaxial leaflet undergoes development (Fig 6). Specifically, in the leaflet, the abaxial epidermis accumulated ~9-24 fold more C_{31} alkane than the adaxial epidermis (Fig 6). Contrary to the observations with the epidermis of stipules, the abaxial epidermis from leaves accumulate more C_{31} alkane toward the base of the plant (i.e. older leaves) than those from younger leaves (nearer the top of the plant) (p-value>0.1, based on t-test analysis). In addition, a gradient of C_{31} alkane accumulation was observed on leaflets examined on each petiole layer. Namely, the abaxial epidermis from the second pair of leaflets tested at the 11th, 13th and 15th petiole layer (i.e.,

L11_2, L13_2, and L15_2) produced less C_{31} alkane than the first pair of leaflets (L11_1, L13_1, and L15_1, respectively) (p-value<0.05) (Fig 6). However, the accumulation of the C_{31} alkane in the adaxial epidermis was unaffected by leaf development (Fig. 6).

2.4 The effect of development on the accumulation of fatty acids, aldehydes, alcohols and hydrocarbons in leaves and stipules

Similar to hydrocarbons, the accumulation of aldehydes, alcohols, and fatty acid differed during leaf and stipule development in the abaxial epidermis, but was unaffected for the adaxial epidermis. On the abaxial epidermis, total surface lipid accumulation, including fatty acids, alcohols, hydrocarbons and aldehydes is higher at the L8 petiole layer (older) than the L12 petiole layer (younger) (p-value<0.05) (Fig 7a). In all of these samples, the predominant surface lipid was hydrocarbons, particularly the C_{31} alkane (Fig 7b). The second most abundant surface lipid was the primary alcohols ranging in chain lengths from C_{26} to C_{30}; the abaxial leaf epidermis of the L8 petiole layer accumulates more C_{26}, C_{27} and C_{29} than the L12 petiole layer, but for C_{18}, C_{29} alcohols accumulation was similar among the L8, L10 and L12 petiole layers (Fig 8d). Of the fatty acids, the C_{16}, C_{18}, $C_{18:1}$, and C_{24} are higher in the L8 petiole layer than in L12 layer, while the accumulation of the C_{10}, C_{12}, C_{14}, C_{20} and C_{22} fatty acids are unaffected between the L8 and L12 petiole layers (Fig 7c).

3. Discussion

3.1 Surface lipids accumulate differentially between the abaxial and adaxial epidermis of the leaf but not the stipule

Difference of surface lipids between the adaxial and abaxial pea leaf epidermis has been reported previously (Gniwotta et al. 2005; P.J. Holloway 1977). Our results are in good accordance to previous findings that indicated that abaxial leaf epidermis contains more alkanes while adaxial leaf epidermis consists of more alcohols and C_{31} consists of more than 90% of total hydrocarbons in abaxial leaf epidermis (Gniwotta et al. 2005). However, we only detected odd-numbered hydrocarbons with chain length from C_{25} to C_{31}, whereas in cultivars of Avanta, Lincoln and Maiperle, trace amount of C_{29}, C_{33} and also even-numbered alkanes, C_{30} and C_{32} were reported (Gniwotta et al. 2005). Fatty acid with longest chain length that we detected is C_{24} fatty acids, and only C_{26} aldehyde was detected, and C_{18} and C_{26} to C_{30} alcohols were detected. However, in cultivars of Avanta, Lincoln and Maiperle, C_{26} and C_{28} fatty acid were detected, in addition to C_{26} aldehyde, C_{28} and C_{30} aldehydes were also reported and there were more alcohols were detected, like C_{24} and C_{25}, alcohols (Gniwotta et al. 2005). These difference between our results and results for cultivars of Avanta, Lincoln and Maiperle are probably due to the fact that they are different genotypes of *Pisum sativum* and the different sampling methods were used in the two studies. In our study, we used pea plant with the *Arg* mutant, which allows for easy removal of the epidermis from underlying tissue and free of palisade cell wall fragments (Jewer et al. 1985).

However, for cultivars of Avanta, Lincoln and Maiperle, gum arabic, an aqueous glue was applied to mechanically remove surface compounds (Gniwotta et al. 2005). The wax removal by gum arabic relies on the mechanical interaction between adhesive and wax films (Jetter et al. 2000).

Differences between the adaxial and the abaxial wax composition have been reported for different plants, such as the evergreen tree, conifer, ryegrass and rose etc. (Dragota and Riederer 2007; Ringelmann et al. 2009; Wen et al. 2006). The biological function of this difference about the surface lipids between the abaxial and adaxial leaf epidermis is not clear. The difference might contribute to the ability of the two surfaces to differentially protect against pathogen infection and water loss and different physical requirements for the abaxial and adaxial leaf surfaces. The pathogen *Blumeria graminis* has been reported to primarily infect the adaxial leaf surfaces of ryegrass (*Lolium* spp.) whereas the abaxial leaf surfaces were rarely infected (Carver et al. 1990). Similar to our observations in pea, the adaxial epicuticular waxes of ryegrass were dominated by alcohols and the abaxial fraction primarily consisted of *n*-alkanes (Ringelmann et al. 2009). In pea, the spore germination efficiency and appressoria formation rate of a pathogen, *Erysiphe pisi,* on the abaxial leaf surface is lower than on the adaxial leaf surface (Gniwotta et al. 2005). In addition, in pea with reduce surface lipids, the insect attachment force to the leaf is considerably enhanced (Gorb et al. 2008). In contrast, on the side with more surface lipids, the insect and pathogen density decreased

(Chang et al. 2004; Chang et al. 2006; White and Eigenbrode 2000a, b). In addition, the abaxial leaf surface contains most of the stomata, and the stomata can open greater in abaxial than in adaxial epidermis of leaves (Donkin et al. 1982; Hey et al. 1997; Jewer et al. 1982; Jewer et al. 1985; Pemadasa 1981, 1982). The high alkane content in the abaxial leaf epidermis might contribute to preventing water looses when the stomata open for gas exchange.

Abaxial leaf epidermis and stipule epidermis produced more fatty acids (for example, C_{22} and C_{24} fatty acids), but less palmitic acid and stearic acid than adaxial leaf epidermis, which is consistent with the fact that hydrocarbons in abaxial leaves and stipule epidermis uses very long chain fatty acids as precursors. Dithioerythritol and mercaptoethanol have been found to inhibit C_{31} alkane synthesis and causes C_{32} aldehyde accumulation in pea (Buckner and Kolattuk 1973). In addition, an aldehyde and alcohol generating fatty acyl-CoA reductase and the decarbonylase were partially purified from *Pisum sativum* leaves (Schneider-Belhaddad and Kolattukudy 2000; Vioque and Kolattukudy 1997). In the abaxial leaflet epidermis, there are more alkanes, aldehdyes and less alkane as compared to the adaxial leaflet epidermis in pea. These results might indicate that in adaxial leaf epidermis, the biofunctional fatty acyl-CoA mainly produces alcohols whereas in the abaxial leaf epidermis, it mainly generates aldehydes, which are converted to alkanes by aldehyde decarbonylase (Fig 9).

3.2 Differential temporal and spatial accumulation patterns of surface lipids in abaxial and adaxial epidermises

The surface lipids of the leaves and stipules, in terms of the fatty acids, alcohols, aldehydes and hydrocarbons that accumulate on their epidermises are similar. However, whereas the composition of the surface lipids of the stipule and adaxial leaf epidermis is unaffected by age and petiole position, the abaxial leaf epidermis is affected by these developmental changes. Older abaxial epidermis (at 8th petiole) accumulated ~20% more surface lipids than the adaxial epidermis (at 12th petiole). The total amount, chemical composition and physical form of leaf surface lipids is highly variable among different plant species, and can be affected by environmental factors such as light and humidity (PostBeittenmiller 1996) as well as developmental factors (Blaker and Greyson 1988; Kim et al. 2012; Reina-Pinto and Yephremov 2009; Rhee et al. 1998). The effect of age on the development of surface lipids has been explored in a variety of species (Baker and Hunt 1981; Blaker and Greyson 1988; Jenks et al. 1996; Jetter and Schaffer 2001; Rhee et al. 1998). For example, in Arabidopsis stem, during development, alkanes, aldehydes and esters increase in accumulation, and free fatty acids, alcohols and ketones decrease in accumulation (Jenks et al. 1996). In maize, accumulation of surface lipids on leaves is both age-related (an individual leaf at different times) and leaf position-related (leaves at different position on a plant of a given age)

(Blaker and Greyson 1988). In leek leaves, induction of surface lipid accumulation is primarily controlled by developmental factors but is also affected by environmental factors (Rhee et al. 1998). However, in *Prunus laurocerasus* leaves, the absolute amount and the relative composition of surface compounds remain constant after leaf development is completed (Jetter and Schaffer 2001; Jetter et al. 2000). Our result that the surface lipids are at the same level in the adaxial leaf and stipule epidermises at different petiole positions, but increased in older abaxial leaf epidermis might imply that pea leaves, like *Prunus laurocerasus* leaves, stop accumulating surface lipids or only accumulate slightly more surface lipids after the leaf development is completed.

In summary, this study found that surface lipids show a differential accumulation patterns between the abaxial and adaxial epidermises from leaves but such differential is does not occur in the two epidermises of the stipule. In addition, the surface lipids in abaxial leaf epidermis are influenced by the age of the leaf in relation to development and position on the plant-body, although the underlying mechanism is still unclear.

4. Experimental procedures

4.1 Plant material and hydrocarbon extraction

Seeds of pea (*Pisum sativum*) Marx 4 W6 17667 were obtained from the USDA Western Regional Plant Introduction Station at Pullman, Washington. Marx 4 W6 17667 is called *Arg* pea plant in this paper. *Arg* pea plant carries

mutation of a, Arg, Bt, er, le, PA and Pl, which are not relevant to wax production in the surface of stipule and leaves. The detailed information about those mutations can be found at USDA agricultural research service website (http://www.ars.usda.gov/Main/docs.htm?docid=14132). Plants were grown in BACCTO premium potting soil (Michigan Peat Company, Houston, TX): perlite (Miracle-Gro®) (3:1). Plants were grown in a growth chamber under the following conditions: 16 h day/8 h night; 25℃ day/18℃ night; light intensity 300 to 400 μmol photons m^{-2} s^{-1} and 70% relative humidity.

4.2 Sampling pea leaf and stipule epidermis

The *Arg* pea plants carry the *Argentum* (Largeau et al.) mutation, which causes the presence of airspace under epidermis, allowing for easy separation of the epidermis from underlying tissue. Abaxial and adaxial epidermal tissue was harvested by peeling using forceps at 5 weeks after seedling germination for metabolite extraction and analyses. Pieces of epidermis from abaxial or adaxial side of the same leaves were collected separately for leaves and combined for stipule. Prior to metabolite extraction, epidermal samples were lyophilized in a FreeZone 4.5 Liter Freeze Dry System (Labconco, MO) and powderized with a Mixer Mill MM301 (Retsch, Germany). Immediately prior to extraction of hydrocarbons, 5 μg of the internal standard, hexacosane (1 mg/mL) (Fluka, WI) was applied directly to approximately 10 mg of tissue. HPLC-grade hexane (Fisher Scientific, NJ; 1.5 mL) was added to the tissue and samples were sonicated for 15 min. The supernatant was sonicated two

more times. To analyze all of the metabolites (e.g. hydrocarbons, alcohols, fatty acids and aldehydes) in the epidermis, the combined supernatant were dried and silylated by 70 uL of bis-trimethyl silyl trifluoroacetamide with 1% Trimethylchlorosilane (BSTFA+1%TMC) at 60℃ for 30mins for GC-MS analysis. For hydrocarbon analysis, the combined supernatant for each sample was passed over a pre-prepared silica gel (J.T.Baker, NJ) column which was washed with 10 mL hexane before usage. The eluent was collected and dried in a rotary nitrogen evaporator (Organomation Associates, INC, MA) at 30℃. The dried hydrocarbon sample was dissolved in 1 mL hexane for GC-MS analysis.

4.3 Gas chromatography-mass spectrometric analysis

Chromatographic analysis was performed with a gas chromatograph (Model 6890 series, Agilent Technologies, Palo Alto, CA), equipped with a mass detector Model 5973 (Agilent Technologies, Palo Alto, CA). Chromatography was conducted with a HP-5MS cross-linked (5%)-diphenyl-(95%)-dimethyl polysiloxane column (30 m length, 0.25 mm I. D.), using helium as the carrier gas. The injection temperature was at 280℃. The oven temperature was initially at 200℃, was increased 280℃ at a rate of 4℃/min, further increased to 320℃ at a rate of 20℃/min and held at this temperature for 3 min. Peak identification was facilitated by using the NIST spectral library. To quantify the accumulation of hydrocarbons, the response of the mass-spectrometer was calibrated to the hexacosane internal standard.

4.4 Statistical methods

All metabolite data were gathered from a minimum of triplicate biological replicates. Metabolite abundances are the average of these multiple determinations (±standard error). Where appropriate, a student's t-test was conducted to determine whether the metabolite abundances are statistically different among samples.

References

Baker EA, Hunt GM (1981) Developmental-Changes in Leaf Epicuticular Waxes in Relation to Foliar Penetration. New Phytol 88:731-747

Blaker TW, Greyson RI (1988) Developmental Variation of Leaf Surface Wax of Maize, Zea-Mays. Can J Bot 66:839-846

Buckner JS, Kolattuk PE (1973) Specific Inhibition of Alkane Synthesis with Accumulation of Very Long-Chain Compounds by Dithioerythritol, Dithiothreitol, and Mercaptoethanol in Pisum-Sativum. Arch Biochem Biophys 156:34-45

Buschhaus C, Herz H, Jetter R (2007a) Chemical composition of the epicuticular and intracuticular wax layers on adaxial sides of Rosa canina leaves. Ann Bot-London 100:1557-1564

Buschhaus C, Herz H, Jetter R (2007b) Chemical composition of the epicuticular and intracuticular wax layers on the adaxial side of Ligustrum vulgare leaves. New Phytol 176:311-316

Buschhaus C, Jetter R (2011) Composition differences between epicuticular and intracuticular wax substructures: How do plants seal their epidermal surfaces? J Exp Bot 62:841-853

Caffrey JJ, J-K. C, Wurtele ES, Nikolau BJ (1998) Tissue distribution of acetyl-CoA carboxylases in leaves of leek (Allium porrum L.). Journal of Plant Physiology 153

Carver TLW, Thomas BJ, Ingersonmorris SM, Roderick HW (1990) The Role of the Abaxial Leaf Surface Waxes of Lolium Spp in Resistance to Erysiphe-Graminis. Plant Pathol 39:573-583

Cassagne C, Lessire R (1975) Studies on Alkane Biosynthesis in Epidermis of Allium-Porrum-L Leaves .4. Wax Movement into and out of Epidermal-Cells. Plant Sci Lett 5:261-268

Chang GC, Neufeld J, Durr D, Duetting PS, Eigenbrode SD (2004) Waxy bloom in peas influences the performance and behavior of Aphidius ervi, a parasitoid of the pea aphid. Entomol Exp Appl 110:257-265

Chang GC, Neufeld J, Eigenbrode SD (2006) Leaf surface wax and plant morphology of peas influence insect density. Entomol Exp Appl 119:197-205

Donkin ME, Travis AJ, Martin ES (1982) Stomatal Responses to Light and Co2 in the Argenteum Mutant of Pisum-Sativum. Z Pflanzenphysiol 107:201-209

Dragota S, Riederer M (2007) Epicuticular wax crystals of Wollemia nobilis: Morphology and chemical composition. Ann Bot-London 100:225-231

Eigenbrode SD, Stoner KA, Shelton AM, Kain WC (1991) Characteristics of Glossy Leaf Waxes Associated with Resistance to Diamondback Moth (Lepidoptera, Plutellidae) in Brassica-Oleracea. J Econ Entomol 84:1609-1618

Gniwotta F, Vogg G, Gartmann V, Carver TLW, Riederer M, Jetter R (2005) What do microbes encounter at the plant surface ? Chemical composition of pea leaf cuticular waxes. Plant Physiol 139:519-530

Gorb E, Voigt D, Eigenbrode SD, Gorb S (2008) Attachment force of the beetle Cryptolaemus montrouzieri (Coleoptera, Coccinellidae) on leaflet surfaces of mutants of the pea Pisum sativum (Fabaceae) with regular and reduced wax coverage. Arthropod-Plant Inte 2:247-259

Grimbly PE (1977) Tomato Silvering, Its Anatomy and Chimerical Structure. J Hortic Sci 52:469-473

Halloway PJ, Hunt GM, Baker EA, Macey MJK (1977) Chemical composition and ultrastructure of the epicuticular wax in four mutants of *Pisum sativum* (L). Chem Phys Lipids 20:141-155

Hey SJ, Bacon A, Burnett E, Neill SJ (1997) Abscisic acid signal transduction in epidermal cells of Pisum sativum L Argenteum: Both dehydrin mRNA accumulation and stomatal responses require protein phosphorylation and dephosphorylation. Planta 202:85-92

Hoch HC, Pratt C, Marx GA (1980) Sub-Epidermal Air Spaces - Basis for the Phenotypic-Expression of the Argenteum Mutant of Pisum. Am J Bot 67:905-911

Javelle M, Vernoud V, Rogowsky PM, Ingram GC (2011) Epidermis: the formation and functions of a fundamental plant tissue. New Phytol 189:17-39

Jenks MA, Tuttle HA, Feldmann KA (1996) Changes in epicuticular waxes on wildtype and Eceriferum mutants in Arabidopsis during development. Phytochemistry 42:29-34

Jetter R, Schaffer S (2001) Chemical composition of the Prunus laurocerasus leaf surface. Dynamic changes of the epicuticular wax film during leaf development. Plant Physiol 126:1725-1737

Jetter R, Schaffer S, Riederer M (2000) Leaf cuticular waxes are arranged in chemically and mechanically distinct layers: evidence from Prunus laurocerasus L. Plant Cell Environ 23:619-628

Jewer PC, Incoll LD, Shaw J (1982) Stomatal Responses of Argenteum - a Mutant of Pisum-Sativum-L with Readily Detachable Leaf Epidermis. Planta 155:146-153

Jewer PC, Neales TF, Incoll LD (1985) Stomatal Responses to Carbon-Dioxide of Isolated Epidermis from a C-3 Plant, the Argenteum Mutant of Pisum-Sativum-L and a Crassulacean-Acid-Metabolism Plant Kalanchoe-Daigremontiana Hamet and Perr. Planta 164:495-500

Kim KW, Koo YK, Yoon CJ (2012) Age-related leaf characteristics of surface features and ultrastructure of Dendropanax morbifera. J Electron Microsc 61:37-46

Kumar S, Mishra RK, Kumar A, Srivastava S, Chaudhary S (2009) Regulation of stipule development by COCHLEATA and STIPULE-REDUCED genes in pea Pisum sativum. Planta 230:449-458

Largeau C, Casadevall E, Berkaloff C (1980) The Biosynthesis of Long-Chain Hydrocarbons in the Green-Alga Botryococcus-Braunii. Phytochemistry 19:1081-1085

Macey MJK, Barber HN (1970a) Chemical Genetics of Wax Formation on Leaves of Brassica-Oleracea. Phytochemistry 9:13-&

Macey MJK, Barber HN (1970b) Chemical Genetics of Wax Formation on Leaves of Pisum-Sativum. Phytochemistry 9:5-&

Merida T, Schonherr J, Schmidt HW (1981) Fine-Structure of Plant Cuticles in Relation to Water Permeability - the Fine-Structure of the Cuticle of Clivia-Miniata Reg Leaves. Planta 152:259-267

Mikić A, Mihailović V, Ćupina B, Kosev V, Warkentin T, McPhee K, Ambrose M, Hofer J, Ellis N (2011) Genetic Background and Agronomic Value of Leaf Types in Pea (Pisum sativum). Genetics and Breeding 48:275-284

Nikolau BJ, Wurtele ES, Stumpf PK (1984) Tissue distribution of acetyl-coenzyme a carboxylase in leaves. Plant Physiol 75:895-901

P.J. Holloway GMH, E. A. Baker and M.J.K Macey. (1977) Chemical composition and ultrastructure of the epicuticular wax in four mutants of *Pisum sativium* (L). Chemistry and Physics of Lipids 20:141-155

Pemadasa MA (1981) Abaxial and Adaxial Stomatal Behavior and Responses to Fusicoccin on Isolated Epidermis of Commelina-Communis L. New Phytol 89:373-384

Pemadasa MA (1982) Differential Abaxial and Adaxial Stomatal Responses to Indole-3-Acetic-Acid in Commelina-Communis L. New Phytol 90:209-219

PostBeittenmiller D (1996) Biochemistry and molecular biology of wax production in plants. Annu Rev Plant Phys 47:405-430

Reina-Pinto JJ, Yephremov A (2009) Surface lipids and plant defenses. Plant Physiol Bioch 47:540-549

Rhee Y, Hlousek-Radojcic A, Ponsamuel J, Liu DH, Post-Beittenmiller D (1998) Epicuticular wax accumulation and fatty acid elongation activities are induced during leaf development of leeks. Plant Physiol 116:901-911

Riedel M, Eichner A, Meimberg H, Jetter R (2007) Chemical composition of epicuticular wax crystals on the slippery zone in pitchers of five Nepenthes species and hybrids. Planta 225:1517-1534

Ringelmann A, Riedel M, Riederer M, Hildebrandt U (2009) Two sides of a leaf blade: Blumeria graminis needs chemical cues in cuticular waxes of Lolium perenne for germination and differentiation. Planta 230:95-105

Schneider-Belhaddad F, Kolattukudy P (2000) Solubilization, partial purification, and characterization of a fatty aldehyde decarbonylase from a higher plant, Pisum sativum. Arch Biochem Biophys 377:341-349

Shin KH, Choi IM, Chung KH, Lee JM, Park HS (2010) Morphological Development and Chemical Composition of Epicuticular Wax Crystals in 'Campbell Early' Grape. Hortic Environ Biote 51:253-256

Vioque J, Kolattukudy PE (1997) Resolution and purification of an aldehyde-generating and an alcohol-generating fatty acyl-CoA reductase from pea leaves (Pisum sativum L). Arch Biochem Biophys 340:64-72

Wen M, Buschhaus C, Jetter R (2006) Nanotubules on plant surfaces: Chemical composition of epicuticular wax crystals on needles of Taxus baccata L. Phytochemistry 67:1808-1817

White C, Eigenbrode SD (2000a) Effects of surface wax variation in Pisum sativum on herbivorous and entomophagous insects in the field. Environ Entomol 29:773-780

White C, Eigenbrode SD (2000b) Leaf surface waxbloom in Pisum sativum influences predation and intra-guild interactions involving two predator species. Oecologia 124:252-259

Wurtele ES, Nikolau BJ (1986) Enzymes of Glucose-Oxidation in Leaf Tissues - the Distribution of the Enzymes of Glycolysis and the Oxidative Pentose-Phosphate Pathway between Epidermal and Mesophyll Tissues of C-3-Plants and Epidermal, Mesophyll, and Bundle Sheath Tissues of C-4-Plants. Plant Physiol 82:503-510

Wurtele ES, Nikolau BJ, Conn EE (1984) Tissue Distribution of Beta-Cyanoalanine Synthase in Leaves. Plant Physiol 75:979-982

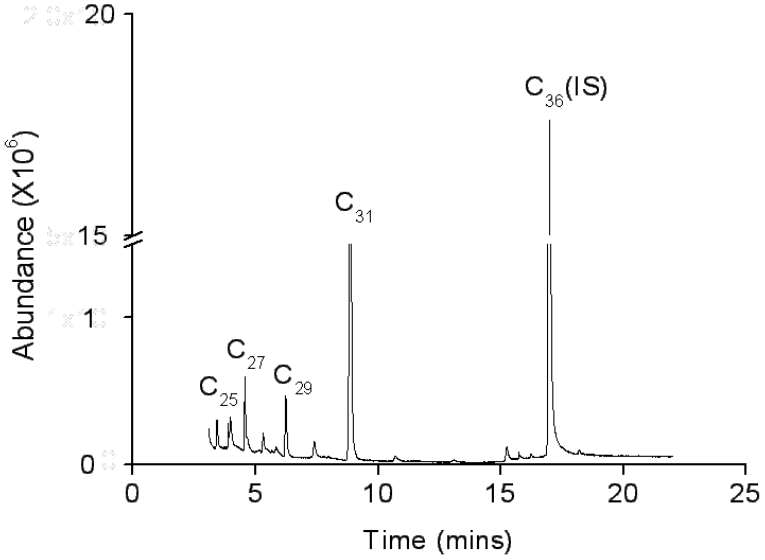

Figure 1. Gas chromatograph analysis of hydrocarbons in hexane extract from pea leaf and stipule epidermis after silica gel purification.

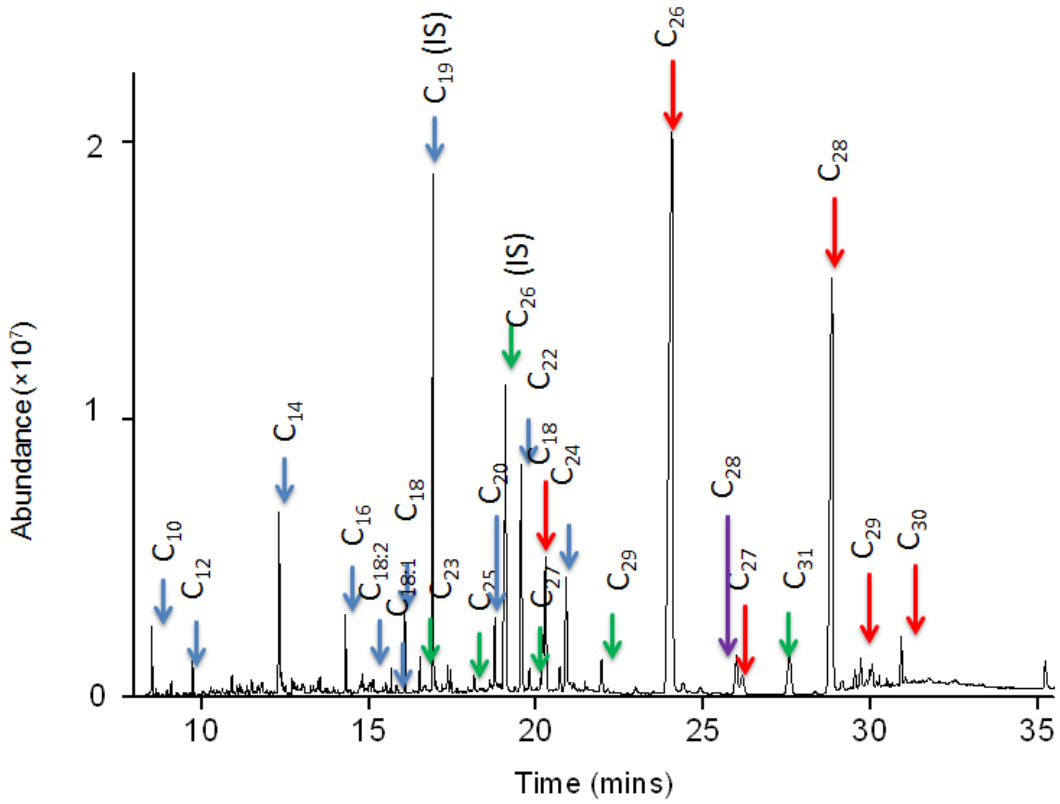

Figure 2. Gas chromatogram of hexane extraction from pea leaf and stipule epidermis without silica gel purification. Blue arrow - fatty acid; red arrow - alcohol, purple arrow - aldehyde, green arrow-alkane.

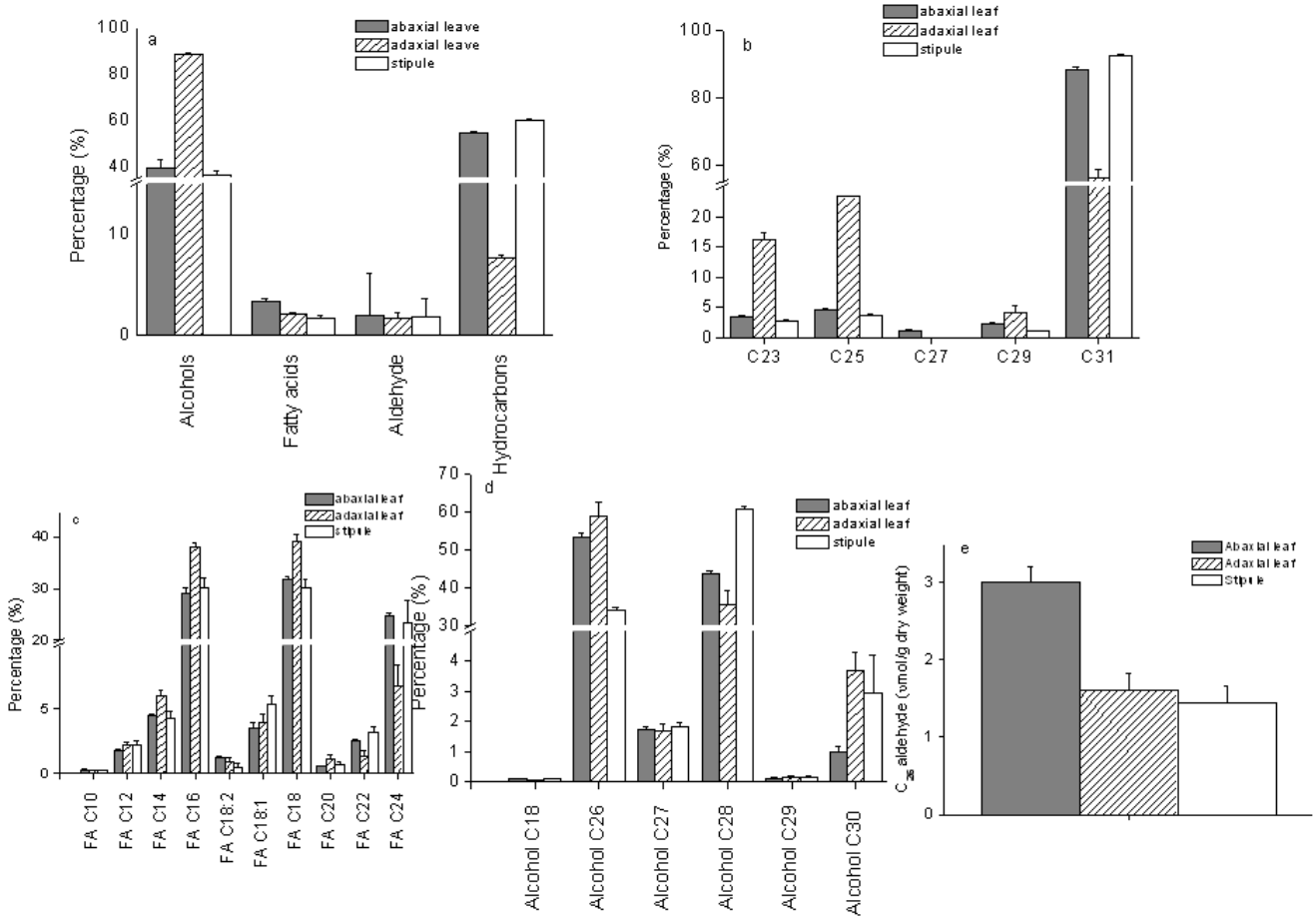

Figure 3. Percentage of individual constituents among hydrocarbons, alcohols, fatty acids and aldehydes in *Arg* pea plant.

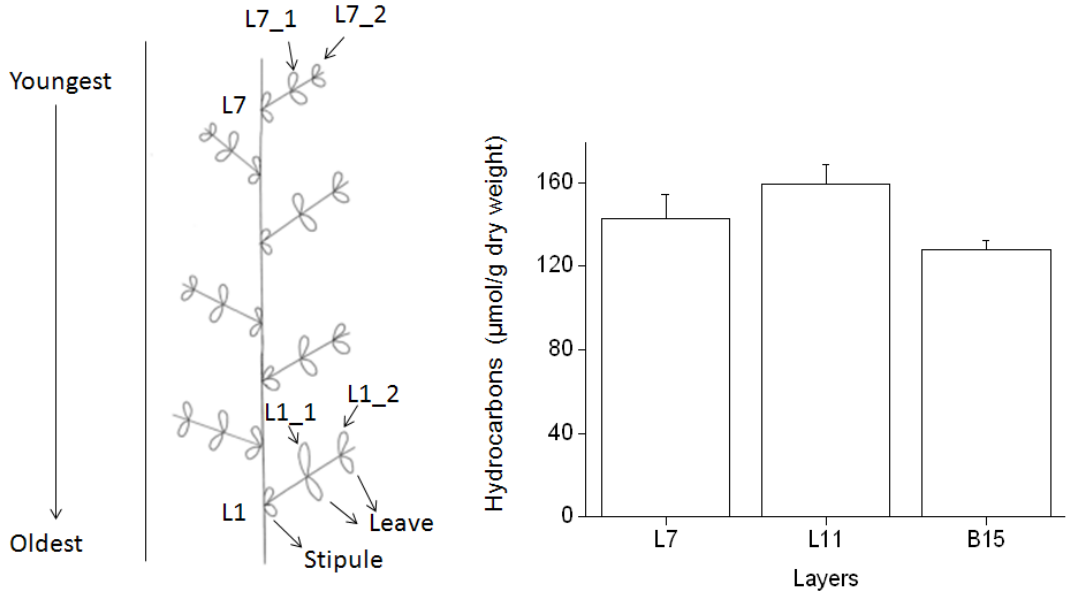

Figure 4. No accumulation difference of hentriacontane in the pea stipule epdiermis at different developmental stage. Schematic representation of a pea plant and labeling system to indicate the development of leaves and stipule was shown on the right.

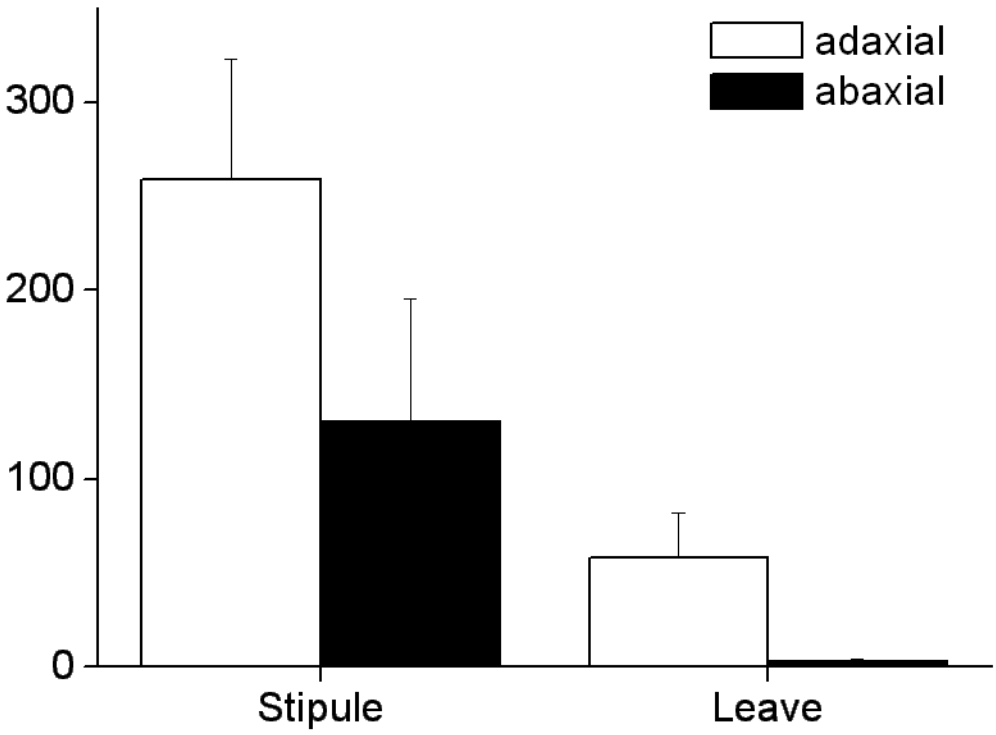

Figure 5. Hydrocarbons accumulated in the adaxial and abaxial leaflet epidermises of *Pisum sativum*.

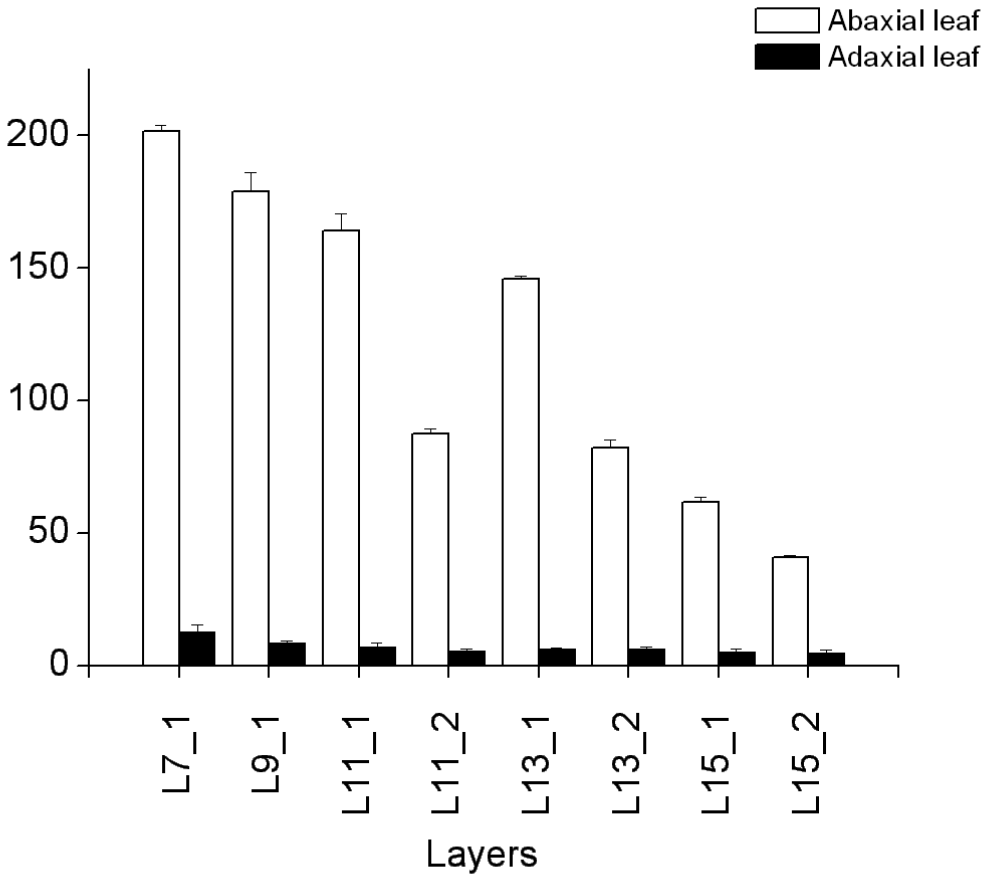

Figure 6. Hentriacontane accumulated in the abaxial leaf epidermis of leaves at different developmental stages.

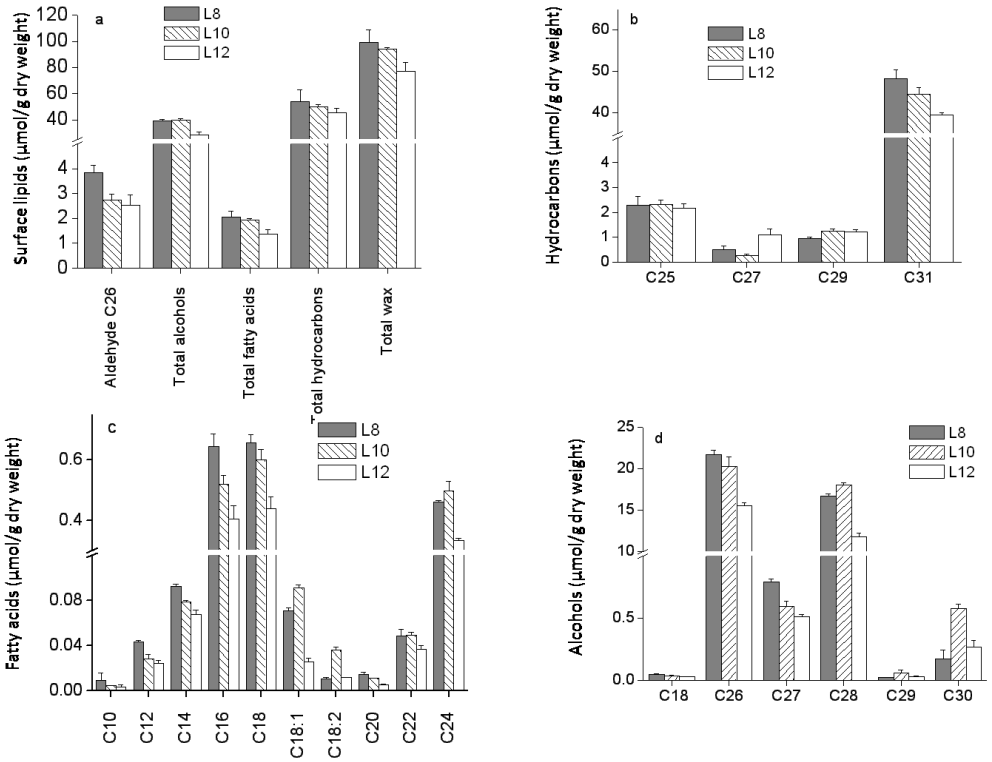

Figure 7. Effect of development on the distribution of hydrocarbons, alcohols, fatty acids and aldehydes in the epicuticular lipids of the abaxial leaf epidermis.

Table 1. Distribution alkanes among different chain lengths in abaxial and adaxial leaf epidermis and stipule epidermis

Alkanes	Abaxial leaf epidermis	Stipule epidermis	Adaxial leaf epidermis
C25	0.33%±0.15%	0.08%±0.02%	2.71%±0.40%
C27	0.28%±0.17%	0.12%±0.07%	5.33%±0.65%
C29	0.64%±0.16%	0.80%±0.18%	4.79%±0.50%
C31	98.75%±0.46%	99.01%±0.24%	87.18%±1.32%

Supplementary Table 1. Epicuticular lipids of abaxial and adaxial leaf epidermis, and stipule epidermis at different developmental stages (nmol/g dry weight)

	Abaxial leaf epidermis			Stipule epidermis			Adaxial leaf epidermis		
	L8	L10	L12	L8	L10	L12	L8	L10	L12
FA C10	9.4±6.6	3.1±2.4	4.6±0.2	3.1±0.4	4.2±0.7	1.8±0.6	5.8±2.8	3.6±0.6	1.8±0.1
FA C12	43.4±1.3	24.5±2.1	28.6±3.7	34.4±5.4	44.1±14.4	18±3.2	26.6±6.7	36.3±6.7	21.4±3
FA C14	92.4±2.2	67.4±4.3	78.7±1.4	83.6±21.1	88.2±28.7	42.2±14.1	99.5±17.6	76±13.9	57.5±10
FA C16	643.5±42	403.2±43.6	518.6±29.5	548.2±142.8	558.3±123.1	317.2±61.3	562.2±151.2	532±69.9	391.4±52.8
FA C18	657±27.9	438.5±39	600.4±35.1	525.8±162.3	578.9±125.6	325.3±64.4	597.1±165.3	542.6±72.1	401.8±64.3
FA C18:1	71.1±2.3	25.9±2.9	90.8±2.8	103.8±22.7	83.3±22.6	54±4.5	35.6±1.6	55.5±12.5	46.6±8.9
FA C18:2	10.9±0.9	12.1±0.1	35.9±2.5	0.0±0.0	2.8±2.8	12.9±4.5	4.6±4.6	14.4±8.3	9.7±5.8
FA C20	14.8±1.4	5.5±0.2	11.4±0.1	16.8±8.3	12±1.6	5.3±0.5	18.3±4.6	21.3±11.7	5.3±0.4
FA C22	48.7±5.7	36.8±3	49.2±2.5	44.4±16.6	53.6±4.6	41.5±2.5	22.4±7.4	26.2±12.7	6.2±0.1
FA C24	459.5±6.2	333.1±1.9	498.6±29.9	164.2±164.2	436±10.7	380.5±85.7	125.8±67.8	68.5±11.4	72.3±36.6
Alcohol C18	46.7±3.6	25.7±2.2	36.2±1.8	34.1±5.9	38.8±9.5	19.5±2.4	31.3±5.3	34±4.8	15.6±1.4
Alcohol C26	21708.5±508.7	15502.4±350.2	20239±1178.9	9936.8±3317	10763.2±969.4	10904.8±1446.3	41829.2±5534.7	37284.3±4810.3	39344.1±6360.5
Alcohol C27	789.2±27.7	513.2±15.6	596.6±36.9	643±224.8	654±88.7	425.5±75.6	1218.6±240.3	1419.4±279.5	738±88.4
Alcohol 28	16678.2±218.7	11800.3±372.7	18022.5±241	17995±5655.5	19806.6±1876.9	18415.9±2892.9	29247.7±5082.8	27990.6±3292.2	16818.8±5848.8
Alcohol C29	1.9±29.9	3.2±59.5	20.6±27.8	27.8±26.1	26.1±71.4	32.5±24	149.8±32.4	148.5±24.4	53.4±19.5
Alcohol C30	168.8±72.5	268.9±49	576.2±35.9	2216.9±1680.3	485±80.7	487.7±135.8	2468.7±1172.8	3058±246.7	1840.7±625.8
Aldehyde C26	3829.5±6.8	2525.1±126.5	2751.8±229.1	1546.3±665.5	1347.3±238.9	1486.7±346.6	1978±687	1918.6±37.2	997.1±247
Alkane C23	2044.7±12.4	1280.7±18.6	1687±350.2	1406.4±286	1917.6±424.8	858±92.9	1101.5±177.7	1015.1±101.5	741.9±179.1
Alkane C25	2294.6±141.4	2177±67.2	2309.8±193.8	1888.2±497.9	2630.2±565.8	1361.6±147.6	1545.9±235	1404.6±136.7	1118.9±283.4
Alkane C27	496.5±3.4	1080.9±46.2	261.9±11.9	0.0±0.0	0.0±0.0	0.0±0.0	0±0	0±0	0±0
Alkane C29	951.7±26.9	1226.7±14	1247.5±73.7	590.9±302.1	456.4±165.1	597.6±25.6	150.9±150.9	469.4±95.9	142.6±83.4
Alkane C31	48108.6±9234.2	39497.9±447	44360.9±1603.6	47571.5±13621.9	51131.1±9016.1	43421.9±2623.5	2817.4±430.1	4140.3±787.9	2803.8±465
Total alcohols	39414.4±646.8	28140.7±303.4	39530.3±1400.1	30853.9±10017.2	31773.9±2908.3	30325.1±4487.6	74945.6±10509.5	69935.2±8003.7	58810.8±6842.1
Total fatty acids	2051.2±34.8	1350.5±88.7	1917.2±74.6	1524.9±423.2	1862±296.8	1199.2±220.8	1498.3±399	1376.7±171.7	1014.4±84.5
Total hydrocarbons	53896.3±9148.3	45263.5±432.5	49867.4±1868.9	51457.2±14663.1	56135.5±9917.9	46239.2±2760.1	5615.9±763.5	7029.6±1062.5	4807.4±823.5
SUM	99191.6±9519.9	77279.8±816.2	94066.8±1190.6	85382.4±25394.1	91118.8±12655.8	79250.4±6390.9	84037.9±10815	80260.3±8955.7	65629.8±7654.4

CHAPTER 6. HYDROCARBON ACCUMULATION IN IN *BOTRYOCOCCUS BRAUNII* EXPOSED TO DIFFERENT AVAILABILITIES OF CARBON, bNITROGEN AND PHOSPHATE

Wenmin Qin, Marna D. Yandeau-Nelson, Basil J. Nikolau.

Center for Metabolic Biology, Plant Science Institute

Center for Biorenewable Chemical

Department of Biochemistry, Biophysics and Molecular Biology

Iowa State University, Ames, IA 50010

Email: dimmas@iastate.edu

Telephone: 515-294-0347

Fax number: 515-294-0453

Abstract

Botryococcus braunii (*B.braunii*) can accumulate up to 70% of its dry weight as hydrocarbons. The hydrocarbon production by the race A strain, UTEX 572 has been investigated with different carbon, nitrogen and phosphate availability. The majority of hydrocarbons produced (>90%) were odd-numbered, linear alkanes and alkenes of 23 to 33 carbon-chain lengths, along with minor amounts of even-numbered hydrocarbons ranging from 24 to 30 carbons. *B. braunii* cells grown in high carbon (2% CO_2), low nitrogen and low phosphate conditions (in Waris medium) accumulated ~3-fold more hydrocarbons as compared to those grown in low carbon (ambient CO_2), high

nitrogen and high phosphate conditions (in modified B3N medium). In both media, the abundance of the major hydrocarbons, alkenes and odd-number hydrocarbons decreased (~75% for alkene and ~92% for odd-numbered hydrocarbons at time of inoculation), reached the lowest (~50% at 3 days for alkenes and ~88% for odd-numbered hydrocarbons at day 5) and then increased (~90% at day 5 for alkenes and ~97% at day 9 for odd-numbered hydrocarbons). This study shows that *B. braunii* can accumulate higher levels of hydrocarbons in medium with high CO_2 concentration and low nitrogen and phosphate nutrients.

Key words *Botryococcus braunii* hydrocarbon carbon nitrogen phosphate

Introduction

Botryococcus braunii is a unicellular photosynthetic microalgae that is widely distributed in fresh and brackish water of all continents (Chitis 1980). *B. braunii* has attracted a lot of interest due to its ability to accumulate large quantities of hydrocarbon and thus potential application and profitability for liquid fuel production (Tsukahara and Sawayama 2005). Based on the chemical structures of hydrocarbons, three races (A, B and C) of *B. braunii* have been defined. Only Race A produces linear alkanes, predominantly unbranched n-alkadienes and trienes with odd carbon number chain lengths, from C_{25} to C_{31}, which can accumulate to account up to 16-70% of the dry weight of the cell-mass (Rao et al. 2007). Production levels as well as chemical composition of these hydrocarbons vary among different *B. braunii* strains and

are influenced by growth conditions. For example, strain SAG 30.81 produces 30–40% hydrocarbons, whereas LB 572 accumulates 20–30% hydrocarbons irrespective of the tested media and culture conditions, even though both strains belong to race A (Dayananda et al. 2007). In addition, both these strains produce more hydrocarbons when they are constantly agitated (rather than not agitated), are grown under continuous illumination (rather than a 16h-8 h light-dark cycle), and are grown in medium BG11 (rather than medium BBMa) (Dayananda et al. 2007).

Analogous to other neutral lipids, the physiological role of hydrocarbons might be as energy reserves, and their synthesis is regulated qualitatively and quantitatively by a number of environmental factors, such as light intensity, temperature, and nutrients (Benamotz et al. 1985; Coleman et al. 1988; Shifrin and Chisholm 1981). CO_2 is efficiently fixed by *B. braunii* and can therefore be used to cultivate *B. braunii* (Yang et al. 2004). Aeration with CO_2 is regarded as best for *B. braunii* growth (Ranga Rao and Ravishankar 2007; Tanoi et al. 2011; Yoo et al. 2010). In addition, in various *B. braunii* strains, 2 % CO_2 has been reported to increase hydrocarbon accumulation by ~20 % (Ge et al. 2011b; Ranga Rao and Ravishankar 2007). It is generally recognized that nitrogen and phosphorus are also necessary for growth (Weetall 1985). Nitrate has been reported to be used as a sole nitrogen source for *B. braunii* over a range of 2-4 mM, and nitrite at 8 mM concentration totally inhibited the growth of *B. branii* (Yang et al. 2004). However, a deficiency in nitrogen favors

hydrocarbon accumulation (Benamotz et al. 1985; Choi et al. 2011; Shifrin and Chisholm 1981; Singh 2003; Singh and Kumar 1992). For *B. braunii* strain UTEX 572 for example, reducing nitrate from 3.66 mM to 0.04 mM, induced lipid production by 2-fold to ~630 mg/g (Choi et al. 2011). In contrast, excess phosphate can noticeably increase hydrocarbon production (Casadevall et al. 1985). The high concentration of phosphate might be used to maintain N:P ratio, which is known to influence the lipid content of various algae (Casadevall et al. 1985). The optimum concentrations of potassium phosphate for growth and lipid production were 0.058 and 0.083 g/L respectively for *B. braunii* strain LB 572 (Tran et al. 2010).

In this study, we identified and characterized hydrocarbons from *B. braunii* strain UTEX 572. In addition to the odd-numbered hydrocarbons, which have been reported in previous studies, we also detected even-numbered hydrocarbons, which accounted for about 10% of the hydrocarbons. This alludes that there might be two different hydrocarbon biosynthetic pathways, or that different fatty acid pools are being accessed for hydrocarbon production. Furthermore, we used two different media, one with high carbon, low nitrogen and phosphate nutrients (Waris medium, aerated with air containing 2% CO_2) and the other with low carbon, high nitrogen and phosphate nutrients (modified B3N medium at ambient air) to investigate the effect of carbon, nitrogen and phosphate nutrients on the hydrocarbon accumulation in *B. braunii*.

Materials and Methods

B. braunii strains and growth media

The *B. braunii* Race A strain, UTEX 572 was used throughout this study, which was obtained from The Culture Collection of Algae (UTEX) at the University of Texas, Austin. Modified Chu-13 medium, modified B3N medium and Waris medium were used (Brown et al. 1969; Largeau et al. 1980b; Mcfadden and Melkonian 1986). The recipe of these three medium were listed in Table 1. Modified B3N medium have the highest nitrogen (8.82 mM) and phosphate (1.72 mM) concentrations, followed by Modified Chu13 medium (nitrogen: 3.7 mM, phosphate: 0.46 mM), and Waris medium have the lowest nitrogen (0.98 mM) and phosphate (0.151 mM) concentrations. Stock cultures of UTEX 572 were cultivated on slants of modified B3N medium. Pre-cultures were grown in 250 mL Erlenmeyer flasks in a shaking incubator at 100 rpm. Growth conditions were maintained at 25°C; light intensity of 120 μmol photons.m^{-2}.s^{-1}, and included a 16-h light/8-h dark diurnal cycle. For maintenance of *B. braunii*, cultures were transferred every 3 weeks where 25 mL of culture was added to 100 mL fresh modified Chu 13 medium (Templier et al. 1991a).

To investigate hydrocarbon accumulation of *B. braunii* exposed to different availabilities of carbon, nitrogen and phosphate nutrients, *B. braunii* cells were first grown in modified Chu13 medium to high cell density. Cells were collected by centrifugation at 800 ×g and transferred to two different media, the modified B3N medium with high nitrogen and phosphate

concentration and without aeration with 2% CO_2 (low carbon), and the Waris medium with low nitrogen and phosphate concentration but aerated with air containing 2% CO_2 (high carbon).

Growth curves were obtained from dry weight measurements taken at 2 days intervals from the time of transferring. These where obtained by withdrawing a 50 ml aliquot of the culture, pelleting the cells by centrifugation at 2500 g for 10 min, and lyophilizing the cell-pellet. Pellets were then weighed to obtain the dry weight measurements.

Hydrocarbons were extracted from cells, which were collected by centrifugation at 1000×g and 4℃ for 10 min. Freshly collected cells were flash-frozen in liquid nitrogen and stored at -80℃. Before extracting the hydrocarbons, cell-pellets were lyophilized using a FreeZone 4.5 Liter Freeze Dry System (LabConco, MO) and ground by using GenoGrinder 2000 (Spex CertiPrep ,NJ).

Hydrocarbon extraction and purification

Immediately prior to extraction of hydrocarbons, 10 µg of the internal standard, hexacosane (1 mg/mL) (Fluka, WI) was applied directly to ~100 mg of tissue. HPLC-grade hexane (Fisher Scientific, NJ; 1.5 mL) was added to the tissue and samples were sonicated for 15 min. After centrifugation at 13,000 g for 1 min, the supernatant was collected. The hexane extraction and centrifugation steps were repeated for two more times. The combined supernatant for each sample was passed over a pre-prepared silica gel

(J.T.Baker, NJ) column and the column was washed with 10 mL hexane. The eluent was collected and dried in a rotary nitrogen evaporator (Organomation Associates, INC, MA) at 30℃. The dried hydrocarbon sample was dissolved in 1 mL hexane for GC-MS analysis.

Hydrogenation reaction

To confirm the nature of unsaturated hydrocarbons, hydrocarbon extracts were hydrogenated with H_2 using palladium catalyst (Sigma-Aldrich) (Perera et al., 2010). In detail, approximately 1 mg of hydrocarbon-containing extract was dissolved in 1 mL of ethyl acetate, and 0.25 mg of palladium activated in carbon was added as catalyst. The solution was placed in a Parr Bomb hydrogenation chamber under an H_2 atmosphere, and incubated at room temperature for 12 h under 690 kPa pressure. The resulting product was filtered to remove the catalyst, and the solution was evaporated under N_2 gas. After silylation (Sweeley et al. 1963), the products were analyzed by GC-MS.

Dimethyl disulfide reaction

The positions of double bonds in hydrocarbons were determined by GC-MS analysis of dimethyl disulfide adducts (Buser et al., 1983). Approximately, 1 ug of hydrocarbon-containing extract was dissolved in 50 uL hexane and incubated at 40°C over night with 50 uL dimethyl disulfide and 5 uL of 0.06% (w/v) I_2 in diethyl ether. The reaction was stopped by addition of 50 uL of 5% (w/v) sodium thiosulfate and samples were diluted with 200 uL

hexane. The organic phase was removed and concentrated prior to GC-MS analysis.

Gas chromatography-mass spectrometric analysis

Chromatographic analysis was performed with a gas chromatograph (Model 6890 series, Agilent Technologies, Palo Alto, CA), equipped with a mass detector Model 5973 (Agilent Technologies, Palo Alto, CA). Chromatography was conducted using a HP-5MS cross-linked (5%)-diphenyl-(95%)-dimethyl polysiloxane column (30 m length, 0.25 mm inner diameter), using helium as the carrier gas. The injection temperature was at 280℃. The oven temperature was initially at 200 ℃, was increased to 280 ℃ at a rate of 4 ℃/min, and further increased to 320 ℃ at a rate of 20 ℃/min, and held at this temperature for 3 min.

Results

Growth of *B. braunii* UTEX 572

To analyze the effect of the carbon, nitrogen and phosphate availability on cellular growth and hydrocarbon production of *B. braunii*, cells were initially grown in modified Chu 13 medium aerated with air containing 2 % CO_2 for 2 weeks. At this stage cultures reached early stationary phase, and cells were transferred to two different media, a modified B3N medium at ambient air (high nitrogen and phosphate, low carbon) or Waris medium aerated with 2% CO_2 (low nitrogen and phosphate, high carbon). Because *B. braunii* tend to flocculate, cell counting and the optical measurements did not provide

consistent measures of cell growth. Therefore, the growth curves of *B. braunii* were obtained from dry-weight measurements of cells harvested every 2 days over a 10-day period. As shown in Fig 1, strain UTEX 572 continues to grow after transferring to both modified B3N and Waris medium. However, after transferring to the modified B3N medium that has higher nitrogen and phosphate but low inorganic carbon, *B. braunii* can grow at a higher rate, and reaches a higher cell density (0.19 g dry weight/L) as compared with growth in the Waris medium (~ 0.8 g dry weight/L) that has lower nitrogen and phosphate concentration but higher concentration of inorganic carbon (2% CO_2).

Hydrocarbon analysis of *B. braunii* UTEX 572

GC-MS analyses of hexane extracts indicate that *B. braunii* UTEX 572 grown in either modified B3N medium or Waris medium produce hydrocarbons, the majority of which are odd-numbered, linear alkane and alkenes ranging from 23 to 33 carbon atoms and some minor even-numbered alkanes and alkenes ranging from 24 to 30 carbon atoms (Fig 2a).

The authentic identification of these hydrocarbons was established by a combination of co-elution with commercial standards, and by GC-MS analysis of the individual components (Fig. 2a). In parallel, the hexane extracts from *B. braunii* were hydrogenated by reacting with H_2 in the presence of a palladium catalyst, followed by GC-MS analysis (Fig 2b). As illustrated in Fig 2a, these analyses revealed the occurrence of linear alkanes, alkenes and dienes

(ranging from 21 to 33 atoms). Specifically, the complexity of the hydrocarbon extracts, resulting from the occurrence of carbon-carbon double bonds, was reduced upon hydrogenation, collapsing all unsaturated hydrocarbons to the respective saturated alkanes (Fig2a and Fig 2b). The chemical identification of these hydrogenated hydrocarbons were confirmed by comparing their retention times to commercial standards and by analysis the mass spectrum following electron impact (Laureillard et al. 1986) ionization-induced fragmentation.

Identification of unsaturated hydrocarbons in *B. braunii* UTEX 572

The positions of the double bonds in the unsaturated hydrocarbons were identified by the mass-spectrometric analysis of dimethyl disulfide adducts (Fig. 3) (Buser et al. 1983; Pepe et al. 1995; Vincenti et al. 1987). Electron ionization mass spectrometry of these adducts generated fingerprint ions, from which the position of the double bonds could be deduced. For example, Fig. 4 illustrates the analysis of a 29-carbon alkene (identified by the m/z value of the molecular ion of the dimethyl disulfide adducts); the m/z values of the fragmentation ions (327 and 173) indicate that the double bond in this alkene occurs at the ninth position. Hence, based upon these analyses, this metabolite was identified as 9-nonacosene. Additional analyses established the occurrence of a homologous series of alkenes of 25, 27, 31 carbon chain length, with double bonds situated either at position 9 or at the terminal end (Table 1 and Fig S1).

Hydrocarbons accumulate differently under different nutrient conditions

At the time of sub-culturing from the initial inoculum, the UTEX 572 strain produced about 12 µmol/g dry biomass of hydrocarbons. After transferring to Waris medium aerated with 2% CO_2 (high carbon, low nitrogen and phosphate), the strain continued to accumulate more hydrocarbons, and the total hydrocarbon more than doubled (~ 30 µmol/g) by about 6 and 7 days after sub-culturing. In contrast, cells transferred to modified B3N medium, with only ambient levels of CO_2 (low carbon, high nitrogen and phosphate) exhibited a slight decrease in hydrocarbon accumulation and then remained at this constant low level (Fig 5). At the biggest differential between the two cultures, there was a 4-fold difference in hydrocarbon accumulation between them.

The odd-numbered hydrocarbons with chain-length ranging from C_{23} to C_{33} accounted for >90% of the hydrocarbons in both media used in this study. In addition, to these odd-numbered hydrocarbons, small amount of even-numbered hydrocarbons (<10%) with chain length ranging from C_{24} to C_{30} were also detected, which has not been reported in previous study concerning the hydrocarbons in RACE A strains of *B. braunii* (Metzger et al. 1986). In addition, in both media, most of the hydrocarbons are unsaturated with alkenes consisting more than 50% of the hydrocarbons (Supplemental Table 1). After transferring to the two different media, Waris medium with 2% CO_2 and modified B3N medium at ambient air, the changes in the relative percentages of alkanes, alkenes, odd- and even-numbered hydrocarbons

followed the same trend. The majority of the hydrocarbons were unsaturated (~50-95%), and the percentage of alkene decreased (~75% at time of inoculation), reached the lowest level at 3 days (~50%), and then increased up to ~90% by day 5 (Supplemental Table 1). The percentage of the major hydrocarbons, odd-numbered and linear, also decreased from ~92% to ~88% at 3 days and then increased up to ~97% at 9 days after transferring to either media (Supplemental Table 1).

Discussion

Both even- and odd- numbered hydrocarbons existed in *B. braunii* UTEX 572

As with prior studies with other *B. braunii* strains (An et al. 2003; Metzger et al. 1986; Yong et al. 1986), we have identified odd-numbered, linear alkanes and alkenes ranging from C_{23} to C_{31} in an A Race strain, UTEX572. In addition, to these previously identified odd-numbered, linear, hydrocarbons that account for the majority of the hydrocarbons, we have identified minor amounts (< 10%) of even-numbered, linear hydrocarbons ranging from C_{24} to C_{30}, which have not been previously reported. In both media utilized in this study, *B. braunii* produced the same type of even-numbered hydrocarbons; these being predominantly, $C_{24:1}$, C_{24}, $C_{28:1}$, C_{28}, $C_{30:1}$ and C_{30}.

All dienic hydrocarbons that have been reported previously contain a terminal double bond and a cis-double bond, located in the 9th position relative

to the terminal methyl group (Metzger et al. 1986). Our results are consistent with these finding. In addition to the dienes, both monoenes with double bonds either at the terminal or at 9th positions have been found. The presence of a terminal double bond in long-chain hydrocarbons of freshwater green algae have been previously reported for *Scenedesmus* (Iwata et al. 1961), *Chlorella* (Iwata and Sakurai 1963), *Jeotgalicoccus* species (Rude et al. 2011), and cyanobacterium *Lyngbya majuscula* (Gehret et al. 2011).

Regulation of alkene accumulation by controlling carbon, nitrogen and phosphate availability

In our study of *B. braunii* UTEX 572, the supply of nitrate and phosphate nutrients stimulated growth (the modified B3N medium), and low nitrogen and phosphate together with higher concentration of CO_2 (Waris medium) suppressed cell growth, which is consistent with previous findings (An et al. 2003; Ranga Rao and Ravishankar 2007; Tanoi et al. 2011; Tran et al. 2010). Whereas nitrate and phosphate (with limited carbon) stimulated growth, these nutritional conditions suppressed hydrocarbon accumulation. We found that at high carbon levels (2% CO_2), but low nitrogen and phosphate nutrients (Waris medium) stimulated the accumulation of hydrocarbons by about 3-fold. This result is consistent with previous finding that supply of carbon sources and nitrogen and phosphate deficient conditions stimulated hydrocarbon production in *B. braunii* (Benamotz et al. 1985; Choi et al. 2011; Ge et al. 2011b; Shifrin and Chisholm 1981; Singh 2003; Singh and Kumar 1992).

Athough total hydrocarbon accumulation are different between *B. braunii* cells growth in B3N media at ambient air and Waris media aerated with 2% CO_2, the relative abundances of individual hydrocarbons was the same in *B. braunii* cells grown in two different media.

Potential hydrocarbon biosynthesis pathways in *B. braunii* UTEX 572

Although the physiological functions of hydrocarbons in algae such as *B. braunii* remain unclear, these molecules probably act to reserve energy (Singh and Kumar 1992). Hydrocarbons are thought to be synthesized using fatty acid as precursors (Tornabene 1982). There is evidence showing that the elongation-decarboxylation/decarbonylation pathway can be used to synthesize odd-numbered hydrocarbons from even number fatty acids in *B. braunii* (Dennis and Kolattukudy 1992; Dennis and Kolattukudy 1991a; Templier et al. 1991a, b; Wang and Kolattukudy 1995b). A microsomal preparation from *B. braunii* was found to convert exogenous fatty acids to hydrocarbon by decarbonylation from aldhyde (Dennis and Kolattukudy 1991c). An aldehyde-generating fatty acyl-CoA reductase and the decarbonylase were partially purified from *B. braunii* (Dennis and Kolattukudy 1992; Dennis and Kolattukudy 1991a; Wang and Kolattukudy 1995b). It's possible to envision that even-numbered hydrocarbons could be synthesized via the same mechanism, but from odd-numbered fatty acid precursors. Alternatively, the even-numbered hydrocarbons might be synthesized by reduction-dehydration-reduction pathway as suggested in *Vibrio furnissii* M1

(Park 2005). Based on the observation that in *V. furnissii* that even-number alkanes are present, and the corresponding alcohol, aldehyde, and alkane derivatives can be detected by feeding [1-^{14}C] hexadecanoic acid, this reductive pathway of hydrocarbon biosynthesis was proposed. In this reduction-dehydration-reduction pathway, the elongated fatty acid is first reduced to an aldehyde, and then further reduced to an alcohol, which is dehydrated to form an alkene and can be further reduced to alkane. However, the recent genome sequencing of a *V. furnissii* strain did not show alkane biosynthesis genes and also did not show alkane-producing phenotype (Wackett et al. 2007).

The alkenes with a terminally-located double bond have been reported to be formed from fatty acids by a novel P450 fatty acid decarboxylase in *Jeotgalicoccus* (Rude et al. 2011), and a curacin thioesterase with decarboxylating function in a marine cyanobacterium *Lyngbya majuscula* (Gehret et al. 2011). By feeding radioactively-labeled oleic (cis-18:1 ω9) or elaidic (trans-18:1 ω9) acid to a Race A *B. braunii* strain, a non-specific elongation-decarboxylation system was suggested to be responsible for cis- or trans- alkadiene hydrocarbons (Templier et al. 1991a, b).

Consistent with the elongation-decarboxylation/decarbonylation pathway, double bond positions in all of the dienes and some of the monoenes reported herein are located at the 9th position, which is the same position with

respect to the terminal methyl group of the carbon chains as the double bond of oleic acid (Kolattuk.Pe 1967; Templier et al. 1991b).

References

An JY, Sim SJ, Lee JS, Kim BW (2003) Hydrocarbon production from secondarily treated piggery wastewater by the green alga Botryococcus braunii. J Appl Phycol 15:185-191

Benamotz A, Tornabene TG, Thomas WH (1985) Chemical Profile of Selected Species of Microalgae with Emphasis on Lipids. J Phycol 21:72-81

Brown AC, Knights BA, Conway E (1969) Hydrocarbon Content and Its Relationship to Physiological State in Green Alga Botryococcus Braunii. Phytochemistry 8:543-&

Buser HR, Arn H, Guerin P, Rauscher S (1983) Determination of Double-Bond Position in Monounsaturated Acetates by Mass-Spectrometry of Dimethyl Disulfide Adducts. Anal Chem 55:818-822

Casadevall E, Dif D, Largeau C, Gudin C, Chaumont D, Desanti O (1985) Studies on Batch and Continuous Cultures of Botryococcus-Braunii - Hydrocarbon Production in Relation to Physiological-State, Cell Ultrastructure, and Phosphate Nutrition. Biotechnol Bioeng 27:286-295

Chitis Y (1980) An unusual hydrocarbon. J Ramsay Society 27-28

Choi GG, Kim BH, Ahn CY, Oh HM (2011) Effect of nitrogen limitation on oleic acid biosynthesis in Botryococcus braunii. J Appl Phycol 23:1031-1037

Coleman LW, Rosen BH, Schwartzbach SD (1988) Environmental-Control of Carbohydrate and Lipid-Synthesis in Euglena. Plant Cell Physiol 29:423-432

Dayananda C, Sarada R, Rani MU, Shamala TR, Ravishankar GA (2007) Autotrophic cultivation of Botryococcus braunii for the production of hydrocarbons and exopolysaccharides in various media. Biomass Bioenerg 31:87-93

Dennis M, Kolattukudy PE (1992) A cobalt-porphyrin enzyme converts a fatty aldehyde to a hydrocarbon and CO. Proc Natl Acad Sci U S A 89:5306-5310

Dennis MW, Kolattukudy PE (1991) Alkane biosynthesis by decarbonylation of aldehyde catalyzed by a microsomal preparation from Botryococcus braunii. Arch Biochem Biophys 287:268-275

Ge YM, Liu JZ, Tian GM (2011) Growth characteristics of Botryococcus braunii 765 under high CO(2) concentration in photobioreactor. Bioresource Technol 102:130-134

Gehret JJ, Gu LC, Gerwick WH, Wipf P, Sherman DH, Smith JL (2011) Terminal Alkene Formation by the Thioesterase of Curacin A Biosynthesis STRUCTURE OF A DECARBOXYLATING THIOESTERASE. J Biol Chem 286:14445-14454

Iwata I, Mizushima M, Nakata H, Sakurai Y (1961) Lipids of Algae .1. Components of Unsaponifiable Matter of Algae Scenedesmus. Agr Biol Chem Tokyo 25:319-&

Iwata I, Sakurai Y (1963) Lipids of Algae .3. Components of Unsaponifiable Matter of Algae Chlorella. Agr Biol Chem Tokyo 27:253-&

Kolattuk.Pe (1967) Biosynthesis of Paraffins in Brassica Oleracea - Fatty Acid Elongation-Decarboxylation as a Plausibel Pathway. Phytochemistry 6:963-&

Largeau C, Casadevall E, Berkaloff C, Dhamelincourt P (1980) Sites of Accumulation and Composition of Hydrocarbons in Botryococcus-Braunii. Phytochemistry 19:1043-1051

Laureillard J, Largeau C, Waeghemaeker F, Casadevall E (1986) Biosynthesis of the Resistant Polymer in the Alga Botryococcus-Braunii Studies on the Possible Direct Precursors. J Nat Prod 49:794-799

Mcfadden GI, Melkonian M (1986) Use of Hepes Buffer for Microalgal Culture Media and Fixation for Electron-Microscopy. Phycologia 25:551-557

Metzger P, Templier J, Largeau C, Casadevall E (1986) An N-Alkatriene and Some N-Alkadienes from the a Race of the Green-Alga Botryococcus-Braunii. Phytochemistry 25:1869-1872

Park MO (2005) New pathway for long-chain n-alkane synthesis via 1-alcohol in Vibrio furnissii M1. J Bacteriol 187:1426-1429

Pepe C, Dizabo P, Dagaut J, Balcar N, Lautier MF (1995) Determination of Double-Bond Position in Di-Unsaturated Alkadienes by Means of Mass-Spectrometry of Dimethyl Disulfide Derivatives. Eur Mass Spectrom 1:209-211

Ranga Rao A, Ravishankar GA (2007) Influence of CO2 on growth and hydrocarbon production in Botryococcus braunii. J Microbiol Biotechn 17:414-419

Rao AR, Dayananda C, Sarada R, Shamala TR, Ravishankar GA (2007) Effect of salinity on growth of green alga Botryococcus braunii and its constituents. Bioresour Technol 98:560-564

Rude MA, Baron TS, Brubaker S, Alibhai M, Del Cardayre SB, Schirmer A (2011) Terminal Olefin (1-Alkene) Biosynthesis by a Novel P450 Fatty Acid Decarboxylase from Jeotgalicoccus Species. Appl Environ Microb 77:1718-1727

Shifrin NS, Chisholm SW (1981) Phytoplankton Lipids - Interspecific Differences and Effects of Nitrate, Silicate and Light-Dark Cycles. J Phycol 17:374-384

Singh Y (2003) Photosynthetic activity, and lipid and hydrocarbon production by alginate-immobilized cells of Botryococcus in relation to growth phase. J Microbiol Biotechn 13:687-691

Singh Y, Kumar HD (1992) Lipid and Hydrocarbon Production by Botryococcus-Spp under Nitrogen Limitation and Anaerobiosis. World J Microb Biot 8:121-124

Sweeley CC, Bentley R, Makita M, Wells WW (1963) Gas-Liquid Chromatography of Trimethylsilyl Derivatives of Sugars and Related Substances. J Am Chem Soc 85:2497-&

Tanoi T, Kawachi M, Watanabe MM (2011) Effects of carbon source on growth and morphology of Botryococcus braunii. J Appl Phycol 23:25-33

Templier J, Largeau C, Casadevall E (1991a) Biosynthesis of Normal-Alkatrienes in Botryococcus-Braunii. Phytochemistry 30:2209-2215

Templier J, Largeau C, Casadevall E (1991b) Nonspecific Elongation Decarboxylation in Biosynthesis of Cis-Alkadienes and Trans-Alkadienes by Botryococcus-Braunii. Phytochemistry 30:175-183

Tornabene TG (1982) Microorganisms as Hydrocarbon Producers. Experientia 38:43-46

Tran HL, Kwon JS, Kim ZH, Oh Y, Lee CG (2010) Statistical Optimization of Culture Media for Growth and Lipid Production of Botryococcus braunii LB572. Biotechnol Bioproc E 15:277-284

Tsukahara K, Sawayama S (2005) Liquid fuel production using microalgae. Journal of the Japan Petroleum Institute 48:251-259

Vincenti M, Guglielmetti G, Cassani G, Tonini C (1987) Determination of Double-Bond Position in Diunsaturated Compounds by Mass-Spectrometry of Dimethyl Disulfide Derivatives. Anal Chem 59:694-699

Wackett LP, Frias JA, Seffernick JL, Sukovich DJ, Cameron SM (2007) Genomic and biochemical studies demonstrating the absence of an alkane-producing phenotype in Vibrio furnissii M1. Appl Environ Microb 73:7192-7198

Wang X, Kolattukudy PE (1995) Solubilization and purification of aldehyde-generating fatty acyl-CoA reductase from green alga Botryococcus braunii. FEBS Lett 370:15-18

Weetall HH (1985) Studies on the Nutritional-Requirements of the Oil-Producing Alga Botryococcus-Braunii. Appl Biochem Biotech 11:377-391

Yang SL, Wang J, Cong W, Cai ZL, Fan OY (2004) Utilization of nitrite as a nitrogen source by Botryococcus braunii. Biotechnol Lett 26:239-243

Yong TPC, Largeau C, Casadevall E (1986) Biosynthesis of Non-Isoprenoid Hydrocarbons by the Microalga Botryococcus-Braunii - Evidences for an Elongation-Decarboxylation Mechanism - Activation of Decarboxylation. New J Chem 10:701-707

Yoo C, Jun SY, Lee JY, Ahn CY, Oh HM (2010) Selection of microalgae for lipid production under high levels carbon dioxide. Bioresource Technol 101:S71-S74

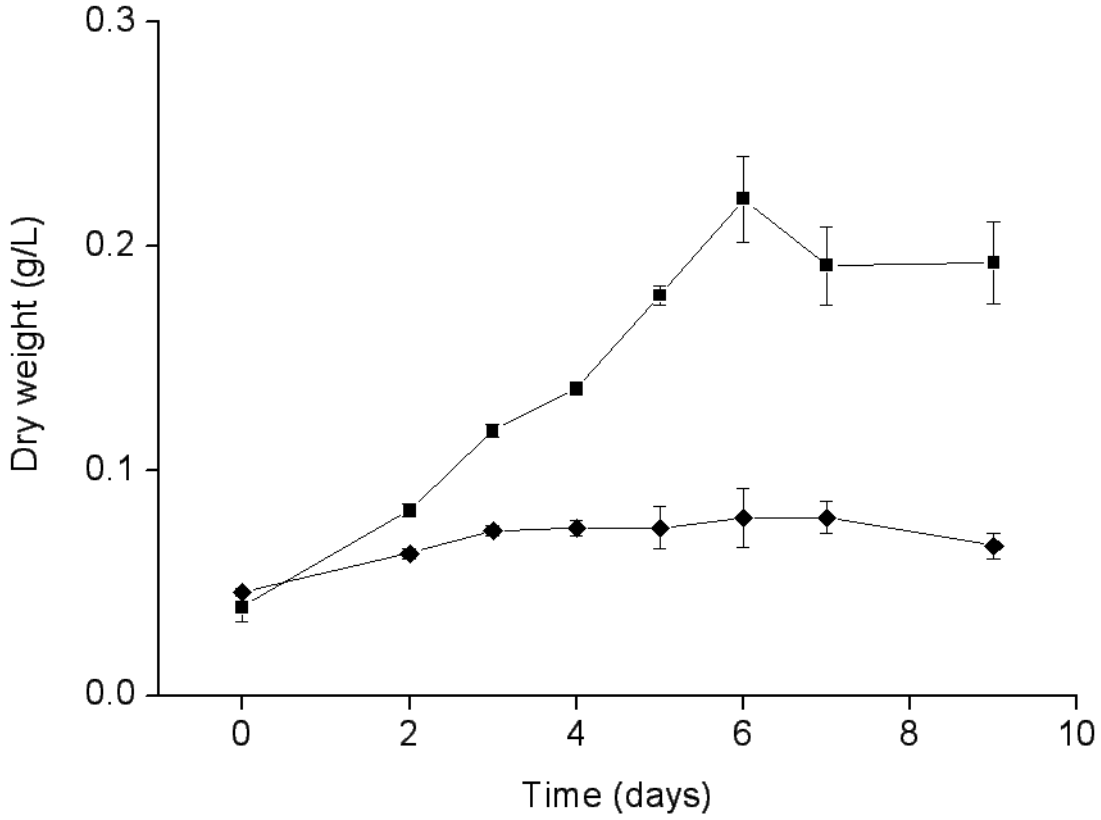

Figure 1. Growth of *B. braunii* UTEX 572 in modified B3N medium without CO_2 and Waris medium with 2 % CO_2.

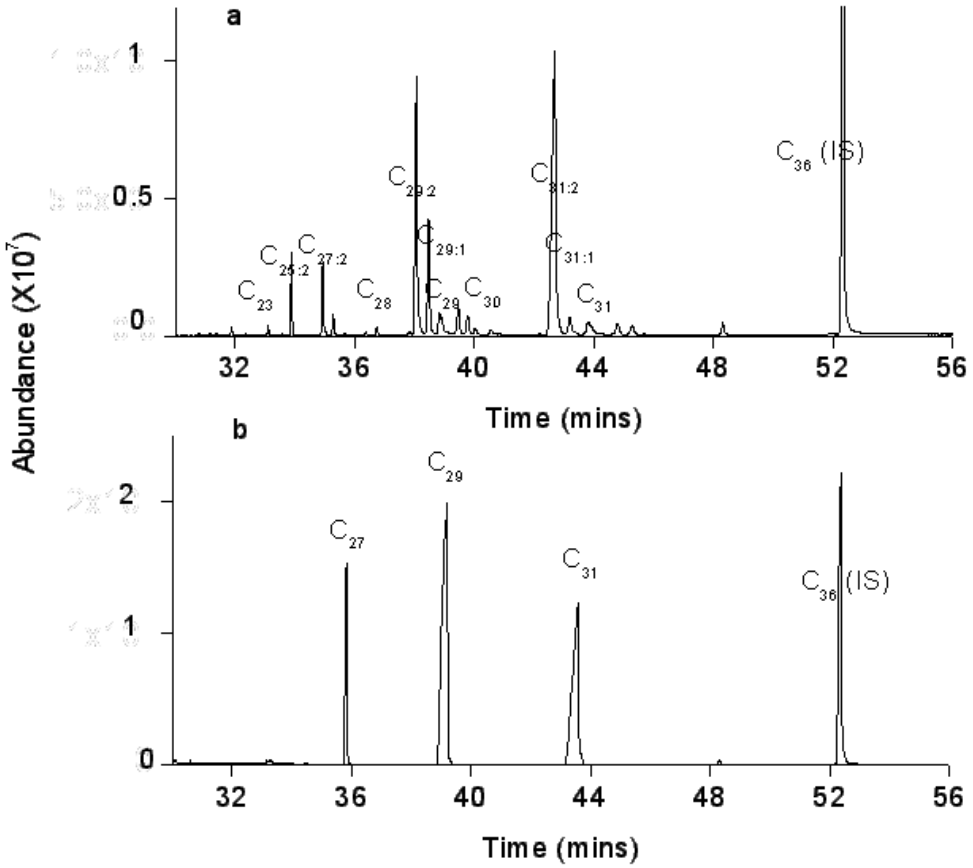

Figure 2. Comparison of hydrocarbon extracts from *B. braunii* before (a) and after (b) hydrogenation reaction.

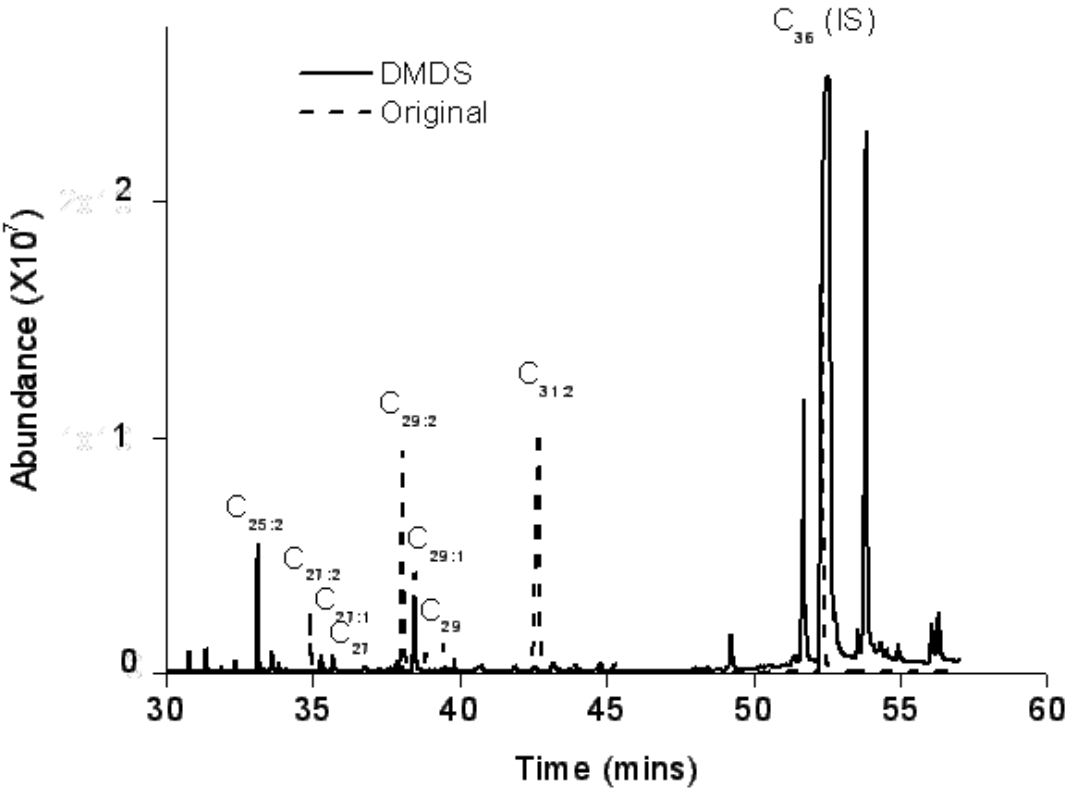

Figure 3. Comparison of hydrocarbon extracts from *B. braunii* before and after DMDS reaction.

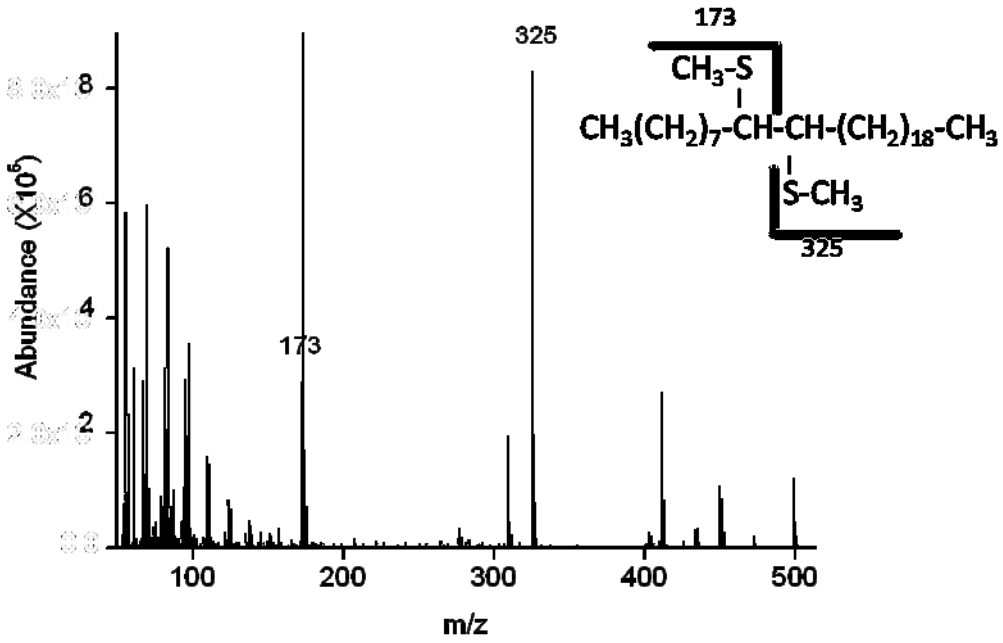

Figure 4. Mass Spectrum of DMDS adduct of 9-$C_{29:1}$.

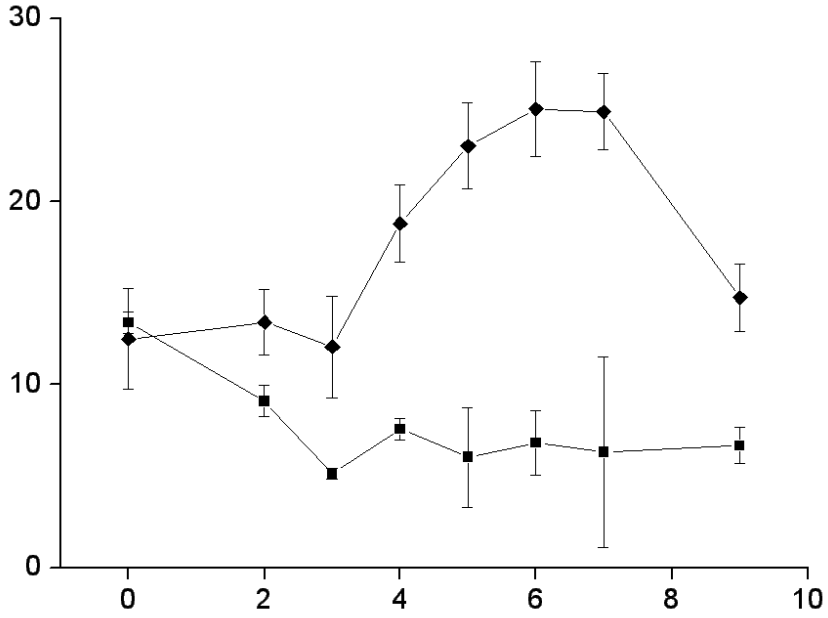

Figure 5. Hydrocarbon content in *B. braunii* at different stages of growth in modified B3N and Waris media.

Table 1. Hydrocarbons identified in *B. braunii* UTEX 572

B. Braunii	Hydrocarbons	
UTEX 572	1-tricosene	1-C23:1
	1-tetracosene	1-C24:1
	1-pentacosene	1-C25:1
	9-pentacosene	9-C25:1
	9-heptacosene	9-C27:1
	1-octacosene	1-C28:1
	9-nonacosene	9-C29:1
	1-triacontene	1-C30:1
	1-hentriacontene	1-C31:2
	1,16-pentocosadiene	1,16-C25:2
	1,20-heptacosadiene	1,20-C27:2
	1,22-hentriacontadiene	1,22-C31:2
	1,25-hentriacontadiene	1, 25-C31:2

Figure S1. Mass spectrum of DMDS diadduct of monoene, diene identified in *B. braunii* UTEX 572

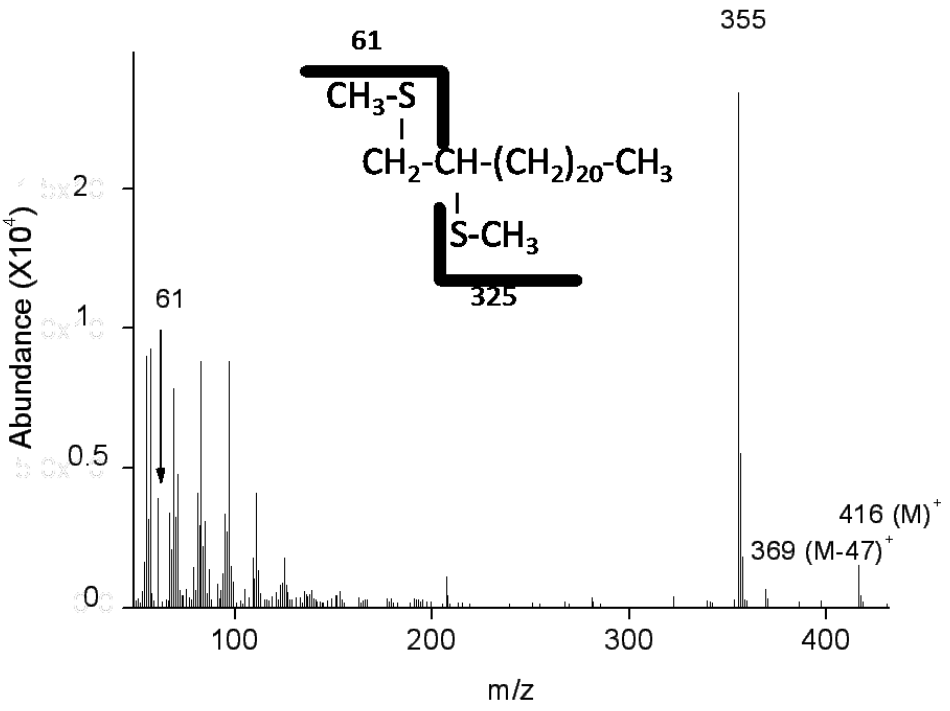
61
355
CH3-S
CH2-CH-(CH2)20-CH3
S-CH3
325
61
Abundance (X10^4)
2
1
0.5
0
416 (M)+
369 (M-47)+
100
200
300
400
m/z

1-$C_{23:1}$

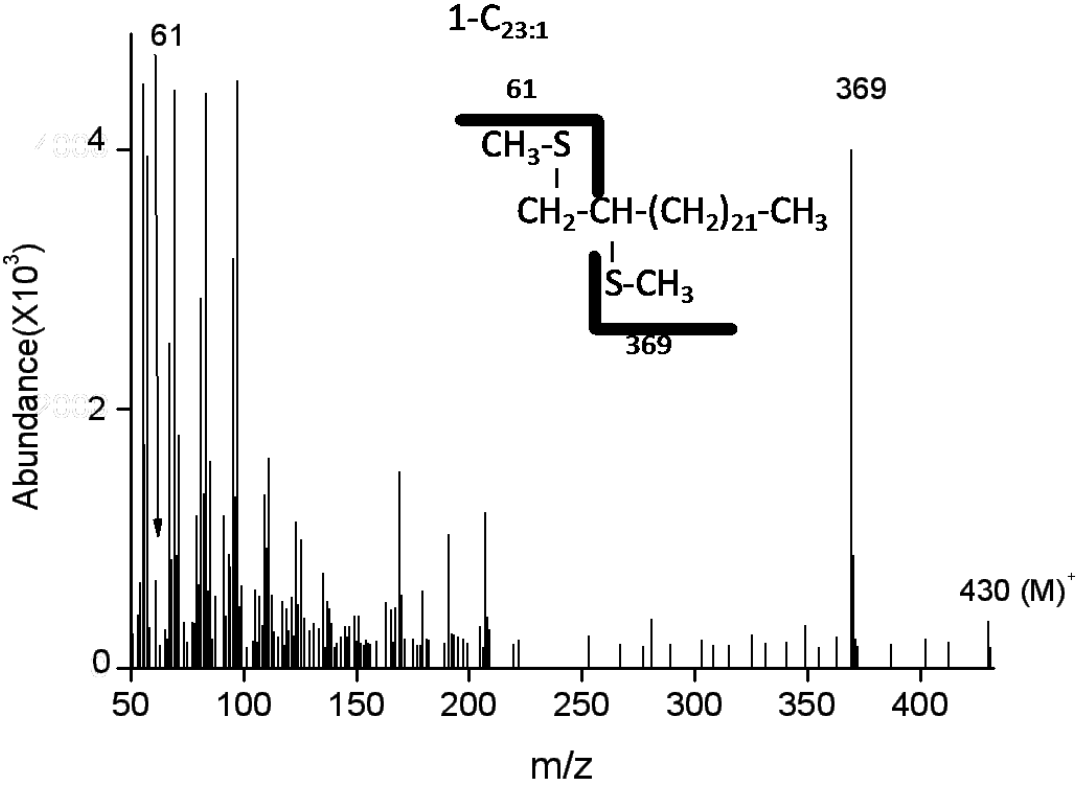
61
61
369
CH3-S
CH2-CH-(CH2)21-CH3
S-CH3
369
Abundance(X10^3)
4
2
0
430 (M)+
50
100
150
200
250
300
350
400
m/z

1-$C_{24:1}$

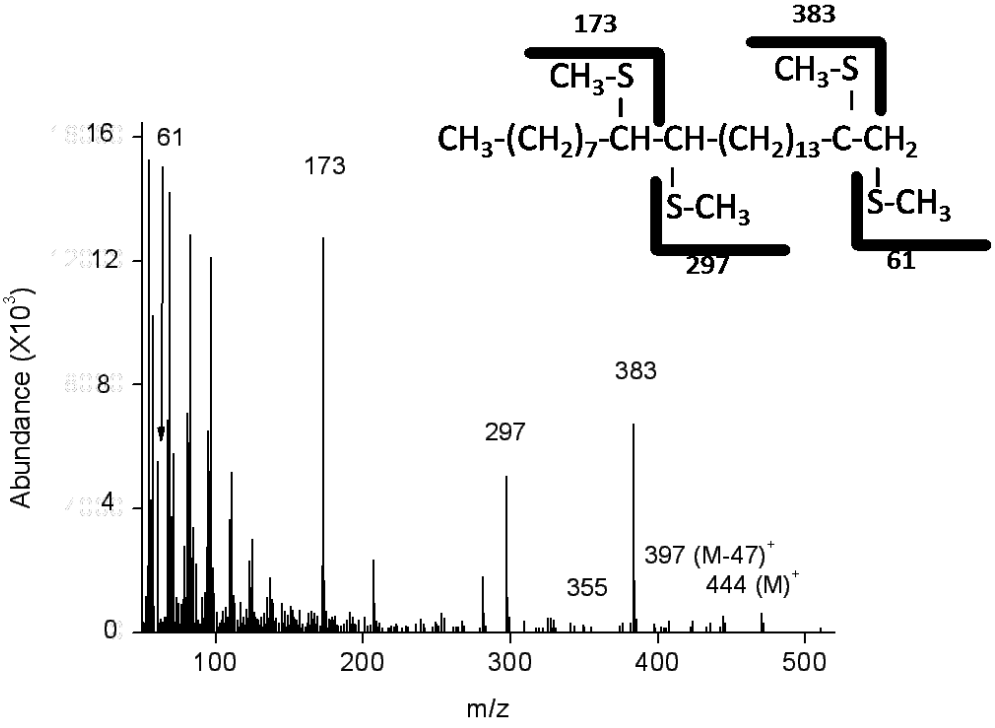

1,16-$C_{25:2}$

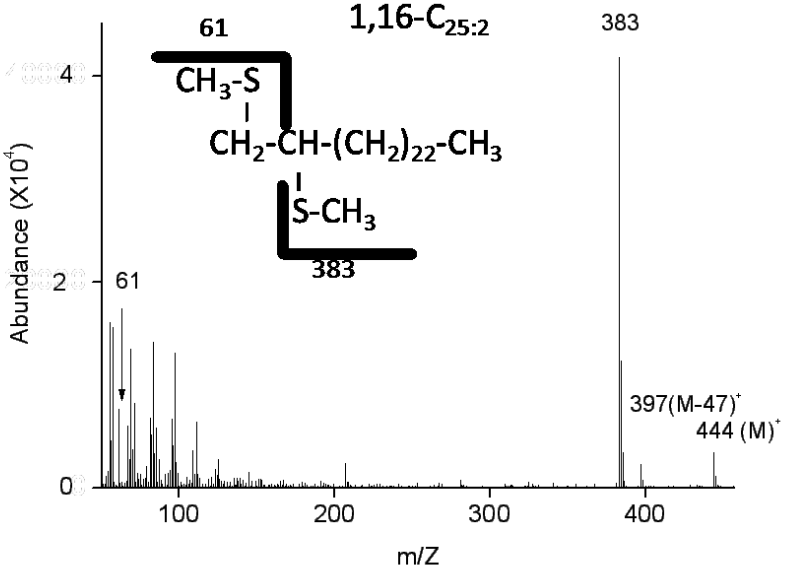

1- $C_{25:1}$

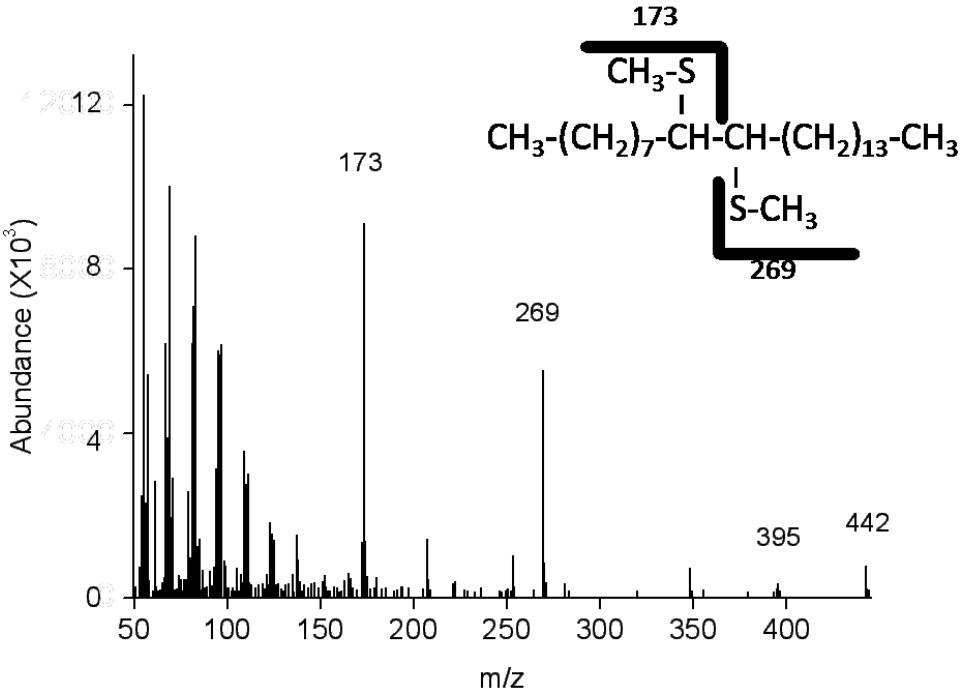

9- $C_{25:1}$

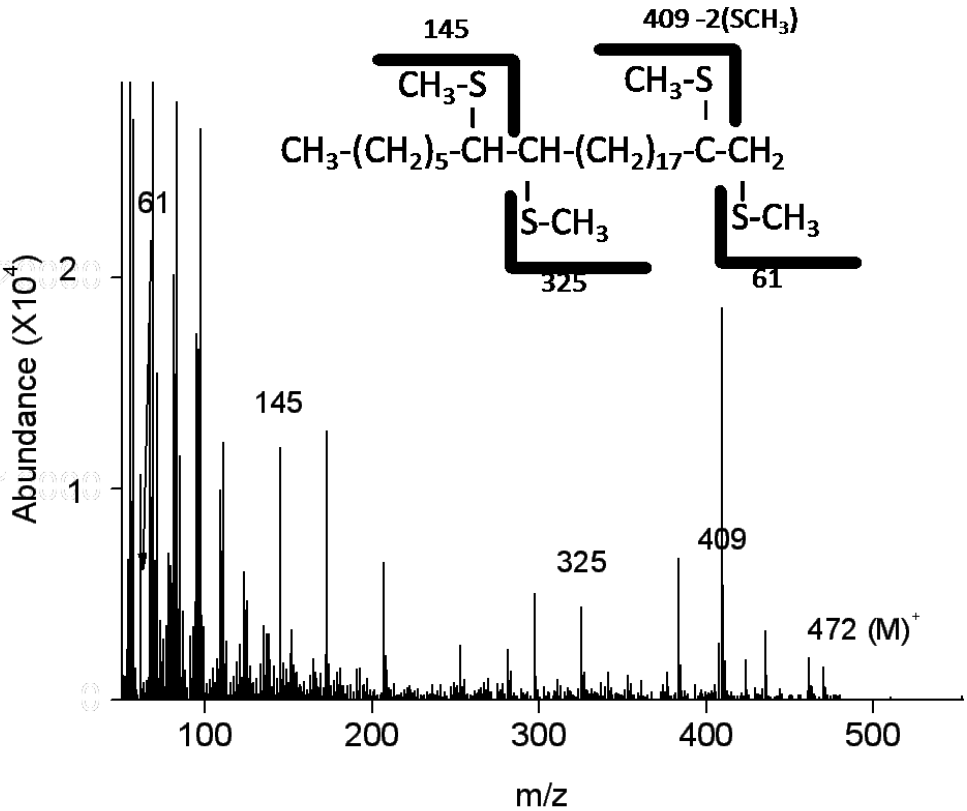

1,20- $C_{27:2}$

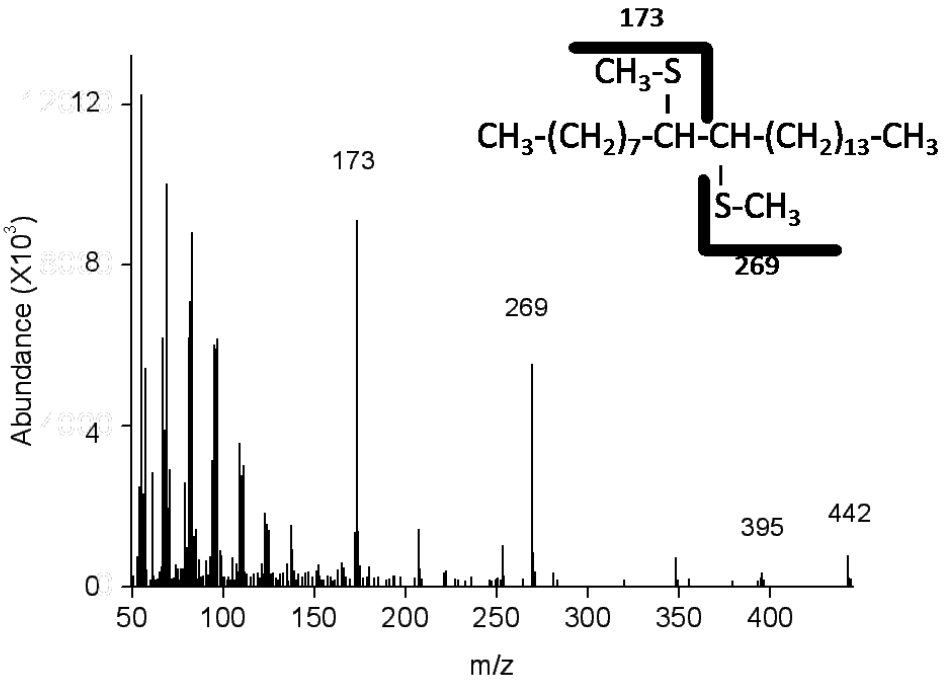

9- $C_{25:1}$

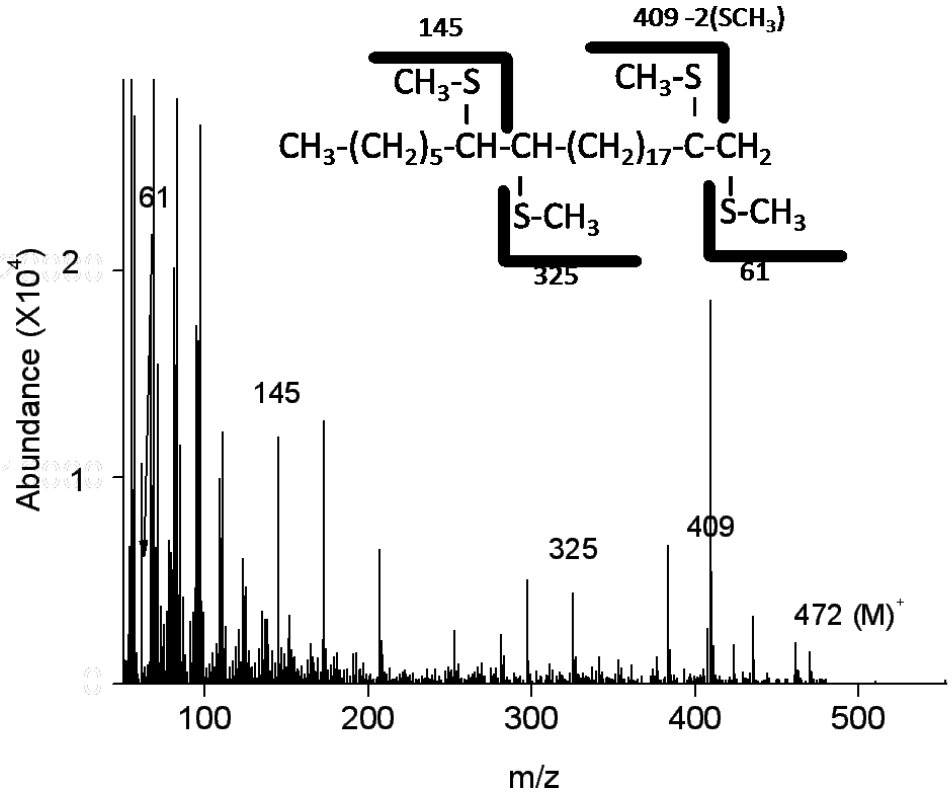

1,20- $C_{27:2}$

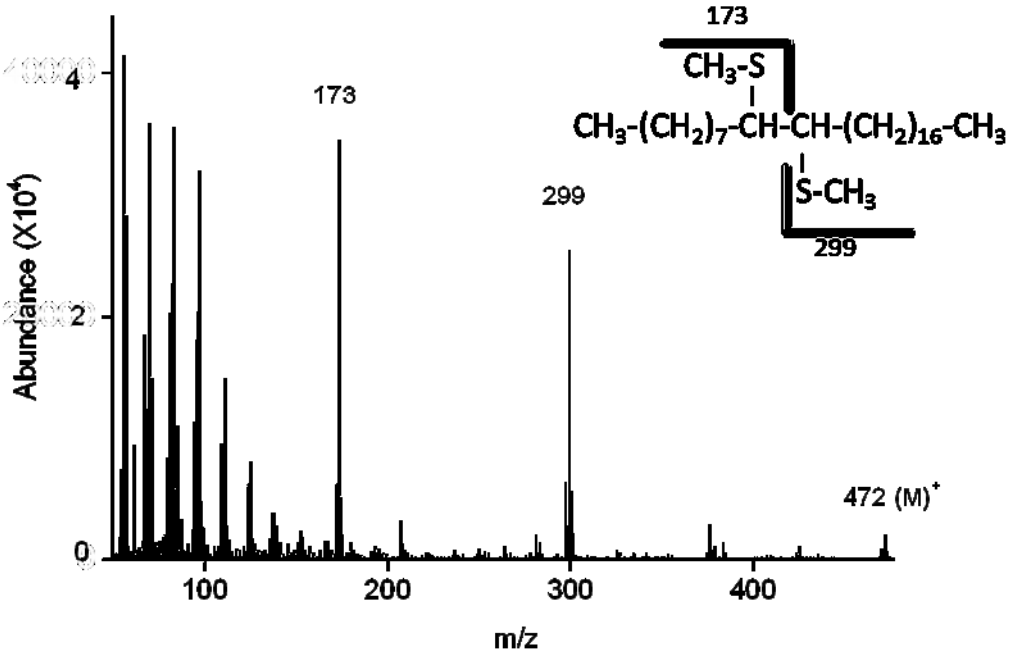
173
CH3-S
CH3-(CH2)7-CH-CH-(CH2)16-CH3
S-CH3
299
173
299
472 (M)+
Abundance (X10^4)
4
2
0
100
200
300
400
m/z

9-$C_{27:1}$

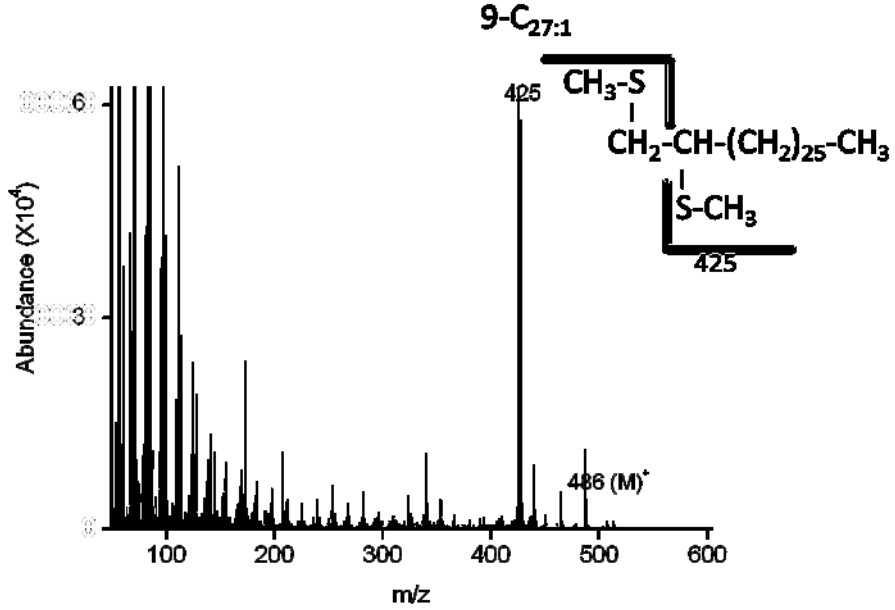
CH3-S
CH2-CH-(CH2)25-CH3
S-CH3
425
425
486 (M)+
Abundance (X10^4)
6
3
0
100
200
300
400
500
600
m/z

1-$C_{28:1}$

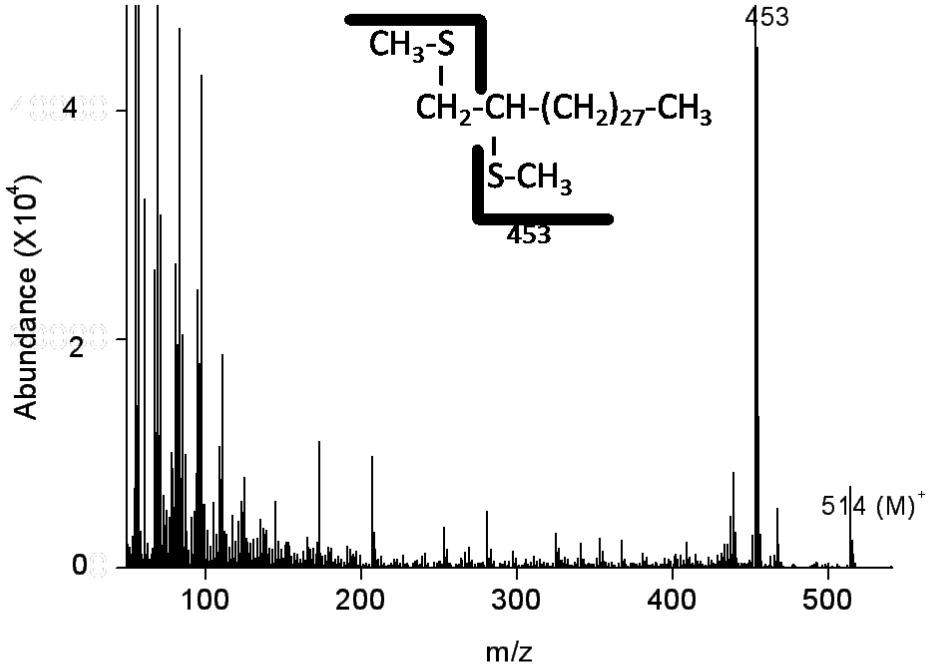
453
CH3-S
CH2-CH-(CH2)27-CH3
S-CH3
453
514 (M)+
Abundance (X10^4)
0
2
4
100
200
300
400
500
m/z

1-$C_{31:2}$

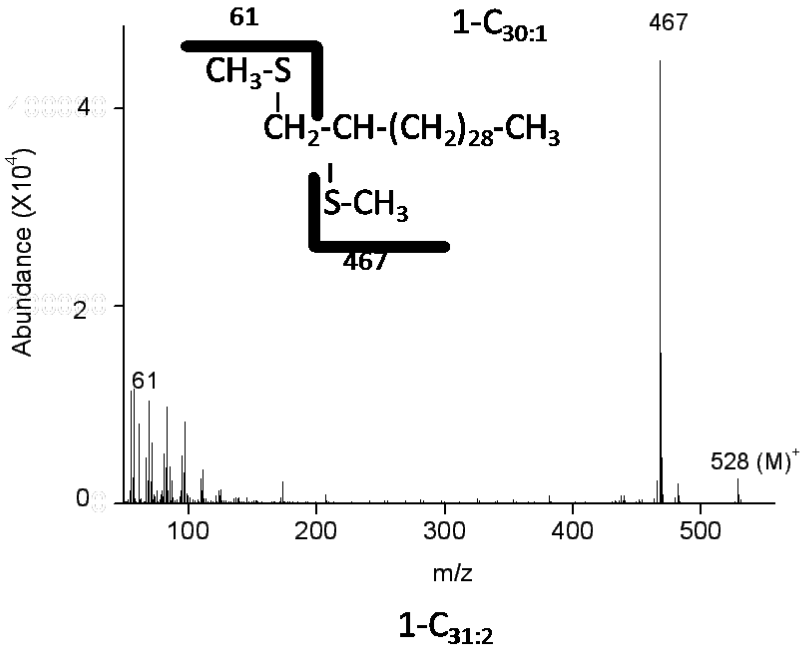
61
1-C30:1
467
CH3-S
CH2-CH-(CH2)28-CH3
S-CH3
467
61
528 (M)+
Abundance (X10^4)
0
2
4
100
200
300
400
500
m/z

1-$C_{30:1}$

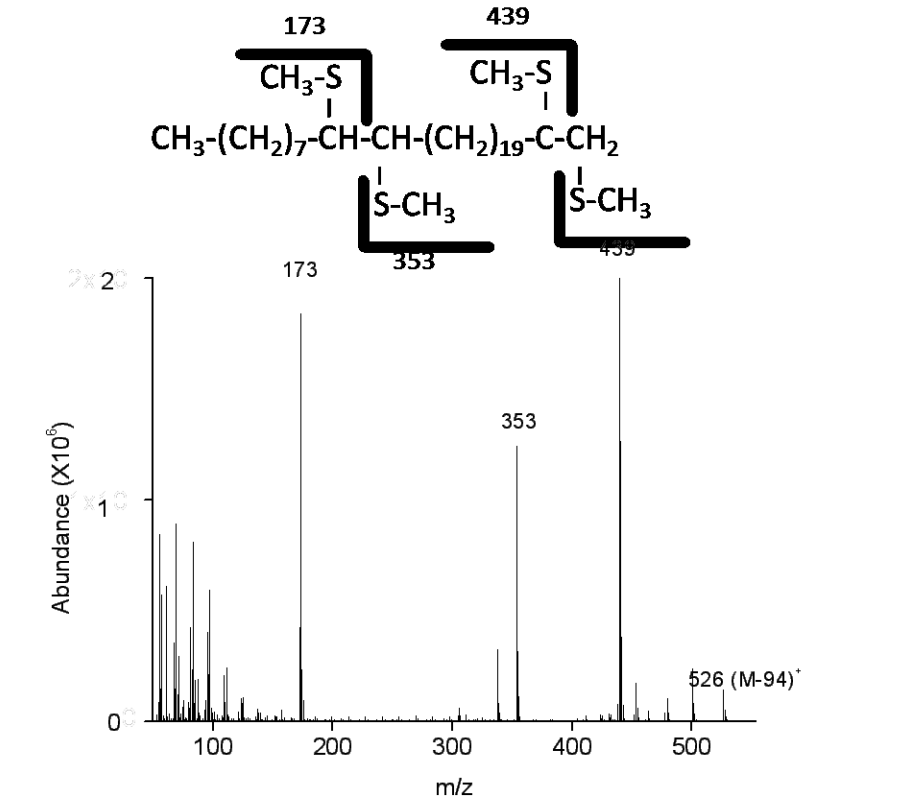

1,22-$C_{31:2}$

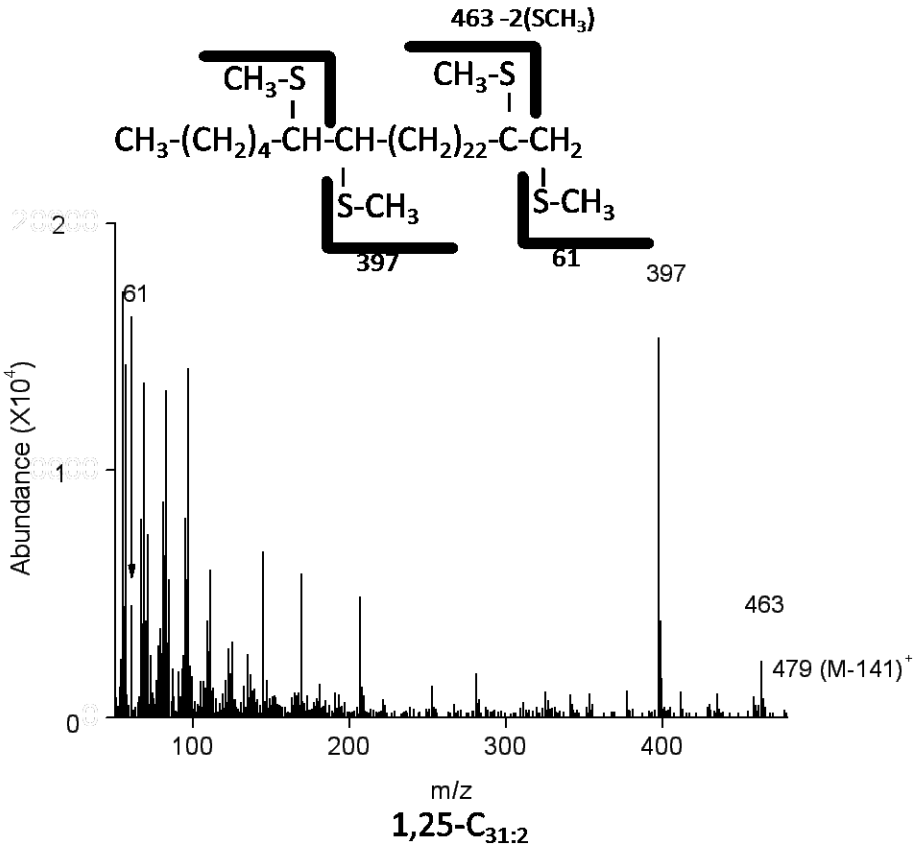

1,25-$C_{31:2}$

Supplemental Table 1. Composition of modified B3N medium, modified Chu13 medium and Waris medium

Component	Waris medium	Modified B3N medium	Modified Chu13 Medium
KNO3	0.98 mM		3.7 mM
NaNO3		8.82 mM	
MgSO4·7H2O	0.081 mM	0.3 mM	0.8 mM
(NH4)2HPO4	0.151 mM		
CaSO4.2H2O	0.36 mM		
CaCl2·2H2O		0.17mM	0.73 mM
K2HPO4		0.43 mM	0.46 mM
KH2PO4		1.29 mM	
NaCl		0.42 mM	
Ferric citrate			0.08 mM
Citrate			0.5 mM
P-IV metal solution	6mL/L	6mL/L	
Microelement solution			1mL/L

CHAPTER 7. PHYSIOLOGICAL REGULATION OF LONG-CHAIN ALKENE-ACCUMULATION BY THE AVAILABILITY OF CARBON, NITROGEN AND PHOSPHATE NUTRIENTS IN *EMILIANIA HUXLEYI*

Wenmin Qin, Samson Condon, Marna D. Yandeau-Nelson, Basil J. Nikolau.

Center for Metabolic Biology, Plant Science Institute

Center for Biorenewable Chemical

Department of Biochemistry, Biophysics and Molecular Biology

Iowa State University, Ames, IA 50010

Email: dimmas@iastate.edu

Telephone: 515-294-0347

Fax number: 515-294-0534

Abstract

Very long-chain n-alkenes have been identified in the marine algae *Emiliania huxleyi*. Examination of three different *E. huxleyi* strains, CCMP 1516, CCMP 1742 and CCMP 373, indicate that two of the strains (CCMP 1516 and CCMP 1742) produce dienes and trienes ranging from C_{31} to C_{35}, while strain CCMP 373 produces only C_{37} and C_{38} dienes. Mass spectrometric analysis of dimethyl disulfide adducts identified the alkenes from CCMP 1516 and CCMP 1742 as 7,22-hentricontadiene ($C_{31:2}$), 1,9-tritriacontadiene ($C_{33:2}$), 1,3,9- tritriacontatrine ($C_{33:3}$), 1,6,9-tritriacontatrine ($C_{33:3}$), 2,8,23-tetratriacontatriene ($C_{34:3}$), 1,8,17,25-tetratriacontatetraiene ($C_{34:4}$), 1,8,26-heptatriacontatriene ($C_{35:3}$) and 1,5,13,26-heptatriacontatetraiene

($C_{35:4}$). The dienes from CCMP 373 are 15,22-heptatricontadiene (15,22-$C_{37:2}$) and 15,22-octatriacontadiene (15,22-$C_{38:2}$). Controlling the availability of carbon, nitrogen and phosphate nutrients in the growth medium could alter the alkene accumulation patterns in these three strains. CCMP 1516 and CCMP 1742 accumulate more alkenes in medium deficient of nitrogen and phosphate than in medium deficient of carbon, whereas CCMP 373 produced more alkenes in medium deficient of carbon than in medium deficient in nitrogen and phosphate. In summary, the alkene composition and amount vary among different strains of *E. huxleyi*, and the carbon, nitrogen and phosphate nutrient influences the total production patterns of alkenes and their relative composition profiles.

Key index words: alkenes; *E. huxleyi*; lipid bodies; Nile Red

Abbreviations: LB, lipid body; NR, Nile Red

Introduction

The unicellular coccolithophore *Emiliania huxleyi* has colonized almost every photic zone of the oceans and constitutes a high proportion of the marine biomass (Okada and Honjo, 1973). *E. huxleyi* produces intricate calcium carbonate platelets, termed coccoliths as an exoskeleton (Paasche 1999), and plays a major role in the global carbon cycling by regulating the exchange of CO_2 across the ocean-atmosphere interface through calcium carbonate precipitation and photosynthesis (de Vargas et al., 2007). Of

particular palaeoceanographic interest, *E. huxleyi* produces neutral lipids consisting of a series of polyunsaturated long-chain (C_{31}–C_{39}) alkenones, alkenoates, and alkenes (PULCA) (Conte et al. 1992; Conte et al., 1994; Bell and Pond, 1996; Sawada et al., 1996). These compounds are widely used as biomarkers for the existence of such algae in palaeoenvironments (Eglinton et al., 1992).

Alkadienes, triene and tetraenes of different carbon chain lengths have been observed in different strains of *E. huxleyi* and the alkene distribution is different among different strains (Conte et al. 1994; Conte et al. 1995). For example, some strains such as CCAP920/2, CH25/90, 92E, VAN 55, VAN56 and GO1 etc. contain a mixture of C_{31}, C_{33}, C_{37} and C_{38} alkenes while others such as CS-57, G1779GE, M181, 88E and EH2 etc. lack the C_{37} and C_{38} hydrocarbons (Conte et al. 1995; Grossi et al. 2000; Rieley et al. 1998b). In addition, $C_{29:1}$ and $C_{21:6}$ have also been found in other *E. huxleyi* strains. (Sawada and Shiraiwa 2004; Volkman et al. 1980). The double bond positions of alkenes from some of *E. huxleyi* strains have been identified, which provides chemical information to facilitate the understanding of the alkene biosynthesis pathway. For example, four C31 dienes in strain CCAP 920/2 are 1,22-, 2,22-, 3,22-, 2,24-$C_{31:2}$, and a single C_{33} diene is 2,24-$C_{33:2}$. In strain VAN 556 1,22-$C_{31:2,}$ 1,15,22-$C_{37:3}$ and 1,16,23-$C_{38:3}$ have been identified (Rieley et al. 1998b). In strains CCAP 920/2 and VAN 556, double bonds in the C_{31} and C_{33} alkenes are in the *cis* configuration, whereas in the C_{37} and C_{38} alkatrienes

they are in the *trans* configuration (Rieley et al. 1998b). Although, the positions of the double bonds of some of the alkenes in *E. huxleyi* have been established, the information about the double bond positions of other alkenes is still missing.

The growth of *E. huxleyi* is greatly influenced by nutrient availability (Paasche 1998, 2001; Paasche and Brubak 1994; Sekino et al. 1996; Sekino and Shiraiwa 1994). *E. huxleyi* can produce large quantities of organic matter by fixing dissolved inorganic carbon (DIC) (Sekino and Shiraiwa 1994), and when inorganic carbon supplies are limiting, cell growth is inhibited (Sekino et al. 1996). However, high concentrations of bicarbonate also suppresses cell growth and the mechanism of this suppression is not yet fully understood (Herfort et al. 2002, 2003). Free CO_2 substrate is incorporated into the photosynthetic intermediates, whereas HCO_3^- is primarily incorporated into $CaCO_3$ (Shiraiwa 2003b). The equilibrium balance in reaction (1) explains how bicarbonate concentration suppresses *E. huxleyi* growth:

$$HCO_3^- + OH^- \rightleftharpoons CO_2 + H_2O \quad (1)$$

Analysis of ocean blooms indicate that *E. huxleyi* growth is susceptible to the N:P ratio; optimal growth being achieved at a ratio of 16:0.2, whereas cell growth is inhibited at a N:P ratio of 16:5 (Egge and Heimdal 1994).

PULCA accumulation in *E. huxleyi* is interdependent with the growth phase and the availability of C, N, and P nutrients. Hence, PULCA

accumulation increases during stationary phase (Pond and Harris 1996), and when N and P are limiting. Depending on the strain, PULCA levels as high as 10-20% can be achieved (Epstein 1998; Prahl et al. 2003).

Although the physiological functions of alkenes remain unclear, like other neutral lipids they may function as a means of storing chemical energy (Eltgroth et al. 2005). In addition, these alkenes may play an important role in the acclimatization of these organisms to low temperature, by regulating membrane fluidity, which may be of importance in the production of large ocean blooms in high-latitude waters, where the water temperature is 10-15 ℃ (Grossi et al. 2000; Y. 2003). While the effects of nutrient (carbon, nitrogen and phosphate) availability on photosynthesis and cell grown are well characterized, little is known about how availability of these nutrients affects alkene production in *E. huxley*i.

In this study, we identified and characterized alkenes from three different strains of *E. huxleyi*, CCMP 1516, CCMP 1742 and CCMP 373), and investigated how growth modulations, achieved by varying the availability of carbon, nitrogen and phosphate nutrients affects these alkenes.

Materials and Methods

E. huxleyi strains and media

Three strain of *E. huxleyi* (CCMP1742, CCMP1516 and CCMP373) were obtained from Provasoli-Guillard National Center for Culture of Marine Phytoplankton (http://ccmp.bigelow.org). These strains were maintained in

the basic sea salt media with trace metals, vitamins and carbon, nitrogen and phosphate nutrient (CNP media) (Table 1) in batch cultures in 250 mL Pyrex flasks. Cultures were maintained at ~16 ℃, and exposed to a daily 16-h light/8-h dark cycle using cool-white fluorescent illumination (～50 μEin m^{-2} s^{-1}). Each strain was initially grown until early stationary phase (i.e., 8 days) in CNP medium. Cells were then transferred to the intended nutrient-limited medium, either carbon-enriched, phosphate and nitrogen deficient media (C media) or carbon deficient, phosphate and nitrogen enriched media (NP media) (Table 1).

Approximately 1g fresh weight of cells were pelleted at 800 g for 10 mins, washed with and transferred to C or NP media. CCMP1742, CCMP1516 and CCMP373 cells were cultured in 500 mL media in 1-L Pyrex flasks. Culture flasks were stirred by gentle swirling once a day, at the same time each day, and immediately sampled for determining cell density, and cellular alkenone content and composition. At each experimental time point, cell density was determined microscopically using a haemocytometer.

Hydrocarbon extraction

Hydrocarbons were extracted from 7-, 9-, 11-, 14- and 21-day-old cultures of *E. huxleyi*. Cells were collected by centrifugation at 1000×g at 4℃ for 10 min, and the pellet was flash-frozen in liquid nitrogen and stored at -80℃. Before analysis, cell pellets were lyophilized in a FreeZone 4.5 Liter Freeze

Dry System (LabConco, MO), and powderized with a GenoGrinder 2000 (Spex CertiPrep, NJ).

Immediately prior to extraction of hydrocarbons, 2 µg of the internal standard, hexacosane (1 mg/mL) (Fluka, WI) was applied directly to approximately 10 mg of lyophilized cells. HPLC-grade hexane (Fisher Scientific, NJ; 1.5 mL) was used to extract the cells, and samples were sonicated for 15 min. Following centrifugation at 13000 g for 1 min, the supernatant was collected. This extraction-sonication-centriguation step was repeated two more times. The combined extract-supernatants for each sample were passed over a pre-packed silica gel (J.T. Baker, NJ) column (9 inch in length and 5.0 mm inner diameter), which was pre-washed with 10 mL hexane. The hexane eluent was collected and dried in a rotary nitrogen evaporator (Organomation Associates, INC, MA) at 30 ℃. The dried hydrocarbon sample was dissolved in 200 µL hexane for GC-MS analysis.

Nile Red staining, microscopy and spectrofluorometry

Culture aliquots (1 mL) were sampled at different time points during growth, and cells were stained by the addition of 6 µL of 500 $\mu g.mL^{-1}$ Nile Red dissolved in acetone. Wet mounts were examined with a Nikon Eclipse TE-200 fluorescent microscope (Nikon Inc., Melville, NY, USA) equipped with a narrow TRITC filter (excitation 510-560 nm, dichroic mirror and barrier filter, 495 nm).

Images were captured with a Hamamatsu C4742-95 camera (Hamamatsu, Bridgewater, NJ).

Hydrogenation reaction

To confirm the nature of unsaturated hydrocarbons, hydrocarbon extracts were hydrogenated with H_2 using palladium catalyst (Sigma-Aldrich) (Perera et al., 2010). An aliquot of the extract containing approximately 1 mg of hydrocarbons was dissolved in 1 mL of ethyl acetate, and 0.25 mg of palladium activated in carbon was added as catalyst. The solution was placed in a Parr Bomb hydrogenation chamber (Parr, http://www.parrinst.com), under an H_2 atmosphere and incubated at room temperature for 12 h under 690 kPa pressure. The resulting product was filtered to remove the catalyst, and the solution was evaporated under N_2 gas. After silylation (Sweeley et al. 1963), the products were analyzed by GC-MS.

Dimethyl disulfide reaction

Double bond positions were determined by GC-MS analysis of dimethyl disulfide adducts (Buser et al., 1983). Approximately 1 g of hydrocarbon extract was dissolved in 50 L hexane and incubated at 40 °C over night with 50 L dimethyl disulfide and 5 L of 0.06% (w/v) I_2 in diethyl ether. The reaction was stopped by the addition of 50 L of 5% (w/v) sodium thiosulfate

and samples were diluted with 200 L hexane. The organic phase was removed and concentrated prior to GC-MS analysis.

Gas chromatography-mass spectrometric analysis

Chromatographic analysis was performed with a gas chromatograph (Model 6890 series, Agilent Technologies, Palo Alto, CA), equipped with a mass detector Model 5973 (Agilent Technologies, Palo Alto, CA). Chromatography was conducted using a HP-5MS cross-linked (5%)-diphenyl-(95%)-dimethyl polysiloxane column (30 m length, 0.25 mm inner diameter), using helium as the carrier gas. The injection temperature was at 280℃. The oven temperature was initially at 200 ℃, was increased to 280 ℃ at a rate of 4 ℃/min, further increased to 320 ℃ at a rate of 20 ℃/min and held at this temperature for 3 min.

Results

Growth of E. huxleyi

We investigated the effect of altering the supply of carbon, nitrogen and phosphate nutrients in the media on the growth of three strains of *E. huxleyi*, CCMP 1516, CCMP 1742 and CCMP 373. In these experiments, the strains were initially grown in CNP media, which contained nitrogen, phosphate and phosphate. Each strain reached stationary phase after 8 days of culture initiation (Fig. 1). Although all three strains showed a doubling time of approximately 2 days, strain CCMP 373 reached stationary phase at a cell density that was only one-fourth of the highest cell density reached by CCMP

1516 and CCMP 1742 (Fig 1a). Upon reaching stationary phase, each strain was transferred to one of three media: 1) fresh CNP medium, which contained the normal levels of carbon, nitrogen and phosphorus; 2) a medium containing unchanged level of carbon but deficient in nitrogen and phosphate (C media); and 3) a media containing unchanged level of nitrogen and phosphate but deficient in carbon (NP media). Figure 1b and 1c, shows the growth of each strain in these three media. For each of the strains, cells continue to grow in both the NP and CNP media but fail to grow or multiply after transfer to C media, which is deficient in N and P nutrients (Fig. 1b and 1c).

Identification of alkenes of E. huxleyi

GC-MS analyses hydrocarbons extracted from the three strains indicated that CCMP 1516 and CCMP 1742 grown in C, NP or CNP media produce the same types of alkenes. These are homologous series of compounds ranging from 31 to 35 carbon atoms with two or more double bonds. In contrast, CCMP 373 produced only two diene constituents, $C_{37:2}$ and $C_{38:2}$ (Fig. 2). The authentic identification of each hydrocarbon was established by a combination of co-elution with commercial standards, and by analysis of the mass spectrum of the individual components (Fig. 2). To confirm the constituents were alkenes, the hydrocarbon extracts were hydrogenated with H_2 in the presence of a palladium catalyst under high pressure and analyzed by GC-MS analysis (Fig. 3). The complexity of the hydrocarbon extracts, resulting from the occurrence of carbon-carbon double

bonds, was reduced upon hydrogenation, collapsing all unsaturated hydrocarbons to the respective saturated alkanes (Fig. 3). The chemical identification of these hydrogenated hydrocarbons was confirmed by comparing their retention times to commercial standards and by analysis of the mass spectrum following electron impact ionization-induced fragmentation (Laureillard et al. 1986).

The positions of the double bonds in the unsaturated hydrocarbons were identified by the mass-spectroscopic analysis of dimethyl disulfide adducts (Buser et al. 1983; Carlson et al. 1989) (Fig. 4). Electron ionization mass spectrometry of these adducts generated fingerprint ions, from which the position of the double bonds could be deduced. For example, Fig. 5a illustrates the analysis of a 31-carbon diene from CCMP 1516 (identified as a diene by the m/z value of the molecular ion of the dimethyl disulfide adduct). The m/z values of one pair of fragmentation ions of 355 and 173 and another pair of fragmentation ions of 61 and 511 indicate that the double bonds in this diene occur at the first and twenty-second positions. Hence, based upon these analyses, this metabolite was identified as 1,22-$C_{31:2}$.

Additional parallel analyses established the occurrence of double-bond positions of other alkenes, 7,22-$C_{31:2}$, 1,9-$C_{33:2}$, 1,3,9-$C_{33:3}$, 1,6,9-$C_{33:3}$, 2,8,23-$C_{34:3}$, 1,8,17,25-$C_{34:4}$, 1,8,26-$C_{35:3}$ and 1,5,13,26-$C_{35:4}$ in CCMP 1516 and CCMP 1742. The same strategy was applied to the alkenes of CCMP 373, and Figure 5b illustrates the analysis of a 37-carbon diene; the m/z values

of one pair of fragmentation ions, 257 and 353 indicate that the double bonds in this diene occur at the fifteenth and twenty-second positions. Therefore, this metabolite was identified as 15,22-$C_{37:2}$. Similarly, the $C_{38:2}$ diene was identified as 15,22-$C_{38:2}$. Double bond positions of all other alkenes for the three strains are listed in Table 2 and their mass spectrums are in the Supplemental Figures S1.

Lipid bodies observed by epifluorescence microscopy

When *E. huxleyi* cells were stained with the lipophilic dye Nile Red, the lipid bodies (LBs) exhibited fluorescence when exposed to ultraviolet light. LBs varied in number and size among cells, but most cells had multiple LBs, mostly at the cell periphery. *E. huxleyi* CCMP 1516 (Fig. 6) and CCMP1742 (Fig. 6) cells had more LBs when grown in media low in N and P (media C), as compared to cells grown in media containing adequate levels of nitrogen and phosphate (medium NP). CCMP 373, in contrast, contains more lipid bodies when grown in medium NP as compared to cells grown in medium C (Fig 7).

Hydrocarbon accumulation differs among E. huxleyi strains grown under different nutrient-limiting conditions. E. huxleyi strains CCMP 1516, CCMP 1742 and CCMP 373 were first grown in CNP media for 8 days, and then transferred to CNP, C and NP media respectively. Strains CCMP 1516 and CCMP 1742 in C and NP media were sampled at the time of inoculation, and at 1, 2, and 3 weeks later. Strain CCMP 373 was similarly sampled at 7, 9, 12, 14 and 16 days. All collected samples were subjected to hydrocarbon

analysis to investigate the effect of nutrient availability on hydrocarbon accumulation.

When strain CCMP 1516 was transferred from CNP medium to the C medium, accumulation of hydrocarbons increased more than two-fold within 2 weeks after transfer, as compared to the initial inoculum of this strain. However, in NP medium, increased alkene accumulation was delayed and did not occur until 3 weeks after transferring. The largest difference in alkene accumulation in the two media by CCMP 1516 occurred at 2 weeks after transfer, when there was a 3-fold higher alkene levels in C medium than the NP medium. As far as the relative proportions of individual alkenes were concerned, at the time of transfer, the major alkenes in CCMP 1516 were 1, 22-$C_{31:2}$ (>40%) and 1,8,26-$C_{35:3}$ (~35%). After transferring to the C and NP media, relative percentage of these two alkenes declined, while the percentage of 7,22-$C_{31:2}$, 1,9-$C_{33:2}$, 2,8,23-$C_{34:3}$ increased (Supplemental Table 1 and Fig 6).

CCMP 1742 accumulated enhanced levels of alkenes after transferring to C and NP medium. However, the speed of this increased accumulation in C medium is much faster than in NP medium (Fig. 6). At all time points that were assesed, CCMP 1742 produced more alkenes in C medium than in NP medium. The biggest difference in accumulation between the two media occurs at 2 weeks after transfer, when there was a 6-fold difference between the two media. At the time of transfer, the major alkenes were the trienes, 1,6,9-$C_{33:3}$ and 2,8,23-$C_{34:3}$. As the cultures aged, the relative proportion of

these trienes decreased, while the proportion of 1,22-$C_{31:2}$, 7,22-$C_{31:2}$, and 1,8,26-$C_{35:3}$ increased (Supplemental Table 2 and Fig. 6). In consistent to the observation of lipid bodies by NR staining, CCMP 373 (Fig. 7) produces more alkenes in NP medium than in C medium in opposite to what has been observed in two other *E. huxleyi* strains, CCMP 1516 and CCMP 1742.

Total alkene accumulation in strain CCMP 373 remained constant after transferring to C media but in NP medium alkenes initially increased and then decreased as the culture aged (Fig 7). In both C and NP media, CCMP 373 produced more 15,22-$C_{37:2}$ than 15,22-$C_{38:2}$. The relative proportion of these two dienes was unchanged in the NP medium, in C medium 15,22-$C_{37:2}$ first decreased and then increased, while that of 15,22-$C_{38:2}$ was contrary (Supplemental Table 3 and Fig. 7).

Discussion

Alkenes identified in *E. huxleyi*

Prior studies of the lipids of *E. huxlei* have identified a number of neutral lipids, including very long chain alkenes, this includes $C_{31:2}$, $C_{33:2}$, $C_{33:3}$, $C_{33:4}$, $C_{37:2}$, $C_{37:3}$, $C_{38:2}$ and $C_{38:3}$ (Grossi et al. 2000; Rieley et al. 1998b; Sawada and Shiraiwa 2004; Volkman et al. 1980). In the current study of strains CCMP 1516, CCMP 1742, and CCMP 373 we have detected and characterized dienes (i.e., $C_{31:2}$, $C_{33:2}$, $C_{37:2}$ and $C_{38:2}$), trienes (i.e., $C_{33:3}$, $C_{34:3}$ and $C_{35:3}$), and tetraenes (i.e., $C_{33:4}$ and $C_{35:4}$), which are apparently without precedent. Both $C_{37:2}$ and $C_{38:2}$ identified in CCMP 373 have double bond positions at 15 and

22. $C_{31:2}$, $C_{33:2}$, $C_{33:3}$, $C_{35:3}$, $C_{35:4}$ identified in CCMP1516 and CCMP 1742 have one double bond position at 9th and another one at the terminal end. Another $C_{31:2}$ identified in CCMP 1516 and CCMP 1742 have a double bond at 7th position in addition to 9th position. And $C_{34:3}$ has double bond positions at 2, 8 and 23 or at 1, 8 and 17.

Although alkene content has been characterized for many strains of algae, their biosynthesis has not been extensively studied. However, considering the position(s) of the double bonds in these alkenes, and pre-supposing that these alkenes are derived from unsaturated fatty acids, one can begin to formulate hypotheses concerning their biosynthetic origins. For example, the n-9 (ω 9) position of unsaturation in the most of the alkenes, (e.g. 1,22-$C_{31:2}$, 7,22-$C_{31:2}$, 1,6,9-$C_{33:3}$, 1,3,9-$C_{33:3}$, 1,9-$C_{33:2,}$ 1,8,17,25-$C_{34:4}$, 1,8, 26-$C_{35:3}$ and 1,5, 13,26-$C_{35:4}$) is strong evidence that these alkenes were derived from an oleic acid (cis-9-C18:1) precursor via chain elongation and desaturation (Rontani et al. 2006).

Unlike CCMP 1516 and CCMP 1742, CCMP 373 produced only two types of alkenes, the dienes 15,22-$C_{37:2}$ and 15,22-$C_{38:2}$. C_{37} and C_{38} alkadienes and trienes with double bond positions at 15 and 22 were previously detected in *E. huxleyi* strain CS-57 (Grossi et al. 2000; Rieley et al. 1998b). In addition, corresponding methyl C_{37} and C_{38} alkenones have also been found in *E. huxleyi* strain CS-57 (Rontani et al. 2006). This might suggest that in *E. huxleyi* CS-57, 15,22-$C_{37:2}$ and 15,22-$C_{38:2}$ are biosynthesized from their

corresponding methyl C_{37} and C_{38} alkenones, which were initially reduced to alkenols and then dehydrated to alkatrienes, which were further reduced to C_{37} and C_{38} alkadienes (Grossi et al. 2000; Rontani et al. 2006). The C_{37} and C_{38} alkenones with the same double bonds positions are probably derived from β-keto acids, which are converted from long-chain 3-ketoacyl-CoA in the fatty acid elongation as what happened in plant (Fridman et al. 2005). By using acetyl-CoA and propionyl-CoA as primers for fatty acid synthesis and elongation followed by Δ^{14} and Δ^{15} desaturation, both C_{37} (odd-numbered) and C_{38} (even-numbered) methyl ketone with two double bones can be formed (Rontani et al. 2006).

Therefore, the $C_{37:2}$ and $C_{38:2}$ from CCMP 373 likely share a common biosynthetic pathway. Instead, in CCMP 1516 and CCMP 1742 there are potentially multiple biosynthetic pathways at work. Those alkenes (1,22-$C_{31:2}$, 1,9-$C_{33:2}$, 1,3,9 and 1,6,9-$C_{33:3}$, 1,8,26-$C_{35:3}$, 1,8,17,25-$C_{34:4}$, 1,5,13,26-$C_{35:4}$) with double bonds at 9th position and terminal end, might use the oleic acid as precursor with (trienes and tetraienes) or without (dienes) further desaturation and then form a terminal double position by the terminal decarboxylation step. Other alkenes, including 7,22-$C_{31:1}$ and 2,8, 23-$C_{34:3}$ might be biosynthesized by a different unknown pathway or using different precursors.

Regulation of alkene accumulation by controlling carbon, nitrogen and phosphate nutrient availability

Our experiments with three strains of *E. huxleyi* , CCMP 1516, CCMP1742 and CCMP 373 have shown the alkene composition in this organism is subject to significant change not only as a consequence of genetics (explored by investigating different strains), but also in response to environmentally relevant physiological growth factors, such as carbon, nitrogen and phosphate nutrient availability.

The growth of strains CCMP 1516, CCMP 1742, and CCMP 373 each behaved similarly but the alkene accumulation of CCMP 1516 and CCMP 1742 reacted differently from CCMP 373 to different carbon, nitrogen and phosphate availabilities. In all of three strains, the supply of nitrate and phosphate (NP media) (Lopez-Nieves et al. 2012) stimulated growth, whereas a high concentration of bicarbonate (C media) suppressed cell growth, which is consistent with previous findings (Paasche 1998, 2001; Paasche and Brubak 1994; Sekino et al. 1996; Sekino and Shiraiwa 1994). For example, CCMP 1516 and CCMP1742 accumulated more alkenes in C medium as compared to NP medium, whereas CCMP 373 accumulated more alkenes in NP medium as compared to C medium. Increased carbon sources have been reported to improve lipid and hydrocarbon production in a number of algae, including *Chlamydomonas* (Lopez-Nieves et al. 2012) and *Botryococcus braunii* (Ge et al. 2011b), which is similar to the situation with CCMP 1516 and CCMP 1742. In addition, our results in CCMP 1516 and CCMP 1742 are consistent to previous finding that the *E. huxleyi* PULCAs, which are similar in structure to

alkenes, also increased under N and P limitation (Epstein 1998; Prahl et al. 2003).

The accumulation of PUCLAs might comprise a starvation-stress response of *E. huxleyi*, and thus their increased biosynthesis in response to nutrient deprivation significantly alters the biochemical composition of these cells (Grossi et al. 2000; Shuter 1979). However, these biochemical changes appear to be different to the nutrient deprivation. With CCMP 373, more alkenes accumulate in response to carbon-deficiency (but sufficient supply of nitrogen and phosphate), and with both CCMP 1742 and CCMP 1516, deficiency in nitrogen and phosphate induce these biochemical changes.

Algae cells are known to undergo complicated modifications in growth and of their intracellular and membrane composition in response to growth regulating environmental factors such as nutrient availability (Shuter 1979; Sunda and Huntsman 1995). For example, a critical factor for *E. huxleyi* ocean-blooms is the NO_3:PO_4 ratio; blooms occuring when this ratio is greater than 16 (Lessard et al. 2005). However, the NO_3:PO_4 ratio suitable for alkene production by *E. huxleyi* strains has not been reported.

One may be able to extrapolate from the chemically-similar, but more characterized system of alkenone synthesis. Cellular alkenone levels and degree of unsaturation is also affected by environmental factors like nutrients and temperature (Conte et al. 1998; Epstein 1998). In some strains of haptophytes, nutrient- or temperature-limited growth stress, induces

production of alkenones, and degree of unsaturation of C_{37}- and C_{38}-alkenones significantly decreases (Conte et al. 1998; Epstein 1998), whereas in other strains little change in alkenone concentration or degree of unsaturation occurs in nitrate-limited conditions (Popp et al. 1998).

This may also be the case for *E. huxleyi*, and different strains may have different favorable NO_3:PO_4 ratio for alkene production and unsaturation. In this study the NO_3:PO_4 ratio was ~24, which may be suitable for CCMP 373 to produce alkenes but not for CCMP 1516 and CCMP 1742. In addition, the C:N ratio has been reported to affect growth of *E. huxleyi* (Kaffes et al. 2010), which may also influence alkene production in *E. huxleyi*.

References

Buser HR, Arn H, Guerin P, Rauscher S (1983) Determination of Double-Bond Position in Monounsaturated Acetates by Mass-Spectrometry of Dimethyl Disulfide Adducts. Anal Chem 55:818-822

Carlson DA, Roan CS, Yost RA, Hector J (1989) Dimethyl Disulfide Derivatives of Long-Chain Alkenes, Alkadienes, and Alkatrienes for Gas-Chromatography Mass-Spectrometry. Anal Chem 61:1564-1571

Conte MH, Thompson A, Eglinton G (1994) Primary Production of Lipid Biomarker Compounds by Emiliania-Huxleyi - Results from an Experimental Mesocosm Study in Fjords of Southwestern Norway. Sarsia 79:319-331

Conte MH, Thompson A, Eglinton G, Green JC (1995) Lipid Biomarker Diversity in the Coccolithophorid Emiliania-Huxleyi (Prymnesiophyceae) and the Related Species Gephyrocapsa-Oceanica. J Phycol 31:272-282

Conte MH, Thompson A, Lesley D, Harris RP (1998) Genetic and physiological influences on the alkenone/alkenoate versus growth temperature relationship in Emiliania huxleyi and Gephyrocapsa oceanica. Geochim Cosmochim Ac 62:51-68

Egge JK, Heimdal BR (1994) Blooms of Phytoplankton Including Emiliania-Huxleyi (Haptophyta) - Effects of Nutrient Supply in Different N-P Ratios. Sarsia 79:333-348

Eltgroth ML, Watwood RL, Wolfe GV (2005) Production and cellular localization of neutral long-chain lipids in the haptophyte algae Isochrysis galbana and Emiliania huxleyi. J Phycol 41:1000-1009

Epstein BL, D' Hondt, S., Quinn, J. G., Zhang, J. & Hargraves, P. E. (1998) The effect of dissolved nutrient concentrations on alkenone-based temperature estimates. . Paleoceanography 13:122-126

Fridman E, Wang J, Iijima Y, Froehlich JE, Gang DR, Ohlrogge J, Pichersky E (2005) Metabolic, genomic, and biochemical analyses of glandular trichomes from the wild tomato species Lycopersicon hirsutum identify a key enzyme in the biosynthesis of methylketones. Plant Cell 17:1252-1267

Ge YM, Liu JZ, Tian GM (2011) Growth characteristics of Botryococcus braunii 765 under high CO(2) concentration in photobioreactor. Bioresource Technol 102:130-134

Grossi V, Raphel D, Aubert C, Rontani JF (2000) The effect of growth temperature on the long-chain alkenes composition in the marine coccolithophorid Emiliania huxleyi. Phytochemistry 54:393-399

Herfort L, Thake B, Roberts J (2002) Acquisition and use of bicarbonate by Emiliania huxleyi. New Phytol 156:427-436

Herfort L, Thake B, Roberts J (2003) Acquisition and use of bicarbonate by Emiliania huxleyi (vol 156, pg 427, 2002). New Phytol 158:225-225

Kaffes A, Thoms S, Trimborn S, Rost B, Langer G, Richter KU, Koehler A, Norici A, Giordano M (2010) Carbon and nitrogen fluxes in the marine coccolithophore Emiliania huxleyi grown under different nitrate concentrations. J Exp Mar Biol Ecol 393:1-8

Laureillard J, Largeau C, Waeghemaeker F, Casadevall E (1986) Biosynthesis of the Resistant Polymer in the Alga Botryococcus-Braunii Studies on the Possible Direct Precursors. J Nat Prod 49:794-799

Lessard EJ, Merico A, Tyrrell T (2005) Nitrate : phosphate ratios and Emiliania huxleyi blooms. Limnol Oceanogr 50:1020-1024

Lopez-Nieves S, Jones H, Garcia O, Collins A, Timlin J, Hanson D (2012) Interactions between the Co2 Concentrating Mechanism and Lipid Production

of Two Species of Algae: Chlamydomonas Reinhardtii and Nannochloropsis Salina. Pharm Biol 50:673-673

Paasche E (1998) Roles of nitrogen and phosphorus in coccolith formation in Emiliania huxleyi (Prymnesiophyceae). Eur J Phycol 33:33-42

Paasche E (1999) Reduced coccolith calcite production under light-limited growth: a comparative study of three clones of Emiliania huxleyi (Prymnesiophyceae). Phycologia 38:508-516

Paasche E (2001) A review of the coccolithophorid Emiliania huxleyi (Prymnesiophyceae), with particular reference to growth, coccolith formation, and calcification-photosynthesis interactions. Phycologia 40:503-529

Paasche E, Brubak S (1994) Enhanced Calcification in the Coccolithophorid Emiliania-Huxleyi (Haptophyceae) under Phosphorus Limitation. Phycologia 33:324-330

Pond DW, Harris RP (1996) The lipid composition of the coccolithophore Emiliania huxleyi and its possible ecophysiological significance. J Mar Biol Assoc Uk 76:579-594

Popp BN, Kenig F, Wakeham SG, Laws EA, Bidigare RR (1998) Does growth rate affect ketone unsaturation and intracellular carbon isotopic variability in Emiliania huxleyi? Paleoceanography 13:35-41

Prahl FG, Wolfe GV, Sparrow MA (2003) Physiological impacts on alkenone paleothermometry. Paleoceanography 18

Rieley G, Teece MA, Peakman TM, Raven AM, Greene KJ, Clarke TP, Murray M, Leftley JW, Campbell CN, Harris RP, Parkes RJ, Maxwell JR (1998) Long-chain alkenes of the haptophytes Isochrysis galbana and Emiliania huxleyi. Lipids 33:617-625

Rontani JF, Prahl FG, Volkman JK (2006) Re-examination of the double bond positions in alkenones and derivatives: Biosynthetic implications. J Phycol 42:800-813

Sawada K, Shiraiwa Y (2004) Alkenone and alkenoic acid compositions of the membrane fractions of Emiliania huxleyi. Phytochemistry 65:1299-1307

Sekino K, Kobayashi H, Shiraiwa Y (1996) Role of coccoliths in the utilization of inorganic carbon by a marine unicellular coccolithophorid, Emiliania huxleyi: A survey using intact cells and protoplasts. Plant Cell Physiol 37:123-127

Sekino K, Shiraiwa Y (1994) Accumulation and Utilization of Dissolved Inorganic Carbon by a Marine Unicellular Coccolithophorid, Emiliania-Huxleyi. Plant Cell Physiol 35:353-361

Shiraiwa Y (2003) Physiological regulation of carbon fixation in the photosynthesis and calcification of coccolithophorids. Comp Biochem Physiol B Biochem Mol Biol 136:775-783

Shuter B (1979) A model of physiological adaptation in unicellular algae. J Theor Biol 78:519-552

Sunda WG, Huntsman SA (1995) Iron Uptake and Growth Limitation in Oceanic and Coastal Phytoplankton. Mar Chem 50:189-206

Sweeley CC, Bentley R, Makita M, Wells WW (1963) Gas-Liquid Chromatography of Trimethylsilyl Derivatives of Sugars and Related Substances. J Am Chem Soc 85:2497-&

Volkman JK, Eglinton G, Corner EDS, Forsberg TEV (1980) Long-Chain Alkenes and Alkenones in the Marine Coccolithophorid Emiliania-Huxleyi. Phytochemistry 19:2619-2622

Y. S (2003) Physiological regulation of carbon fixation in the biosynthesis and calcification of coccolithophorids Comparative biochemistry and Physiology Part B 136:775-783

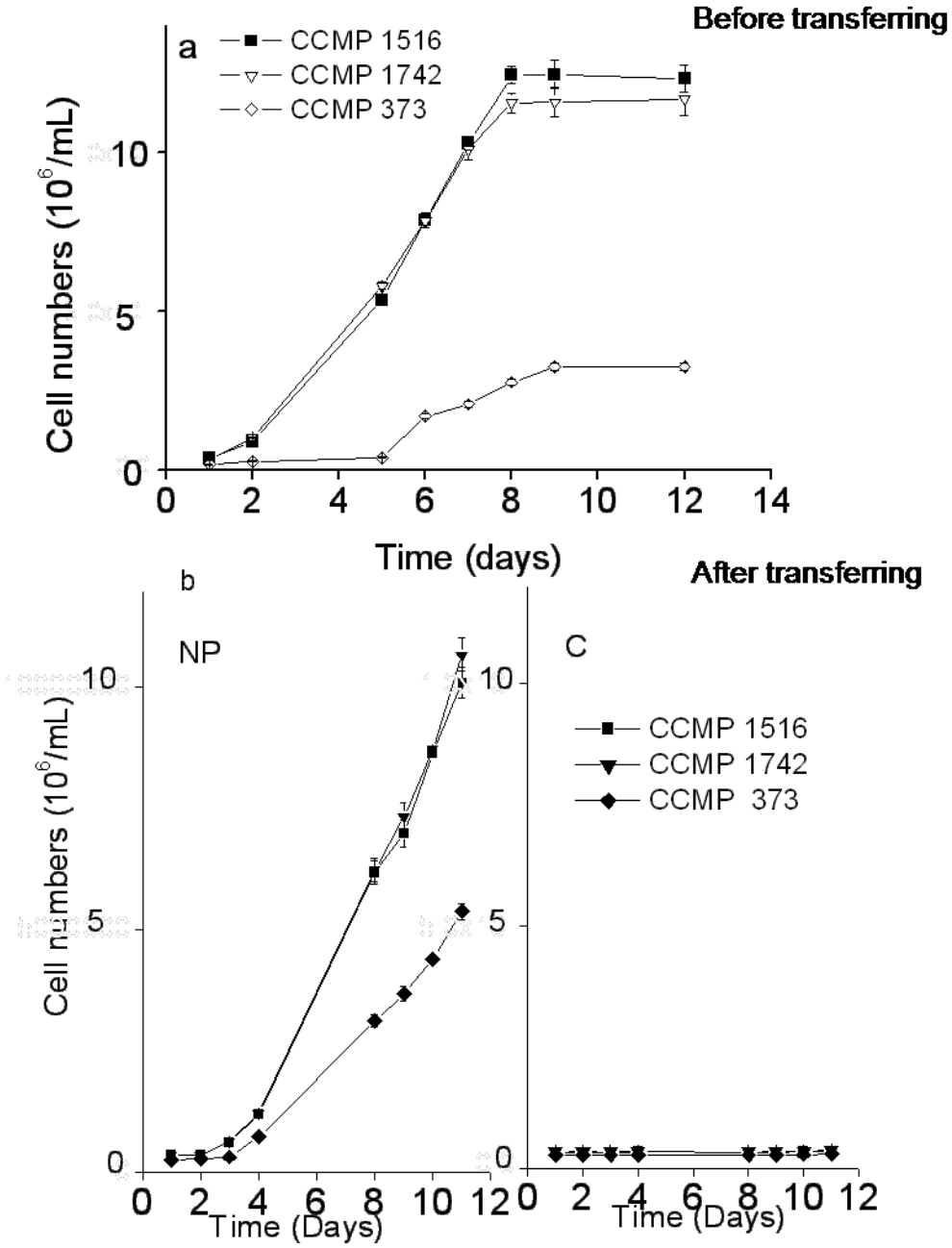

Figure 1. Growth curve of 3 strains of *E. huxleyi* in basic sea salt media with carbon, nitrogen and phosphate source a). CCMP 1516, CCMP 1742 and CCMP 373 in CNP before transferring and b). In NP and C media after transferring

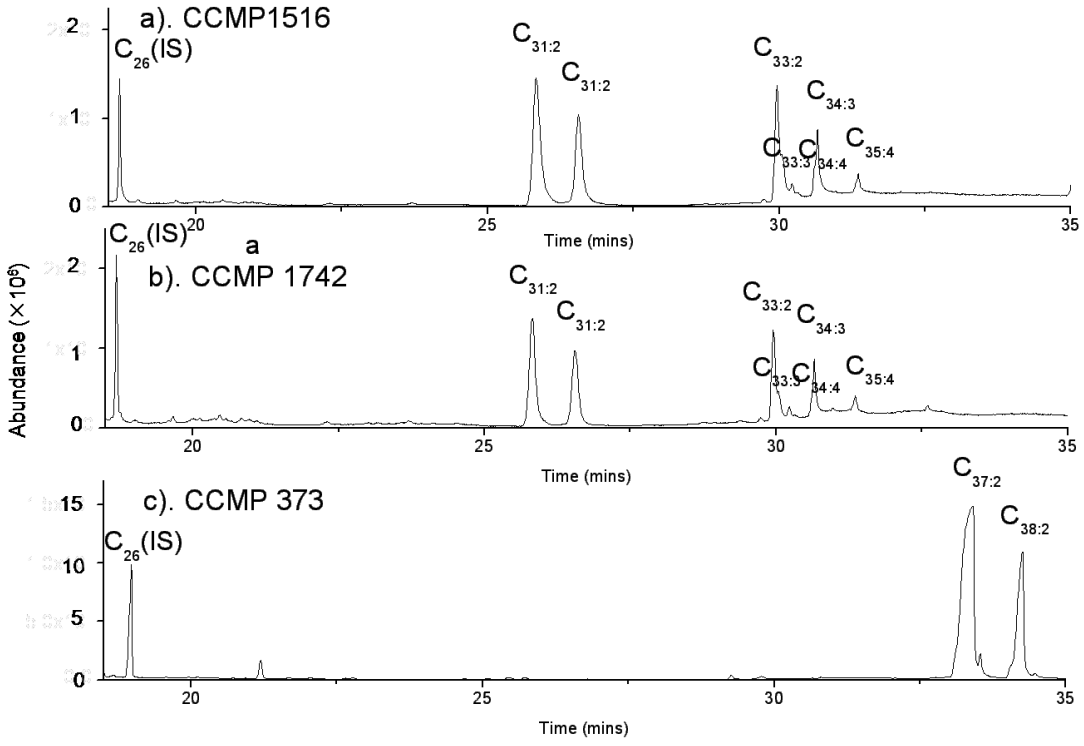

Figure 2. GC-MS analysis of hydrocarbon extracts from *E. huxleyi* of CCMP 1516 (a), CCMP 1742 (b) and CCMP 373 (c).

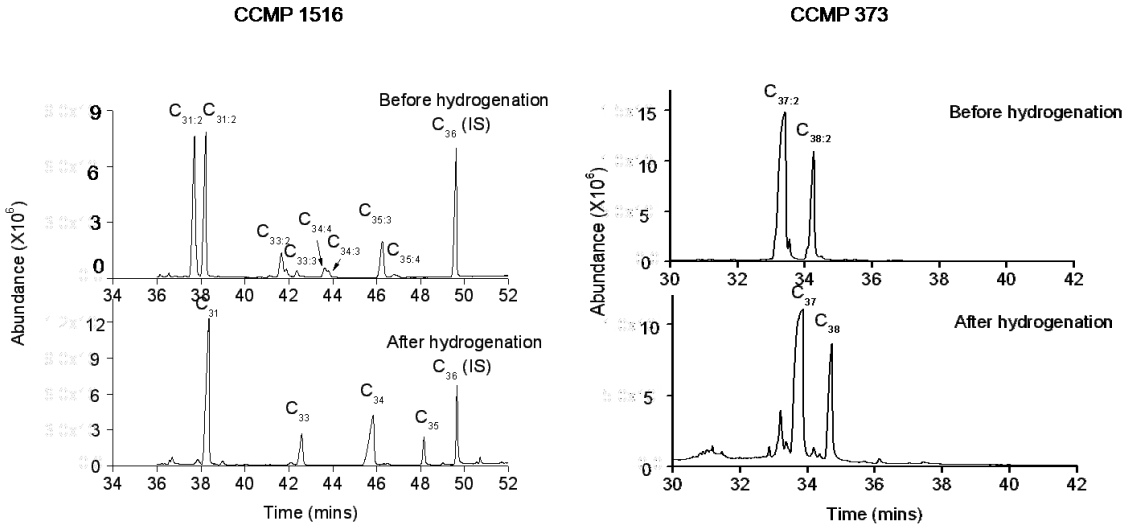

Figure 3. Comparison of hydrocarbon extracts from *E. huxleyi* before and after hydrogenation reaction.

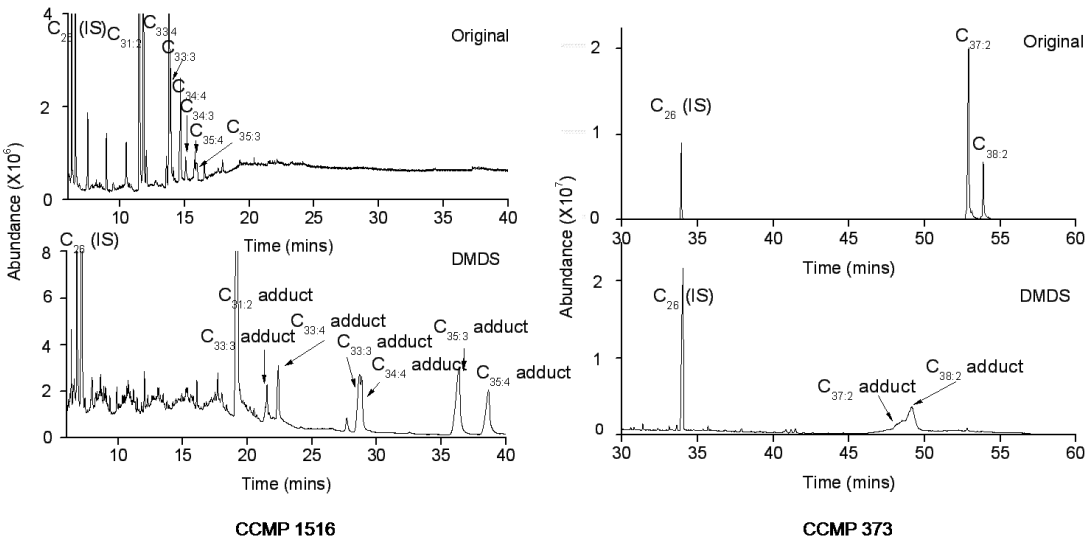

Figure 4. Comparison of hydrocarbon extracts from *E. huxleyi* before and after DMDS reaction.

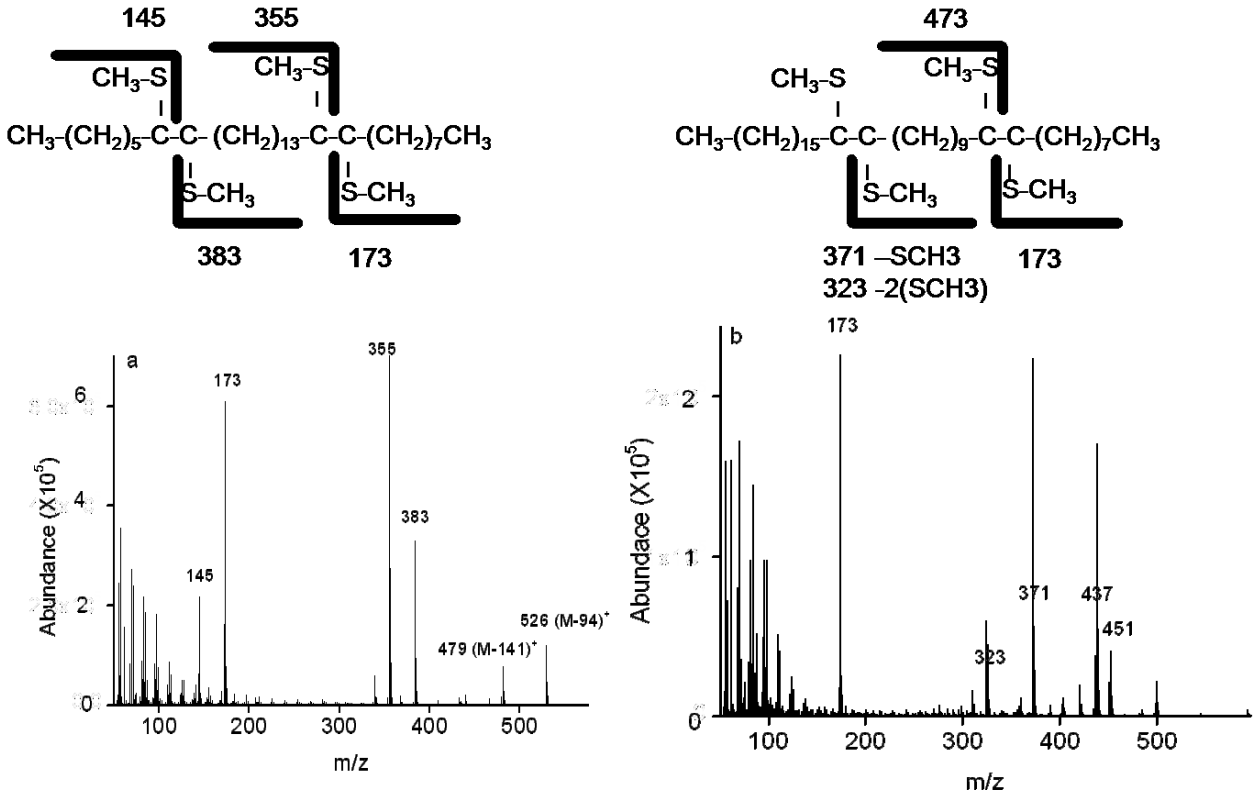

Figure 5. Mass spectrum of DMDS diadduct of 7, 22-hentricontadiene (a) and 9,20-hepatatriacontadiene (b).

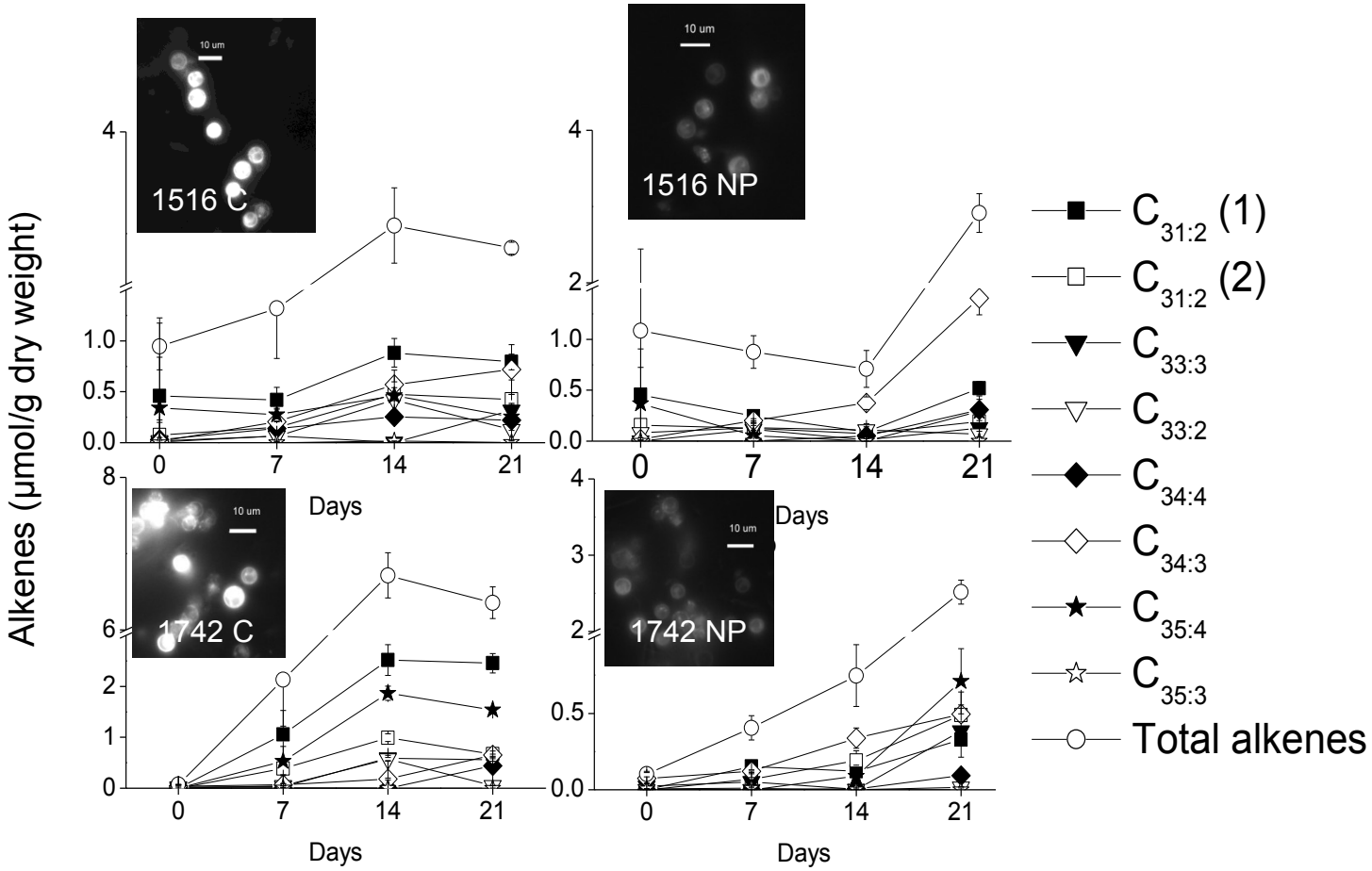

Figure 6. Individual alkene and total alkenes produced by *E. huxleyi*, CCMP 1516 and CCMP 1742 at different time after transferring to fresh C and NP media.

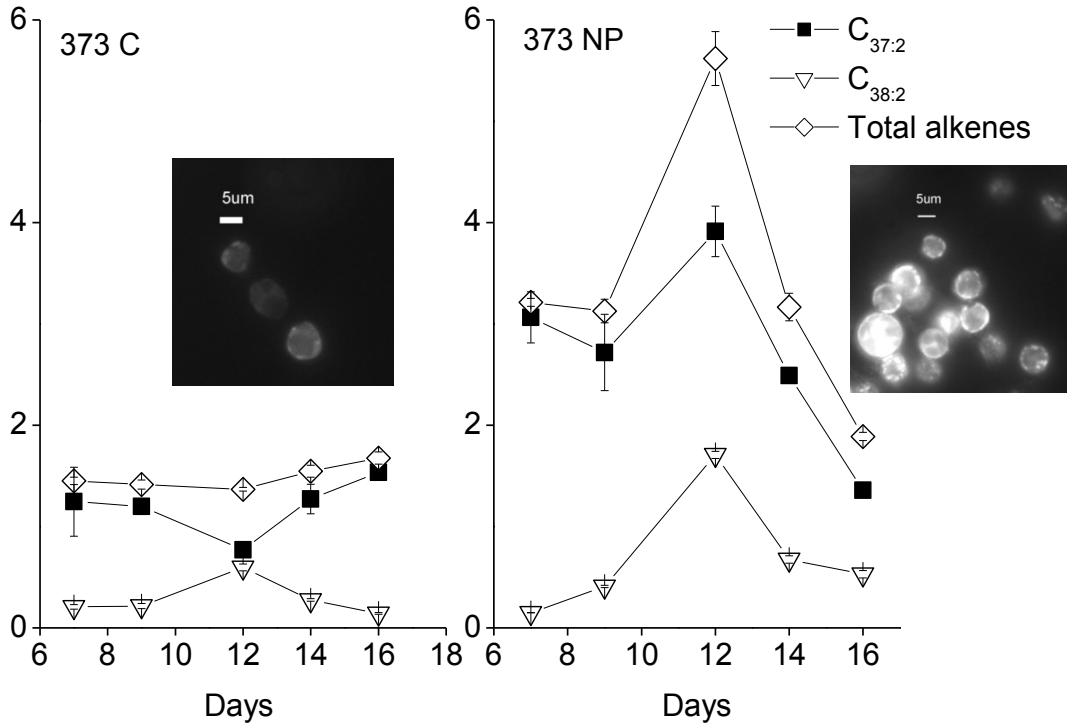

Figure 7. Individual alkene and total alkenes produced by *E. huxleyi*, CCMP 373 at different time after transferring to fresh C and NP media.

Table 1. Media to grow *E. huxleyi* CCMP 1516, CCMP 1742 and CCMP 373

Components		Media		
		C	NP	CNP
Sea salt (g/L)		40	40	40
Trace metals	$FeCl_3 \cdot 6H_2O$ (M)	1.17×10^{-5}	1.17×10^{-5}	1.17×10^{-5}
	$Na_2EDTA \cdot 2H_2O$ (M)	1.17×10^{-5}	1.17×10^{-5}	1.17×10^{-5}
	$CuSO_4 \cdot 5H_2O$ (M)	3.93×10^{-8}	3.93×10^{-8}	3.93×10^{-8}
	$Na_2MoO_4 \cdot 2H_2O$ (M)	2.60×10^{-8}	2.60×10^{-8}	2.60×10^{-8}
	$ZnSO_4 \cdot 7H_2O$ (M)	7.65×10^{-8}	7.65×10^{-8}	7.65×10^{-8}
	$CoCl_2 \cdot 6H_2O$ (M)	4.20×10^{-8}	4.20×10^{-8}	4.20×10^{-8}
	$MnCl_2 \cdot 4H_2O$ (M)	9.10×10^{-7}	9.10×10^{-7}	9.10×10^{-7}
Vitamins	Thiamine HCl (Vitamin B_1) (M)	2.96×10^{-7}	2.96×10^{-7}	2.96×10^{-7}
	Biotin (Viatamin H) (M)	2.05×10^{-9}	2.05×10^{-9}	2.05×10^{-9}
	Cyanocobalamin (Vitamin B_{12}) (M)	3.69×10^{-10}	3.69×10^{-10}	3.69×10^{-10}
NaHCO3 (g/L)		0.84	0	0.168
NaNO3 (g/L)		0	0.075	0.075
NaH2PO4•H2O (g/L)		0	0.005	0.005

Table 2. Alkenes identified in *E. huxleyi* strains

Alkene	E. huxleyi strain	
	CCMP 1516, CCMP1742	CCMP 373
C31:2 diene	1,22; 7,22- hentricontadiene	Not detected
C33:2 diene	1,9- tritriacontadiene	Not detected
C33:3 triene	1,3,9; 1,6,9- tritriacontatriene	Not detected
C34:3 triene	2,8,23-etratriacontatriene	Not detected
C34:4 tetraiene	1,8,17,25-etratriacontatetraiene	Not detected
C35:3 triene	1,8,26- heptatriacontatriene	Not detected
C35:4 tetraiene	1,5,13,26- heptatriacontatetraiene	Not detected
C37:2 diene	Not detected	15,22- heptatricontadiene
C38:2 diene	Not detected	15,22- octatriacontadiene

Figure S1. Mass spectrum of DMDS diadduct of dienes, trienes and tetraienes Identified in CCMP 1516/CCMP 1742 and CCMP 373

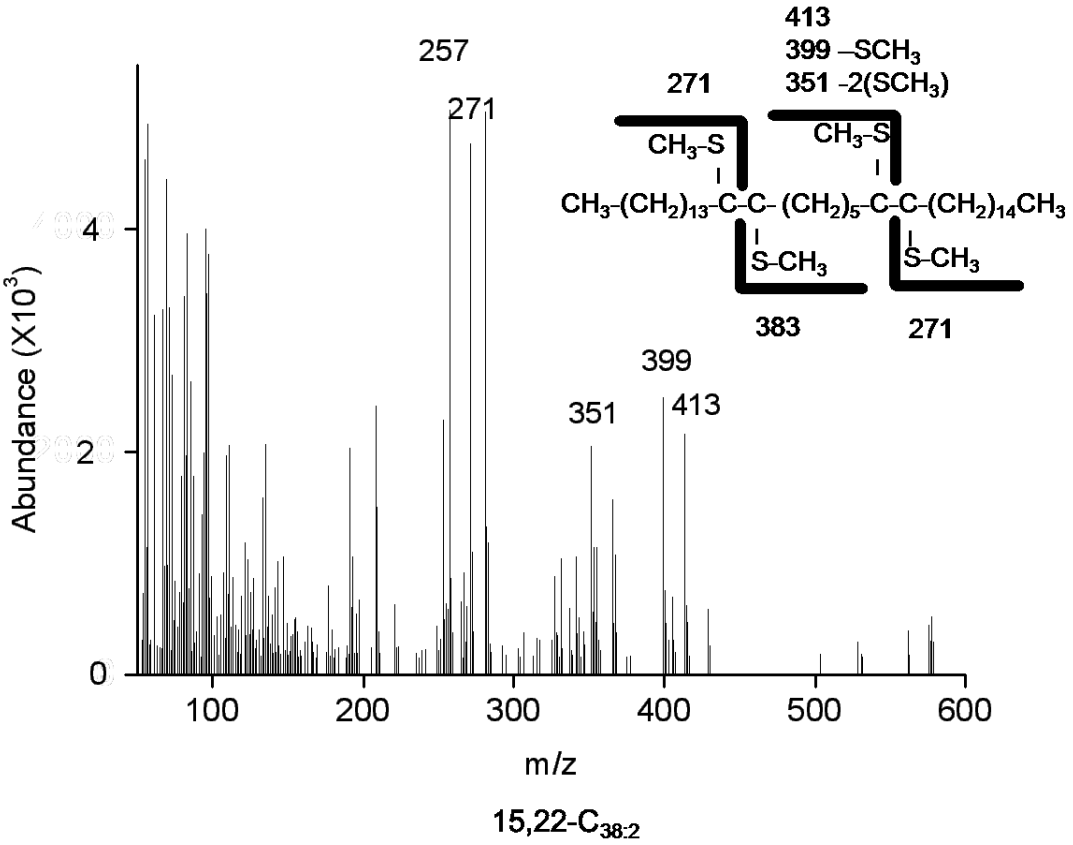
413
399 –SCH3
351 -2(SCH3)
271
257
271
CH3-S
CH3-S
CH3-(CH2)13-C-C- (CH2)5-C-C-(CH2)14CH3
S-CH3
S-CH3
383
271
399
413
351
Abundance (X10^3)
4
2
0
100
200
300
400
500
600
m/z
15,22-C38:2

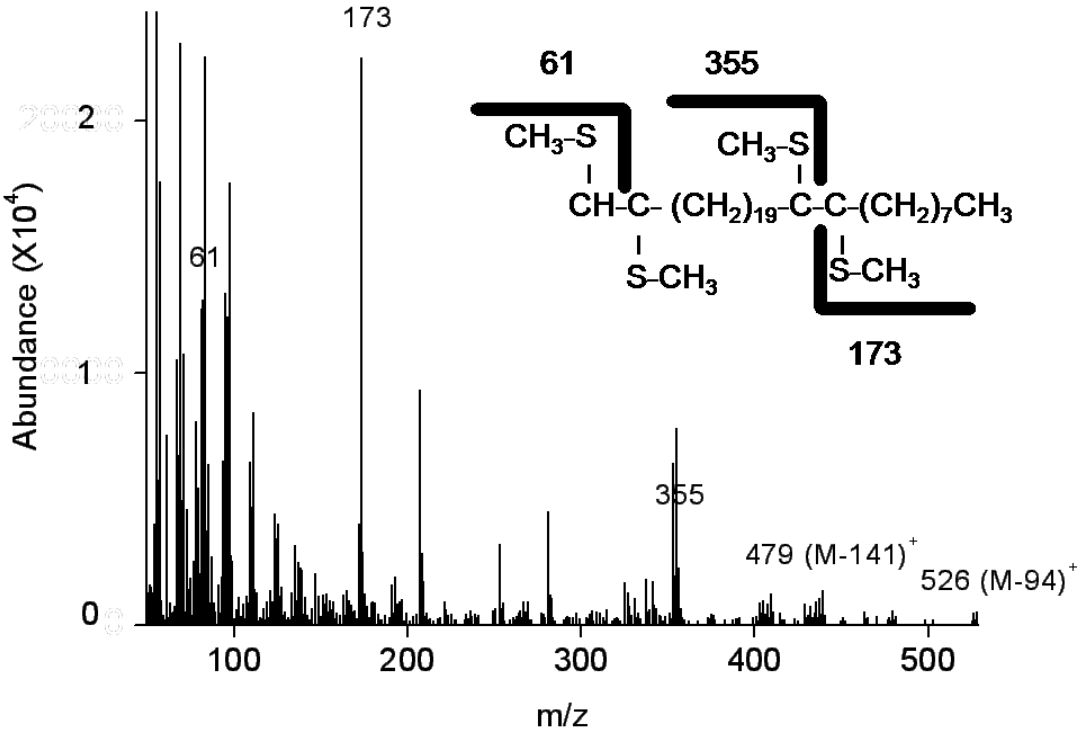
173
61
355
CH3-S
CH3-S
CH-C- (CH2)19-C-C-(CH2)7CH3
S-CH3
S-CH3
173
61
355
479 (M-141)+
526 (M-94)+
Abundance (X10^4)
2
1
0
100
200
300
400
500
m/z

1,22-$C_{31:2}$

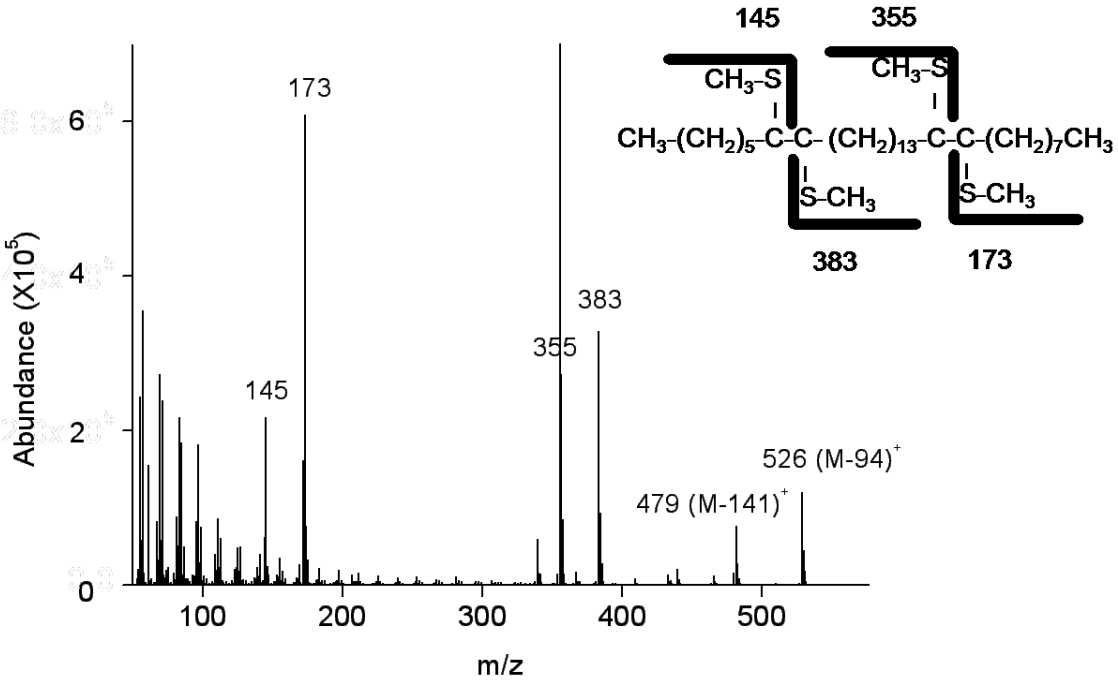
145
355
CH3-S
CH3-S
CH3-(CH2)5-C-C-(CH2)13-C-C-(CH2)7CH3
S-CH3
S-CH3
383
173
Abundance (X10^5)
6
4
2
0
173
145
355
383
526 (M-94)+
479 (M-141)+
100
200
300
400
500
m/z

7,22-$C_{31:2}$

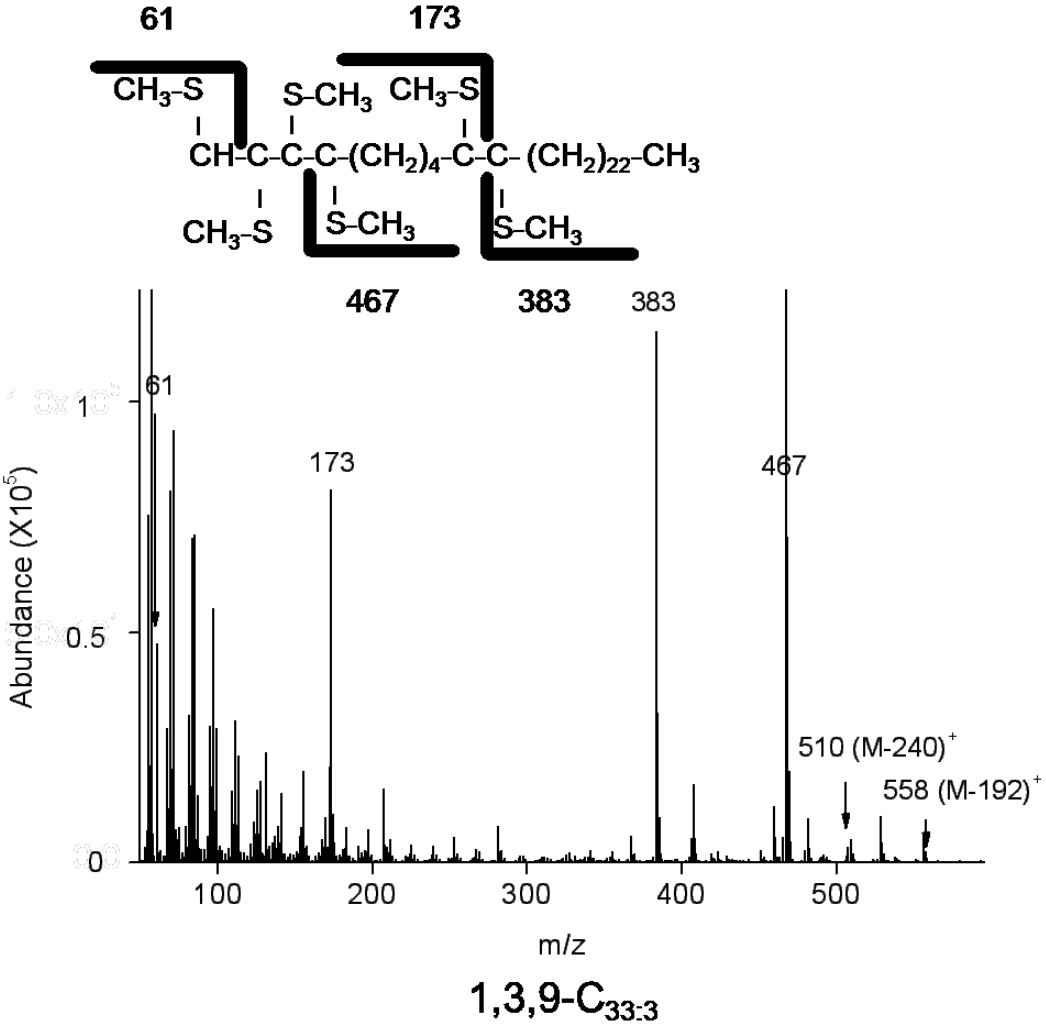
61
173
CH3-S
S-CH3
CH3-S
CH-C-C-C-(CH2)4-C-C-(CH2)22-CH3
CH3-S
S-CH3
S-CH3
467
383
383
61
173
467
510 (M-240)+
558 (M-192)+
Abundance (X10^5)
1
0.5
0
100
200
300
400
500
m/z

1,3,9-$C_{33:3}$

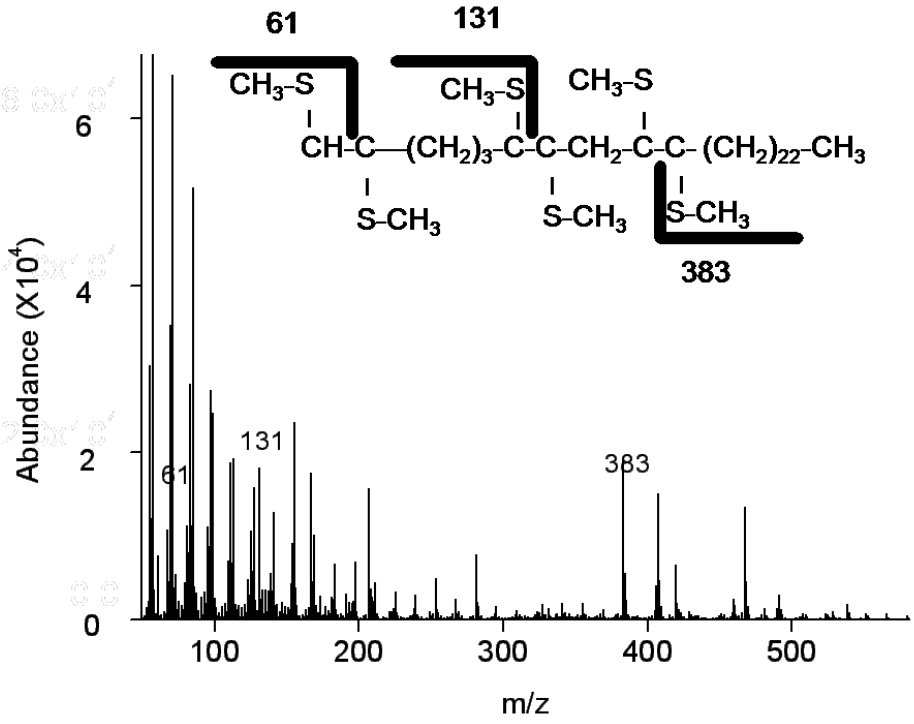
61
131
383
CH3-S
CH3-S
CH3-S
CH-C—(CH2)3-C-C-CH2-C-C-(CH2)22-CH3
S-CH3
S-CH3
S-CH3
Abundance (X10^4)
6
4
2
0
61
131
383
100
200
300
400
500
m/z

1,6,9-$C_{33:3}$

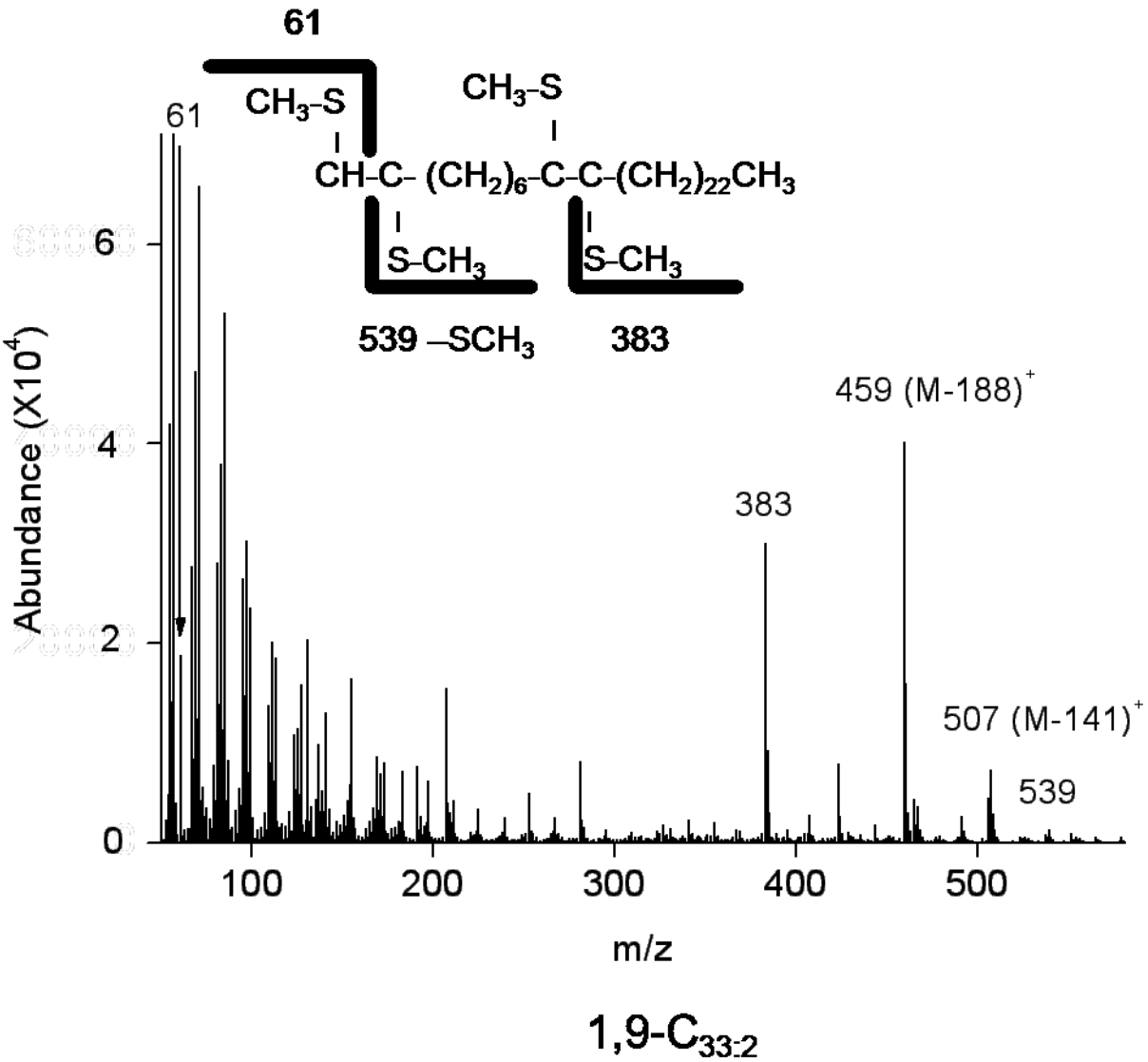
61
CH3–S
CH3–S
61
CH–C– (CH2)6–C–C–(CH2)22CH3
S–CH3
S–CH3
539 –SCH3
383
459 (M-188)+
383
507 (M-141)+
539
Abundance (X10^4)
6
4
2
0
100
200
300
400
500
m/z

1,9-$C_{33:2}$

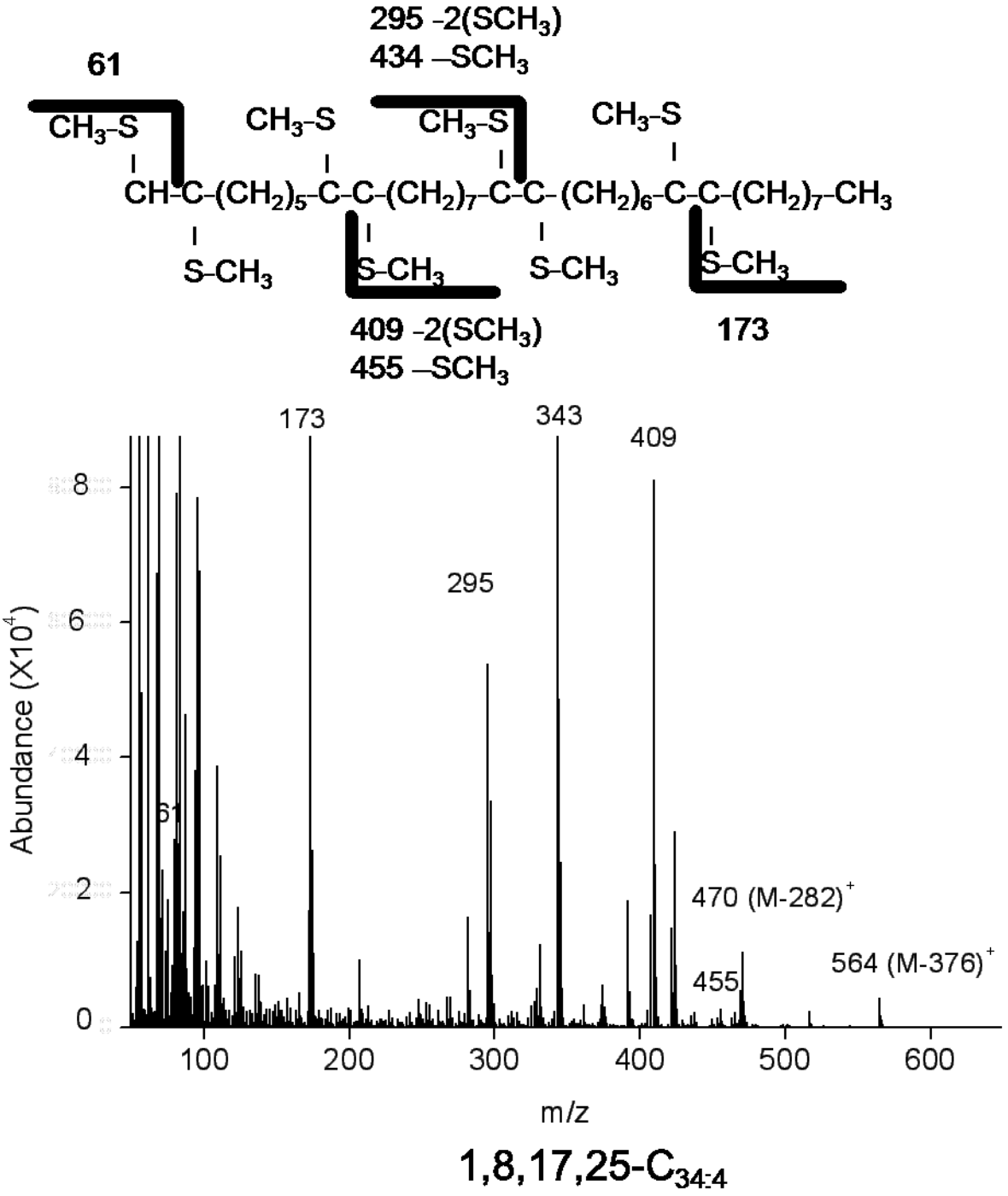
295 -2(SCH3)
434 –SCH3
61
CH3-S
CH3-S
CH3-S
CH3-S
CH-C-(CH2)5-C-C-(CH2)7-C-C-(CH2)6-C-C-(CH2)7-CH3
S-CH3
S-CH3
S-CH3
S-CH3
409 -2(SCH3)
455 –SCH3
173
Abundance (X10^4)
m/z
173
343
409
295
61
470 (M-282)+
564 (M-376)+
455
0
2
4
6
8
100
200
300
400
500
600

1,8,17,25-$C_{34:4}$

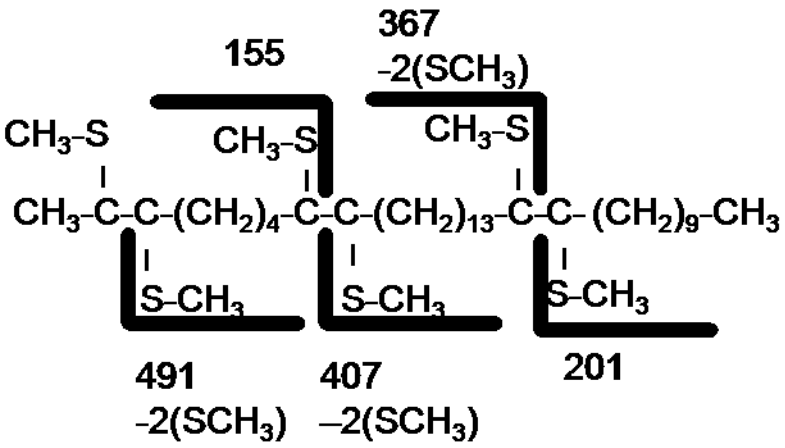
155
367
-2(SCH3)
CH3-S
CH3-S
CH3-S
CH3-C-C-(CH2)4-C-C-(CH2)13-C-C-(CH2)9-CH3
S-CH3
S-CH3
S-CH3
491
-2(SCH3)
407
–2(SCH3)
201

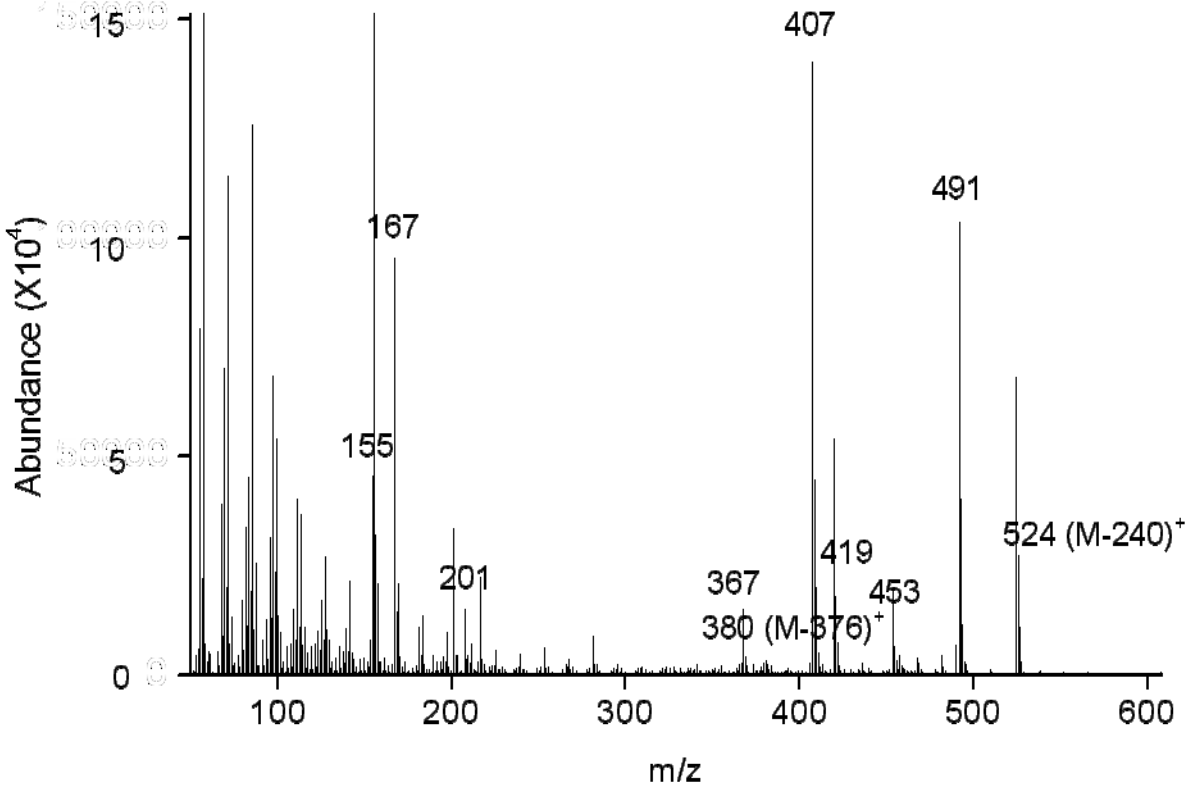
Abundance (X10^4)
15
10
5
0
100
200
300
400
500
600
m/z
407
491
167
155
201
419
367
453
380 (M-376)+
524 (M-240)+

2,8,23-$C_{34:3}$

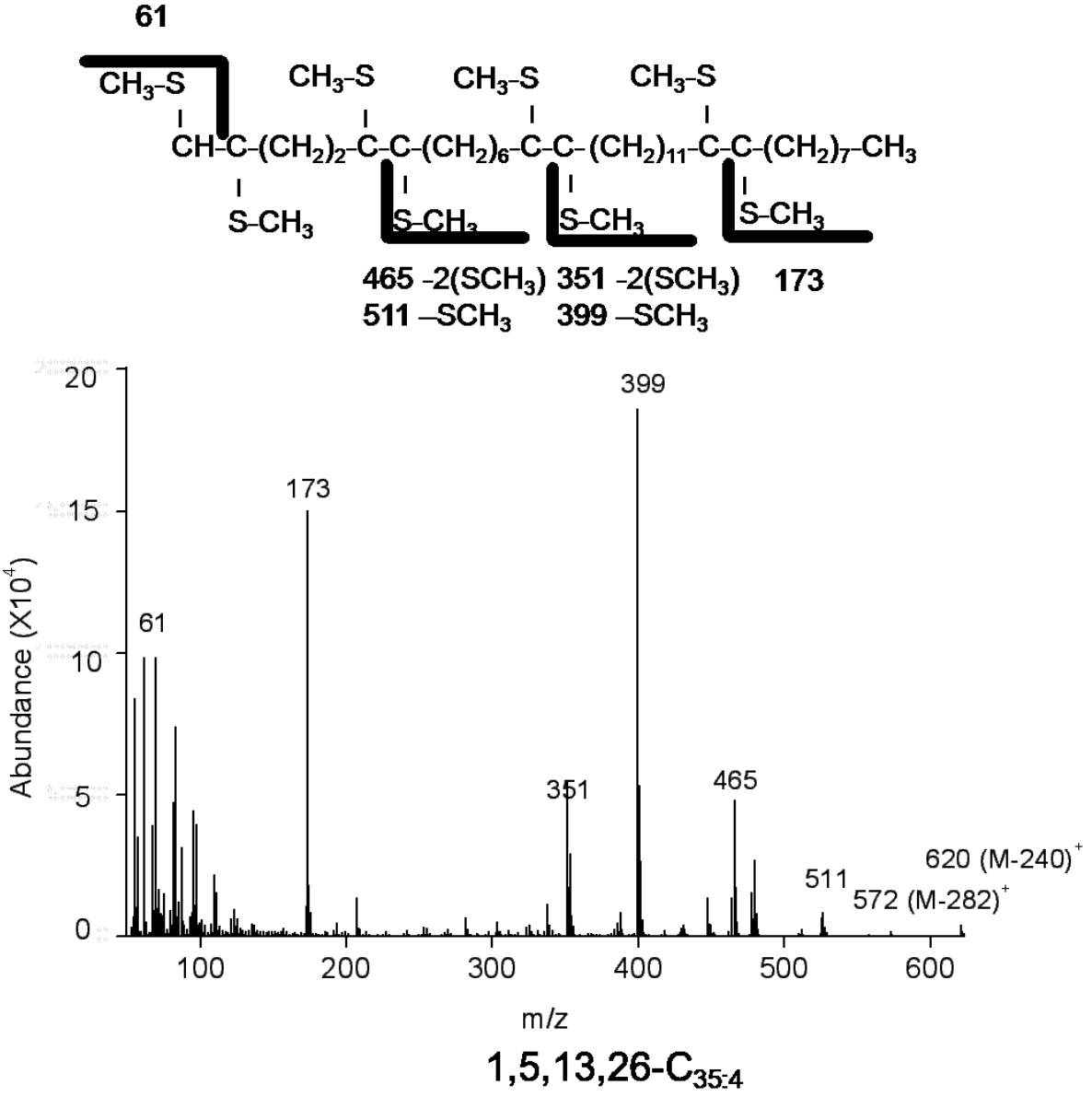
61
CH3-S
CH3-S
CH3-S
CH3-S
CH-C-(CH2)2-C-C-(CH2)6-C-C-(CH2)11-C-C-(CH2)7-CH3
S-CH3
S-CH3
S-CH3
S-CH3
465 -2(SCH3) 351 -2(SCH3) 173
511 –SCH3 399 –SCH3
Abundance (X10^4)
20
15
10
5
0
61
173
351
399
465
511
572 (M-282)+
620 (M-240)+
100
200
300
400
500
600
m/z

1,5,13,26-$C_{35:4}$

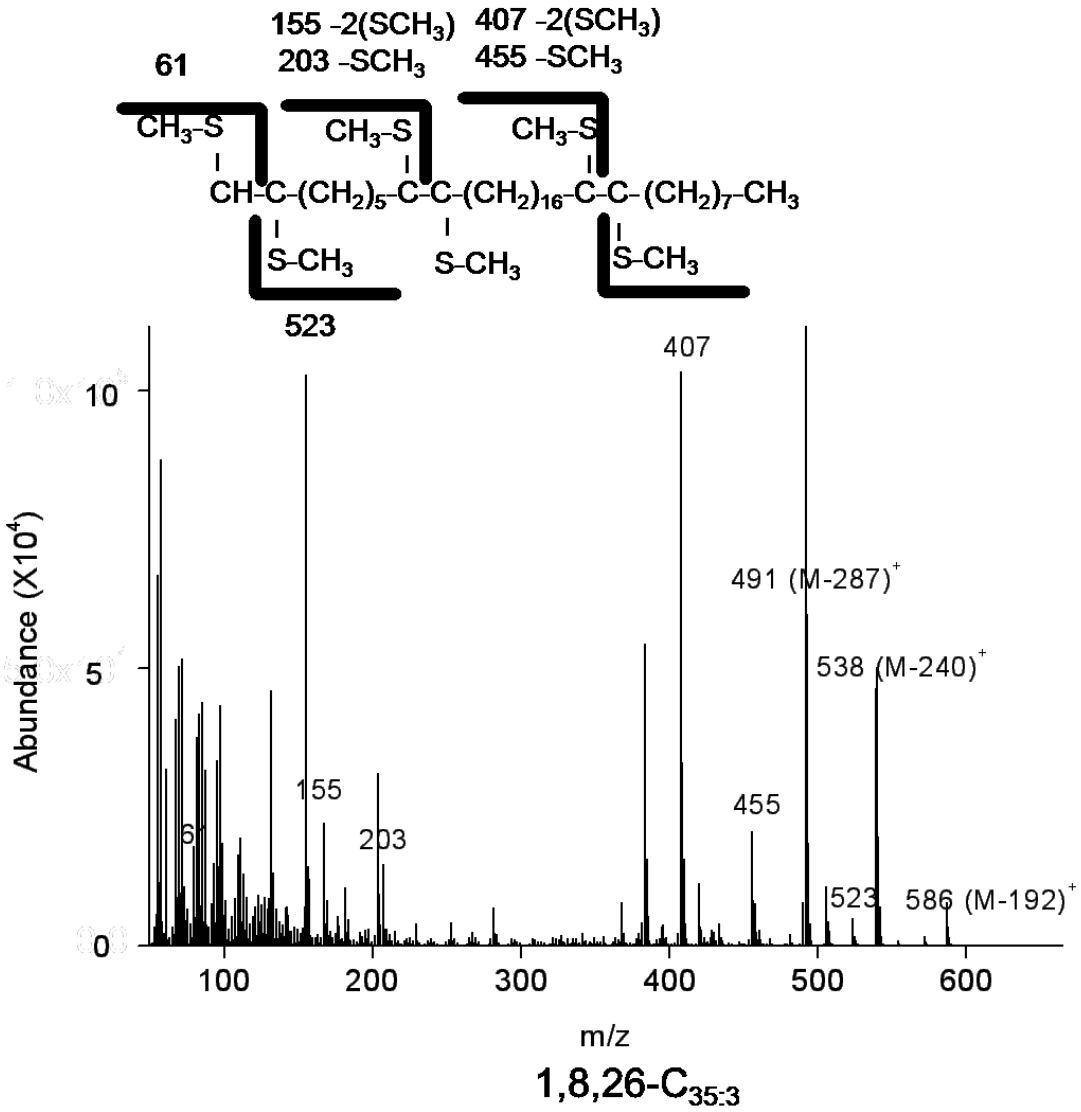
155 -2(SCH3)
203 -SCH3
407 -2(SCH3)
455 -SCH3
61
CH3-S
CH3-S
CH3-S
CH-C-(CH2)5-C-C-(CH2)16-C-C-(CH2)7-CH3
S-CH3
S-CH3
S-CH3
523
407
491 (M-287)+
538 (M-240)+
155
455
203
61
523
586 (M-192)+
Abundance (X10^4)
10
5
0
100
200
300
400
500
600
m/z
1,8,26-C35:3

Supplemental Table 1. Relative percentage of alkenes from total hexane extraction of *E. huxleyi* CCMP 1516					
Media	Alkenes	Days after transferring to fresh C and NP meida			
		0	7	14	21
C	1,22-C31:2	49%±9%	33%±2%	29%±2%	27.8%±0.4%
	7,22-C31:2	8%±8%	12%±1%	16%±2%	14.9%±0.4%
	1,6,9-C33:3	0.5%±0.5%	9%±8%	0.12%±0.02%	11.1%±0.3%
	1,9-C33:2	2%±2%	4%±2%	14%±2%	4.4%±0.2%
	1,8,17,25-C34:4	3%±3%	6%±6%	8%±1%	8%±1%
	2,8,23-C34:3	1.4%±0.1%	13%±3%	19%±3%	25%±1%
	1,8,26-C35:3	36%±0%	23%±4%	13%±7%	8.9%±0.2%
	1,5,13,26-C35:4	0.008%±0.002%	0.007%±0.003%	0.51%±0.06%	0.060%±0.003%
NP	1,22-C31:2	43%±5%	28%±1%	14%±5%	18%±2%
	7,22-C31:2	14%±2%	14.5%±0.5%	7%±7%	6%±5%
	1,6,9-C33:3	0.1%±0.1%	12%±5%	1%±1%	5%±5%
	1,9-C33:2	6%±6%	17%±7%	13%±5%	2%±1%
	1,8,17,25-C34:4	0.007%±0.002%	0.009%±0.001%	8%±2%	10%±3%
	2,8,23-C34:3	1.8%±0.3%	24%±3%	57%±8%	49%±6%
	1,8,26-C35:3	34%±2%	5%±5%	0.009%±0.001%	9%±5%
	1,5,13,26-C35:4	0.009%±0.003%	0.005%±0.001%	0.008%±0.001%	0.007%±0.002%

Supplemental Table 2. Relative percentage of alkenes from total hexane extraction of *E. huxleyi* CCMP 1742					
Media	Alkenes	Days after transferring to fresh C and NP meida			
		0	7	14	21
C	1,22-C31:2	0.008%±0.001%	51%±5%	37%±3%	39%±2%
	7,22-C31:2	0.009%±0.002%	21%±3%	15%±2%	11%±1%
	1,6,9-C33:3	33%±33%	2%±1%	9%±1%	8.7%±0.2%
	1,9-C33:2	0%±0%	1%±1%	8.5%±0.1%	0.8%±0.0%
	1,8,17,25-C34:4	0.005%±0.002%	0.003%±0.002%	0.007%±0.002%	6.9%±0.2%
	2,8,23-C34:3	67%±33%	4%±1%	2.7%±0.3%	10.2%±0.1%
	1,8,26-C35:3	0.005%±0.001%	20%±9%	27.8%±1.7%	24%±1%
	1,5,13,26-C35:4	0.006%±0.002%	1%±1%	0.00%±0.00%	0.031%±0.001%
NP	1,22-C31:2	0.003%±0.002%	38%±2%	16%±2%	13%±1%
	7,22-C31:2	0.008%±0.001%	16%±8%	25%±3%	20%±2%
	1,6,9-C33:3	33%±33%	12%±6%	0.3%±0.3%	16%±7%
	1,9-C33:2	0.009%±0.002%	0.005%±0.001%	0.008%±0.001%	0.7%±0.2%
	1,8,17,25-C34:4	0.005%±0.001%	0.008%±0.001%	1%±1%	4%±1%
	2,8,23-C34:3	62%±31%	31%±4%	47%±4%	19%±5%
	1,8,26-C35:3	0.007%±0.001%	0.008%±0.003%	11%±4%	27%±6%
	1,5,13,26-C35:4	5%±3%	3%±2%	0.008%±0.003%	0.003%±0.002%

CHAPTER 8: GENERAL CONCLUSIONS

The research in this dissertation addresses how simple aliphatic hydrocarbons differently accumulate in biological systems. This differential accumulation was investigated in response to different genotypes of a single species (e.g., maize inbreds), among different organs or tissue-types (e.g., emerging silks and pollen of maize, and different epidermal layers of pea), and in response to different nutrient availability (regulation by different carbon, nitrogen and phosphate nutrient levels in two different algae). This work has identified conditions in which such hydrocarbons hyper- and hypo-accumulate in four different species (the higher plants maize and pea, and the algae *B. braunii* and *E. huxleyi*), and established a platform to identify candidate genes that function in hydrocarbon biosynthesis via comparative transcriptomics.

Hyper- and hypo-accumulation of hydrocarbons in maize silks, pea epidermis, *B. braunii* and *E. huxleyi*

We demonstrated that total hydrocarbon accumulation, and the relative abundances of individual hydrocarbon constituents varies in pollen and silks of a diverse set of maize inbreds. This collection of maize inbreds includes the set of 26 founder inbreds that were used to establish the nest-associated mapping (Benamotz et al.) population (Yu et al. 2008), and a set of 14 genetically diverse inbreds that capture ca. 30% of the allelic diversity at 94

genetic loci randomly distributed across the maize genome, found across 260 maize inbreds (Flint-Garcia et al. 2005; Liu et al. 2003). Within the set of 14 inbreds, we demonstrated that hydrocarbons also vary between different organs (i.e. pollen and silk). This observed diversity alludes to the fact that hydrocarbon accumulation in maize is a quantitative trait, the phenotype of which is controlled by multiple genes, each with small effect on hydrocarbon accumulation (Alrefai et al. 1995; Byrne et al. 1996; McMullen et al. 1998).

Hydrocarbons are synthesized from very long chain fatty acids (VLFAs) precursors. In addition to genes involved in converting fatty acids to hydrocarbons, the genes involved in fatty acid initiation, synthesis and elongation might also contribute to hydrocarbon accumulation. Therefore, differential expression of different combination of such gene functions among the maize inbreds might cause the different levels of hydrocarbon accumulation patterns among the inbreds. The diversity in hydrocarbon accumulation patterns identified here across maize inbreds can be harnessed to identify the quantitative trait loci (QTL) that are implicated in HC biosynthesis by QTL mapping. QTL mapping is the physical identification (genome locations) of the loci that affect the trait of interest. By combining genotyping data generated by the Maize Community (Guo and Beavis 2011) and the hydrocarbon accumulation patterns among different inbreds, it is possible to map the hydrocarbon QTLs to relatively small regions of the

genome (Kelley et al. 2012). Furthermore, the diversity across founders of the NAM population also allows exploration of association mapping approaches, by taking advantage of known linkage disequilibrium to link the hydrocarbon phenotype to genotype, and to identify regions of the genome that correlate with specific hydrocarbon chemotypes (Aranzana et al. 2005; Myles et al. 2009; Stich et al. 2008; Yu and Buckler 2006). The genes in such hydrocarbon QTLs regions can be combined with candidate genes identified by comparative transcriptome profiling between encased and emerged maize silks (Chapter 4) to pinpoint the hydrocarbon controlling gene loci.

The maize inbred B73 can accumulate about 3-fold more hydrocarbons than the inbred Mo17 (Chapter 2). This diversity in hydrocarbon accumulation can be applied to investigate how genetic interactions impact hydrocarbons in maize. Previously, analysis of hydrocarbon accumulation patterns in the F1 hybrids (B73×Mo17 and Mo17×B73) as compared to their parental inbreds, B73 and Mo17 established that both hybrids produced more total surface lipids than their parents, B73 and Mo17. To test whether different hybrid combinations, and different organs in the same set of hybrids would show different heterotic patterns of hydrocarbon-inheritence, the hydrocarbons were profiled in six F1 hybrids generated by intercrossing the LH1, LH123HT, PHG39 and PHG84 inbreds. In these hybrids the trait of hydrocarbon accumulation in silks showed different heterotic patterns of inheritance,

including additive, underdominance and low-parent dominance. In addition, hydrocarbon inheritence in maize pollen showed overdominance heterotic effects, which contrasts with the situation shown in the silks of the same F1 hybrids plants. These different heterotic pattern of inheritance in maize pollen and silk suggest that different pathways may dominate in the different organs, consistent with the biochemical studies of maize silks (Perera et al. 2010c) that indicate four parallel biosynthetic pathways generates the silk hydrocarbons (i.e., the elongation-isomerization pathway, elongation-desaturation-decarbonylation pathway, elongation-desaturation-decarbonylation pathway, and elongation-decarbonylation).

The studies described in Chapter 5, used the *Argentum* mutant of pea (strain 17667) to explore the surface lipids on the leaf epidermis, and found that they are primarily composed of alkanes (e.g. 90% C_{31} alkane). However, there is a quantitative difference in the amount of hydrocarbons that are expressed on abaxial (i.e., lower) epidermis as compared to the adaxial (i.e. upper) epidermis; ~50 µmol/g of C31 alkane in the upper epidermis as compared to ~2 µmol/g C31 alkane in the lower epidermis (Chapter 5). However, this difference in hentriacontane accumulation is not observed between the abaxial and adaxial epidermis of stipules. Further, these studies showed that abaxial leafand stipule epidermis accumulate ca. 50% hydrocarbons and 40% alcohols, whereas adaxial leaf epidermis

accumulates less than 10% hydrocarbons but ca. 90% of alcohols (i.e. mainly C_{26} and C_{28} alcohols). In addition to these different hydrocarbon accumulation patterns between the abaxial and adaxial leaf epidermis, hydrocarbon accumulation is also developmentally regulated in the abaxial leaf epidermis (the older abaxial leaf epidermis accumulate more hydrocarbons as compared to younger ones), but this developmentally regulated expression in hydrocarbon accumulation is not apparent in adaxial leaf epidermis and stipule epidermis.

Hyper- and hypo-accumulation of hydrocarbons was explored in two algae, *B. braunii* and *E. huxleyi* (Chapters 6 and 7, respectively). These were achieved by controlling the supply of carbon, nitrogen and phosphate nutrient in the growth media for the two algae. In general, the results for *B. braunii* (strain UTEX 572) and *E. huxleyi* (strains CCMP 1516 and CCMP 1742) are consistent with the observation that carbon enrichment and nitrogen and phosphate limitation can stimulate hydrocarbon accumulation in algae (Benamotz et al. 1985; Choi et al. 2011; Ge et al. 2011a; Grossi et al. 2000; Shifrin and Chisholm 1981; Singh and Kumar 1992). In contrast, strain CCMP 373 produced higher levels of hydrocarbons when carbon was limited. The difference between CCMP 373 and other algae strain is possibly due to different C:N and N:P ratio requirements. The NO_3:PO_4 ratio used for CCMP 1516, CCMP 1742 and CCMP 373 is ~24, which might be suitable for CCMP

373 to produce alkenes but not for CCMP 1516 and CCMP 1742. In addition, the C: N ratio has been reported to affect growth of *E. huxleyi* (Kaffes et al. 2010), which might also influence alkene production differently in different *E. huxleyi* strains.

Platforms to identify genes involved in hydrocarbon biosynthesis in maize silk, pea epidermis, *B. braunii* and *E. huxleyi*

Transcriptomic profiling was used in four different biological systems (i.e. maize silk, pea epidermis, *B. braunii* and *E. huxleyi*) to identify differentially expressed genes from tissues that hyper-accumulate and hypo-accumulate hydrocarbons. From this collected dataset we will identify genes that are differentially expressed between the two disparate hydrocarbon-producing conditions, presupposing that candidate genes that may participate in hydrocarbon biosynthesis will be co-express with hydrocarbon production. RNAs were extracted from the conditions that result in the hyper- and hypo-accumulation of hydrocarbons from all four of the biological systems, maize silks, pea epidermis, *B. braunii* and *E. huxleyi*, (see details in Appendix A), and these were sequenced using the Illumina sequencing technology. Comparative transcriptome profiling of these datasets is being applied to identify differentially expressed genes. The entire pipeline has been completed for maize (Chapter 4) and is now being applied to pea, *B. braunii* and *E. huxleyi*. In chapter 4, the comparative transcriptome profiling between

encased and emerged silks from maize inbred B73 was applied to identify genes involved in surface lipid biosynthesis. Enzymes involved in producing VLCFAs as precursors for hydrocarbons are found to be differentially expressed between encased and emerged silks. Two ACCase transcripts (GRMZM2G377341_T01 and GRMZM5G858094_T01) catalyzing the limiting step of fatty acid initiation and one KAS transcript (GRMZM2G072205_T01) catalyzing limiting step of fatty acid synthesis are expressed 2-3 folds higher in emerged silks than encased silks. In addition, one ACCase transcript (GRMZM2G377341), two ACL transcripts (GRMZM2G002416_T01 and GRMZM2G10708_T01) and three KCS transcripts (GRMZM2G167438_T01, GRMZM2G137694_T01 and GRMZM2G445602_T01) in fatty acid elongation have a twofold expression in emerged silks of encased silks except for one KCS transcript (GRMZM2G167438_T01) with a 25-fold expression in emerged silks of encased silks. At the same time another three ACCase transcripts (GRMZM5G854500_T01, GRMZM2G375116_T01 and GRMZM2G375116_T02) and another three KCS transcripts (GRMZM2G151476_T01, GRMZM2G149636_T01 and GRMZM2G104626_T01) in fatty acid elongation have higher expression in encased silks than emerged silks. One transcript (GRMZM2G062151_T01) homologous to *cer1* in Arabidopsis has a 7-fold expression in emerged silks of encased silks whereas another transcript (GRMZM2G099097_T03)

homologous to *cer1* in Arabidopsis has a 5-fold expression in encased silks of emerged silks. In addition, desaturases controlling the saturation of surface lipids also differentially expressed between the encased and emerged silks.

By applying the same strategy to the other three biological systems (pea epidermis, *B. braunii* and *E. huxleyi*), the pool of candidate genes involved in hydrocarbon biosynthesis pathway can be refined by cross-system analysis, with the assumption that at least two of the four biological systems have similar hydrocarbon biosynthetic and/or regulatory pathways. The pool of candidate genes influencing hydrocarbon biosynthesis can be further refined by excluding genes with known function through examination of annotations and gene ontology analysis. Furthermore, sequence similarity networks can be built from these four biological systems by pairwise BLAST analysis. The within system networks can be clustered to identify highly inter-connected modules using the Markov Chain Clustering method (Archer and McLellan). Using this cross-system analysis, candidate genes involved in hydrocarbon biosynthetic pathway(s) should be shared among the maize silk, pea epidermis, *B. braunii* and *E. huxleyi* systems, and these can be discovered.

Possible mechanisms for hydrocarbon biosynthesis in maize silk, pea epidermis, *B. braunii* and *E. huxleyi*

Maize silk and *B. braunii* produced same type of hydrocarbons (Chapter 2, 3 and 6). The two double bonds in the dienes are positioned at the terminal

end and 9th position and the double bond in monoenes are either at the terminal end or at the 9th position. The double bond at the 9th position in alkenes from maize silks and *B. braunii* is possibly derived from an oleic acid precursor (i.e. 18:1-cis-9 fatty acid). Terminal alkenes have been reported to be formed from fatty acids by a novel P450 fatty acid decarboxylase in species of *Jeotgalicoccus* (Rude et al. 2011) and a decarboxylating thioesterase in a marine cyanobacterium, *Lyngbya majuscula* (Gehret et al. 2011), suggesting that perhaps similar enzymes function in maize and *B. braunii*. Existence of both odd-numbered and even-numbered hydrocarbons in maize silk and *B. braunii* cells suggests there are possibly two different hydrocarbon biosynthetic pathways, one for the odd-numbered hydrocarbons and the other for the even-numbered hydrocarbons or the same pathway by using different fatty acid precursors. In maize, the odd-numbered hydrocarbons might be synthesized by the elongation-decarbonylation pathway (Perera et al. 2010c), which might also be true for *B. braunii* according to previous finding that the decarbonylase and the fatty acyl-CoA reductase generating aldehyde before the step of decarbonylation were partially purified from *B. braunii* (Dennis and Kolattukudy 1992; Wang and Kolattukudy 1995a). This suggests that a decarbonylation pathway is also active to biosynthesize odd-numbered hydrocarbons in *B. braunii.* Instead, the even-numbered hydrocarbons might be synthesized by the double reduction-dehydration-reduction pathway, in which, the elongated fatty acid is reduced to an aldehyde and then reduced to

an alcohol, which is dehydrated and reduced to a hydrocarbon. Alternatively, these even-numbered hydrocarbons could also be produced via the decarboxylation or decarbonylation pathway by using odd-numbered fatty acids as precursors (Fig 1 in Chapter 1).

Pea mainly produces C_{31} alkane with minor amounts of C_{25}, C_{27} and C_{29} alkanes on both the abaxial and adaxial surfaces of the leaf and on the stipule (Chapter 5). Two lines of evidence suggest that these alkanes are produced via the elongation-decarbonylatoin pathway. First, the inhibition of C_{31} alkane synthesis in the presence of dithioerythritol and mercaptoethanol stimulated the accumulation of C_{32} aldehyde (Buckner and Kolattuky 1973), suggesting that alkanes are derived from aldehydes in pea. Second, both aldehyde-generating fatty acyl-CoA reductases as well as an aldehyde decarbonylase have been partially purified from *Pisum sativum* leaf (Schneider-Belhaddad and Kolattukudy 2000; Vioque and Kolattukudy 1997). This suggests that in pea, the odd-numbered alkanes might be synthesized by the elongation-decarbonylation pathway, which is also hypothesized for maize and *B. braunii*.

Most of the double bonds in alkenes are at terminal and 9th positions in one of the *E. huxleyi* strains, CCMP 1516 (Chapter 7). This suggests that CCMP 1516 might share the same pathway(s) as maize and *B. braunii*. The double bonds other than terminal and 9th positions might be formed by a

different hydrocarbon biosynthesis pathway or by using different desaturases. Instead, alkenes from CCMP 373 have double bonds at 15 and 22th positions. According to previous literature, 15,22-$C_{37:2}$ and 15,22-$C_{38:2}$ are possibly biosynthesized from their corresponding methyl C_{37} and C_{38} alkenones, which were initially reduced to alkenols and then dehydrated to alkatrienes, which were further reduced to C_{37} and C_{38} alkadienes (Grossi et al. 2000; Rieley et al. 1998b; Rontani et al. 2006). Therefore, CCMP 373 might share the same biosynthetic pathway while in CCMP 1516 there are potentially multiple biosynthetic pathways that produce both odd-numbered and even-numbered alkenes with double bond at different positions or same pathways with different very long chain fatty acid precursors.

REFERENCES

Alrefai, R., Berke, T. G., Rocheford, T. R., 1995. Quantitative Trait Locus Analysis of Fatty-Acid Concentrations in Maize. Genome 38, 894-901.

Aranzana, M. J., Kim, S., Zhao, K. Y., Bakker, E., Horton, M., Jakob, K., Lister, C., Molitor, J., Shindo, C., Tang, C. L., Toomajian, C., Traw, B., Zheng, H. G., Bergelson, J., Dean, C., Marjoram, P., Nordborg, M., 2005. Genome-wide association mapping in Arabidopsis identifies previously known flowering time and pathogen resistance genes. Plos Genet 1, 531-539.

Archer, K., McLellan, F., 2002. Controversy surrounds proposed xenotransplant trial. Lancet 359, 949-949.

Benamotz, A., Tornabene, T. G., Thomas, W. H., 1985. Chemical Profile of Selected Species of Microalgae with Emphasis on Lipids. Journal of Phycology 21, 72-81.

Buckner, J. S., Kolattuky, P. E., 1973. Specific Inhibition of Alkane Synthesis with Accumulation of Very Long-Chain Compounds by Dithioerythritol,

Dithiothreitol, and Mercaptoethanol in Pisum-Sativum. Arch Biochem Biophys 156, 34-45.

Byrne, P. F., McMullen, M. D., Snook, M. E., Musket, T. A., Theuri, J. M., Widstrom, N. W., Wiseman, B. R., Coe, E. H., 1996. Quantitative trait loci and metabolic pathways: Genetic control of the concentration of maysin, a corn earworm resistance factor, in maize silks. P Natl Acad Sci USA 93, 8820-8825.

Choi, G. G., Kim, B. H., Ahn, C. Y., Oh, H. M., 2011. Effect of nitrogen limitation on oleic acid biosynthesis in Botryococcus braunii. J Appl Phycol 23, 1031-1037.

Dennis, M., Kolattukudy, P. E., 1992. A cobalt-porphyrin enzyme converts a fatty aldehyde to a hydrocarbon and CO. Proc Natl Acad Sci U S A 89, 5306-5310.

Flint-Garcia, S. A., Thuillet, A. C., Yu, J. M., Pressoir, G., Romero, S. M., Mitchell, S. E., Doebley, J., Kresovich, S., Goodman, M. M., Buckler, E. S., 2005. Maize association population: a high-resolution platform for quantitative trait locus dissection. Plant J 44, 1054-1064.

Ge, Y. M., Liu, J. Z., Tian, G. M., 2011. Growth characteristics of Botryococcus braunii 765 under high CO2 concentration in photobioreactor. Bioresource Technol 102, 130-134.

Gehret, J. J., Gu, L. C., Gerwick, W. H., Wipf, P., Sherman, D. H., Smith, J. L., 2011. Terminal Alkene Formation by the Thioesterase of Curacin A Biosynthesis STRUCTURE OF A DECARBOXYLATING THIOESTERASE. J Biol Chem 286, 14445-14454.

Grossi, V., Raphel, D., Aubert, C., Rontani, J. F., 2000. The effect of growth temperature on the long-chain alkenes composition in the marine coccolithophorid Emiliania huxleyi. Phytochemistry 54, 393-399.

Guo, B. H., Beavis, W. D., 2011. In silico genotyping of the maize nested association mapping population. Mol Breeding 27, 107-113.

Kaffes, A., Thoms, S., Trimborn, S., Rost, B., Langer, G., Richter, K. U., Koehler, A., Norici, A., Giordano, M., 2010. Carbon and nitrogen fluxes in the marine coccolithophore Emiliania huxleyi grown under different nitrate concentrations. J Exp Mar Biol Ecol 393, 1-8.

Kelley, R. Y., Williams, W. P., Mylroie, J. E., Boykin, D. L., Harper, J. W., Windham, G. L., Ankala, A., Shan, X., 2012. Identification of Maize Genes

Associated with Host Plant Resistance or Susceptibility to Aspergillus flavus Infection and Aflatoxin Accumulation. PLoS One 7, e36892.

Liu, K. J., Goodman, M., Muse, S., Smith, J. S., Buckler, E., Doebley, J., 2003. Genetic structure and diversity among maize inbred lines as inferred from DNA microsatellites. Genetics 165, 2117-2128.

McMullen, M. D., Byrne, P. F., Snook, M. E., Wiseman, B. R., Lee, E. A., Widstrom, N. W., Coe, E. H., 1998. Quantitative trait loci and metabolic pathways. P Natl Acad Sci USA 95, 1996-2000.

Myles, S., Peiffer, J., Brown, P. J., Ersoz, E. S., Zhang, Z., Costich, D. E., Buckler, E. S., 2009. Association mapping: critical considerations shift from genotyping to experimental design. Plant Cell 21, 2194-2202.

Perera, M. A. D. N., Qin, W. M., Yandeau-Nelson, M., Fan, L., Dixon, P., Nikolau, B. J., 2010. Biological origins of normal-chain hydrocarbons: a pathway model based on cuticular wax analyses of maize silks. Plant J 64, 618-632.

Rieley, G., Teece, M. A., Peakman, T. M., Raven, A. M., Greene, K. J., Clarke, T. P., Murray, M., Leftley, J. W., Campbell, C. N., Harris, R. P., Parkes, R. J., Maxwell, J. R., 1998. Long-chain alkenes of the haptophytes Isochrysis galbana and Emiliania huxleyi. Lipids 33, 617-625.

Rontani, J. F., Prahl, F. G., Volkman, J. K., 2006. Re-examination of the double bond positions in alkenones and derivatives: Biosynthetic implications. J Phycol 42, 800-813.

Rude, M. A., Baron, T. S., Brubaker, S., Alibhai, M., Del Cardayre, S. B., Schirmer, A., 2011. Terminal Olefin (1-Alkene) Biosynthesis by a Novel P450 Fatty Acid Decarboxylase from Jeotgalicoccus Species. Appl Environ Microb 77, 1718-1727.

Schneider-Belhaddad, F., Kolattukudy, P., 2000. Solubilization, partial purification, and characterization of a fatty aldehyde decarbonylase from a higher plant, Pisum sativum. Arch Biochem Biophys 377, 341-349.

Shifrin, N. S., Chisholm, S. W., 1981. Phytoplankton Lipids - Interspecific Differences and Effects of Nitrate, Silicate and Light-Dark Cycles. J Phycol 17, 374-384.

Singh, Y., Kumar, H. D., 1992. Lipid and Hydrocarbon Production by Botryococcus-Spp under Nitrogen Limitation and Anaerobiosis. World J Microb Biot 8, 121-124.

Stich, B., Mohring, J., Piepho, H. P., Heckenberger, M., Buckler, E. S., Melchinger, A. E., 2008. Comparison of mixed-model approaches for association mapping. Genetics 178, 1745-1754.

Vioque, J., Kolattukudy, P. E., 1997. Resolution and purification of an aldehyde-generating and an alcohol-generating fatty acyl-CoA reductase from pea leaves (Pisum sativum L). Arch Biochem Biophys 340, 64-72.

Wang, X., Kolattukudy, P. E., 1995. Solubilization and Purification of Aldehyde-Generating Fatty Acyl-Coa Reductase from Green-Alga Botryococcus-Braunii. Febs Lett 370, 15-18.

Yu, J., Buckler, E. S., 2006. Genetic association mapping and genome organization of maize. Curr Opin Biotechnol 17, 155-160.

Yu, J. M., Holland, J. B., McMullen, M. D., Buckler, E. S., 2008. Genetic design and statistical power of nested association mapping in maize. Genetics 178, 539-551.

APPENDIX A. RNA PREPARATIONS FOR ILLUMINA SEQUENCING FROM MAIZE, PEA, *BOTRYOCOCCUS BRAUNII* AND *EMILIANIA HUXLEYI*: APPLIED TO SAMPLES ISOLATED FROM CONDITIONS LEADING TO HYPER- AND HYPO-ACCUMULATION OF HYDROCARBONS

Growth conditions that result in the hyper- and hypo-accumulation of hydrocarbons have been identified for maize silks, pea epidermis, and cells of the algae, *B. braunii* and *E. huxleyi*, as described in chapters 2, 4, 5 and 6 of this thesis, respectively. To identify genes involved in hydrocarbon biosynthesis, RNA was extracted from these tissue samples under the conditions that lead to either hyper- or hypo-accumulation of hydrocarbons. The RNA samples from these tissues were subjected to transcriptome profiling via next-generation sequencing using Illumina sequencing technology. In parallel, hydrocarbons were extracted and analyzed from aliquots of the same biological samples that were used for transcriptome analysis.

As reported in Chapter 2 of this thesis, we established that maize silks differentially accumulate hydrocarbons depending on whether these silks are encased by or emerged from husk leaves. Three days after emergence from the husks, emerged silks have ~3-fold more hydrocarbons than silks encased by the husks. Encased and emerged silks were harvested from maize ears at 3-days post silk-emergence. Hydrocarbons from the emerged silks comprised ~1.2% of silk dry weight, as compared to ~0.4% for encased silks (Table 1). This 3-fold difference in hydrocarbon accumulation is similar to previous findings (Perera et al. 2010c).

Based on results presented in Chapter 4 for *Pisum sativum* (pea) that identified epidermal tissues that expressed different levels of hydrocarbons, the following tissues were chosen for Illumina sequencing: 1) adaxial leaf epidermis; 2) abaxial leaf epidermis; and 3) the combined adaxial and abaxial epidermis from stipules. These epidermal tissues were harvested from 5-week-old plants of the *Arg* (Marx 1982) and *Arg wlo* (Marx 1987b) lines (*wlo* mutant reduces wax on the upper surface of leaflets). The abaxial leaf epidermis and the combined adaxial and abaxial stipule epidermis tissues accumulate similar amounts of hydrocarbons, ~ 4% and ~6.5% of total dry weight in the *Arg* and *Arg wlo* pea plants, respectively. In contrast, the abaxial leaf epidermis accumulates ~10-fold and ~15-fold less hydrocarbons in these *Arg* and *Arg wlo* pea plants, respectively (Chapter 5, Table 1).

Based on the results presented in Chapter 6 for *B. braunii* cells, hydrocarbon accumulation patterns could be affected by changes in media composition. Cells transferred to modified B3N medium for 7-days (low carbon, high nitrogen and phosphate) represented the hydrocarbon hypo-accumulation state, and cells transferred to Waris medium with 2% CO_2 bubbling (high carbon, low nitrogen and phosphate) for 7 days represented the hydrocarbon hyper-accumulation state. The latter produced ~3% hydrocarbons (total dry biomass), which is ~3-fold more than the former (Chapter 6, Table 1). These cell samples were choosen for Illumina sequencing.

Based to results presented in Chapter 7, for *E. huxleyi* cells, hydrocarbon accumulation patterns could be affected by changes in media composition, but these media-effects were opposite for the two strains that were studied (i.e., CCMP 1516 and CCMP 373). The two media used were rich in carbon but deficient in nitrogen and phosphate, or the medium was deficient in carbon but rich in nitrogen and phosphate. Cells were grown in these media for 11 days were collected for isolating RNA and subjecting it to Illumina sequencing. With strain CCMP 1516 cells hydrocarbons hyper-accumulated to ~0.2% of cellular dry biomass when this strain was grown in medium rich in carbon, but deficient in nitrogen and phosphate, and this hydrocarbon level was ~5-fold higher than when this strain was grown in medium deficient in carbon but rich of nitrogen and phosphate (~0.04% of cellular dry biomass). In contrast, with strain CCMP 373 the hyper-accumulation of hydrocarbons occurred when it was grown in medium deficient in carbon but rich in nitrogen and phosphate (at ~0.3% of cellular dry biomass), which is ~4-fold higher than when these cells grown in medium rich of carbon but deficient in nitrogen and phosphate (Chapter 7, Table 1).

All biological tissue samples (maize silk, pea epidermis, *E. huxleyi* or *B. braunii* cells) were harvested in duplicate, and one aliquot was profiled for hydrocarbon content (as summarized above). The second aliquot of tissue samples (approximately 1.0 g of tissue) was used for RNA extraction. Maize silk, pea epidermis and *B. braunii* cells were extracted with PureLink™ Plant

RNA Reagent (Invitrogen, Grand Island, NY), according to manufacturer's instructions. RNA was extracted from *E. huxleyi* cells using the Trizol Reagent (Invitrogen), according to manufacturer's instructions.

RNA samples were treated with 2M lithium chloride to precipitate RNA, and RNA quality was tested using the Agilent 2100 Bioanalyzer and associated RNA 6000 Nano assay kit according to manufacturer's instructions (Agilent, Santa Clara, CA). RNA integrity (Shifrin and Chisholm 1981) numbers are listed in Table 1. Illumina sequencing requires that RNA samples have RNA integrity numbers greater than 8.0.

RNA samples with RIN numbers >8.0 were used for cDNA library construction according to the protocol provided by Illumina Inc (San Diego, CA). Poly(A) mRNA was first isolated from the isolated RNA samples and then added to Dynabeads® oligo(dT) beads (Invitrogen, Grand Island, NY). The cDNA library was built by using the mRNA-seq Sample Preparation Kit provided by Illumina Inc (San Diego, CA) according to manufacturer's guide. cDNA libraries were subjected to transcriptomics profiling by sequencing on the Illumina Genome Analyzer II, at the ISU DNA Facility. The resulting transcriptomes are currently being analyzed via computational and bioinformatic approaches.

References

Marx GA (1982) Argenteum (Arg) Mutant of Pisum - Genetic-Control and Breeding-Behavior. J Hered 73:413-420

Marx GA (1987) A suite of mutants that modify pattern formation in pea leaves. Plant Mol Biol Rep 5:311–335.

Perera MADN, Qin WM, Yandeau-Nelson M, Fan L, Dixon P, Nikolau BJ (2010) Biological origins of normal-chain hydrocarbons: a pathway model based on cuticular wax analyses of maize silks. Plant J 64:618-632

Shifrin NS, Chisholm SW (1981) Phytoplankton Lipids - Interspecific Differences and Effects of Nitrate, Silicate and Light-Dark Cycles. J Phycol 17:374-384

Table 1. Hydrocarbon contents and RINs of RNA samples from maize, pea, *B. braunii* and *E. huxleyi* for Illumina sequencing under hyper- and hypo-hydrocarbon accumulation conditions

Biological System	Genotype	Organ	Media	Hydrocarbon accumulation state	Hydrocarbon	RIN number
Maize	B73	Encased silks	N/A	Hypo	0.34%	9.6/9.6
		Emerged silks	N/A	Hyper	1.05%	9.2/9.2
Pea (*Arg* mutant)	W6 15098	Abaxial leaf epidermis	N/A	Hypo	0.41%	8.9/9.2
		Adaxial leaf epidermis	N/A	Hyper	6.38%	8.8/9.1
		Combined abaxial and adaxial stipule epidermis	N/A	Hyper	6.41%	8.7/9.0
	W6 17667	Abaxial leaf epidermis	N/A	Hypo	0.35%	8.7/8.7
		Adaxial leaf epidermis	N/A	Hyper	4.11%	8.6/8.6
		Combined abaxial and adaxial stipule epidermis	N/A	Hyper	4.53%	8.5/8.3
B. braunii	UTEX 572	Whole cell	Modified B3N medium at atmospheric CO_2	Hypo	0.77%	9.2/9.2
		Whole cell	Waris medium with 2% CO_2	Hyper	2.87%	9.7/9.7
E. huxleyi	CCMP 1516	Whole cell	Basic sea salt medium with 10 mM $NaHCO_3$	Hypo	0.04%	8.7/8.6
		Whole cell	Basic sea salt medium with $NaNO_3$ and	Hyper	0.21%	8.8/8.9
	CCMP 373	Whole cell	Basic sea salt medium with 10 mM $NaHCO_3$	Hypo	0.07%	8.5/8.3
		Whole cell	Basic sea salt medium with $NaNO_3$ and	Hyper	0.29%	8.7/8.8

APENDIX B. AMINO ACID AND TOTAL METABOLITE ANALYSIS OF ENCASED AND EMERGED SILKS OF MAIZE

The data presented in Chapter 2 established that maize silks differentially accumulate hydrocarbons depending on whether these silks are encased by or emerged from husk leaves. Three days after emergence from the husks, emerged silks have ~3-fold more hydrocarbons than silks encased by the husks. To expand on this observation and determine how generalizable this metabolic difference is distributed among different metabolic processes, the encased and emerged silks were harvested at 3-days post-emergence and additional metabolite profiling was conducted on these tissues. These metabolite profiling studies were targeted to metabolites that would be expected to be associated with hydrocarbon biosynthesis (i.e., fatty acids), and to those that would not be expected to be associated with hydrocarbon biosynthesis (i.e., amino acids). In addition, metabolites were also profiled with an analytical platform that did not bias metabolites that were analyzed (i.e., non-targeted, “total” metabolite platform). All studies were conducted with the encased and emerged silks from the maize inbred B73, harvested at 3 days post-emergence. These plants were planted and grown at the Iowa State University Agronomy Farm (Boone, IA) during the summer, 2009. For each analysis, there are 5 replications, and each replication came from a single distinct maize plant, that was planted in the same plot of the field by random design.

Amino acids in encased and emerged silks

A total of 10 mg of lyophilized silk powdered tissue from encased or emerged silks were used for amino acid analysis. Before amino acids were extracted, 100 µl of 0.2 mM norvaline was added as an internal standard. Amino acids were extracted in 500 µl of 10% trichloroacetic acid (TCA) by shaking the suspension at 1500×g for 1 min with a multi-tube vortexer (Fisher Scientific, Atlanta, GA). Samples were centrifuged at 3000×g rpm for 5 min and the supernatant was collected. This extraction procedure was repeated on the pellet one more time and the combined supernatants were used for amino acid analysis. The solid phase extraction, amino acid derivatization and liquid-liquid extraction procedures of the EZ:faast kit were used according to user's manual (Phenomenex, Torrance, CA). The derivatized amino acids were immediately analyzed with a gas chromatograph (Model 6890 series, Agilent Technologies, Palo Alto, CA), equipped with a mass detector Model 5973 (Agilent Technologies, Palo Alto, CA). Chromatography was conducted using a HP-5MS cross-linked (5%)-diphenyl-(95%)-dimethyl polysiloxane column (30 m length, 0.25 mm inner diameter), using helium as the carrier gas. The injection temperature was at 280℃. The oven temperature was initially at 200℃, was increased to 280℃ at a rate of 4℃/min, and further increased to 320℃ at a rate of 20℃/min and held at this temperature for 3 min.

A mixture of amino acid standards provided in the EZ:faast kit were also analyzed (Fig 1) for identification of amino acids in maize silks based on retention time and retention index. A total of 23 amino acids were detected in both emerged and encased silks, including alanine (Dayananda et al.), glycine (Gly), α-aminobutyric acid (Aba), valine (Val), leucine (Leu), isoleucine (Massonnet et al.), serine, proline (Pro), asparagine (Asn), aspartic acid (Asp), methionine (Met), hydroxyproline (Hyp), glutamic acid (Glu), phenylalanie (Papadopoulos et al.), α-aminoadipic acid (Aaa), α-aminopimelic acid (Benamotz et al.), glutamine (Gln), ornithine (Shifrin and Chisholm), the di-peptide glycyl-proline (GPR), lysine (Lys), histidine (Lessard et al.), tyrosine (Yanes et al. 2011) and tryptophan (Trp). The total concentration of amino acids (i.e. the combined amounts of all 23 amino acids) did not vary between emerged and encased silks (p-value> 0.05). Hence, the concentrations of the majority of individual amino acids did not vary between the two silk tissue samples, however, a few amino acids showed a significant difference. These are, Asn and Lys which were 2-fold higher in the encased silks as compared to the emerged silks. In contrast, all other amino acids have the same amount in encased and emerged silks (Fig 2).

Non-targeted profiling of "total" metabolites in encased and emerged silks

A 10-mg aliquot of lyophilized silk powder from encased or emerged silks was used for quantification metabolites in these tissues. Before extracting

metabolites, 20 µg nonadecanoic acid and 100 µg ribitol were added as internal standards for nonpolar and polar compounds, respectively. To extract metabolites, 0.35 mL hot methanol (60℃) was added to each sample, and the suspension was incubated at 60℃ for 10 min (Morvaivitanyi et al. 1993). Samples were vortexed and sonicated in a water bath at 25℃ for 10 min. An equal volume of chloroform was added and vortexed for 30 sec, followed by the addition of 0.3 mL water. Samples were then vortexed for 30 sec. The samples were centrifuged at 3000×g for 5 min to separate the phases. A total of 200 µl was removed from each of the polar and non-polar phases for GC-MS analysis. Prior to GC-MS analysis, the polar fraction was dried in a speed-vacuum concentrator for 30 min. Next, 50 microliter of 20 mg/mL methoxyamine hydrochloride in dry pyridine was applied to the dried polar fraction for methoximation at 30 ℃ for 1.5 hours with continuous shaking (Lisec et al. 2006). Both polar and nonpolar fractions were silylated with 70 µl of bis-trimethyl silyl trifluoroacetamide with 1% trimethylchlorosilan (BSTFA +1% TMCS), incubated for 30 min at 60 ℃. GC-MS analysis proceeded as described above for amino acids.

The non-polar fraction of the metabolites extracted from emerged and encased silks consisted mainly of hydrocarbons, fatty acids, and sterols (a few small peaks of sugars were also detected, but these probably represent contaminated sugars from the polar fraction, and were not quantified) (Fig.3).

The polar fraction was primarily composed of sugars, and these were identified as hexoses, but their exact chemical nature was not deduced (Fig. 4).

The analysis of the non-polar fraction from the emerged silks indicates that these silks produce ~3 fold more hydrocarbons than encased silks. This is the same finding as obtained with the hexane extraction method used in Chapter 7 that is targeted towards hydrocarbon metabolites. Hydrocarbons are primarily composed of homologous series of odd-numbered alkanes and alkenes, ranging from C_{23} to C_{33}. This is the same as the hydrocarbon-targeted analyses described in Chapter 7. However, the one systematic difference is that even-numbered hydrocarbons were not detected by this non-targeted metabolite extraction method. This might be caused by the fact that the even-numbered hydrocarbons occur at very low levels and are hidden by the other more abundant metabolites, such as C_{16}, $C_{18:2}$ and $C_{18:1}$ fatty acids.

The other major class of metabolites that were detected in the non-polar, non-targeted metabolite analysis platform are the fatty acids. Total amount of fatty acids recovered by this method did not vary between the emerged and encased silks. The fatty acid constituents consisted of even-numbered fatty acids ranging in chain lengths from C_{16} to C_{24}. In addition to the fatty acids of up to C_{18} chain length that were extracted by barium hydroxide method in Chapter 7, in this non-targeted metabolite platform very long chain fatty acids ($C_{20:1}$, C_{20}, $C_{22:1}$, C_{22} and C_{24} fatty acids) were also detected in both encased

and emerged silks. Individual fatty acid constituents did not vary in amounts between the two silk tissues. This is in contrast to the fatty acid data obtained by the barium hydroxide method described in Chapter 7. These differences are attributable to the fact that the barium hydroxide fatty acid analysis method collects all fatty acids present in the sample, by hydrolyzing acylated products that include ester, amide, thioester and phosphoester bonds, whereas the total metabolite extraction method collects the free fatty acids and probably the thioester and phosphoester bonded fatty acids. Although the total fatty acid content recovered by the barium hydroxide fatty acid analysis method did not vary between encased and emerged silks, some individual fatty acids differed in amounts between encased and emerged silks. For example, $C_{16:1}$ and $C_{18:1}$ fatty acids were ~10% higher in emerged silks than in encased silks while $C_{18:2}$ fatty acid was ~15 % higher in encased silks as compared to emerged silks (Fig 5).

The polar metabolites extracted from emerged and encased silks with the non-targeted extraction protocol included glycerol, monosaccharides, disaccharides and two unidentified sugars (UD1 and UD2) (Fig 6). The monosaccharides consist of five hexoses, which cannot be distinguished by their mass spectra. The two disaccharides are arabinofuranose and sucrose. The encased silks produced ~10% more total sugars as compared to emerged

silks (p-value <0.05). In addition to total sugars, the encased silks also produced more hexose 1 and hexose 3 than the emerged silks.

References

Benamotz A, Tornabene TG, Thomas WH (1985) Chemical Profile of Selected Species of Microalgae with Emphasis on Lipids. J Phycol 21:72-81

Dayananda C, Sarada R, Rani MU, Shamala TR, Ravishankar GA (2007) Autotrophic cultivation of Botryococcus braunii for the production of hydrocarbons and exopolysaccharides in various media. Biomass Bioenerg 31:87-93

Lessard EJ, Merico A, Tyrrell T (2005) Nitrate : phosphate ratios and Emiliania huxleyi blooms. Limnol Oceanogr 50:1020-1024

Lisec J, Schauer N, Kopka J, Willmitzer L, Fernie AR (2006) Gas chromatography mass spectrometry-based metabolite profiling in plants. Nat Protoc 1:387-396

Morvaivitanyi M, Molnanperl I, Knausz D, Sass P (1993) Simultaneous Gc Derivatization and Quantification of Acids and Sugars. Chromatographia 36:204-206

Yanes O, Tautenhahn R, Patti GJ, Siuzdak G (2011) Expanding Coverage of the Metabolome for Global Metabolite Profiling. Anal Chem 83:2152-2161

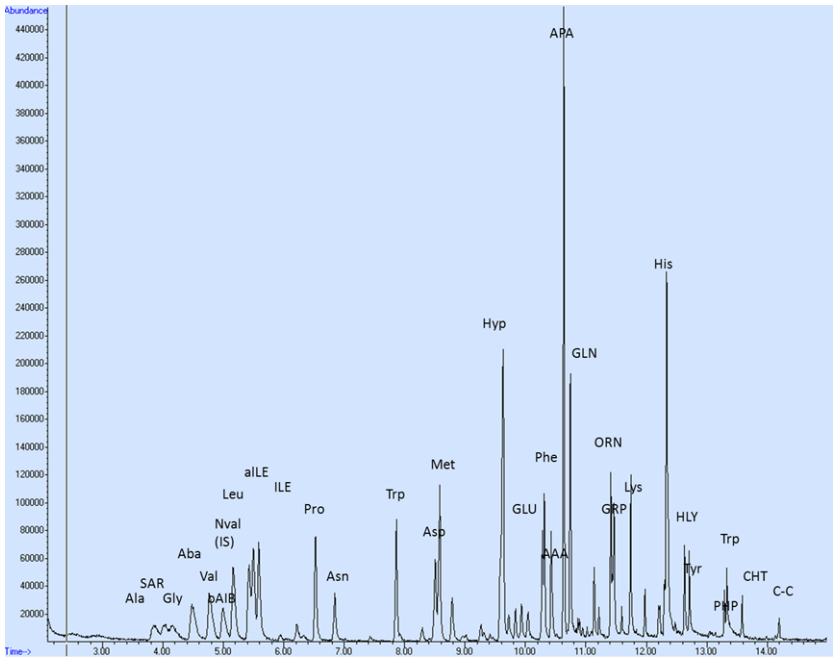

Figure 1. Gas chromatograph of standard amino acids in EZ:faast kit.

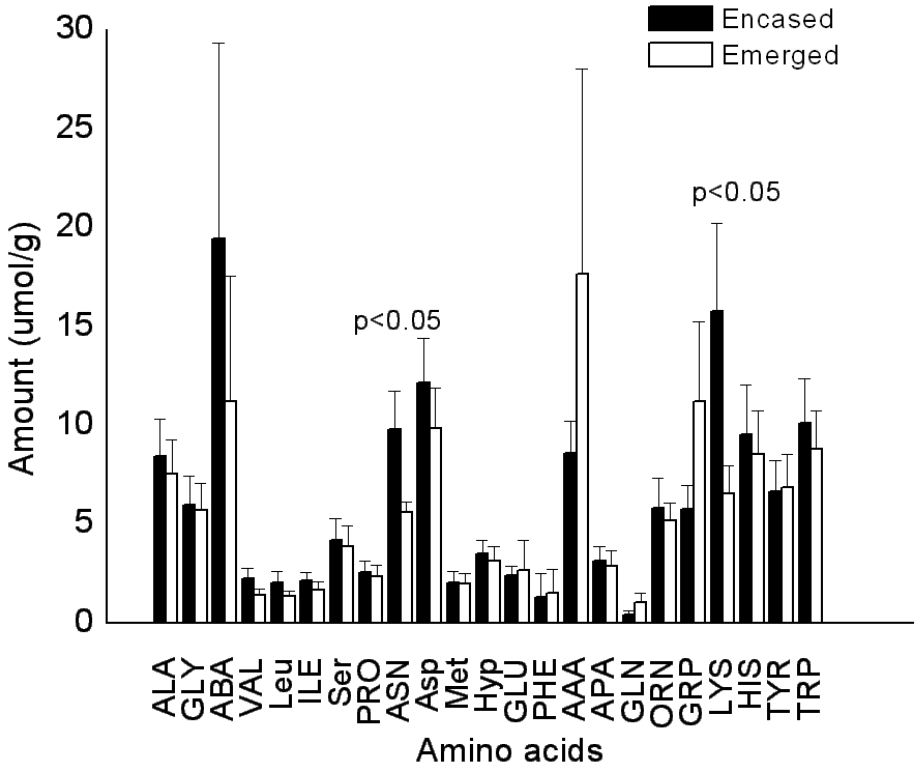

Figure 2. Amino acids present in encased and emerged silks collected 3 days post-emergence

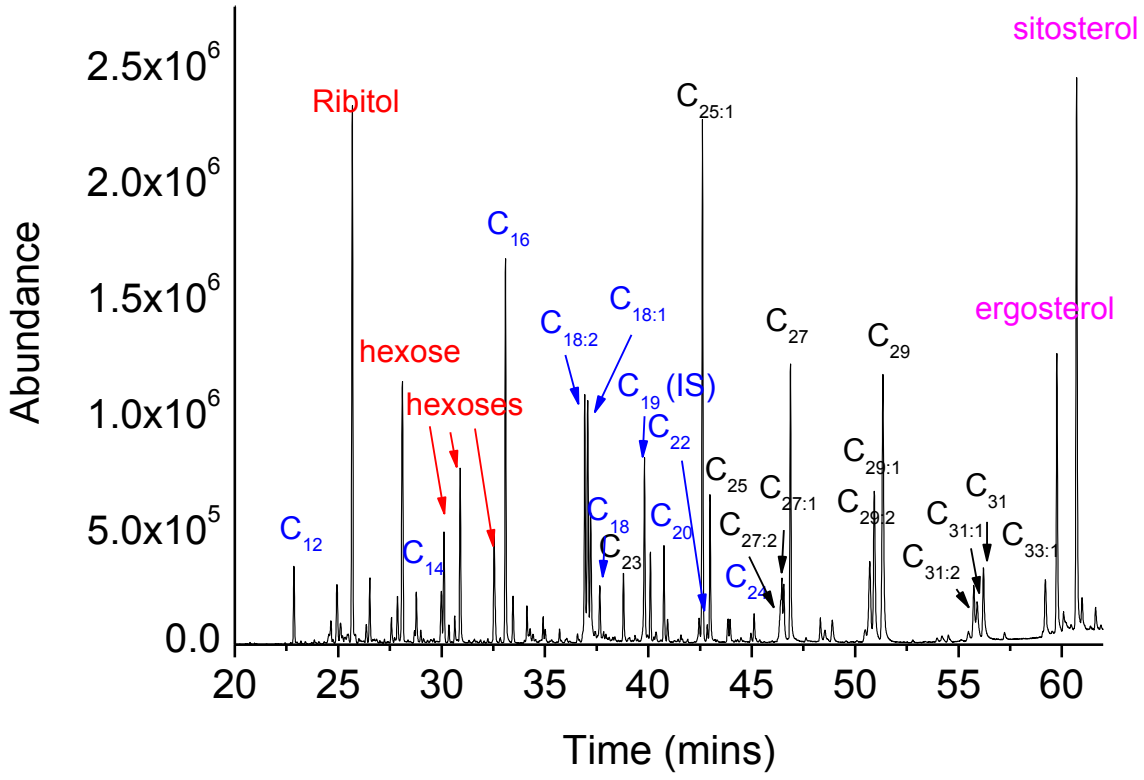

Figure 3. Gas chromatography of nonpolar fraction of total metabolite extract from maize silks. Red-sugars, contamination from polar fraction; blue-fatty acids; black-hydrocarbons; and magenta-sterols.

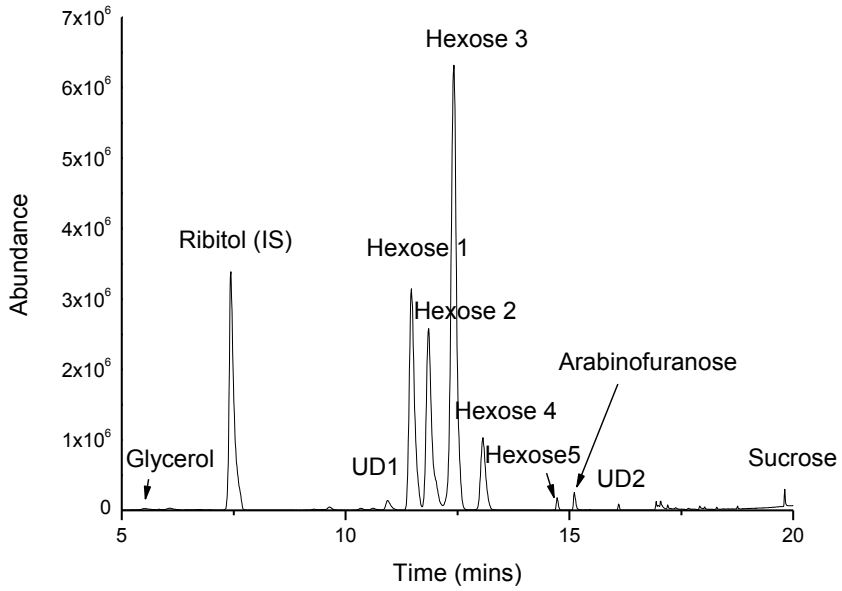

Figure 4. Gas chromatography of polar fraction of total metabolite extract from maize silks.

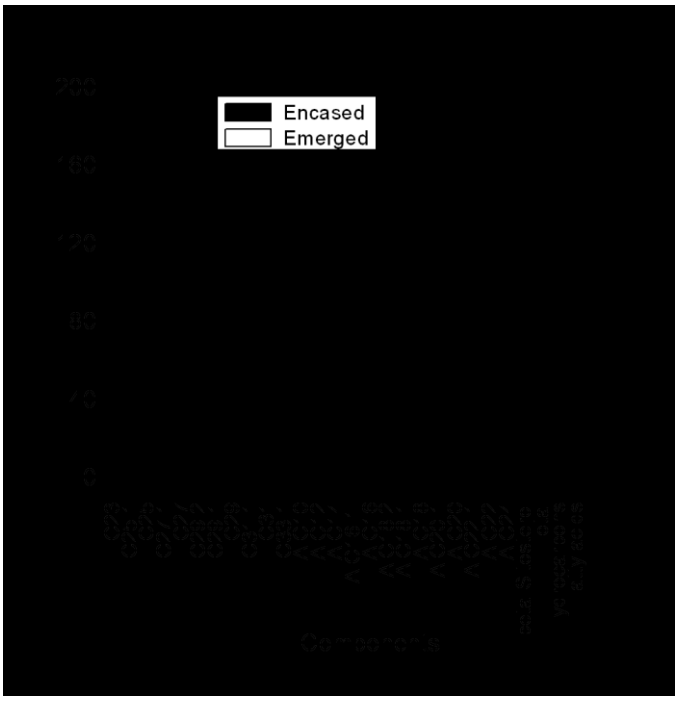

Figure 5. Hydrocarbons and fatty acids in the nonpolar fraction of total metabolite extracts in B73 encased and emerged silks

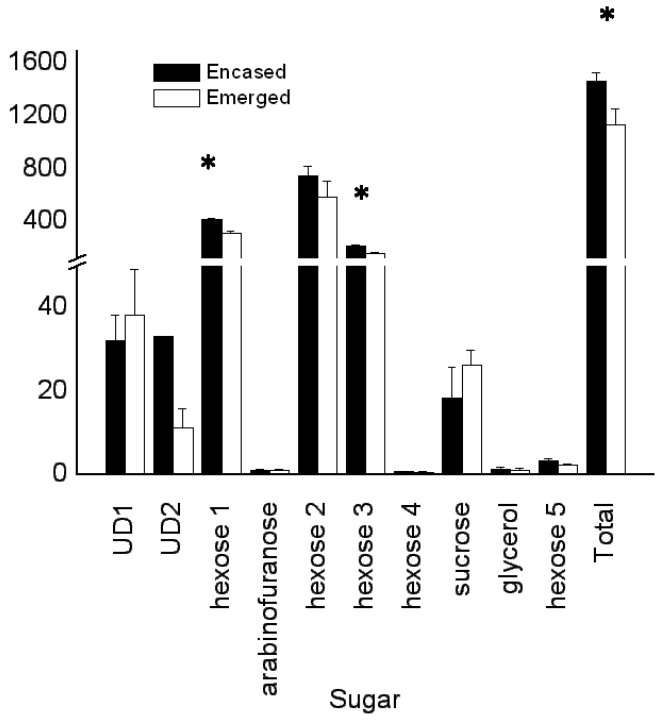

Figure 6. Sugars in the polar fraction of total metabolite extracts in B73 encased and emerged silks